IMPROVED METHODS IN NEURAL NETWORK-BASED ADAPTIVE OUTPUT FEEDBACK CONTROL, WITH APPLICATIONS TO FLIGHT CONTROL

A Thesis
Presented to
The Academic Faculty

by

Nakwan Kim

In Partial Fulfillment
of the Requirements for the Degree
Doctor of Philosophy

School of Aerospace Engineering
Georgia Institute of Technology
November 2003

IMPROVED METHODS IN NEURAL NETWORK-BASED ADAPTIVE OUTPUT FEEDBACK CONTROL, WITH APPLICATIONS TO FLIGHT CONTROL

Approved by:

Anthony J. Calise, Chairman

J.V.R. Prasad

Eric N. Johnson

J. Eric Corban

Naira Hovakimyan

Date Approved: November 25, 2003

To my wife

사랑하는 아내에게

ACKNOWLEDGEMENTS

First and foremost, I would like to thank my advisor Dr. Anthony J. Calise for his wisdom, generosity, and limitless patience in helping me to understand and fulfill my study. The level of professional advice and insight has been incredible. I am fortunate to have worked with him.

I would like to express my sincere gratitude to my thesis committee members: Dr. J.V.R. Prasad, Dr. Eric N. Johnson, Dr. J. Eric Corban, and Dr. Naira Hovakimyan for taking time to read and evaluate this document. I have gained much from their comments and I have enjoyed their company.

I am grateful to all of my colleagues at Georgia Tech including Hesham El-Shirbiny, Tomohisa Hayakawa, Jeong Hur, Matt Johnson, Suresh Kannan, Choong-Yil Kim, Ali Kutay, Venkatesh Madyastha, Pylyp Papush, Ramachandra Sattigeri, Yoong-Hyun Shin, Suraj Unnikrishnan, Bong-Jun Yang, Ilkay Yavrucuk, and a spiritual sponsor Joseph De Kroon. A special thank you goes to Matt for his generous and painstaking proofreading a draft version of the dissertation. I want to thank Dr. Calise and all the other members of controls group for making the control labs a fun place to work.

Finally, I would like to thank my wife and parents back in Korea for all their love, support, and encouragement. Without them, this work would have been much harder.

TABLE OF CONTENTS

DEDICATION . . . . . **iii**

ACKNOWLEDGEMENTS . . . . . **iv**

LIST OF FIGURES . . . . . **viii**

SUMMARY . . . . . **xiv**

I INTRODUCTION **1**

1.1 Nonlinear Adaptive Control 1

1.2 NN Augmented Feedback Linearization 3

1.3 NN Augmentation of Existing Controllers 5

1.4 Assumption on Sign of Control Effectiveness 6

1.5 Contributions of this Thesis 7

1.6 Thesis Outline 8

II SIGN OF CONTROL EFFECTIVENESS **10**

2.1 Problem Formulation 11

2.2 NN Approximation of the Inversion Error 14

2.3 Modeling Error Reformulation 15

2.4 Extension to Output Feedback Control 21

III NEURAL NETWORK AUGMENTED INPUT/OUTPUT FEEDBACK LINEARIZATION **31**

3.1 Plant Description 32

3.2 Controller Design and Tracking Error Dynamics 33

3.3 Design of an Observer for the Error Dynamics 40

3.4 Adaptive Laws and Boundedness Analysis 41

3.4.1 NN Adaptation with σ-modification 42

3.4.2 NN Adaptation with e-modification 46

3.4.3 NN Adaptation with Projection 48

3.5 Pseudo Control Hedging 52

3.5.1 Static Actuation 56
3.5.2 Dynamic Actuation 60
3.6 Design and Performance Results of R-50 Helicopter Model 62
3.7 Application to High Bandwidth Longitudinal Flight Control 73
3.7.1 Relative Degree = 1 Design 74
3.7.2 Relative Degree = 2 Design 76
3.7.3 Numerical Results 78
3.8 Nonlinearly-Parameterized NN with SPR Approach 81
3.8.1 Controller Design 82
3.8.2 Numerical Example 86
IV NN AUGMENTATION OF EXISTING CONTROLLERS 93
4.1 Existing Controller Augmentation Scheme 94
4.1.1 Error Observer Approach 99
4.1.2 SPR Filter Approach 101
4.2 Extension to MIMO Systems 104
4.3 Application to Guided Munitions 111
4.3.1 Numerical Results 113
4.3.2 Command Limiting Using Angle of Attack 119
V NN ADAPTIVE CONTROL WITH ASYMPTOTIC TRACKING 129
5.1 System Description and Error Dynamics 129
5.2 Adaptive Control Augmentation 132
VI CONCLUSIONS AND RECOMMENDATIONS FOR FUTURE RESEARCH 135
6.1 Conclusion 135
6.2 Recommendations for Future Research 136
6.2.1 Relaxation of Assumption 3.5.2 136
6.2.2 Relaxation of Assumption 3.8.1 137
6.2.3 Extension of Chapter 4 to Non-minimum Phase Systems . . . 137

6.2.4 Extension of Chapter 5 to Output Feedback 137

APPENDIX A — PROOFS OF BOUNDEDNESS ANALYSIS . . 138

A.1 Error Observer Approach with e-modification (Theorem 2.4.2) . . . 138

A.2 Error Observer Approach with σ-modification (Theorem 3.4.1) . . . 141

A.3 Error Observer Approach with e-modification (Theorem 3.4.2) . . . 145

A.4 Error Observer Approach with Projection (Theorem 3.4.3) 148

A.5 SPR Filter Approach with e-modification (Theorem 3.8.1) 151

A.6 Augmentation of Existing Controllers with SPR Filter and σ-modification (Theorem 4.1.2) 153

A.7 Augmentation of Existing Controllers in MIMO Systems with Error Observer and e-modification (Theorem 4.2.1) 155

A.8 Asymptotic Tracking with Adaptive Bounding (Theorem 5.2.1) . . . 159

REFERENCES 161

VITA 167

LIST OF FIGURES

1 Nonlinearly-parameterized NN architecture 16

2 Geometric representation of the sets in the error space 21

3 Control system architecture without PCH 35

4 Projection operator 50

5 Computation of the PCH signal 53

6 The n^{th}-order reference model with PCH signal 54

7 R-50 unmanned helicopter 62

8 Generic block diagram of single channel of adaptive attitude command system with pseudo control hedging 63

9 Pitch tracking performance without NN controller 67

10 Pitch tracking performance with NN controller and σ-modification . . 68

11 NN weights $(\hat{W}, \hat{V})$ history and Δ vs. v_{ad} with σ-modification 68

12 Pitch tracking performance with e-modification 69

13 NN weights $(\hat{W}, \hat{V})$ history and Δ vs. v_{ad} with e-modification 69

14 Pitch tracking performance with projection 70

15 NN weights $(\hat{W}, \hat{V})$ history and Δ vs. v_{ad} with projection 70

16 R-50 flight test in attitude control without NN 71

17 R-50 flight test in attitude control with NN 71

18 Generic block diagram of single channel of an adaptive rate command system 76

19 Baseline design performance. 79

20 Relative degree = 1 design ($w_c = 7$ rad/sec). 80

21 Bode plots of the full model and the short period model. 80

22 Relative degree = 2 design ($w_c = 7$ rad/sec). 81

23 System response with a linear compensator 88

24 System response with nonlinearly-parameterized NN 88

25 System response with linearly-parameterized NN 89

26 Weight history with linearly-parameterized NN 89
27 Weight (W) history with nonlinearly-parameterized NN 90
28 Weight (V) history with nonlinearly-parameterized NN 90
29 Control position with nonlinearly-parameterized NN 91
30 Control position with linearly-parameterized NN 91
31 Δ vs. v_{ad} with nonlinearly-parameterized NN 92
32 Δ vs. v_{ad} with linearly-parameterized NN 92
33 Adaptive control architecture with existing controller augmentation using simple reference model 96
34 A schematic diagram of JDAM 112
35 10%-to-90% rise time specification 117
36 Transient-test commands 117
37 Transient response at Mach 1 and 20 Kft with SPR filter approach . . 118
38 10%-to-90% rise time comparison 118
39 Transient response at Mach 1 and 20 Kft with error observer approach 119
40 Nonlinear model at Mach 0.8 and 20 Kft 121
41 Adaptive control architecture with existing controller augmentation and command limiting 122
42 Nonlinear model without command limiting or NN at Mach 0.8 and 20 Kft 125
43 AoA and control effort without command limiting or NN at Mach 0.8 and 20 Kft 125
44 Nonlinear model without command limiting and with NN at Mach 0.8 and 20 Kft 126
45 AoA and control effort without command limiting and with NN at Mach 0.8 and 20 Kft 126
46 Nonlinear model with command limiting and NN at Mach 0.8 and 20 Kft 127
47 AoA and control effort with command limiting and NN at Mach 0.8 and 20 Kft 127
48 Command limiting and NN at Mach 0.8 and 20 Kft with parametric uncertainty in y_l (80%) 128

49 Command limiting and NN at Mach 0.8 and 20 Kft with parametric uncertainty in y_l (150%) 128

NOMENCLATURE

a	Sigmoidal activation potential
a^*	Maximum of activation potentials
e	Reference model tracking error
$\boldsymbol{E}$	Error dynamics state
$\hat{\boldsymbol{E}}$	Error dynamics observer state
$f(\cdot)$	Plant dynamics
$G_d(s)$	Desired feedback linearized system transfer function
$h(\cdot)$	System output function
$h_r(\cdot)$	r^{th} derivative of the system output function
$\hat{h}_r(\cdot)$	Approximation of $h_r(\cdot)$
I	Identity matrix
k_σ	σ-modification gain
k_e	e-modification gain
K	Error dynamics observer gain
K_P,K_D	Proportional gain and derivative gain of the dynamic compensator
n	Dimension of the system
n_1, n_2, n_3	Numbers of neural network inputs, of hidden-layer neurons and of outputs
P, Q	Positive definite matrices for Lyapunov equation
$\Re^n$	n-dimensional Euclidean space
r	Relative degree
u	Control input variable
u_{cmd}	Commanded control input
$\hat{u}$	Estimated control input using a model for the actuator characteristics
v	Total pseudo-control
v_{rm}	Reference model pseudo-control component

v_{dc}	Dynamic Compensator pseudo-control component
v_h	Hedge signal
v_{ad}	Neural network output
W, V, Z	Neural network weights
$\boldsymbol{x}$	State vector for plant dynamics
x_{rm}	Reference model state
y	Regulated output variable
$\bar{y}$	Additional measurements that are available for feedback
y_{com}	Pre-filtered tracking command
y_{rm}	Reference model state variables
$\boldsymbol{\mu}$	Neural network input vector
$\Delta(\cdot)$	Model error function
Γ_W, Γ_V	Diagonal matrices containing neural network learning rates
ϵ	Neural network reconstruction error
η	Dynamic compensator state
$\lambda_{min}(\cdot)$	Minimum eigenvalue
$\lambda_{max}(\cdot)$	Maximum eigenvalue
$\boldsymbol{\chi}$	State vector associated with the internal dynamics
$\boldsymbol{\xi}$	State vector associated with the output dynamics
$\boldsymbol{\sigma}(\cdot), \sigma'(\cdot)$	Neuron sigmoidal function and its gradient
AoA	Angle of Attack
IMU	Inertial Measurement Unit
JDAM	Joint Direct Attack Munition
LHP	Left Half Plane
MIMO	Multi-input multi-output

NN	Neural Network
PCH	Pseudo Control Hedging
RHP	Right Half Plane
SISO	Single-input single-output
SPR	Strictly Positive Real

SUMMARY

Utilizing the universal approximation property of neural networks, we develop several novel approaches to neural network-based adaptive output feedback control of nonlinear systems, and illustrate these approaches for several flight control applications. In particular, we address the problem of non-affine systems and eliminate the fixed point assumption present in earlier work. All of the stability proofs are carried out in a form that eliminates an algebraic loop in the neural network implementation. An approximate input/output feedback linearizing controller is augmented with a neural network using input/output sequences of the uncertain system. These approaches permit adaptation to both parametric uncertainty and unmodeled dynamics. All physical systems also have control position and rate limits, which may either deteriorate performance or cause instability for a sufficiently high control bandwidth. Here we apply a method for protecting an adaptive process from the effects of input saturation and time delays, known as "pseudo control hedging". This method was originally developed for the state feedback case, and we provide a stability analysis that extends its domain of applicability to the case of output feedback. The approach is illustrated by the design of a pitch-attitude flight control system for a linearized model of an R-50 experimental helicopter, and by the design of a pitch-rate control system for a 58-state model of a flexible aircraft consisting of rigid body dynamics coupled with actuator and flexible modes.

A new approach to augmentation of an existing linear controller is introduced. It is especially useful when there is limited information concerning the plant model, and the existing controller. The approach is applied to the design of an adaptive autopilot for a guided munition. Design of a neural network adaptive control that ensures asymptotically stable tracking performance is also addressed.

CHAPTER I

INTRODUCTION

1.1 Nonlinear Adaptive Control

Historically, linear control design has dominated flight control applications and is thus well established. Linear controllers are designed to achieve desired stability and performance requirements for a linearized model of the system dynamics at selected operating points. As modern high-performance aircraft are required to be ever more maneuverable, they encounter complex nonlinear dynamics that cannot be easily approximated by linear models. Thus the use of nonlinear control theory is motivated to meet the stability and performance requirements in the presence of highly nonlinear dynamics.

Recently, a systematic approach to nonlinear control called "feedback linearization" [1, 2] has gained popularity and has been applied to flight control [3, 4, 5]. It utilizes a smooth nonlinear coordinate transformation to transform an original nonlinear plant into an equivalent linear time-invariant form, and then uses well-known and powerful linear control design techniques to complete the control design. Limitations of the method of feedback linearization are that it is applicable only to minimum phase systems, and that it requires an accurate nonlinear model. Thus robustness to uncertainties is not guaranteed. Unfortunately, uncertainties are common in real-world systems. Such uncertainties include parametric uncertainty and unmodeled dynamics. Systems with uncertainties can be dealt with by robust control. Given upper bounds on the modeling error, one designs a feedback control law that guarantees stability and performance specifications for all uncertainties within the given bounds. The design process requires both a nominal model and some characterization of the

model uncertainties.

An alternative to robust control is adaptive control. Adaptive control offers the advantage that the bounds on uncertainty are not necessarily required to be known since the uncertainty is adaptively cancelled online. In an adaptive control setting, the controller parameters are updated online using signals that are available within the system. Gain scheduling can be categorized as an adaptive control within the context of this broad definition. It alters linear controller gains according to the environmental properties at different operating points. Adaptive control has been most successful for plants in which the unknown parameters appear linearly. Standard adaptive control design methods are limited by the assumption that there exists a linear parametrization of the plant uncertainty. The difficulty lies in finding the correct parametrization to use. Neural networks (NNs) offer the potential to overcome the difficulties associated with applying adaptive control to highly uncertain nonlinear systems, for which a linear parametrization of the uncertainty is not known.

NNs are universal approximators [6, 7, 8] and provide a convenient way to parameterize uncertainty. NNs provide a way to approximate a continuous nonlinear function to any degree of accuracy on a compact set. We can leave the burden of parameterizing an unknown nonlinear function to the NN and use nonlinear stability theory to derive adaptation laws for updating the NN weights. NNs are nonlinear functions whose parameters are the weights and biases of the network. Adaptation of the NN parameters (weights) is typically obtained by gradient algorithms using the tracking error, which in turn is a filtered difference between the output of the NN and the unknown function to be approximated by the NN. There are other approximator structures such as conventional polynomials and fuzzy systems [9, 10, 11].

Early results in adaptive control suffered from lack of robustness (i.e. parameter drift) to bounded disturbances and unmodeled dynamics. This led many researchers to study the instabilities arising from the lack of robustness which led to a body of

research known as robust adaptive control. Several techniques and alterations were proposed to assure boundedness of all signals in the presence of system uncertainties. These include σ-modification [12, 13], e-modification [14, 15], parameter projection [16, 17] and dead-zone [18, 19]. The idea is to modify the adaptive law so that the time derivative of the Lyapunov function used to analyze the adaptive scheme becomes negative when the adaptive parameters go beyond certain bounds. Although σ-modification was introduced to avoid parameter drift, it has a disadvantage that even in the ideal case when there is perfect NN reconstruction without other disturbances, σ-modification does not drive the errors to zero. This shortcoming motivated another variation called e-modification, which eliminates the main drawback of σ-modification by multiplying the norm of error signal with the σ-modification term in the adaptive law. Parameter projection keeps the NN weights inside a prescribed convex set that contains the unknown optimal weights. This approach requires a known norm bound for the NN weights, while both σ and e-modifications require no a priori information about the NN weights. A comprehensive treatment of robust adaptive control can be found in Ioannou and Sun [20] and in Ortega and Tang [21].

1.2 NN Augmented Feedback Linearization

NN adaptive control combined with feedback linearization [22, 23, 24] is a popular method for control of nonlinear systems. This method takes advantage of feedback linearization and assigns the NN to deal with uncertainty in the system. In [22] linearly-parameterized NNs have been used in combination with feedback linearization to compensate online for the error introduced by using an approximate inverting transformation. Stability analysis pertaining to control of affine discrete-time nonlinear systems using nonlinearly-parameterized NNs first appeared in [25]. The first analysis of nonlinearly-parameterized NNs for continuous-time systems appeared in [26]. Applications in robotics are described in [27, 28, 29]. Extensions to non-affine

systems together with applications in flight control can be found in [22, 30, 23, 31, 24]. Comprehensive overviews of NNs for control systems are provided in survey papers [32, 33, 34].

Extensions of the methods described above to observer-based output feedback controls are treated in [35, 36]. However, these results are limited to systems with full relative degree (vector relative degree = degree of the system) with the added constraint that the relative degree of each output is less than or equal to two [37]. In the SISO (single-input single-output) case, this implies that observer-based adaptive output feedback control is limited to second order systems with position measurement. Moreover, since state observers are employed, the dimension of the plant must be known. Therefore, methods that rely on a state observer are vulnerable to unmodeled dynamics. In [38] a direct adaptive approach is developed that removes the limitations inherent in state observer-based design. In [39] these same limitations are overcome by employing an error observer, in place of a state observer. The only requirement in the latter two approaches is that the relative degree of the regulated output be known. These works have been limited to the use of σ-modification. This thesis provides proof of boundedness for e-modification and parameter projection, thereby allowing more latitude in choosing an adaptive algorithm for output feedback control.

Adaptive systems are known to be sensitive to control limits. All physical systems have control position and rate limits. These limits are potentially destabilizing, particularly under high-bandwidth control. In [40, 41] a novel approach for treating control limits within an adaptive control setting called "pseudo-control hedging" (PCH) was introduced and developed for the state feedback case. A PCH signal is first calculated by taking the difference between the pseudo control and an estimate of the achievable pseudo control, and then the PCH signal is used to modify the reference model. The PCH method removes selected plant input characteristics (discrepancies between commanded and actual plant input) from tracking error dynamics

and prevents adaptation to these characteristics.

Both classical and modern control design methods are fundamentally limited by the presence of unmodeled high frequency effects. The same is particularly true in adaptive methods that attempt to learn and interact with these effects. One goal of this thesis has been to develop an approach to flight control design that is inspired by the performance levels that pilots are able to attain through long hours of training. This implies that we explicitly account for and adapt to the presence of unmodeled and potentially nonlinear dynamics in an output feedback setting, even if all the states of the modeled portion of the system are available for feedback. Adaptation to unmodeled dynamics is achieved by recognizing the effect that these dynamics have; both in terms of degree and relative degree of the system. This implies that, in the context of controlling the system with unmodeled dynamics, we must treat the design like an output feedback problem. Our main assumptions are that the system is minimum phase, stabilizable and observable, and that the relative degree of the regulated output variable is known. The dimension of the plant need not be known.

1.3 NN Augmentation of Existing Controllers

The main idea of NN augmentation of an existing controller is to combine the use of a NN adaptive element, which can accommodate for model errors online, and the simplicity of a linear fixed-gain control, such as a PID controller. Several attempts to develop a method for adding an adaptive element to an existing linear controller architecture have appeared in the literature [42, 43, 44]. These methods are limited to state feedback, and matched uncertainty [43, 44]. In [42], dynamic systems that are particular to robots are considered. In [45, 46] output feedback adaptive control approaches for augmenting an existing linear controller are developed, and applied to control of uncertain flexible systems. These approaches are limited to minimum phase systems. An extension to control of non-minimum phase systems can be found in [47].

In all of these approaches, a reference model is chosen by making use of an existing controller that guarantees performance requirements when applied to a known plant model. Knowledge of the plant model and the existing controller is assumed. However, there are many situations in which the plant model is unknown (or only its structure is known), and the controller is designed by tuning its parameters. Consequently, the controller design (often gain scheduled) is not directly linked to a known plant model, and the plant model is not available to define a reference model for adaptive control design purposes. Here we develop an approach that makes use of a simple reference model which has the same relative degree as the true plant. The advantage here is that the designer is free to specify the reference model without requiring information on how the existing linear controller was designed. The reference model can be chosen freely as long as it is stable and of the same relative degree as the true plant.

1.4 Assumption on Sign of Control Effectiveness

Knowledge of the sign of control effectiveness is a common assumption in adaptive control. For an affine system with constant control effectiveness it is not difficult to show that knowledge of the sign of control effectiveness is needed to obtain a reasonable adaptive law. For an affine system with state-dependent control effectiveness or for a non-affine system, the requirement for knowledge of the sign of control effectiveness has not been adequately addressed in the existing literature. In [38, 48, 39] this issue is addressed by introducing a fixed point assumption. In the NN-augmented feedback linearization approach, the modeling error is a function of the output of the NN, which is in turn designed to cancel the modeling error. This approach requires existence of a fixed point solution to the equation relating the output of the NN and the modeling error. In [38], it has been pointed out that applying the condition for a contraction mapping to the modeling error leads to the conclusion that control effectiveness for an approximate model has the same sign as the plant. Thus the

requirement for knowledge of the sign of the control effectiveness is implicit in the overall approach, but does not appear explicitly in the stability analysis. However, it can be shown that applying the contraction mapping to an equivalent condition leads to the opposite conclusion, that the estimate for the control effectiveness has the opposite sign of the true control effectiveness. This suggests that knowledge of the sign of the control effectiveness is not relevant to the issue of existence of a fixed point solution. Here we employ the mean value theorem to avoid the assumption of a fixed point solution, and elucidate the role of the sign of control effectiveness both in the boundedness analysis and in the adaptive law.

In [49] signal boundedness was proven by using the mean value theorem in a non-affine system. The mean value theorem was utilized to represent the non-affine system in an affine form. This proof was limited to state feedback control without internal dynamics. Here we adopt the method in [49] to reformulate the modeling error such that it is not an explicit function of the NN output, thus eliminating the issue of a fixed point solution. A new adaptive law is developed in which knowledge of the sign of the control effectiveness is explicitly needed to prove that the response is bounded. We also extend the stability analysis so that it is applied to an output feedback setting with internal dynamics as well.

1.5 Contributions of this Thesis

The main contributions of this thesis include:

- Elimination of the so-called "fixed point problem" in adaptive control of non-affine systems, and clarification on the role that knowledge of the sign of control effectiveness plays in adaptive control of non-affine systems.
- A novel approach to approximate input/output feedback linearization that employs a pole shifting idea.

- Boundedness analysis of PCH with NN adaptive control in an output feedback setting.
- Boundedness proof of NN adaptive output feedback control with e-modification.
- Boundedness proof of NN adaptive output feedback control with parameter projection.
- Implementations of NN adaptive control for high-bandwidth helicopter pitch attitude control and flexible aircraft pitch rate control.
- Extension of the direct adaptive output feedback control method in [38] to include nonlinearly-parameterized NNs.
- Development of a method to augment an existing controller with a NN when there is limited information of the plant and existing controller. Demonstration of the efficacy of the adaptive scheme in a JDAM munition autopilot design.
- Extension of the augmentation of existing controllers to multi-input multi-output (MIMO) systems.
- A technique of command limiting so as to avoid an excessive excursion in a selected state variable.
- A design of a NN adaptive control which ensures asymptotic tracking performance. This work is done with nonlinearly-parameterized NN and parameter projection.

1.6 Thesis Outline

Chapter 2 eliminates the requirement that there exists a fixed-point solution for the output of NN to cancel the modeling error. The need of knowledge of the sign

of control effectiveness is shown both in new NN adaptive laws and the proof of boundedness. The NN universal approximation property is briefly explained.

Chapter 3 presents an approach combining NN-based adaptive control and input/output feedback linearization in an output feedback setting. Designs of the adaptive controller and an observer for the error dynamics are described. Ultimate boundedness of all the signals is proven in three adaptive schemes. The approach is illustrated by the design of a pitch-angle flight control system for a linearized model of an R-50 experimental helicopter and a pitch-rate command system design of a 58-state model of a flexible aircraft. A direct adaptive approach with a nonlinearly-parameterized NN, without the use of the error observer, is presented and a numerical example is included to demonstrate the efficiency of the approach.

Chapter 4 describes an approach to augment an existing controller with a NN-based adaptive element. The augmenting architecture developed offers two choices in the output feedback setting: the error observer approach and the direct approach. An application to a JDAM munition autopilot design is treated. These results include command limiting in the case of excessive angle of attack. The augmenting architecture is extended to MIMO systems with the error observer approach in Section 4.2.

Chapter 5 introduces an adaptive scheme which achieves asymptotic convergence of the tracking error to zero while guaranteeing boundedness of other signals. The method utilized parameter projection, adaptive bounding and Barbalat's lemma.

The results of the research effort are summarized in Chapter 6, where conclusions are presented along with directions for future research. The main proofs of boundedness are given in Appendices A.1 - A.8.

CHAPTER II

SIGN OF CONTROL EFFECTIVENESS

Experience in simulation has shown that an unknown reversal in the sign of the control effectiveness invariably leads to an unstable response. Nevertheless, knowledge of the sign of control effectiveness is not incorporated explicitly in the proof of stability [38, 39, 48]. A fixed point of $f(x)$ is defined as a point $x \in \mathcal{D}$ satisfying $f(x) = x$ where $f(x)$ is a function with domain $\mathcal{D}$ [50]. In the NN-augmented feedback linearization approach, the modeling error, Δ, is a function of the output of NN, v_{ad}, which is designed to cancel $\Delta(\cdot, v_{ad})$ and obtain stable error dynamics. This raises the question of existence of a fixed point solution to the equation $v_{ad} = \Delta(\cdot, v_{ad})$. In [38] a contraction mapping assumption is imposed on $\Delta(\cdot, v_{ad})$ with respect to v_{ad} to guarantee the existence of a fixed point solution to $v_{ad} = \Delta(\cdot, v_{ad})$. The contraction mapping condition on $\Delta(\cdot, v_{ad})$ requires that $\text{sgn}(\partial \hat{h}_r(\boldsymbol{x}, u)/\partial u) = \text{sgn}(\partial h_r(\boldsymbol{x}, u)/\partial u)$, where h_r is the r^{th} derivative of output and $\hat{h}_r$ is an approximate model of h_r. This implies knowledge of the sign of the control effectiveness. However, it can be argued that a solution to $v_{ad} = \Delta(\cdot, v_{ad})$ exists if and only if there exists a solution to $v = h_r(\boldsymbol{x}, u) - v_{ad}$, where $u = \hat{h}_r^{-1}(\boldsymbol{x}, v)$ is the inverting solution for the control. It can be shown that applying the condition for a contraction to $h_r(\boldsymbol{x}, u) - v_{ad}$ with respect to v leads to the condition $\text{sgn}(\partial \hat{h}_r(\boldsymbol{x}, u)/\partial u) = -\text{sgn}(\partial h_r(\boldsymbol{x}, u)/\partial u)$. This suggests that the sign of control effectiveness is not relevant to the existence of a fixed point solution to $v_{ad} = \Delta(\cdot, v_{ad})$. Note that in general, the contraction mapping condition is overly restrictive because it is a sufficient condition for existence of a unique solution, which is more than what may be required. Regardless of this apparent contradiction, knowledge of the sign of the control effectiveness is not explicit in the proofs of

boundedness in [38, 39, 48]. Thus we are inclined to develop an alternate approach to the proof in which the knowledge of the sign of the control effectiveness is explicit.

This chapter will show that knowledge of the control effectiveness appears as an explicit requirement in the adaptation law, and that it is essential for boundedness analysis in the adaptive control setting. This is done by eliminating the issue of a fixed point solution with the use of the mean value theorem so that a reformulated modeling error, $\bar{\Delta}$, is not an explicit function of v_{ad}. We apply this method to augmentation of an existing controller in Chapter 4 as well.

2.1 Problem Formulation

For simplicity of presentation of the main idea we consider a SISO nonlinear system of the following form:

$$\begin{aligned} \dot{x}_i &= x_{i+1}, \quad i = 1, 2, \cdots, n-1 \\ \dot{x}_n &= f(\boldsymbol{x}, u) \end{aligned} \tag{2.1.1}$$

where $\boldsymbol{x} \in \mathcal{D}_x \subset \Re^n$, and $u \in \Re$ is the control input. The function $f(\boldsymbol{x}, u)$ may be unknown. The control objective is to synthesize a state-feedback control law such that $\boldsymbol{x}(t)$ tracks a smooth reference trajectory $\boldsymbol{x}_m(t)$ asymptotically. Let $\hat{f}(\boldsymbol{x}, u)$ denote an approximate model for $f(\boldsymbol{x}, u)$ so that

$$f(\boldsymbol{x}, u) = \hat{f}(\boldsymbol{x}, u) + \Delta \tag{2.1.2}$$

where the modelling error is $\Delta(\boldsymbol{x}, u) = f(\boldsymbol{x}, u) - \hat{f}(\boldsymbol{x}, u)$. The model $\hat{f}(\boldsymbol{x}, u)$ should be chosen to be invertible with respect to its second argument. The invertibility is warranted by the following assumption.

Assumption 2.1.1. $\partial \hat{f}(\boldsymbol{x}, u)/\partial u$ is continuous and non-zero for every $(\boldsymbol{x}, u) \in \mathcal{D}_x \times \Re$.

Let the approximate function be recast as

$$v = \hat{f}(\boldsymbol{x}, u) \tag{2.1.3}$$

where v is called pseudo-control. Then the control law can be defined directly from (2.1.3)

$$u = \hat{f}^{-1}(\boldsymbol{x}, v) \tag{2.1.4}$$

The pseudo-control is composed of three signals:

$$v \triangleq x_m^{(n)} + v_c - v_{ad} \tag{2.1.5}$$

where $x_m^{(n)}$ is the n^{th} time derivative of $x_m(t)$, v_c is the output of a linear controller, and v_{ad} is an adaptive term designed to cancel $\Delta(\boldsymbol{x}, u)$.

The reference model can be expressed in state space form as:

$$\dot{\boldsymbol{x}}_m = A_m \boldsymbol{x}_m + \boldsymbol{b}_m x_c \tag{2.1.6}$$

$$\boldsymbol{x}_m \triangleq \begin{bmatrix} x_m & \dot{x}_m & \cdots & x_m^{(n-1)} \end{bmatrix}^T$$

$$A_m = \begin{bmatrix} 0 & 1 & 0 & \cdots & 0 \\ 0 & 0 & 1 & \cdots & 0 \\ \vdots & \vdots & \vdots & \ddots & \vdots \\ 0 & 0 & 0 & 0 & 1 \\ -a_1 & -a_2 & -a_3 & \cdots & -a_n \end{bmatrix}, \boldsymbol{b}_m = \begin{bmatrix} 0 \\ 0 \\ 0 \\ \vdots \\ a_1 \end{bmatrix},$$

where $\boldsymbol{x}_m \in \Re^n$ are the state vector of the reference model, $x_c \in \Re$ is a bounded external command signal, and A_m is Hurwitz.

Let $e \triangleq x_m - x_1$. Then

$$e^{(n)} = -v_c + v_{ad} - \Delta \tag{2.1.7}$$

For simplicity, the linear controller is defined as:

$$v_c = k_1 e + k_2 \dot{e} + \cdots + k_n e^{(n-1)} \tag{2.1.8}$$

where the gains k_i are chosen such that the dynamics in (2.1.7) are asymptotically stable when $v_{ad} - \Delta = 0$. In state space form:

$$\dot{\boldsymbol{E}} = A\boldsymbol{E} + \boldsymbol{b}(v_{ad} - \Delta(\boldsymbol{x}, u)) \tag{2.1.9}$$

where $\boldsymbol{E} = \begin{bmatrix} e & \dot{e} & \cdots & e^{(n-1)} \end{bmatrix}^T$, and

$$A = \begin{bmatrix} 0 & 1 & 0 & \cdots & 0 \\ 0 & 0 & 1 & \cdots & 0 \\ \vdots & \vdots & \vdots & \ddots & \vdots \\ 0 & 0 & 0 & 0 & 1 \\ -k_1 & -k_2 & -k_3 & \cdots & -k_n \end{bmatrix}, \boldsymbol{b} = \begin{bmatrix} 0 \\ 0 \\ 0 \\ \vdots \\ 1 \end{bmatrix}.$$

Remark 2.1.1. Reference [38] points out that Δ depends on v_{ad} through (2.1.4) and (2.1.5) and that v_{ad} is designed to cancel Δ. The contraction assumption was introduced to guarantee the existence and uniqueness of a solution for v_{ad} to $v_{ad} = \Delta(\cdot, v_{ad})$. The contraction is satisfied by the following condition:

$$\left| \frac{\partial \Delta}{\partial v_{ad}} \right| < 1 \tag{2.1.10}$$

This implies:

$$\left| \frac{\partial \Delta}{\partial v_{ad}} \right| = \left| \frac{\partial (f - \hat{f})}{\partial u} \frac{\partial u}{\partial v} \frac{\partial v}{\partial v_{ad}} \right| = \left| \frac{\partial (f - \hat{f})}{\partial u} \frac{\partial u}{\partial \hat{f}} \right| < 1, \tag{2.1.11}$$

which can be rewritten in the following way:

$$\left| \frac{\partial f / \partial u}{\partial \hat{f} / \partial u} - 1 \right| < 1. \tag{2.1.12}$$

Condition (2.1.12) is satisfied if and only if the two following conditions hold:

$$\operatorname{sgn}\left(\frac{\partial f}{\partial u} \right) = \operatorname{sgn}\left(\frac{\partial \hat{f}}{\partial u} \right), \tag{2.1.13}$$

$$0 < \frac{1}{2} \left| \frac{\partial f}{\partial u} \right| < \left| \frac{\partial \hat{f}}{\partial u} \right| < \infty \tag{2.1.14}$$

This leads to the conclusion that one of the sufficient conditions that ensures existence of a solution to the equality $v_{ad} = \Delta(\cdot, v_{ad})$ is that the $\text{sgn}(\partial \hat{f}(\boldsymbol{x}, u)/\partial u) = \text{sgn}(\partial f(\boldsymbol{x}, u)/\partial u)$. Thus, knowledge of the sign of the control effectiveness is implicit in the approach to guarantee existence of a solution. However, a solution to $v_{ad} = \Delta(\cdot, v_{ad})$ exists if and only if there exists a solution to $v = f(\boldsymbol{x}, u) - v_{ad}$. It can be shown that applying the condition for a contraction mapping to $v = f(\boldsymbol{x}, u) - v_{ad}$ leads to the condition $\text{sgn}(\partial \hat{f}(\boldsymbol{x}, u)/\partial u) = -\text{sgn}(\partial f(\boldsymbol{x}, u)/\partial u)$. Examining the contraction mapping condition we are led to:

$$\begin{aligned} \left| \frac{\partial f}{\partial v} - \frac{\partial v_{ad}}{\partial v} \right| &= \left| \frac{\partial f}{\partial v} + 1 \right| \\ &= \left| \frac{\partial f/\partial u}{\partial \hat{f}/\partial u} + 1 \right| < 1 \\ -2 < \frac{\partial f/\partial u}{\partial \hat{f}/\partial u} &< 0 \end{aligned} \tag{2.1.15}$$

which is equivalent to:

$$\text{sgn}\left(\frac{\partial \hat{f}}{\partial u}\right) = -\text{sgn}\left(\frac{\partial f}{\partial u}\right) \tag{2.1.16}$$

$$0 < \frac{1}{2}\left|\frac{\partial f}{\partial u}\right| < \left|\frac{\partial \hat{f}}{\partial u}\right| < \infty \tag{2.1.17}$$

Since both (2.1.13) and (2.1.16) are sufficient for existence of a fixed point solution to $v_{ad} = \Delta$, it follows that

$$0 < \frac{1}{2}\left|\frac{\partial f}{\partial u}\right| < \left|\frac{\partial \hat{f}}{\partial u}\right| < \infty \tag{2.1.18}$$

alone is sufficient for existence of a fixed point solution. This suggests that knowledge of the sign of the control effectiveness is not relevant to the issue of existence of a fixed point solution to $v_{ad} = \Delta(\cdot, v_{ad})$.

2.2 NN Approximation of the Inversion Error

The term "artificial NN" has come to mean any architecture that has massively parallel interconnections of simple "neural" processors [51]. Given $\boldsymbol{x} \in \mathcal{D} \subset \Re^{n_1}$, a

nonlinearly-parameterized (three layer) NN has an output given by

$$y_i = \sum_{j=1}^{n_2} \left[w_{ji}\ \sigma_j \left(\sum_{k=1}^{n_1} v_{kj} x_k + \theta_{vj} \right) \right] + \theta_{wi}, \qquad i = 1, \ldots, n_3 \tag{2.2.1}$$

where $\sigma(\cdot)$ is activation function, v_{kj} are the first-to-second layer interconnection weights, w_{ji} are the second-to-third layer interconnection weights, and θ_{vj}, θ_{wi} are bias terms.

Definition 2.2.1. A function $\sigma : \Re \to \Re$ is a squashing function if it is an activation function, $\lim_{x \to -\infty} \sigma(x) = 0$, and $\lim_{x \to \infty} \sigma(x) = 1$.

The NN structure is depicted in Figure 1. Such an architecture is known to be a universal approximator of continuous nonlinearities with "squashing" activation functions [6, 7, 8]. This implies that a continuous function $\boldsymbol{g}(\boldsymbol{x})$ with $\boldsymbol{x} \in \mathcal{D} \subset \Re^{n_1}$ can be written as

$$\boldsymbol{g}(\boldsymbol{x}) = W^T \boldsymbol{\sigma}(V^T \boldsymbol{x}) + \boldsymbol{\epsilon}(\boldsymbol{x}) \tag{2.2.2}$$

where $\mathcal{D}$ is a compact set and $\boldsymbol{\epsilon}(\boldsymbol{x})$ is the function reconstruction error (also called representation error or approximation error). In general, given a constant real number $\epsilon^* > 0$, $\boldsymbol{g}(\boldsymbol{x})$ is within ϵ^* range of the NN, if there exist constant weights V, W, such that for all $\boldsymbol{x} \in \mathcal{D} \subset \Re^{n_1}$, (2.2.2) holds with $\|\boldsymbol{\epsilon}\| < \epsilon^*$. W and V are the optimal weights defined as:

$$\{W, V\} = \arg \min_{W,V} \left\{ \max_{\boldsymbol{x} \in \mathcal{D}} \| \boldsymbol{g}(\boldsymbol{x}) - W^T \boldsymbol{\sigma}(V^T \boldsymbol{x}) \| \right\} \tag{2.2.3}$$

2.3 Modeling Error Reformulation

Define the following signals,

$$\begin{aligned} v_l &\triangleq x_m^{(n)} + v_c \\ v^* &\triangleq \hat{f}(\boldsymbol{x}, f^{-1}(\boldsymbol{x}, v_l)) \end{aligned} \tag{2.3.1}$$

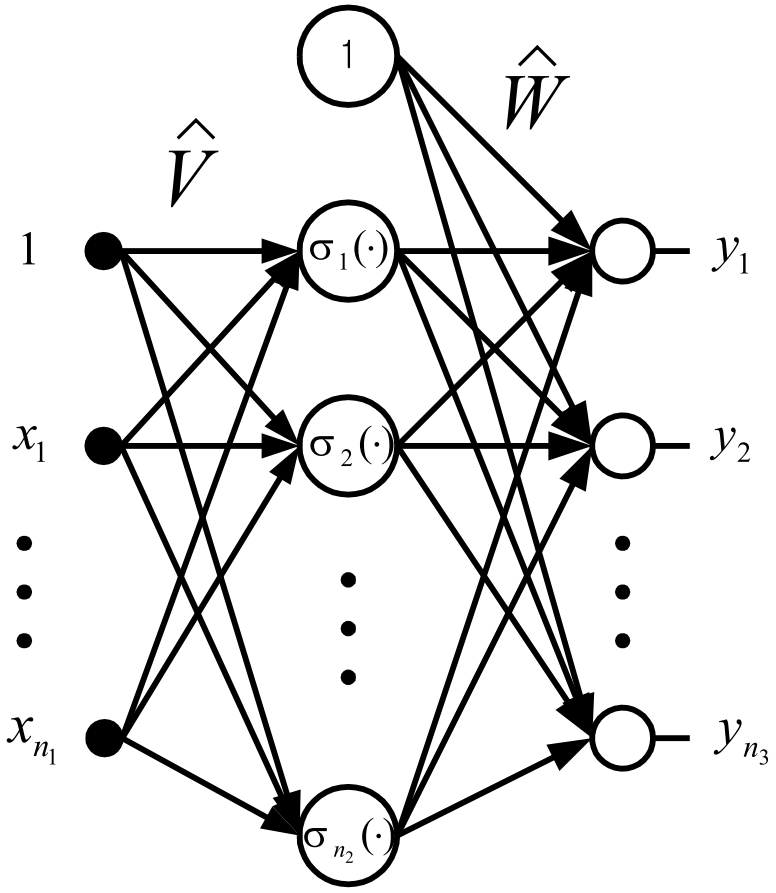

Figure 1: Nonlinearly-parameterized NN architecture

Assumption 2.3.1. $\partial f(\boldsymbol{x}, u)/\partial u$ is continuous and non-zero for every $(\boldsymbol{x}, u) \in \mathcal{D}_x \times \Re$ and its sign is known.

Invertibility of $f(\boldsymbol{x}, u)$ with respect to its second argument is guaranteed by Assumption 2.3.1. From (2.3.1), it follows that v_l can be written as

$$v_l = f(\boldsymbol{x}, \hat{f}^{-1}(\boldsymbol{x}, v^*)) \tag{2.3.2}$$

and,

$$\begin{aligned} v_{ad} - \Delta(\boldsymbol{x}, u) &= v_{ad} - f(\boldsymbol{x}, u) + \hat{f}(\boldsymbol{x}, u) \\ &= v_{ad} - f(\boldsymbol{x}, \hat{f}^{-1}(\boldsymbol{x}, v)) + v_l - v_{ad} \\ &= -f(\boldsymbol{x}, \hat{f}^{-1}(\boldsymbol{x}, v)) + v_l \end{aligned} \tag{2.3.3}$$

Applying the mean value theorem to $f(\boldsymbol{x}, \hat{f}^{-1}(\boldsymbol{x}, v))$

$$\begin{aligned} f(\boldsymbol{x}, \hat{f}^{-1}(\boldsymbol{x}, v)) &= f(\boldsymbol{x}, \hat{f}^{-1}(\boldsymbol{x}, v^*)) + f_{\bar{v}}(v - v^*) \\ &= v_l + f_{\bar{v}}(v - v^*) \end{aligned} \tag{2.3.4}$$

where

$$f_{\bar{v}} \triangleq \left.\frac{\partial f}{\partial u}\frac{\partial u}{\partial v}\right|_{v=\bar{v}}, \ \bar{v} = \theta v + (1-\theta)v^*, \text{ and } \ 0 \leq \theta(v) \leq 1 \tag{2.3.5}$$

Using (2.3.1) and (2.3.4) in (2.3.3),

$$\begin{aligned} v_{ad} - \Delta &= f_{\bar{v}}[v_{ad} - v_l + \hat{f}(x, f^{-1}(\boldsymbol{x}, v_l))] \\ &= f_{\bar{v}}[v_{ad} - \bar{\Delta}(\boldsymbol{x}, v_l)] \end{aligned} \tag{2.3.6}$$

where $\bar{\Delta} = v_l - \hat{f}(\boldsymbol{x}, f^{-1}(\boldsymbol{x}, v_l))$. By Assumption 2.3.1 and 2.1.1, it follows that $f_{\bar{v}} = \frac{\partial f}{\partial u}/\frac{\partial \hat{f}}{\partial u}|_{v=\bar{v}}$ is either strictly positive or strictly negative. Using (2.3.6), we have the following error dynamics.

$$\dot{\boldsymbol{E}} = A\boldsymbol{E} + \boldsymbol{b}f_{\bar{v}}(v_{ad} - \bar{\Delta}(\boldsymbol{x}, v_l)) \tag{2.3.7}$$

Since $\bar{\Delta}$ is not a function of v_{ad}, there is no need of solving a fixed point solution for v_{ad} to cancel $\bar{\Delta}$.

The adaptive element is defined as:

$$\begin{aligned} v_{ad} &= \hat{W}^T \boldsymbol{\sigma}(\hat{V}^T \boldsymbol{\mu}) \\ \boldsymbol{\sigma}(\boldsymbol{z}) &= \begin{bmatrix} 1 & \sigma_1(z_1) & \cdots & \sigma_{n_2}(z_{n_2}) \end{bmatrix}^T \in \Re^{n_2+1} \\ \sigma_i(z_i) &= \frac{1}{1+e^{-a_i z_i}}, \quad i = 1, 2, \cdots, n_2 \end{aligned} \tag{2.3.8}$$

The NN input is $\boldsymbol{\mu} = \begin{bmatrix} 1 & \boldsymbol{x}^T & v_l \end{bmatrix}^T$. The NN weights are updated by the following adaptation law.

$$\begin{aligned} \dot{\hat{W}} &= -\Gamma_W \left[\text{sgn}(f_{\bar{v}}) \hat{\boldsymbol{\sigma}} \boldsymbol{E}^T P \boldsymbol{b} + k_e \|\boldsymbol{E}\| \hat{W} \right] \\ \dot{\hat{V}} &= -\Gamma_V \left[\text{sgn}(f_{\bar{v}}) \boldsymbol{\mu} \boldsymbol{E}^T P \boldsymbol{b} \hat{W}^T \hat{\sigma}' + k_e \|\boldsymbol{E}\| \hat{V} \right] \end{aligned} \tag{2.3.9}$$

where $\Gamma_V, \Gamma_W > 0$ and $k_e > 0$ is the e-modification gain. $\hat{\boldsymbol{\sigma}} = \boldsymbol{\sigma}(\hat{V}^T \boldsymbol{\mu})$ and $\hat{\sigma}'$ is the Jacobian of $\hat{\boldsymbol{\sigma}}$

$$\hat{\sigma}' \triangleq \frac{d\boldsymbol{\sigma}}{d\boldsymbol{z}}|_{\boldsymbol{z}=\hat{V}^T\boldsymbol{\mu}} = \begin{bmatrix} 0 & \cdots & 0 \\ \frac{d\sigma_1}{dz_1} & \cdots & 0 \\ \vdots & \ddots & \vdots \\ 0 & \cdots & \frac{d\sigma_{n_2}}{dz_{n_2}} \end{bmatrix} \in \Re^{(n_2+1)\times n_2} \tag{2.3.10}$$

and has the following property.

$$|z_i \sigma_i'(z_i)| \leq \delta = 0.224, \tag{2.3.11}$$

The equality in (2.3.11) holds when $a_i z_i = 1.543$ [52].

Since A is Hurwitz, then for any $Q > 0$, there exists a unique $P > 0$ that solves the Lyapunov equation:

$$A^T P + PA = -Q \tag{2.3.12}$$

Introduce the *vec* operator for a matrix $M \in \Re^{n\times m}$

$$vecM \triangleq \begin{bmatrix} \text{col}_1(M) \\ \text{col}_2(M) \\ \vdots \\ \text{col}_m(M) \end{bmatrix} \in \Re^{nm} \tag{2.3.13}$$

which is a vector of dimension $nm \times 1$ obtained by stacking the columns of M where $\text{col}_i(M)$ is the i^{th} column vector of M.

Assumption 2.3.2. The NN approximation $\bar{\Delta}(\boldsymbol{x}, v_l) = W^T\phi(\boldsymbol{x}, v_l) + \epsilon$ with $\|\epsilon\| < \epsilon^*$ holds on a compact set $\mathcal{D}$ and the compact set $\mathcal{D}$ is sufficiently large such that $\boldsymbol{E} \in B_R \triangleq \{\boldsymbol{\zeta} \ : \ \|\boldsymbol{\zeta}\| \leq R\}$ ensures $\boldsymbol{x} \in \mathcal{D}$, where $\boldsymbol{\zeta} = \begin{bmatrix} \boldsymbol{E}^T & \tilde{W}^T & (vec\tilde{V})^T \end{bmatrix}^T$.

Assumption 2.3.2 requires $\mathcal{D}$ to encompass a ball of radius $\|\boldsymbol{x}_m\| + R$.

$$\|\boldsymbol{x}\| \leq \|\boldsymbol{x}_m\| + \|\boldsymbol{E}\| \leq \|\boldsymbol{x}_m\| + R \tag{2.3.14}$$

Assumption 2.3.3. $f_{\bar{v}}$ and $\frac{d}{dt}\left(\frac{1}{f_{\bar{v}}}\right)$ are continuous functions in $\mathcal{D}$.

Any continuous function has a maximum on a compact set. Define

$$f^B \triangleq \max_{\boldsymbol{x}, u \in \mathcal{D}} |f_{\bar{v}}|, \quad F \triangleq \max_{\boldsymbol{x}, u \in \mathcal{D}} \left| \frac{d}{dt}\left(\frac{1}{f_{\bar{v}}}\right) \right| \tag{2.3.15}$$

We assume that there exist a compact set $\mathcal{D}$ inside which the NN approximation and (2.3.15) are valid as long as $\boldsymbol{x}$ stays in $\mathcal{D}$. We will show that if the initial error $\boldsymbol{E}(0)$ starts in a compact set $\Omega_\alpha \subset B_R$, then the feedback law (2.1.4) and the adaptive law (2.3.9) guarantee that $\boldsymbol{E}(t)$ is ultimately bounded inside $\Omega_\beta \subset \Omega_\alpha$ so that $\boldsymbol{x} \in \mathcal{D}$ for all time.

Using the Taylor series expansion of $\boldsymbol{\sigma}(\boldsymbol{z})$ at $\boldsymbol{z} = \hat{\boldsymbol{z}}$, one gets:

$$\boldsymbol{\sigma} = \hat{\boldsymbol{\sigma}} - \hat{\sigma}'\tilde{V}^T\boldsymbol{\mu} + \mathcal{O}(\|\tilde{V}\|^2) \tag{2.3.16}$$

where $\mathcal{O}(\|\tilde{V}\|^2)$ represents the higher order terms and $\boldsymbol{z} = V^T\boldsymbol{\mu}, \hat{\boldsymbol{z}} = \hat{V}^T\boldsymbol{\mu}$. Then

$$\begin{aligned} v_{ad} - \bar{\Delta} &= \hat{W}^T\hat{\boldsymbol{\sigma}} - W^T\boldsymbol{\sigma} - \epsilon \\ &= \hat{W}^T\hat{\boldsymbol{\sigma}} - W^T\left(\hat{\boldsymbol{\sigma}} - \hat{\sigma}'\tilde{V}^T\boldsymbol{\mu} + \mathcal{O}(\|\tilde{V}\|^2)\right) - \epsilon \\ &= \tilde{W}^T\hat{\boldsymbol{\sigma}} + W^T\hat{\sigma}'\tilde{V}^T\boldsymbol{\mu} - W^T\mathcal{O}(\|\tilde{V}\|^2) - \epsilon \\ &= \tilde{W}^T\hat{\boldsymbol{\sigma}} + \hat{W}^T\hat{\sigma}'\tilde{V}^T\boldsymbol{\mu} + \bar{w} \end{aligned} \tag{2.3.17}$$

where $\bar{w} = -\tilde{W}^T\hat{\sigma}'\tilde{V}^T\boldsymbol{\mu} - W^T\mathcal{O}(\|\tilde{V}\|^2) - \epsilon$.

Theorem 2.3.1. Let Assumptions 2.3.1, 2.1.1, 2.3.2 and 2.3.3 hold. Then there exists a positive invariant set $\mathcal{D}_\zeta$ in the space of the error variables $\boldsymbol{\zeta}$ wherein the control law given by (2.1.4), (2.1.5) and the adaptive law (2.3.9) ensure, for all $\boldsymbol{\zeta}(0) \in \Omega_\alpha$, that $\boldsymbol{E}, \tilde{W}, \tilde{V}$ are ultimately bounded.

Proof. Choose the following Lyapunov function candidate

$$L = \left|\frac{1}{f_{\bar{v}}}\right| \boldsymbol{E}^T P \boldsymbol{E} + \tilde{W}^T \Gamma_W^{-1} \tilde{W} + \mathrm{tr}(\tilde{V}^T \Gamma_V^{-1} \tilde{V}) \tag{2.3.18}$$

Differentiating with respect to time,

$$\begin{aligned} \dot{L} = \frac{d}{dt}\left|\frac{1}{f_{\bar{v}}}\right| \boldsymbol{E}^T P \boldsymbol{E} + \left|\frac{1}{f_{\bar{v}}}\right| \left(-\boldsymbol{E}^T Q \boldsymbol{E} + 2\boldsymbol{E}^T P \boldsymbol{b} f_{\bar{v}}(v_{ad} - \bar{\Delta})\right) \\ + 2\tilde{W}^T \Gamma_W^{-1} \dot{\tilde{W}} + 2\mathrm{tr}(\tilde{V}^T \Gamma_V^{-1} \dot{\tilde{V}}) \end{aligned} \tag{2.3.19}$$

Applying the adaptive law (2.3.9) and the representation of (2.3.17),

$$\begin{aligned} \dot{L} &= \frac{d}{dt}\left|\frac{1}{f_{\bar{v}}}\right| \boldsymbol{E}^T P \boldsymbol{E} + \left|\frac{1}{f_{\bar{v}}}\right| \left(-\boldsymbol{E}^T Q \boldsymbol{E} + 2\boldsymbol{E}^T P \boldsymbol{b} f_{\bar{v}} \bar{w}\right) \\ &\quad - 2k_e \|\boldsymbol{E}\| (\tilde{W}^T \hat{W} + \mathrm{tr}(\tilde{V}^T \hat{V})) \\ &\leq F\lambda_{max}(P)\|\boldsymbol{E}\|^2 - \frac{1}{f^B}\lambda_{min}(Q)\|\boldsymbol{E}\|^2 \\ &\quad + 2\|\boldsymbol{E}\|\|P\boldsymbol{b}\|(\gamma_1\|\tilde{Z}\|^2 + \epsilon^*) - 2k_e\|\boldsymbol{E}\|(\|\tilde{Z}\|^2 - Z^*\|\tilde{Z}\|) \\ &\leq F\lambda_{max}(P)\|\boldsymbol{E}\|^2 - \frac{1}{f^B}\lambda_{min}(Q)\|\boldsymbol{E}\|^2 \\ &\quad + 2\|\boldsymbol{E}\|\|P\boldsymbol{b}\|(\gamma_1\|\tilde{Z}\|^2 + \epsilon^*) - k_e\|\boldsymbol{E}\|(2\|\tilde{Z}\|^2 - Z^{*^2} - \|\tilde{Z}\|^2) \end{aligned} \tag{2.3.20}$$

We combine the terms to obtain

$$\begin{aligned} \dot{L} \leq -\|\boldsymbol{E}\| \Bigg[\{\frac{1}{f^B}\lambda_{min}(Q) - F\lambda_{max}(P)\}\|\boldsymbol{E}\| \\ + (k_e - 2\gamma_1)\|P\boldsymbol{b}\|\|\tilde{Z}\|^2 - (k_e Z^{*^2} + 2\epsilon^*\|P\boldsymbol{b}\|) \Bigg] \end{aligned} \tag{2.3.21}$$

The above inequality requires that

$$k_e > 2\gamma_1, \quad \frac{\lambda_{min}(Q)}{\lambda_{max}(P)} > F f^B \tag{2.3.22}$$

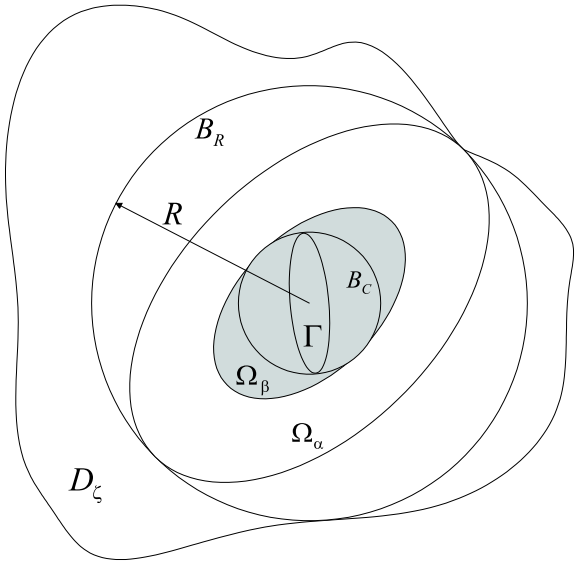

Figure 2: Geometric representation of the sets in the error space

Either of the following two conditions renders $\dot{L} < 0$.

$$\begin{aligned} \|\boldsymbol{E}\| &> \frac{(k_e {Z^*}^2 + 2\epsilon^* \|P\boldsymbol{b}\|)}{\frac{1}{f^B}\lambda_{min}(Q) - F\lambda_{max}(P)} \\ \|\tilde{Z}\| &> \frac{(k_e {Z^*}^2 + 2\epsilon^* \|P\boldsymbol{b}\|)}{(k_e - 2\gamma_1)\|P\boldsymbol{b}\|} \end{aligned} \tag{2.3.23}$$

Therefore $\boldsymbol{E}, \tilde{Z}$ are ultimately bounded inside Ω_β in Figure 2. □

Remark 2.3.1. $\frac{\lambda_{min}(Q)}{\lambda_{max}(P)}$ is related to the convergence rate of (2.3.7) when $v_{ad} = \bar{\Delta}$ and the second inequality in (2.3.22) demands a sufficiently stable error dynamics in (2.3.7).

2.4 Extension to Output Feedback Control

Consider the following *observable* and *stabilizable* nonlinear SISO system:

$$\begin{aligned} \dot{\boldsymbol{x}} &= \boldsymbol{f}(\boldsymbol{x}, u) \\ y &= h(\boldsymbol{x}) \end{aligned} \tag{2.4.1}$$

where $\boldsymbol{x}$ is the state of the system on a domain $\mathcal{D}_x \subset \Re^n$, and $u, y \in \Re$ are the control and regulated output variables, respectively. The functions $\boldsymbol{f}$ and h may be unknown.

Assumption 2.4.1. The functions $\boldsymbol{f} : \mathcal{D}_x \times \Re \rightarrow \Re^n$ and $h : \mathcal{D}_x \rightarrow \Re$ are input/output feedback linearizable [2], and the output y has relative degree r for all $(\boldsymbol{x}, u) \in \mathcal{D}_x \times \Re$.

Based on this assumption, the system (2.4.1) can be transformed into normal form [1]

$$\begin{aligned} \dot{\boldsymbol{\chi}} &= \boldsymbol{f}_0(\boldsymbol{\xi}, \boldsymbol{\chi}) \\ \dot{\xi}_i &= \xi_{i+1} \qquad i = 1, \cdots, r-1 \\ \dot{\xi}_r &= h_r(\boldsymbol{\xi}, \boldsymbol{\chi}, u) \\ y &= \xi_1 \end{aligned} \tag{2.4.2}$$

where $\boldsymbol{\xi} = [\ \xi_1 \quad \dots \quad \xi_r\ ]^T$, $h_r(\boldsymbol{\xi}, \boldsymbol{\chi}, u) = L_f^r h$,and $\boldsymbol{\chi}$ is the state vector associated with the internal dynamics

$$\dot{\boldsymbol{\chi}} = \boldsymbol{f}_0(\boldsymbol{\xi}, \boldsymbol{\chi}) \tag{2.4.3}$$

Assumption 2.4.2. The internal dynamics in (2.4.3), with $\boldsymbol{\xi}$ viewed as input, are input-to-state stable. [53]

Assumption 2.4.3. $\partial h_r(\boldsymbol{x}, u)/\partial u$ is continuous and non-zero for every $(\boldsymbol{x}, u) \in \mathcal{D}_x \times \Re$ and its sign is known.

The control objective is to synthesize an output feedback control law such that $y(t)$ tracks a smooth reference model trajectory $y_{rm}(t)$ within bounded error. Let $\hat{h}_r(y, u)$ denote an approximate model for $h_r(\boldsymbol{x}, u)$ so that:

$$h_r(\boldsymbol{x}, u) = \hat{h}_r(y, u) + \Delta \tag{2.4.4}$$

where the modelling error is $\Delta(\boldsymbol{x}, u) = h_r(\boldsymbol{x}, u) - \hat{h}_r(y, u)$. The model $\hat{h}_r(y, u)$ should be chosen to be invertible with respect to its second argument so as to be consistent with the following assumption.

Assumption 2.4.4. $\partial \hat{h}_r(y,u)/\partial u$ is continuous and non-zero for every $(y,u) \in \mathcal{D}_y \times \Re$.

Let the approximate function be recast as

$$v = \hat{h}_r(y,u) \tag{2.4.5}$$

where v is called pseudo-control. Then the control law can be defined directly from (2.4.5)

$$u = \hat{h}_r^{-1}(y,v) \tag{2.4.6}$$

The pseudo-control is composed of three signals:

$$v \triangleq y_{rm}^{(r)} + v_{dc} - v_{ad} \tag{2.4.7}$$

where $y_{rm}^{(r)}$ is the r^{th} time derivative of $y_{rm}(t)$, v_{dc} is the output of a linear controller, and v_{ad} is an adaptive term designed to cancel $\Delta(\boldsymbol{x},u)$.

The reference model can be expressed in state space form as:

$$\begin{aligned} \dot{\boldsymbol{x}}_{rm} &= A_{rm}\boldsymbol{x}_{rm} + \boldsymbol{b}_{rm}y_c \\ y_{rm} &= C_{rm}\boldsymbol{x}_{rm} \end{aligned} \tag{2.4.8}$$

$$\boldsymbol{x}_{rm} \triangleq \begin{bmatrix} x_{rm} & \dot{x}_{rm} & \cdots & x_{rm}^{(r-1)} \end{bmatrix}^T$$

$$A_{rm} = \begin{bmatrix} 0 & 1 & 0 & \cdots & 0 \\ 0 & 0 & 1 & \cdots & 0 \\ \vdots & \vdots & \vdots & \ddots & \vdots \\ 0 & 0 & 0 & 0 & 1 \\ -a_1 & -a_2 & -a_3 & \cdots & -a_r \end{bmatrix}, \boldsymbol{b}_{rm} = \begin{bmatrix} 0 \\ 0 \\ 0 \\ \vdots \\ a_1 \end{bmatrix},$$

$$C_{rm} = \begin{bmatrix} 1 & 0 & 0 & \cdots & 0 & 0 \end{bmatrix}$$

where $\boldsymbol{x}_{rm} \in \Re^r$ is the state vector of the reference model, $y_c \in \Re$ is a bounded external command signal, and A_{rm} is Hurwitz.

Let $e \triangleq y_{rm} - y$. Then

$$e^{(r)} = -v_{dc} + v_{ad} - \Delta \tag{2.4.9}$$

For the case $r > 1$, the following linear dynamic compensator is introduced to stabilize the dynamics in (2.4.9):

$$\begin{aligned} \dot{\boldsymbol{\eta}} &= A_c\boldsymbol{\eta} + \boldsymbol{b}_c e, \quad \boldsymbol{\eta} \in \Re^{n_c} \\ v_{dc} &= \boldsymbol{c}_c\boldsymbol{\eta} + d_c e \end{aligned} \tag{2.4.10}$$

where n_c is the order of the compensator. The vector $\mathbf{e} = [\ e \quad \dot{e} \quad \cdots \quad e^{(r-1)}\ ]^T$ together with the compensator state $\boldsymbol{\eta}$ will obey the following error dynamics:

$$\begin{aligned} \begin{bmatrix} \dot{\boldsymbol{\eta}} \\ \dot{\mathbf{e}} \end{bmatrix} &= \underbrace{\begin{bmatrix} A_c & \boldsymbol{b}_c\boldsymbol{c} \\ -\mathbf{b}\boldsymbol{c}_c & A - \mathbf{b}d_c\boldsymbol{c} \end{bmatrix}}_{\bar{A}} \underbrace{\begin{bmatrix} \boldsymbol{\eta} \\ \mathbf{e} \end{bmatrix}}_{\boldsymbol{E}} + \underbrace{\begin{bmatrix} \mathbf{0}_{n_c\times 1} \\ \mathbf{b} \end{bmatrix}}_{\bar{\boldsymbol{b}}} (v_{ad} - \Delta) \\ \boldsymbol{z} &= \underbrace{\begin{bmatrix} I_{n_c} & 0_{n_c\times r} \\ 0_{1\times n_c} & \boldsymbol{c} \end{bmatrix}}_{\bar{C}} \begin{bmatrix} \boldsymbol{\eta} \\ \mathbf{e} \end{bmatrix} = \begin{bmatrix} \boldsymbol{\eta} \\ e \end{bmatrix} \end{aligned} \tag{2.4.11}$$

where

$$\begin{aligned} A &= \begin{bmatrix} 0 & 1 & 0 & \cdots & 0 \\ 0 & 0 & 1 & & 0 \\ \vdots & \vdots & & \ddots & \\ 0 & 0 & & & 1 \\ 0 & 0 & 0 & \cdots & 0 \end{bmatrix} \in \Re^{r\times r}, \quad \mathbf{b} = \begin{bmatrix} 0 \\ 0 \\ \vdots \\ 0 \\ 1 \end{bmatrix} \in \Re^{r\times 1}, \\ \boldsymbol{c} &= \begin{bmatrix} 1 & 0 & 0 & \cdots & 0 \end{bmatrix} \in \Re^{1\times r}, \end{aligned} \tag{2.4.12}$$

and $\boldsymbol{z}$ is a vector of available signals. With these definitions, the tracking error dynamics in (2.4.11) can be rewritten in a compact form:

$$\begin{aligned} \dot{\boldsymbol{E}} &= \bar{A}\boldsymbol{E} + \bar{\boldsymbol{b}}(v_{ad} - \Delta) \\ \boldsymbol{z} &= \bar{C}\boldsymbol{E} \end{aligned} \tag{2.4.13}$$

where $A_c, \boldsymbol{b}_c, \boldsymbol{c}_c, d_c$ should be designed such that $\bar{A}$ is Hurwitz. The same argument as in Remark 2.1.1 can be applied here.

Define the following signals

$$\begin{aligned} v_l &\triangleq y_{rm}^{(r)} + v_{dc} \\ v^* &\triangleq \hat{h}_r(y, h_r^{-1}(\boldsymbol{x}, v_l)) \end{aligned} \tag{2.4.14}$$

Invertibility of $h_r(\boldsymbol{x}, u)$ with respect to its second argument is guaranteed by Assumption 2.4.3. From (2.4.14), it follows that v_l can be written as

$$v_l = h_r(\boldsymbol{x}, \hat{h}_r^{-1}(y, v^*)) \tag{2.4.15}$$

and,

$$\begin{aligned} v_{ad} - \Delta(\boldsymbol{x}, u) &= v_{ad} - h_r(\boldsymbol{x}, u) + \hat{h}_r(y, u) \\ &= v_{ad} - h_r(\boldsymbol{x}, \hat{h}_r^{-1}(y, v)) + v_l - v_{ad} \\ &= -h_r(\boldsymbol{x}, \hat{h}_r^{-1}(y, v)) + h_r(\boldsymbol{x}, \hat{h}_r^{-1}(y, v^*)) \end{aligned} \tag{2.4.16}$$

Applying the mean value theorem to (2.4.16),

$$\begin{aligned} v_{ad} - \Delta &= h_{\bar{v}}(v^* - v) \\ &= h_{\bar{v}}[\hat{h}_r(y, h_r^{-1}(\boldsymbol{x}, v_l)) - v_l + v_{ad}] \\ &= h_{\bar{v}}[v_{ad} - \bar{\Delta}(\boldsymbol{x}, v_l)] \end{aligned} \tag{2.4.17}$$

where $\bar{\Delta} = v_l - \hat{h}_r(y, h_r^{-1}(\boldsymbol{x}, v_l))$ and

$$h_{\bar{v}} \triangleq \left.\frac{\partial h_r}{\partial u}\frac{\partial u}{\partial v}\right|_{v=\bar{v}}, \ \bar{v} = \theta v + (1-\theta)v^*, \text{ and } \ 0 \leq \theta(v) \leq 1 \tag{2.4.18}$$

By Assumption 2.4.3 and 2.4.4, it follows that $h_{\bar{v}} = \frac{\partial h_r}{\partial u} / \frac{\partial \hat{h}_r}{\partial u}|_{v=\bar{v}}$ is either strictly positive or strictly negative.

Assumption 2.4.5. $h_{\bar{v}}$ and $\frac{d}{dt}\left(\frac{1}{h_{\bar{v}}}\right)$ are continuous functions in $\mathcal{D}$.

With this assumption we can define

$$h^B \triangleq \max_{\boldsymbol{x}, u \in \mathcal{D}} |h_{\bar{v}}|, \ H \triangleq \max_{\boldsymbol{x}, u \in \mathcal{D}} \left| \frac{d}{dt}\left(\frac{1}{h_{\bar{v}}}\right) \right| \tag{2.4.19}$$

Now we have the following error dynamics.

$$\dot{\boldsymbol{E}} = \bar{A}\boldsymbol{E} + \bar{\boldsymbol{b}}h_{\bar{v}}(v_{ad} - \bar{\Delta}(\boldsymbol{x}, v_l)) \tag{2.4.20}$$

Since $\bar{A}$ is Hurwitz, then for any $Q > 0$, there exists a unique $P > 0$ that solves the Lyapunov equation:

$$\bar{A}^T P + P\bar{A} = -Q \tag{2.4.21}$$

For an adaptive law in the output feedback setting, we adopt the error observer approach. Consider the following full-order linear observer for the tracking error dynamic system in (2.4.13):

$$\begin{aligned} \dot{\hat{\boldsymbol{E}}} &= \bar{A}\hat{\boldsymbol{E}} + K\left(\boldsymbol{z} - \hat{\boldsymbol{z}}\right) \\ &= (\bar{A} - K\bar{C})\hat{\boldsymbol{E}} + K\boldsymbol{z} \\ \hat{\boldsymbol{z}} &= \bar{C}\hat{\boldsymbol{E}} \end{aligned} \tag{2.4.22}$$

where K should be chosen in a way to make $\bar{A} - K\bar{C}$ asymptotically stable.

Remark 2.4.1. Notice that (2.4.22) provides estimates only for the error of states that are feedback linearized, and *not* for the error of states that are associated with the zero dynamics.

Let

$$\tilde{A} \triangleq \bar{A} - K\bar{C}, \quad \tilde{\boldsymbol{E}} \triangleq \hat{\boldsymbol{E}} - \boldsymbol{E} \tag{2.4.23}$$

Then the observer error dynamics can be written:

$$\dot{\tilde{\boldsymbol{E}}} = \tilde{A}\tilde{\boldsymbol{E}} - \bar{\boldsymbol{b}}h_{\bar{v}}(v_{ad} - \bar{\Delta}). \tag{2.4.24}$$

and there exists a positive definite matrix $\tilde{P}$ solving the Lyapunov equation for arbitrary $\tilde{Q} > 0$:

$$\tilde{A}^T\tilde{P} + \tilde{P}\tilde{A} = -\tilde{Q} \tag{2.4.25}$$

The following theorem extends the results found in [6, 7, 8] to map the unknown dynamics of an *observable* plant from available input/output history.

Theorem 2.4.1. [54] Given $\epsilon^* > 0$ and the compact set $\mathcal{D} \subset \mathcal{D}_x \times \Re$, there exists a set of bounded weights V, W and n_2 sufficiently large such that a continuous function $\bar{\Delta}(\boldsymbol{x}, v_l)$ can be approximated by a nonlinearly-parameterized NN

$$\begin{aligned} \bar{\Delta}(\boldsymbol{x}, v_l) &= W^T \boldsymbol{\sigma}(V^T \boldsymbol{\mu}) + \epsilon(\boldsymbol{\mu}, d), \\ \|W\|_F < W^*, &\quad \|V\|_F < V^*, \quad \|\epsilon(\boldsymbol{\mu}, d)\| < \epsilon^* \end{aligned} \tag{2.4.26}$$

using the input vector

$$\boldsymbol{\mu}(t) = \begin{bmatrix} 1 & v_l & \boldsymbol{v}_d^T(t) & \boldsymbol{y}_d^T(t) \end{bmatrix}^T \in \Re^{2N_1 - r + 2}, \quad \|\boldsymbol{\mu}\| \leq \mu^* \tag{2.4.27}$$

where

$$\begin{aligned} \boldsymbol{v}_d(t) &= \begin{bmatrix} v(t) & v(t-d) & \cdots & v(t-(N_1-r-1)d) \end{bmatrix}^T \\ \boldsymbol{y}_d(t) &= \begin{bmatrix} y(t) & y(t-d) & \cdots & y(t-(N_1-1)d) \end{bmatrix}^T \end{aligned} \tag{2.4.28}$$

with $N_1 \geq n$ and $d > 0$.

The input/output history of the original nonlinear plant is needed to map Δ in systems *with* zero dynamics, because for such systems the unobservable subspace is not estimated by (2.4.22) but can be accounted for by the input/output history, as noted in Remark 2.4.1. If the system has full relative degree ($r = n$), the observer in (2.4.22) provides all the estimates needed for the reconstruction of $\bar{\Delta}$, and no past input/output history is required [55].

The adaptive element is defined as:

$$\begin{aligned} v_{ad} &= \hat{W}^T \boldsymbol{\sigma}(\hat{V}^T \boldsymbol{\mu}) \\ \sigma_i(z_i) &= \frac{1}{1 + e^{-a_i z_i}}, \quad i = 1, 2, \cdots, n_2 \end{aligned} \tag{2.4.29}$$

where $N_1 \geq n$ and $d > 0$.

Remark 2.4.2. In the case of full relative degree ($r = n$), the input to the NN need not include the pseudo control signal since the states can be reconstructed without

the use of control input and $\bar{\Delta}$ is not dependent on v. It should be noted that for the case of $r < n$, although there is no need to solve a fixed point solution for v_{ad} to cancel $\bar{\Delta}$, there exists a fixed point solution problem for the NN output since v is used to reconstruct state $\boldsymbol{x}$. This problem can be avoided by removing the current time step pseudo control signal at the expense of increased NN approximation error bound. A NN approximation bound can be derived when $\boldsymbol{\mu} = \begin{bmatrix} 1 & v_l & \boldsymbol{v}_d^T(t-d) & \boldsymbol{y}_d^T(t) \end{bmatrix}$ is used as an input to the NN. Define

$$\begin{aligned} \Delta_d^{(0)} v(t) &\triangleq v(t) \\ \Delta_d^{(k)} v(t) &\triangleq \frac{\Delta_d^{(k-1)} v(t) - \Delta_d^{(k-1)} v(t-d)}{d} \end{aligned} \tag{2.4.30}$$

Using

$$\begin{aligned} \frac{1}{d} \int_{t-2d}^{t-d} \int_{t}^{\tau_1} v^{(2)}(\tau_2)\, d\tau_2 d\tau_1 &= \frac{1}{d} \int_{t-2d}^{t-d} v^{(1)}(\tau_1) - v^{(1)}(t)\, d\tau_1 \\ &= \frac{1}{d} \left[v(\tau_1) - \tau_1 v^{(1)}(t) \right]_{t-2d}^{t-d} \\ &= \frac{1}{d} \left[v(t-d) - v(t-2d) - d v^{(1)}(t) \right] \\ &= \Delta_d^{(1)} v(t-d) - v^{(1)}(t) \end{aligned}$$

$$\Delta_d^{(1)} v(t-d) = v^{(1)}(t) + \frac{1}{d} \int_{t-2d}^{t-d} \int_{t}^{\tau_1} v^{(2)}(\tau_2)\, d\tau_2 d\tau_1 \tag{2.4.31}$$

The following can be shown:

$$\begin{aligned} |\Delta_d^{(1)} v(t-d) - v^{(1)}(t)| &\leq \frac{3d}{2} \max_{t-2d \leq \tau \leq t} |v^{(2)}(\tau)| \\ |\Delta_d^{(k)} v(t-d) - v^{(k)}(t)| &\leq \frac{3d}{2} k \max_{t-(k+1)d \leq \tau \leq t} |v^{(k+1)}(\tau)| \end{aligned} \tag{2.4.32}$$

which can be made arbitrarily small by using a sufficiently small value of d. Using the bounds in (2.4.32), the NN approximation upper bound becomes

$$\| \bar{\Delta}(\boldsymbol{x}, v_l) - \hat{W}^T \hat{\boldsymbol{\sigma}}(\hat{V}^T \boldsymbol{\mu}) \| \leq C_1 \sqrt{\frac{2n-r}{n_2}} + C_2 \frac{d}{2} M \tag{2.4.33}$$

where $M = (2n-r-1)^{\frac{3}{2}} \max_{t \geq 0} \{ \max_{1 \leq k \leq n-1} |y^{(k+1)}(t)|,\ \max_{1 \leq k \leq n-r-1} |3v^{(k+1)}(t)| \}$. See [54] for definitions of C_1, C_2 and detailed derivations of the bounds. Note that the only disadvantage of using $\boldsymbol{v}_d(t-d)$ in $\boldsymbol{\mu}$ is that M is increased.

The NN weights are updated by the following adaptation law.

$$\begin{aligned}\dot{\hat{W}} &= -\Gamma_W \left[\text{sgn}(h_{\bar{v}})\hat{\boldsymbol{\sigma}}\hat{\boldsymbol{E}}^T P\boldsymbol{b} + k_e\|\hat{\boldsymbol{E}}\|\hat{W}\right] \\ \dot{\hat{V}} &= -\Gamma_V \left[\text{sgn}(h_{\bar{v}})\boldsymbol{\mu}\hat{\boldsymbol{E}}^T P\boldsymbol{b}\hat{W}^T\hat{\sigma}' + k_e\|\hat{\boldsymbol{E}}\|\hat{V}\right]\end{aligned} \tag{2.4.34}$$

where $\Gamma_V, \Gamma_W > 0$ and $k_e > 0$ is the e-modification gain.

Assumption 2.4.6. The NN approximation $\bar{\Delta}(\boldsymbol{x}, v_l) = W^T\phi(\boldsymbol{x}, v_l) + \epsilon$ holds on a compact set $\mathcal{D}$ and the compact set $\mathcal{D}$ is sufficiently large such that $\boldsymbol{E} \in B_R \triangleq \{\boldsymbol{\zeta} \ : \ \|\boldsymbol{\zeta}\| \leq R\}$ ensures $\boldsymbol{x} \in \mathcal{D}$ with an error vector $\boldsymbol{\zeta} = \begin{bmatrix}\boldsymbol{E}^T & \tilde{\boldsymbol{E}}^T & \tilde{W}^T & (vec\tilde{V})^T\end{bmatrix}^T$

Assumption 2.4.7. Assume

$$R > C\sqrt{\frac{\lambda_{max}(T)}{\lambda_{min}(T)}} \geq C \tag{2.4.35}$$

where $\lambda_{max}(T)$ and $\lambda_{min}(T)$ are the maximum and minimum eigenvalues of the following matrix:

$$T \triangleq \begin{bmatrix} P & 0 & 0 & 0 \\ 0 & \tilde{P} & 0 & 0 \\ 0 & 0 & \Gamma_W^{-1} & 0 \\ 0 & 0 & 0 & \Gamma_V^{-1} \end{bmatrix} \tag{2.4.36}$$

which will be used in a Lyapunov function candidate as $L = \boldsymbol{\zeta}^T T\boldsymbol{\zeta}$, and

$$C \triangleq \max\left(\frac{2}{\bar{q}}\Upsilon, \ \ 2\left(\frac{\theta_1^2}{k_e^2} + \frac{\theta_2}{k_e}\right)^{\frac{1}{2}}\right) \tag{2.4.37}$$

is a radius of a ball B_C containing Γ, where

$$\begin{aligned}\theta_1 &= \left(\sqrt{n_2+1} + \delta + \frac{a^*}{4}V^*\mu^*\right)\|P\bar{\boldsymbol{b}}\|, \\ \theta_2 &= \frac{k_e}{2}Z^{*^2} + \|P\bar{\boldsymbol{b}}\|W^*\left(\delta + \frac{a^*}{4}V^*\mu^*\right), \\ \kappa_2 &= \gamma_1\|P\bar{\boldsymbol{b}}\| + \alpha_1(\|\tilde{P}\bar{\boldsymbol{b}}\|h^B + \|P\bar{\boldsymbol{b}}\|) \\ \kappa_3 &= 2\gamma_2\|P\bar{\boldsymbol{b}}\| + 2\alpha_2(\|\tilde{P}\bar{\boldsymbol{b}}\|h^B + \|P\bar{\boldsymbol{b}}\|) + k_eZ^{*^2} \\ \Upsilon &\triangleq \kappa_2^2 + \kappa_3\end{aligned} \tag{2.4.38}$$

Let α be the minimum value of the Lyapunov function L on the boundary of B_R:

$$\alpha \triangleq \min_{\|\boldsymbol{\zeta}\|=R} L = R^2 \lambda_{min}(T)\,. \tag{2.4.39}$$

Define the compact set:

$$\Omega_\alpha = \{\boldsymbol{\zeta} \in B_R \mid L \leq \alpha\}. \tag{2.4.40}$$

Theorem 2.4.2. Let Assumptions 2.4.1−2.4.7 hold. If the initial errors belong to the compact set Ω_α defined in (2.4.40), then the feedback control law given by (2.4.6) and the adaptation law (2.4.34) ensure that the signals $\boldsymbol{E}, \tilde{\boldsymbol{E}}, \tilde{W}$ and $\tilde{V}$ in the closed-loop system are ultimately bounded with the ultimate bound $C\sqrt{\frac{\lambda_{max}(T)}{\lambda_{min}(T)}}$.

Proof. See Appendix A.1. □

Remark 2.4.3. This design approach can be also applied to σ-modification and projection approaches as presented in Chapter 3.

CHAPTER III

NEURAL NETWORK AUGMENTED INPUT/OUTPUT FEEDBACK LINEARIZATION

This chapter presents an approach for augmenting a nonlinear controller designed via input/output feedback linearization with a NN-based adaptive element, similar to that described in [39, 56]. We suggest a method which transforms a nonlinear system to a linear system which does not have to be a chain of integrators. This added design flexibility enables the use of lower order dynamic compensation in the linear part of the design. The usefulness in design increases with the relative degree (r) of the regulated output variable. It is particularly useful in fixed structure compensator design, when the structure specified is not able to stabilize a chain of r integrators. We first state what is assumed to be known about the system dynamics, followed by a statement of the design objective. Next, a summary of the main results on NN-based adaptive output feedback control via the approach in [56] is given. Three variations of adaptive laws with proofs of boundedness are given, followed by a description of the control architecture including PCH. Two numerical examples are presented to demonstrate the efficacy of the adaptive output feedback control methods. The first illustrates the main ideas by considering high-bandwidth pitch-attitude tracking control design for a linearized representation of the R-50 dynamics in hover, in which there are control limits, actuator dynamics, time delay, and significant coupling with control rotor dynamics. Results obtained using a full nonlinear model and flight test results on the R-50 model helicopter are reported in [57]. The second example

considers a 58 state model of a flexible aircraft consisting of rigid body dynamics coupled with actuator and flexible modes. A pitch-rate command system design is treated providing a smooth response in the presence of flexible modes, without the use of structural mode filters. Finally, we consider the approach in [38], which eliminates the need for an error observer, but is limited to the use of linearly-parameterized NNs, and extend these results to the case of nonlinearly-parameterized NNs. A numerical example of Van der Pol is presented and compared with the approach found in [38].

3.1 Plant Description

Consider the following *observable* and *stabilizable* nonlinear SISO system:

$$\begin{aligned} \dot{\boldsymbol{x}} &= \boldsymbol{f}(\boldsymbol{x}, u) \\ y &= h(\boldsymbol{x}) \end{aligned} \tag{3.1.1}$$

where $\boldsymbol{x}$ is the state of the system on a domain $\mathcal{D}_x \subset \Re^n$, $u \in \Re$ is the control input, and $y \in \Re$ is the regulated output variable. The functions $\boldsymbol{f}$ and h have origin as equilibrium point $\boldsymbol{f}(0,0) = 0$ and $h(0) = 0$, but may be unknown. In practice, however, some information about $\boldsymbol{f}$ and h will generally be known, and it is best to use whatever information is available. The signals available for feedback are y along with any additional measurements that may be available, but that are not regulated. We will denote these additional measurements by $\bar{y}$.

Assumption 3.1.1. The output y has a known relative degree r for all $(\boldsymbol{x}, u) \in \mathcal{D}_x \times \Re$.

This assumption implies that $\partial h_r(\boldsymbol{x}, u)/\partial u$ is non-zero for every $(\boldsymbol{x}, u) \in \mathcal{D}_x \times \Re$.

Assumption 3.1.2. The sign of $\partial h_r(\boldsymbol{x}, u)/\partial u$ is known.

Assumption 3.1.3. The system (3.1.1) is input/output feedback linearizable [2].

Based on Assumption 3.1.3, the mapping $\boldsymbol{\Phi}(\boldsymbol{x})$ where

$$\boldsymbol{\Phi}(\boldsymbol{x}) = \begin{bmatrix} \chi_1(\boldsymbol{x}) \\ \vdots \\ \chi_{n-r}(\boldsymbol{x}) \\ h(\boldsymbol{x}) \\ \vdots \\ L_f^{r-1}h(\boldsymbol{x}) \end{bmatrix} \triangleq \begin{bmatrix} \boldsymbol{\chi} \\ \boldsymbol{\xi} \end{bmatrix} \tag{3.1.2}$$

with $L_f^i h, i = 1, \ldots, r-1$ being the Lie derivatives, transforms the system (3.1.1) into normal form:

$$\begin{aligned} \dot{\boldsymbol{\chi}} &= \boldsymbol{f}_0(\boldsymbol{\xi}, \boldsymbol{\chi}) \\ \dot{\xi}_i &= \xi_{i+1} \qquad i = 1, \cdots, r-1 \\ \dot{\xi}_r &= h_r(\boldsymbol{\xi}, \boldsymbol{\chi}, u) \\ y &= \xi_1 \end{aligned} \tag{3.1.3}$$

where $\boldsymbol{\xi} = [\ \xi_1 \quad \ldots \quad \xi_r\ ]^T$, $h_r(\boldsymbol{\xi}, \boldsymbol{\chi}, u) = L_f^r h$, and $\boldsymbol{\chi}$ is the state vector associated with the internal dynamics

$$\dot{\boldsymbol{\chi}} = \boldsymbol{f}_0(\boldsymbol{\xi}, \boldsymbol{\chi}) \tag{3.1.4}$$

Assumption 3.1.4. The internal dynamics in (3.1.4), with $\boldsymbol{\xi}$ viewed as input, are input-to-state stable. [53]

3.2 Controller Design and Tracking Error Dynamics

The control objective is to synthesize an output feedback control law such that $y(t)$ tracks a smooth bounded reference trajectory $y_{rm}(t)$ with bounded error using the available signals. Since the system is not exactly known, and only y and $\bar{y}$ are available for feedback, input/output feedback linearization is approximated by introducing the

following control input signal

$$u = \hat{h}_r^{-1}(y, \bar{y}, b_1 v - \sum_{i=0}^{r-1} a_{i+1} \hat{h}_i(y, \bar{y})) \tag{3.2.1}$$

where v is commonly referred to as a pseudo control, and b_1 and a_i's are constants. The continuous function $\hat{h}_r(y, \bar{y}, u)$, which is required to be invertible with respect to its third argument, represents any available approximation of $h_r(\boldsymbol{x}, u) = L_f^r h$, and the continuous functions $\hat{h}_i(y, \bar{y})$'s are approximations of $h_i(\boldsymbol{x}) = L_f^i h$'s. Constants a_i's and b_1 are determined later in the process of controller design.

With the available knowledge of the system dynamics, start by choosing approximate expressions for every derivative of the output up to r^{th} derivative:

$$\begin{aligned}
\dot{y} &= h_1(\boldsymbol{x}) = \hat{h}_1(y, \bar{y}) + \Delta_1 \\
\ddot{y} &= h_2(\boldsymbol{x}) = \hat{h}_2(y, \bar{y}) + \Delta_2 \\
&\vdots \\
y^{(r-1)} &= h_{r-1}(\boldsymbol{x}) = \hat{h}_{r-1}(y, \bar{y}) + \Delta_{r-1} \\
y^{(r)} &= h_r(\boldsymbol{x}, u) = \hat{h}_r(y, \bar{y}, u) + \Delta_r
\end{aligned} \tag{3.2.2}$$

where Δ_i's are model errors defined as $\Delta_i = h_i(\boldsymbol{x}) - \hat{h}_i(y, \bar{y})$ for $i = 1, 2, \cdots, r-1$ and $\Delta_r = h_r(\boldsymbol{x}, u) - \hat{h}_r(y, \bar{y}, u)$. The following assumption guarantees the invertibility of $\hat{h}_r(y, \bar{y}, u)$ with respect to u.

Assumption 3.2.1. $\partial \hat{h}_r(y, \bar{y}, u)/\partial u$ is continuous and non-zero for every $(y, \bar{y}, u) \in \mathcal{D}_y \times \Re$.

If a linear model is used, then

$$\begin{aligned}
y^{(i)} &= c_i y + \bar{c}_i \bar{y} + \Delta_i, \ i = 1, \cdots, r-1 \\
y^{(r)} &= c_r y + \bar{c}_r \bar{y} + d_r u + \Delta_r
\end{aligned} \tag{3.2.3}$$

In the absence of any modelling information, we may select the approximation as $\hat{h}_1(y, \bar{y}) = \hat{h}_2(y, \bar{y}) = \cdots = \hat{h}_{r-1}(y, \bar{y}) = 0$ and $\hat{h}_r(y, \bar{y}, u) = d_r u$.

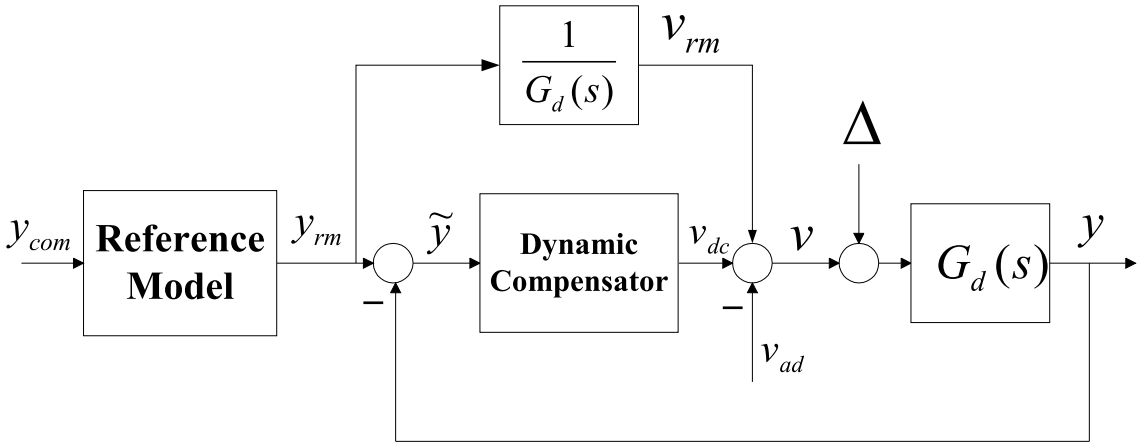

Figure 3: Control system architecture without PCH

To design the linear dynamic compensator we need to specify the desired linearized system from v to y when $\Delta = 0$, $G_d(s)$ in Figure 3, where

$$G_d(s) = \frac{b_1}{D_d(s)} \tag{3.2.4}$$

$$D_d(s) = s^r + a_r s^{r-1} + \cdots + a_2 s + a_1 \tag{3.2.5}$$

$G_d(s)$ should be considered together with the form of the dynamic compensator used to achieve a desired closed-loop level of performance.

Consider the model reference adaptive control architecture of Figure 3. A dynamic compensator is designed to ensure that the resulting error dynamics, for $\Delta = 0$, are asymptotically stable. Combining (3.2.4) and (3.2.5) for $\Delta \neq 0$ (See Figure 3),

$$\begin{aligned} b_1(v+\Delta) &= y^{(r)} + a_r y^{(r-1)} + \cdots + a_2 \dot{y} + a_1 y \\ &= \hat{h}_r(y, \bar{y}, u) + \Delta_r + a_r(\hat{h}_{r-1}(y, \bar{y}) + \Delta_{r-1}) \\ &\quad + \cdots + a_2(\hat{h}_1(y, \bar{y}) + \Delta_1) + a_1 y \\ &= \hat{h}_r(y, \bar{y}, u) + \sum_{i=0}^{r-1} a_{i+1} \hat{h}_i(y, \bar{y}) + \sum_{i=1}^{r} a_{i+1} \Delta_i \end{aligned} \tag{3.2.6}$$

where $\hat{h}_0(y) = y$, it can be seen that

$$v = \frac{1}{b_1}\left(\hat{h}_r(y, \bar{y}, u) + \sum_{i=0}^{r-1} a_{i+1}\hat{h}_i(y, \bar{y})\right) \tag{3.2.7}$$

$$\Delta = \frac{1}{b_1}\sum_{i=1}^{r} a_{i+1}\Delta_i \tag{3.2.8}$$

The control law in (3.2.1) follows directly from (3.2.7). Applying the linear expressions in (3.2.3), we have

$$u = \frac{1}{d_r}(b_1 v - \sum_{i=0}^{r} a_{i+1}(c_i y + \bar{c}_r \bar{y})) \tag{3.2.9}$$

where $a_{r+1} = 1, c_0 = 1$ and $\bar{c}_0 = 0$.

The model inversion errors Δ_i's can be regarded as continuous functions of $\boldsymbol{x}$ and v.

$$\begin{aligned}
\Delta_i(\boldsymbol{x}) &= h_i(\boldsymbol{x}) - \hat{h}_i(y, \bar{y}) \quad \text{for } i = 1, 2, \cdots, r-1 \\
\Delta_r(\boldsymbol{x}, v) &= h_r(\boldsymbol{x}, u) - \hat{h}_r(y, \bar{y}, u) \\
&= h_r\left(\boldsymbol{x}, \hat{h}_r^{-1}\{y, \bar{y}, b_1 v - \sum_{i=0}^{r-1} a_{i+1}\hat{h}_i(y, \bar{y})\}\right) \\
&\quad - \hat{h}_r\left(y, \bar{y}, \hat{h}_r^{-1}\{y, \bar{y}, b_1 v - \sum_{i=0}^{r-1} a_{i+1}\hat{h}_i(y, \bar{y})\}\right)
\end{aligned} \tag{3.2.10}$$

Thus, the total model inversion error is a continuous function of $\boldsymbol{x}$ and v.

$$\Delta(\boldsymbol{x}, v) = \frac{1}{b_1}\left(\Delta_r(\boldsymbol{x}, v) + \sum_{i=1}^{r-1} a_{i+1}\Delta_i(\boldsymbol{x})\right) \tag{3.2.11}$$

The pseudo control in (3.2.1) is chosen to have the form:

$$v = v_{rm} + v_{dc} - v_{ad} \tag{3.2.12}$$

where v_{rm} is a reference model output, v_{dc} is the output of a linear dynamic compensator, and v_{ad} is the adaptive control signal. With the choice of pseudo control in (3.2.12), the dynamics in (3.2.6) reduce to

$$\sum_{i=0}^{r} a_{i+1} y^{(i)} = b_1(v_{rm} + v_{dc} - v_{ad} + \Delta) \tag{3.2.13}$$

Define the reference model pseudo control v_{rm}:

$$\begin{aligned} v_{rm} &= \frac{1}{G_d(s)} y_{rm} = \frac{D_d(s)}{b_1} y_{rm} \\ &= \frac{1}{b_1}(y_{rm}^{(r)} + a_r y_{rm}^{(r-1)} + \cdots + a_2 \dot{y}_{rm} + a_1 y_{rm}) \end{aligned} \tag{3.2.14}$$

Then the dynamics in (3.2.13) can be rewritten:

$$\sum_{i=0}^{r} a_{i+1} e^{(i)} + b_1(v_{dc} - v_{ad} + \Delta) = 0 \tag{3.2.15}$$

where $e = y_{rm} - y$. When $v_{ad} = \Delta = 0$, the error dynamics in (3.2.15) reduces to:

$$D_d(s)e + b_1 v_{dc} = 0 \tag{3.2.16}$$

For the case $r > 1$, the following linear dynamic compensator is introduced to stabilize the dynamics in (3.2.16):

$$\begin{aligned} \dot{\boldsymbol{\eta}} &= A_c \boldsymbol{\eta} + \boldsymbol{b}_c e, \quad \boldsymbol{\eta} \in \Re^{n_c} \\ v_{dc} &= \boldsymbol{c}_c \boldsymbol{\eta} + d_c e \end{aligned} \tag{3.2.17}$$

where n_c is the order of the compensator.

Returning to (3.2.15), the vector $\mathbf{e} = [\ e \quad \dot{e} \quad \cdots \quad e^{(r-1)}\ ]^T$ together with the compensator state $\boldsymbol{\eta}$ will obey the following dynamics, hereafter referred to as the tracking error dynamics:

$$\begin{aligned} \begin{bmatrix} \dot{\boldsymbol{\eta}} \\ \dot{\mathbf{e}} \end{bmatrix} &= \begin{bmatrix} A_c & \boldsymbol{b}_c \boldsymbol{c} \\ -b_1 \mathbf{b} \boldsymbol{c}_c & A - \mathbf{b}(b_1 d_c \boldsymbol{c} + \mathbf{a}) \end{bmatrix} \begin{bmatrix} \boldsymbol{\eta} \\ \mathbf{e} \end{bmatrix} + \begin{bmatrix} \mathbf{0}_{n_c \times 1} \\ \mathbf{b} \end{bmatrix} b_1(v_{ad} - \Delta) \\ \boldsymbol{z} &\triangleq \begin{bmatrix} \boldsymbol{\eta} \\ e \end{bmatrix} \end{aligned} \tag{3.2.18}$$

where

$$
\begin{aligned}
A &= \begin{bmatrix} 0 & 1 & 0 & \cdots & 0 \\ 0 & 0 & 1 & & 0 \\ \vdots & \vdots & & \ddots & \\ 0 & 0 & & & 1 \\ 0 & 0 & 0 & \cdots & 0 \end{bmatrix} \in \Re^{r\times r}, \quad \mathbf{b} = \begin{bmatrix} 0 \\ 0 \\ \vdots \\ 0 \\ 1 \end{bmatrix} \in \Re^{r\times 1}, \\
\boldsymbol{c} &= \begin{bmatrix} 1 & 0 & 0 & \cdots & 0 \end{bmatrix} \in \Re^{1\times r}, \quad \mathbf{a} = \begin{bmatrix} a_1 & a_2 & \cdots & a_r \end{bmatrix} \in \Re^{1\times r}
\end{aligned}
\tag{3.2.19}
$$

and $\boldsymbol{z}$ is a vector of available error signals. For ease of notation, define the following:

$$
\begin{aligned}
\bar{A} &\triangleq \begin{bmatrix} A_c & \boldsymbol{b}_c\boldsymbol{c} \\ -b_1\mathbf{b}\boldsymbol{c}_c & A - \mathbf{b}(b_1 d_c\boldsymbol{c} + \mathbf{a}) \end{bmatrix} \in \Re^{(n_c+r)\times(n_c+r)}, \\
\bar{\boldsymbol{b}} &\triangleq \begin{bmatrix} \mathbf{0}_{n_c\times 1} \\ \mathbf{b} \end{bmatrix}, \ \bar{C} \triangleq \begin{bmatrix} I_{n_c} & 0_{n_c\times r} \\ 0_{1\times n_c} & \boldsymbol{c} \end{bmatrix}, \ \boldsymbol{E} \triangleq \begin{bmatrix} \boldsymbol{\eta} \\ \mathbf{e} \end{bmatrix} \in \Re^{n_c+r}
\end{aligned}
\tag{3.2.20}
$$

where I_{n_c} is an $n_c \times n_c$ identity matrix. With these definitions, the tracking error dynamics in (3.2.18) can be rewritten as

$$
\begin{aligned}
\dot{\boldsymbol{E}} &= \bar{A}\boldsymbol{E} + \bar{\boldsymbol{b}}b_1(v_{ad} - \Delta) \\
\boldsymbol{z} &= \bar{C}\boldsymbol{E}
\end{aligned}
\tag{3.2.21}
$$

where it has already been noted that $A_c, \boldsymbol{b}_c, \boldsymbol{c}_c, d_c$ should be designed such that $\bar{A}$ is Hurwitz.

Define the following signals

$$
\begin{aligned}
v_l &\triangleq v_{rm} + v_{dc} \\
v^* &\triangleq \hat{h}_r(y, \bar{y}, h_r^{-1}(\boldsymbol{x}, b_1 v_l - \sum_{i=0}^{r-1} a_{i+1}h_i(\boldsymbol{x})))
\end{aligned}
\tag{3.2.22}
$$

where $h_0(\boldsymbol{x}) = h(\boldsymbol{x})$. The invertibility of $h_r(\boldsymbol{x}, u)$ with respect to u is guaranteed by Assumption 3.1.1. From (3.2.22), it follows that v_l can be written as

$$
v_l = \frac{1}{b_1}\left[h_r(\boldsymbol{x}, \hat{h}_r^{-1}(y, \bar{y}, v^*)) + \sum_{i=0}^{r-1} a_{i+1}h_i(\boldsymbol{x})\right] \tag{3.2.23}
$$

and,

$$\begin{aligned} v_{ad} - \Delta(\boldsymbol{x}, u) &= v_{ad} - \frac{1}{b_1}\left[h_r(\boldsymbol{x}, u) - \hat{h}_r(y, \bar{y}, u) + \sum_{i=0}^{r-1} a_{i+1}(h_i(\boldsymbol{x}) - \hat{h}_i(y, \bar{y}))\right] \\ &= v_{ad} - \frac{1}{b_1}\left[h_r(\boldsymbol{x}, u) + \sum_{i=0}^{r-1} a_{i+1}h_i(\boldsymbol{x}))\right] + v \\ &= \frac{1}{b_1}\left[h_r(\boldsymbol{x}, \hat{h}_r^{-1}(y, \bar{y}, v^*)) + \sum_{i=0}^{r-1} a_{i+1}h_i(\boldsymbol{x})\right] \\ &\quad - \frac{1}{b_1}\left[h_r(\boldsymbol{x}, u) + \sum_{i=0}^{r-1} a_{i+1}h_i(\boldsymbol{x}))\right] \\ &= \frac{1}{b_1}\left[h_r(\boldsymbol{x}, \hat{h}_r^{-1}(y, \bar{y}, v^*)) - h_r(\boldsymbol{x}, \hat{h}_r^{-1}(y, \bar{y}, v))\right] \end{aligned} \tag{3.2.24}$$

Applying the mean value theorem to (3.2.24),

$$\begin{aligned} v_{ad} - \Delta &= \frac{1}{b_1}h_{\bar{v}}(v^* - v) \\ &= \frac{1}{b_1}h_{\bar{v}}\left[\hat{h}_r\left(y, \bar{y}, h_r^{-1}(\boldsymbol{x}, b_1 v_l - \sum_{i=0}^{r-1} a_{i+1}h_i(\boldsymbol{x}))\right) - v_l + v_{ad}\right] \\ &= \frac{1}{b_1}h_{\bar{v}}[v_{ad} - \bar{\Delta}(\boldsymbol{x}, v_l)] \end{aligned} \tag{3.2.25}$$

where $\bar{\Delta} = v_l - \hat{h}_r\left(y, \bar{y}, h_r^{-1}(\boldsymbol{x}, b_1 v_l - \sum_{i=0}^{r-1} a_{i+1}h_i(\boldsymbol{x}))\right)$ and

$$h_{\bar{v}} \triangleq \frac{\partial h_r}{\partial u}\frac{\partial u}{\partial v}\bigg|_{v=\bar{v}},\ \bar{v} = \theta v + (1-\theta)v^*,\ \text{and}\ \ 0 \le \theta(v) \le 1 \tag{3.2.26}$$

By Assumptions 3.1.2 and 3.2.1, it follows that $h_{\bar{v}} = \frac{\partial h_r}{\partial u} / \frac{\partial \hat{h}_r}{\partial u}|_{v=\bar{v}}$ is either strictly positive or strictly negative. Now we have the following error dynamics.

$$\dot{\boldsymbol{E}} = \bar{A}\boldsymbol{E} + \bar{\boldsymbol{b}}h_{\bar{v}}(v_{ad} - \bar{\Delta}(\boldsymbol{x}, v_l)) \tag{3.2.27}$$

As in Section 2.4, define

$$h^B \triangleq \max_{\boldsymbol{x}, u\in\mathcal{D}}|h_{\bar{v}}|,\ H \triangleq \max_{\boldsymbol{x}, u\in\mathcal{D}}\left|\frac{d}{dt}\left(\frac{1}{h_{\bar{v}}}\right)\right| \tag{3.2.28}$$

3.3 Design of an Observer for the Error Dynamics

In the case of full state feedback [28, 31, 24], Lyapunov-like stability analysis of the error dynamics in (3.2.21) results in update laws for the adaptive control parameters in terms of the error vector $\boldsymbol{E}$. In [42, 36, 37] an adaptive state observer is developed for the nonlinear plant to provide state estimates needed in the adaptation laws. However, the stability analysis was limited to second order systems with position measurements. To relax these assumptions, we make use of a simple linear observer for the tracking error dynamics in (3.2.21) [39, 55]. This observer provides estimates of the unavailable error signals for the update laws of the adaptive parameters that will be presented in (3.4.20).

Consider the following full-order linear observer for the tracking error dynamic system in (3.2.21):

$$\begin{aligned} \dot{\hat{\boldsymbol{E}}} &= \bar{A}\hat{\boldsymbol{E}} + K\left(\boldsymbol{z} - \hat{\boldsymbol{z}}\right) \\ \hat{\boldsymbol{z}} &= \bar{C}\hat{\boldsymbol{E}}, \end{aligned} \tag{3.3.1}$$

where K should be chosen in a way to make $\bar{A} - K\bar{C}$ asymptotically stable. The following remarks will be useful in the sequel.

Remark 3.3.1. One can also design a minimal order optimal estimator that treats the $\boldsymbol{\eta}$ component of z as a noiseless measurement [58].

Remark 3.3.2. Additional measurements contained in $\bar{y}$ may also be used both in the compensator design and in the observer design. This idea is employed in the application treated in Section 3.6.

The error observer design ignores nonlinearities that enter the tracking error dynamics (3.2.21) as a forcing function. This is suggested by the fact that the original nonlinear system with adaptation is approximately feedback linearized, or that v_{ad} nearly cancels $\bar{\Delta}$.

The stability of the closed-loop system should be considered along with the observer error dynamics. Let

$$\tilde{A} \triangleq \bar{A} - K\bar{C}, \quad \tilde{\boldsymbol{E}} \triangleq \hat{\boldsymbol{E}} - \boldsymbol{E}. \tag{3.3.2}$$

Then the observer error dynamics can be written:

$$\dot{\tilde{\boldsymbol{E}}} = \tilde{A}\tilde{\boldsymbol{E}} - \bar{\boldsymbol{b}}h_{\bar{v}}\left[v_{ad} - \bar{\Delta}\right]. \tag{3.3.3}$$

and there exists a positive definite matrix $\tilde{P}$ solving the Lyapunov equation

$$\tilde{A}^T\tilde{P} + \tilde{P}\tilde{A} = -\tilde{Q} \tag{3.3.4}$$

for arbitrary $\tilde{Q} > 0$.

The adaptive term in (3.2.12) is designed as:

$$v_{ad} = \hat{W}^T\boldsymbol{\sigma}(\hat{V}^T\boldsymbol{\mu}), \tag{3.3.5}$$

where $\hat{W}$ and $\hat{V}$ are the NN weights to be updated online in accordance with one of the weight adaptation laws presented in Section 3.4. These are modified backpropagation algorithms, which are commonly used to train a nonlinearly-parameterized NN [59]. The variations which distinguish these laws from standard backpropagation algorithms are due to methods employed to compensate for the NN reconstruction error, and the Taylor series expansion higher order terms in the error dynamics.

3.4 Adaptive Laws and Boundedness Analysis

We will give three different adaptive laws utilizing the error observer introduced in Section 3.3. Proofs of boundedness for each adaptive law are given by using direct Lyapunov analysis. Consider the following vector

$$\boldsymbol{\zeta} = \left[\boldsymbol{E}^T \quad \tilde{\boldsymbol{E}}^T \quad \tilde{W}^T \quad (vec\tilde{V})^T\right]^T \in \mathcal{D}_\zeta \tag{3.4.1}$$

Introduce the largest convex compact set which is contained in $\mathcal{D}_{\boldsymbol{\zeta}}$ such that

$$B_R \triangleq \{\boldsymbol{\zeta} \ : \ \|\boldsymbol{\zeta}\| \leq R\}, \quad R > 0 \tag{3.4.2}$$

We want to ensure that a Lyapunov function level set Ω_β is a positive invariant set for the error $\boldsymbol{\zeta}$ in $\mathcal{D}_{\boldsymbol{\zeta}}$ by showing that the level set Ω_β inside B_R contains a compact set Γ outside which a time derivative of the Lyapunov function candidate is negative as in Figure 2. A Lyapunov function level set Ω_α is introduced to ensure that Ω_β is contained in B_R, and a ball B_C is introduced to provide that Ω_β contains Γ. Before we state theorems, we give assumptions that will be used in proofs of the theorems.

3.4.1 NN Adaptation with σ-modification

The update law which we use in this section is a modification of backpropagation. The algorithm was first proposed by Lewis et.al. [28] in state feedback setting with e-modification. Here the error observer is implemented to generate the estimated error vector used as a teaching signal to the NN when $r \geq 2$.

Define

$$\tilde{W} \triangleq \hat{W} - W, \quad \tilde{V} \triangleq \hat{V} - V\,, \quad \tilde{Z} \triangleq \begin{bmatrix} \tilde{W} & 0 \\ 0 & \tilde{V} \end{bmatrix} \tag{3.4.3}$$

and note that:

$$\|\hat{W}\|_F < \|\tilde{W}\|_F + W^*, \quad \|\hat{V}\|_F < \|\tilde{V}\|_F + V^* \tag{3.4.4}$$

where W^*, V^* are the upper bounds for the weights in (2.4.26). For the stability proof we will need the following representation:

$$\begin{aligned} v_{ad} - \Delta &= \hat{W}^T\boldsymbol{\sigma}(\hat{V}^T\boldsymbol{\mu}) - W^T\boldsymbol{\sigma}(V^T\boldsymbol{\mu}) - \epsilon \\ &= \hat{W}^T\hat{\boldsymbol{\sigma}} - W^T\left(\hat{\boldsymbol{\sigma}} + \hat{\sigma}'(V^T\boldsymbol{\mu} - \hat{V}^T\boldsymbol{\mu}) + \mathcal{O}^2\right) - \epsilon \\ &= \tilde{W}^T\hat{\boldsymbol{\sigma}} - W^T\hat{\sigma}'V^T\boldsymbol{\mu} + \left(W^T\hat{\sigma}'\hat{V}^T\boldsymbol{\mu} - \hat{W}^T\hat{\sigma}'\hat{V}^T\boldsymbol{\mu}\right) \\ &+ \left(\hat{W}^T\hat{\sigma}'\hat{V}^T\boldsymbol{\mu} - \hat{W}^T\hat{\sigma}'V^T\boldsymbol{\mu}\right) + \hat{W}^T\hat{\sigma}'V^T\boldsymbol{\mu} - W^T\mathcal{O}^2 - \epsilon \\ &= \tilde{W}^T\left(\hat{\boldsymbol{\sigma}} - \hat{\sigma}'\hat{V}^T\boldsymbol{\mu}\right) + \hat{W}^T\hat{\sigma}'\tilde{V}^T\boldsymbol{\mu} + \tilde{W}^T\hat{\sigma}'V^T\boldsymbol{\mu} - W^T\mathcal{O}^2 - \epsilon \\ &= \tilde{W}^T\left(\hat{\boldsymbol{\sigma}} - \hat{\sigma}'\hat{V}^T\boldsymbol{\mu}\right) + \hat{W}^T\hat{\sigma}'\tilde{V}^T\boldsymbol{\mu} + \bar{w} \end{aligned} \tag{3.4.5}$$

where $\boldsymbol{\sigma} = \boldsymbol{\sigma}(V^T\boldsymbol{\mu})$, $\hat{\boldsymbol{\sigma}} = \boldsymbol{\sigma}(\hat{V}^T\boldsymbol{\mu})$, the disturbance term $\bar{w} = \tilde{W}^T\hat{\sigma}'V^T\boldsymbol{\mu} - W^T\mathcal{O}^2 - \epsilon$ and $\mathcal{O}^2 = \mathcal{O}(-\tilde{V}^T\boldsymbol{\mu})^2 = \boldsymbol{\sigma} - \hat{\boldsymbol{\sigma}} + \hat{\sigma}'\tilde{V}^T\boldsymbol{\mu}$. This representation is achieved via Taylor

series expansion of $\boldsymbol{\sigma}(V^T\boldsymbol{\mu})$ around the estimates $\hat{V}^T\boldsymbol{\mu}$ [28]. The following bounds are useful to prove the stability of adaptive schemes.

$$\|W^T\boldsymbol{\sigma}\| \leq \sqrt{n_2+1}\|W\|, \tag{3.4.6}$$

$$\|W^T\hat{\sigma}'\hat{V}^T\boldsymbol{\mu}\| \leq \delta\sqrt{n_2+1}\|W\| \tag{3.4.7}$$

where $\delta = 0.224$ according to (2.3.11). Using the above bounds, a bound for $\bar{w}$ over the compact set $\mathcal{D}_\mu$ can be expressed:

$$\begin{aligned}\|\bar{w}\| &= \|W^T\tilde{\boldsymbol{\sigma}} - W^T\hat{\sigma}'\hat{V}^T\boldsymbol{\mu} + \hat{W}^T\hat{\sigma}'V^T\boldsymbol{\mu} - \epsilon\| \\ &\leq 2\sqrt{n_2+1}W^* + \delta\sqrt{n_2+1}W^* + \|\hat{W}\|\frac{a^*}{4}V^*\mu^* + \epsilon^* \\ &\leq \gamma_1\|\tilde{Z}\|_F + \gamma_2\end{aligned} \tag{3.4.8}$$

where $\gamma_1 = \frac{a^*}{4}Z^*\mu^*$, $\gamma_2 = ((2+\delta)\sqrt{n_2+1}+\gamma_1)W^* + \epsilon^*$. $v_{ad} - \Delta$ can be shown to be bounded by:

$$\begin{aligned}\|v_{ad} - \Delta\| &= \|\hat{W}^T\hat{\boldsymbol{\sigma}} - W^T\boldsymbol{\sigma} - \epsilon\| \\ &\leq \alpha_1\|\tilde{Z}\| + \alpha_2\end{aligned} \tag{3.4.9}$$

where $\alpha_1 = \sqrt{n_2+1}$ and $\alpha_2 = 2\sqrt{n_2+1}W^* + \epsilon^*$

Assumption 3.4.1. Assume

$$R > C\sqrt{\frac{\lambda_{max}(T)}{\lambda_{min}(T)}} \geq C \tag{3.4.10}$$

where $\lambda_{max}(T)$ and $\lambda_{min}(T)$ are the maximum and minimum eigenvalues of the following matrix:

$$T \triangleq \begin{bmatrix} P & 0 & 0 & 0 \\ 0 & \tilde{P} & 0 & 0 \\ 0 & 0 & \Gamma_W^{-1} & 0 \\ 0 & 0 & 0 & \Gamma_V^{-1} \end{bmatrix} \tag{3.4.11}$$

which will be used in a Lyapunov function candidate as $L = \boldsymbol{\zeta}^T T \boldsymbol{\zeta}$ with an error vector $\boldsymbol{\zeta} = \begin{bmatrix} \boldsymbol{E}^T & \tilde{\boldsymbol{E}}^T & \tilde{W}^T & (vec\tilde{V})^T \end{bmatrix}^T$, and

$$C \triangleq \max \Big(\frac{\Upsilon}{\sqrt{\{\frac{1}{h^B}\lambda_{min}(Q) - H\lambda_{max}(P)\} - (\gamma_1 + \gamma_2)\|P\bar{\boldsymbol{b}}\|}}, \\ \frac{\Upsilon}{\sqrt{\lambda_{\min}(\tilde{Q}) - (\kappa_1 + \kappa_2)}}, \frac{\Upsilon}{\sqrt{k - \kappa_1 - \gamma_1\|P\bar{\boldsymbol{b}}\|}} \Big) \tag{3.4.12}$$

is a radius of a ball B_C containing Γ. The ball B_C is introduced to quantify β of Ω_β in (3.4.16), where

$$\begin{aligned} \bar{Z} &= \|W - W_0\|_F^2 + \|V - V_0\|_F^2 \\ k_\sigma &> \kappa_1 + \gamma_1\|P\bar{\boldsymbol{b}}\| \\ \kappa_1 &= \Theta\alpha_1 + \|P\bar{\boldsymbol{b}}\|\gamma_1 \\ \kappa_2 &= \Theta\alpha_2 + \|P\bar{\boldsymbol{b}}\|\gamma_2 \\ \Theta &= \|P\bar{\boldsymbol{b}}\| + h^B\|\tilde{P}\bar{\boldsymbol{b}}\| \\ \Upsilon &= \sqrt{\gamma_2\|P\bar{\boldsymbol{b}}\| + \kappa_2 + k\bar{Z}} \end{aligned} \tag{3.4.13}$$

The above quantities are used to show negativeness of the time derivative of the Lyapunov function candidate in Γ, and $P, \tilde{P} > 0$ satisfy:

$$\begin{aligned} \bar{A}^T P + P\bar{A} &= -Q, \\ \tilde{A}^T \tilde{P} + \tilde{P}\tilde{A} &= -\tilde{Q}, \end{aligned} \tag{3.4.14}$$

for some $Q, \tilde{Q} > 0$ with minimum eigenvalues

$$\begin{aligned} \lambda_{\min}(Q) &> h^B H\lambda_{\max}(P) + h^B(\gamma_1 + \gamma_2)\|P\bar{\boldsymbol{b}}\| \\ \lambda_{\min}(\tilde{Q}) &> (\kappa_1 + \kappa_2). \end{aligned} \tag{3.4.15}$$

Let β be the maximum value of the Lyapunov function L on the edge of B_C:

$$\beta \triangleq \max_{\|\boldsymbol{\zeta}\| = C} L = C^2\lambda_{max}(T)\,. \tag{3.4.16}$$

Introduce the set as depicted in Figure 2:

$$\Omega_\beta = \{\boldsymbol{\zeta} \mid L \leq \beta\}\,. \tag{3.4.17}$$

Let α be the minimum value of the Lyapunov function L on the edge of B_R:

$$\alpha \triangleq \min_{\|\boldsymbol{\zeta}\|=R} L = R^2 \lambda_{min}(T)\,. \tag{3.4.18}$$

Define the compact set:

$$\Omega_\alpha = \{\boldsymbol{\zeta} \in B_R \mid L \leq \alpha\}. \tag{3.4.19}$$

Theorem 3.4.1. Let Assumptions 3.1.1, 3.1.2, 3.1.3, 3.1.4, 3.2.1 and 3.4.1 hold. Consider the following weight adaptation laws:

$$\begin{aligned} \dot{\hat{W}} &= -\Gamma_W \left[\mathrm{sgn}(h_{\bar{v}})(\hat{\boldsymbol{\sigma}} - \hat{\sigma}'\hat{V}^T\boldsymbol{\mu})\hat{\boldsymbol{E}}^T P\bar{\boldsymbol{b}} + k_\sigma(\hat{W} - W_0)\right] \\ \dot{\hat{V}} &= -\Gamma_V \left[\mathrm{sgn}(h_{\bar{v}})\boldsymbol{\mu}\hat{\boldsymbol{E}}^T P\bar{\boldsymbol{b}}\hat{W}^T\hat{\sigma}' + k_\sigma(\hat{V} - V_0)\right] \end{aligned} \tag{3.4.20}$$

where $\Gamma_V, \Gamma_W > 0$. If the initial errors belong to the compact set Ω_α defined in (3.4.19), then the feedback control law given by (3.2.1), (3.2.12) and (3.3.5) ensures that the signals $\boldsymbol{E}, \tilde{\boldsymbol{E}}, \tilde{W}$ and $\tilde{V}$ in the closed-loop system are ultimately bounded with the ultimate bound $C\sqrt{\frac{\lambda_{max}(T)}{\lambda_{min}(T)}}$.

Proof. See Appendix A.2. □

Remark 3.4.1. Knowledge of the sign of the control effectiveness has been made explicit in the adaptive law. It is also used in the proof of boundedness in Appendix A.2.

Remark 3.4.2. For fixed values of R and C, the inequality in (3.4.10) implies upper and lower bounds for the adaptation gains Γ_W and Γ_V in (3.4.20). For example, for $\Gamma_W = \gamma_W I$, and γ_W large, so that the minimum eigenvalue of T in (3.4.11) is determined by $1/\gamma_W$, we have $\gamma_W < R^2/(C^2\lambda_{max}(T))$ as an upper bound. Likewise, for small γ_W, so that the maximum eigenvalue of T is determined by the value of $1/\gamma_W$, we have $\gamma_W > C^2/(R^2\lambda_{min}(T))$ as a lower bound.

3.4.2 NN Adaptation with e-modification

The drawback of σ-modification is that the origin of the error signal i.e. $\boldsymbol{E} = 0, \tilde{W} = 0, \tilde{V} = 0$ is not an equilibrium point of (3.2.21) and (3.4.20) even if $\bar{w} = 0$ in (3.4.5). This implies that when the tracking error becomes small, $\dot{\hat{W}}, \dot{\hat{V}}$ are dominated by the σ-modification term in (3.4.20) and $\hat{W}, \hat{V}$ are driven towards W_0, V_0 which may not be a good guess of the optimal weights. Therefore, even if the NN reconstruction error and Taylor series expansion higher order terms are eliminated, the errors do not converge to the origin. This drawback motivates the use of another variation called e-modification, which was suggested by Narendra and Annaswamy [14, 15]. The idea is to multiply the tracking error component to the σ-modification term so that it tends to zero with the tracking error. The adaptive law with e-modification is given by:

$$\begin{aligned} \dot{\hat{W}} &= -\Gamma_W \left[\text{sgn}(h_{\bar{v}}) \hat{\boldsymbol{\sigma}} \hat{\boldsymbol{E}}^T P \bar{\boldsymbol{b}} + k_e \|\hat{\boldsymbol{E}}\| \hat{W} \right] \\ \dot{\hat{V}} &= -\Gamma_V \left[\text{sgn}(h_{\bar{v}}) \boldsymbol{\mu} \hat{\boldsymbol{E}}^T P \bar{\boldsymbol{b}} \hat{W}^T \hat{\sigma}' + k_e \|\hat{\boldsymbol{E}}\| \hat{V} \right] \end{aligned} \tag{3.4.21}$$

where $\Gamma_V, \Gamma_W > 0$ and $k_e > 0$. Note that the contribution from the e-modification term is reduced as $\|\hat{\boldsymbol{E}}\|$ becomes small.

For the boundedness proof we need the Taylor series expansion of $W^T \boldsymbol{\sigma}(V^T \boldsymbol{\mu})$ at $W = \hat{W}$ and $V = \hat{V}$.

$$W^T \boldsymbol{\sigma} = \hat{W}^T \hat{\boldsymbol{\sigma}} - \tilde{W}^T \hat{\boldsymbol{\sigma}} - \hat{W}^T \hat{\sigma}' \tilde{V}^T \boldsymbol{\mu} + \mathcal{O}(\|\tilde{Z}\|^2) \tag{3.4.22}$$

where the higher order terms $\mathcal{O}(\|\tilde{Z}\|^2) = -W^T(\hat{\boldsymbol{\sigma}} - \boldsymbol{\sigma}) + \hat{W}^T \hat{\sigma}' \tilde{V}^T \boldsymbol{\mu}$. Then

$$\begin{aligned} v_{ad} - \Delta &= \hat{W}^T \hat{\boldsymbol{\sigma}} - W^T \boldsymbol{\sigma} - \epsilon \\ &= \tilde{W}^T \hat{\boldsymbol{\sigma}} + \hat{W}^T \hat{\sigma}' \tilde{V}^T \boldsymbol{\mu} - \mathcal{O}(\|\tilde{Z}\|^2) - \epsilon \\ &= \tilde{W}^T \hat{\boldsymbol{\sigma}} + \hat{W}^T \hat{\sigma}' \tilde{V}^T \boldsymbol{\mu} + \bar{w} \end{aligned} \tag{3.4.23}$$

where $\bar{w} = -\mathcal{O}(\|\tilde{Z}\|^2) - \epsilon = W^T(\hat{\boldsymbol{\sigma}} - \boldsymbol{\sigma}) - \hat{W}^T \hat{\sigma}' \tilde{V}^T \boldsymbol{\mu} - \epsilon$. Utilizing (3.4.6) and (3.4.7),

$\bar{w}$ is bounded by:

$$\begin{aligned}\|\bar{w}\| &\leq 2\sqrt{n_2+1}W^* + \hat{W}\hat{\sigma}'(\hat{V}^T\boldsymbol{\mu} - V^T\boldsymbol{\mu}) + \epsilon^* \\ &\leq 2\sqrt{n_2+1}W^* + (\|\tilde{W}\| + W^*)(\delta\sqrt{n_2+1} + \frac{a^*}{4}V^*\boldsymbol{\mu}^*) + \epsilon^* \\ &\leq \gamma_1\|\tilde{Z}\| + \gamma_2\end{aligned} \tag{3.4.24}$$

where $\gamma_1 = \frac{a^*}{4}V^*\mu^* + \delta\sqrt{n_2+1}, \gamma_2 = 2\sqrt{n_2+1}W^* + \gamma_1 + \epsilon^*$ and δ is defined in (2.3.11).

Assumption 3.4.2. Assume

$$R > C\sqrt{\frac{\lambda_{max}(T)}{\lambda_{min}(T)}} \geq C \tag{3.4.25}$$

where $\lambda_{max}(T)$ and $\lambda_{min}(T)$ are the maximum and minimum eigenvalues of the following matrix:

$$T \triangleq \begin{bmatrix} P & 0 & 0 & 0 \\ 0 & \tilde{P} & 0 & 0 \\ 0 & 0 & \Gamma_W^{-1} & 0 \\ 0 & 0 & 0 & \Gamma_V^{-1} \end{bmatrix} \tag{3.4.26}$$

which will be used in a Lyapunov function candidate as $L = \boldsymbol{\zeta}^T T \boldsymbol{\zeta}$ with an error vector $\boldsymbol{\zeta} = \begin{bmatrix} \boldsymbol{E}^T & \tilde{\boldsymbol{E}}^T & \tilde{W}^T & (vec\tilde{V})^T \end{bmatrix}^T$, and

$$C \triangleq \max\left(\frac{2}{\bar{q}}\Upsilon,\ \ 2\left(\frac{\theta_1^2}{k_e^2} + \frac{\theta_2}{k_e}\right)^{\frac{1}{2}}\right) \tag{3.4.27}$$

is a radius of a ball B_C containing Γ, where

$$\begin{aligned}\theta_1 &= \left(\sqrt{n_2+1} + \delta + \frac{a^*}{4}V^*\mu^*\right)\|P\bar{\boldsymbol{b}}\|, \\ \theta_2 &= \frac{k_e}{2}Z^{*^2} + \|P\bar{\boldsymbol{b}}\|W^*\left(\delta + \frac{a^*}{4}V^*\mu^*\right), \\ \Theta &= \|P\bar{\boldsymbol{b}}\| + h^B\|\tilde{P}\bar{\boldsymbol{b}}\|,\ \kappa_9 = \alpha_1\|P\bar{\boldsymbol{b}} + \tilde{P}\bar{\boldsymbol{b}}\|, \\ \kappa_{10} &= 2\alpha_2\|P\bar{\boldsymbol{b}} + \tilde{P}\bar{\boldsymbol{b}}\|,\ \kappa_{12} = 2\|P\bar{\boldsymbol{b}}\|\gamma_2, \kappa_{14} = \|P\bar{\boldsymbol{b}}\|\gamma_1 \\ \Upsilon &\triangleq (\kappa_9 + \kappa_{14})^2 + (\kappa_{10} + \kappa_{12})\end{aligned} \tag{3.4.28}$$

Define the Lyapunov function level sets Ω_α and Ω_β [1]

$$\begin{aligned}\Omega_\alpha &= \{\boldsymbol{\zeta} \in B_R \mid L \leq \alpha \triangleq \min_{\|\boldsymbol{\zeta}\|=R} L\} \\ \Omega_\beta &= \{\boldsymbol{\zeta} \in B_R \mid L \leq \beta \triangleq \max_{\|\boldsymbol{\zeta}\|=C} L\}\end{aligned} \tag{3.4.29}$$

Theorem 3.4.2. Let Assumptions 3.1.1, 3.1.2, 3.1.3, 3.1.4, 3.2.1 and 3.4.2 hold. If the initial errors belong to the compact set Ω_α defined in (3.4.29), then the feedback control law given by (3.2.1), (3.2.12), (3.3.5) and the adaptation law (3.4.21) ensure that the signals $\boldsymbol{E}, \tilde{\boldsymbol{E}}, \tilde{W}$ and $\tilde{V}$ in the closed-loop system are ultimately bounded with the ultimate bound $C\sqrt{\frac{\lambda_{max}(T)}{\lambda_{min}(T)}}$.

Proof. See Appendix A.3. □

3.4.3 NN Adaptation with Projection

A projection operator [17] is employed to constrain the weight estimates to lie inside a known convex bounded set in the weight space that contains the unknown optimal weights. Let us start with a convex set having a smooth boundary defined by

$$\Pi_c \triangleq \{\hat{W} \in \Re^n \mid g(\hat{W}) \leq c\}, \quad 0 \leq c \leq 1 \tag{3.4.30}$$

where $g : \Re^n \to \Re$ is a smooth known function:

$$g(\hat{W}) = \frac{\hat{W}^T\hat{W} - W_{max}^2}{\epsilon_W} \tag{3.4.31}$$

where W_{max} is known bound on the weight vector $\hat{W}$ and $\epsilon_W > 0$ denotes the projection tolerance. Define the projection operator:

$$Proj(\hat{W}, \xi) \triangleq \begin{cases} \xi & \text{if } g(\hat{W}) \leq 0, \\ \xi & \text{if } g(\hat{W}) > 0 \text{ and } \nabla g^T \xi \leq 0, \\ \xi - \frac{\nabla g \nabla g^T \xi}{\|\nabla g\|^2} g(\hat{W}) & \text{if } g(\hat{W}) \leq 0 \text{ and } \nabla g^T \xi > 0 \end{cases} \tag{3.4.32}$$

[1] Since R and C are defined differently from Section 3.4.1, we should have different sets Ω_α and Ω_β when we state a new theorem.

where ∇g is defined as a column vector.

$$\nabla g(x) \triangleq \left[\frac{\partial g(x)}{\partial x_1} \quad \dots \quad \frac{\partial g(x)}{\partial x_n} \right]^T = \frac{2}{\epsilon_W} \hat{W} \tag{3.4.33}$$

The projection operator concept is illustrated in Figure 4. Projection streamlines ξ toward Π_0 so that we get a smooth transformation from the original vector field ξ to a less outward vector for $0 < c \leq 1$ or to a tangent to the boundary vector field for $c = 1$. It follows from (3.4.32) that when $g(\hat{W}) = 1$ and ξ points outward, we have $\nabla g^T Proj(\hat{W}, \xi) = 0$, which implies that the projection operator points along the tangent plane of Π_1 so that once $\hat{W}(0) \in \Pi_1$, $\hat{W}$ will never leave Π_1. The vector ∇g evaluated at a boundary point of the convex set Π_c is pointed away from the set. $Proj(\hat{W}, \xi)$ does not alter the vector ξ if $\hat{W}$ belongs to the convex set Π_0 or ξ points inward. In the set $\{0 < g(\hat{W}) \leq 1\}$, the projection operator subtracts a vector parallel to ∇g and weighted by g from ξ in a way that it still points outward but with reduced magnitude. $\xi - Proj(\hat{W}, \xi)$ has the same direction as $\nabla g(\hat{W})$ and its magnitude is less than $c\|\xi\|$.

$$\begin{aligned} \|\xi - Proj(\hat{W}, \xi)\| &= \frac{\|\nabla g\| |\nabla g^T \xi|}{\|\nabla g\|^2} |g(\hat{W})| \\ &\leq c\|\xi\| \end{aligned} \tag{3.4.34}$$

If we consider the function $\tilde{W}^T \Gamma_W^{-1} \tilde{W}$, its time derivative has the following additional term due to the projection operator.

$$\begin{aligned} \tilde{W}^T (Proj(\hat{W}, \xi) - \xi) &= \begin{cases} 0 \quad \text{if } g(\hat{W}) \leq 0, \\ 0 \quad \text{if } g(\hat{W}) > 0 \text{ and } \nabla g^T \xi \leq 0, \\ -\frac{(\hat{W} - W)^T \nabla g \nabla g^T \xi}{\|\nabla g\|^2} g(\hat{W}) \quad \text{if } g(\hat{W}) \leq 0 \text{ and } \nabla g^T \xi > 0 \end{cases} \\ &\leq 0 \end{aligned} \tag{3.4.35}$$

This additional term can only make the time derivative of the function more negative. The above property will be used in Lyapunov stability analysis.

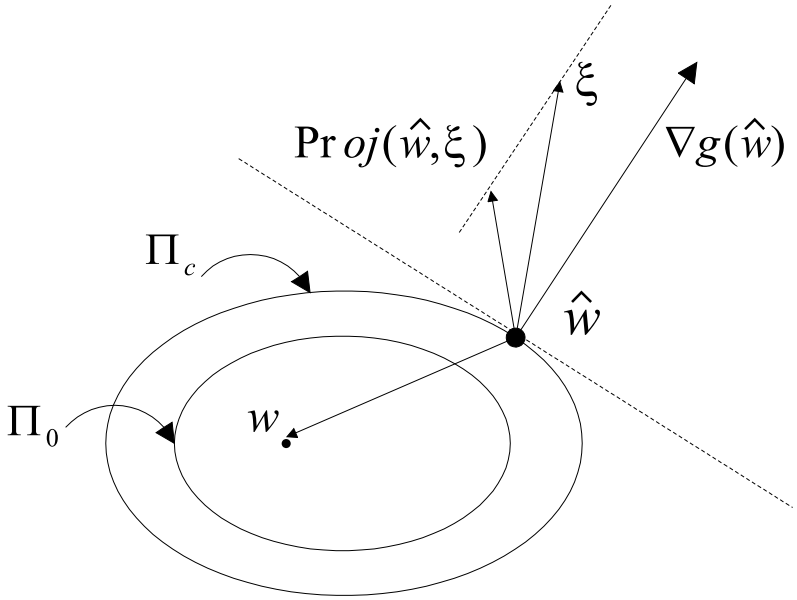

Figure 4: Projection operator

For a weight matrix, we can define the projection operator

$$Proj(\hat{V},\Xi) \triangleq \begin{bmatrix} Proj(\hat{V}_1,\xi_1) & \cdots & Proj(\hat{V}_{n_2},\xi_{n_2}) \end{bmatrix} \tag{3.4.36}$$

where $\hat{V} = \begin{bmatrix} \hat{V}_1 & \cdots & \hat{V}_{n_2} \end{bmatrix} \in \Re^{(n_1+1)\times n_2}$ and $\Xi = \begin{bmatrix} \xi_1 & \cdots & \xi_{n_2} \end{bmatrix} \in \Re^{(n_1+1)\times n_2}$. Then, the matrix projection has the following property similar to (3.4.35).

$$\mathrm{tr}\tilde{V}^T(Proj(\hat{V},\Xi)-\Xi) = \sum_{i=1}^{n_2} \tilde{V}_i^T(Proj(\hat{V}_i,\xi_i)-\xi_i) \leq 0 \tag{3.4.37}$$

Using (3.4.32) and (3.4.36), the NN weight update law can be given by:

$$\begin{aligned} \dot{\hat{W}} &= \Gamma_W Proj(\hat{W}, -\mathrm{sgn}(h_{\bar{v}})\hat{\boldsymbol{\sigma}}\hat{\boldsymbol{E}}^T P\boldsymbol{b}) \\ \dot{\hat{V}} &= \Gamma_V Proj(\hat{V}, -\mathrm{sgn}(h_{\bar{v}})\boldsymbol{\mu}\hat{\boldsymbol{E}}^T P\boldsymbol{b}\hat{W}^T\hat{\sigma}') \end{aligned} \tag{3.4.38}$$

where Γ_V, Γ_W are positive definite matrices.

Alternatively, we can introduce the *vec* operator as defined in (2.3.13), and use the projection operator defined for a vector in (3.4.32). In that case, the NN weights are updated by the following adaptation laws.

$$\begin{aligned} \dot{\hat{W}} &= \Gamma_W Proj(\hat{W}, -\mathrm{sgn}(h_{\bar{v}})\hat{\boldsymbol{\sigma}}\hat{\boldsymbol{E}}^T P\boldsymbol{b}) \\ \dot{\hat{V}} &= \Gamma_V vec^{-1} Proj[vec\hat{V}, -vec(\mathrm{sgn}(h_{\bar{v}})\boldsymbol{\mu}\hat{\boldsymbol{E}}^T P\boldsymbol{b}\hat{W}^T\hat{\sigma}')] \end{aligned} \tag{3.4.39}$$

We are going to show boundedness of the signals $E, \tilde{E}, \hat{W}, \hat{V}$. First, the NN weights $\hat{W}, \hat{V}$ will be shown to be bounded in a prescribed set by using the projection operator. Using the boundedness of the NN weights, we will show the derivative of a Lyapunov function is negative outside a compact set to guarantee the boundedness of $E, \tilde{E}$.

Assumption 3.4.3. Assume

$$R > C\sqrt{\frac{\lambda_{max}(T)}{\lambda_{min}(T)}} \geq C \tag{3.4.40}$$

where $\lambda_{max}(T)$ and $\lambda_{min}(T)$ are the maximum and minimum eigenvalues of the following matrix:

$$T \triangleq \begin{bmatrix} P & 0 & 0 & 0 \\ 0 & \tilde{P} & 0 & 0 \\ 0 & 0 & \Gamma_W^{-1} & 0 \\ 0 & 0 & 0 & \Gamma_V^{-1} \end{bmatrix} \tag{3.4.41}$$

which will be used in a Lyapunov function candidate as $L = \boldsymbol{\zeta}^T T \boldsymbol{\zeta}$ with an error vector $\boldsymbol{\zeta} = \begin{bmatrix} \boldsymbol{E}^T & \tilde{\boldsymbol{E}}^T & \tilde{W}^T & (vec\tilde{V})^T \end{bmatrix}^T$, and

$$C \triangleq \max\Big(\frac{c_1}{\lambda_{\min}(Q)} + \sqrt{\frac{\Upsilon}{\lambda_{\min}(Q)}}, \quad \frac{c_2}{\lambda_{\min}(\tilde{Q})} + \sqrt{\frac{\Upsilon}{\lambda_{\min}(\tilde{Q})}}\Big) \tag{3.4.42}$$

is a radius of a ball B_C containing Γ, where

$$\begin{aligned} c_1 &= \bar{w}^* \|P\boldsymbol{b}\|, \\ c_2 &= \|P\boldsymbol{b} + \tilde{P}\boldsymbol{b}\|\theta^*, \\ \Upsilon &= \frac{c_1^2}{\lambda_{\min}(Q)} + \frac{c_2^2}{\lambda_{\min}(\tilde{Q})} \end{aligned} \tag{3.4.43}$$

Define the Lyapunov function level sets Ω_α and Ω_β

$$\begin{aligned} \Omega_\alpha &= \{\boldsymbol{\zeta} \in B_R \mid L \leq \alpha \triangleq \min_{\|\boldsymbol{\zeta}\|=R} L\} \\ \Omega_\beta &= \{\boldsymbol{\zeta} \in B_R \mid L \leq \beta \triangleq \max_{\|\boldsymbol{\zeta}\|=C} L\} \end{aligned} \tag{3.4.44}$$

Theorem 3.4.3. Let Assumptions 3.1.1, 3.1.2, 3.1.3, 3.1.4, 3.2.1 and 3.4.3 hold. Then there exists a positive invariant set $\mathcal{D}_\zeta$ in the space of the error variables $\boldsymbol{\zeta}$ wherein the control law given by (3.2.1), (3.2.12) and (3.3.5) ensures, for all $\boldsymbol{\zeta}(0) \in \Omega_\alpha$ in (3.4.44), that $\boldsymbol{E}, \tilde{\boldsymbol{E}}, \tilde{W}, \tilde{V}$ are ultimately bounded with the ultimate bound $C\sqrt{\frac{\lambda_{max}(T)}{\lambda_{min}(T)}}$.

Proof. See Appendix A.4. □

3.5 Pseudo Control Hedging

Adaptive controllers are sensitive to input nonlinearities such as actuator position limits, actuator rate limits, actuator dynamics and time delay. The concept of hedging the reference model to prevent an adaptive law from seeing (attempting to adapt to) these unfavorable system-input characteristics was introduced in [40, 41]. This approach permits adaption even during finite periods of control saturation. When the nonlinear actuator characteristics include time delay, the relative degree is not well-defined since the r^{th} derivative of the output does not have a current time control input. In the presence of time delay, the relative degree is redefined as the number of differentiations of the output $y(t)$ required for the delayed input $u(t - T_D)$ to appear in the derivative explicitly. A pseudo control hedge, v_h, is obtained by first estimating the actuator position, $\hat{u}$, using a model for the actuator characteristics. This estimate is then used to compute the difference between commanded pseudo control, v, and the estimated achievable pseudo control. The process is illustrated in Figure 5 for an actuator model that has position limits, rate limits, actuator dynamics and time delay. Using (3.2.7) the PCH signal, v_h, can be expressed as

$$\begin{aligned} v_h &= v - \frac{1}{b_1}\{\hat{h}_r(y, \bar{y}, \hat{u}) + \sum_{i=0}^{r-1} a_{i+1}\hat{h}_i(y, \bar{y})\} \\ &= \frac{1}{b_1}\{\hat{h}_r(y, \bar{y}, u_{cmd}) - \hat{h}_r(y, \bar{y}, \hat{u})\} \end{aligned} \tag{3.5.1}$$

where u_{cmd} is commanded control input from (3.2.1) and $\hat{u}$ is the estimated control input as depicted in Figure 5. The PCH signal is then subtracted from the reference

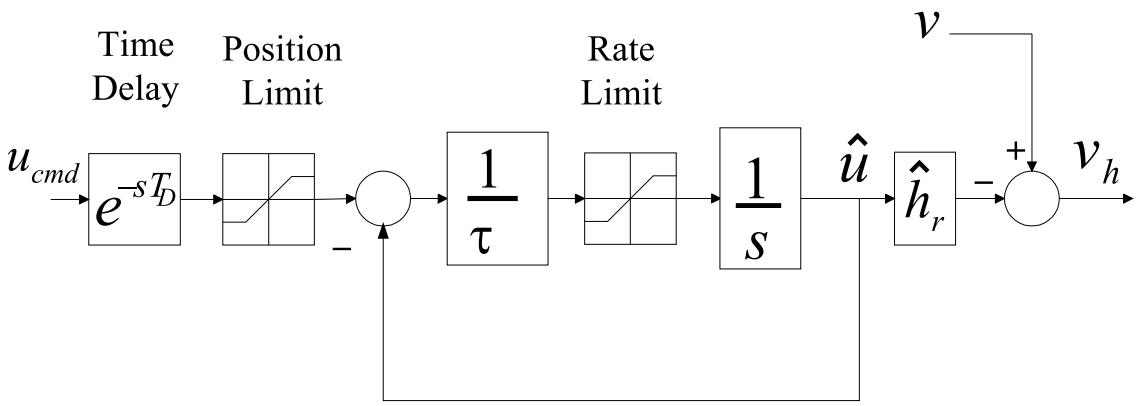

Figure 5: Computation of the PCH signal

model dynamics as described by the following equation

$$x_{rm}^{(r)} = f_{rm}(x_{rm}, \dot{x}_{rm}, \cdots, x_{rm}^{(r-1)}, y_{com}) - b_1 v_h \tag{3.5.2}$$

where y_{com} is the unfiltered command signal. The manner in which it is incorporated in a linear reference model is shown in Figure 6. Notice that the PCH signal is integrated before it is introduced as the reference model pseudo control component so there is no algebraic loop. The n^{th}-order linear reference model augmented with the PCH signal can be expressed in the following state space form:

$$\begin{bmatrix} \dot{x}_{rm} \\ \ddot{x}_{rm} \\ \vdots \\ x_{rm}^{(r-1)} \\ x_{rm}^{(r)} \end{bmatrix} = \underbrace{\begin{bmatrix} 0 & 1 & 0 & \cdots & 0 \\ 0 & 0 & 1 & & 0 \\ \vdots & \vdots & & \ddots & \\ 0 & 0 & & & 1 \\ -m_1 & -m_2 & -m_3 & \cdots & -m_r \end{bmatrix}}_{A_{rm}} \begin{bmatrix} x_{rm} \\ \dot{x}_{rm} \\ \vdots \\ x_{rm}^{(r-2)} \\ x_{rm}^{(r-1)} \end{bmatrix} + \underbrace{\begin{bmatrix} 0 & 0 \\ 0 & 0 \\ \vdots & \vdots \\ 0 & 0 \\ 1 & 1 \end{bmatrix}}_{B_{rm}} \begin{bmatrix} m_1 y_{com} \\ -b_1 v_h \end{bmatrix} \tag{3.5.3}$$

$$\begin{aligned} y_{rm} &= x_{rm} \\ v_{rm} &= \frac{1}{b_1}\begin{bmatrix} a_1 & a_2 & \cdots & a_r \end{bmatrix} \boldsymbol{x}_{rm} + \frac{1}{b_1}(x_{rm}^{(r)} + b_1 v_h) \\ &= \frac{1}{b_1}\begin{bmatrix} (a_1 - m_1) & (a_2 - m_2) & \cdots & (a_r - m_r) \end{bmatrix} \boldsymbol{x}_{rm} + \frac{m_1}{b_1} y_{com} \end{aligned}$$

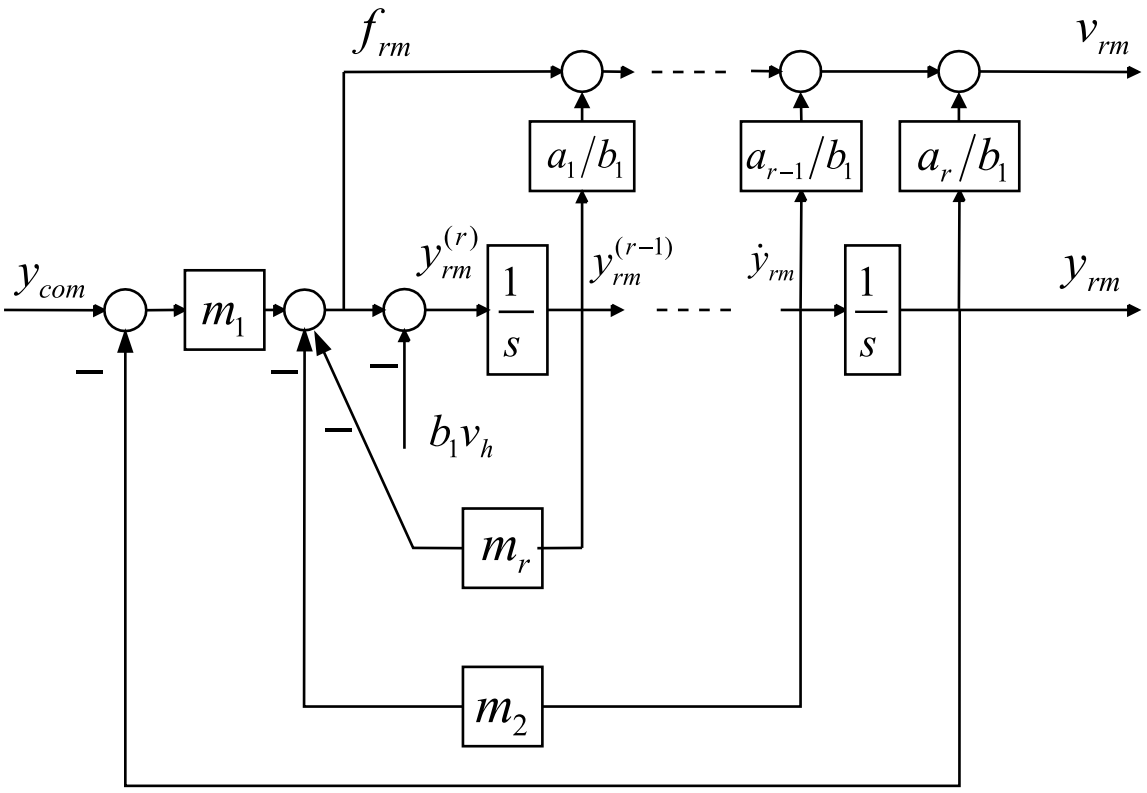

Figure 6: The n^{th}-order reference model with PCH signal

where $m_1, m_2, \cdots, m_r$ are the reference model gains chosen such that A_{rm} is Hurwitz. There exists $P_{rm} > 0$ satisfying the following Lyapunov equation

$$A_{rm}^T P_{rm} + P_{rm} A_{rm} = -Q_{rm} \tag{3.5.4}$$

for all $Q_{rm} > 0$. It is reasonable to introduce the following assumption.

Assumption 3.5.1. The command $y_{com}(t)$ is uniformly bounded so that

$$\|y_{com}(t)\| \leq y_{com}^*, \quad y_{com}^* \geq 0$$

In [39], in the absence of input nonlinearity, ultimate boundedness of error signals has been shown in an output feedback setting using Lyapunov's direct method for the case of unbounded actuation. In the presence of input nonlinearity, it is not obvious how to guarantee boundedness of reference model states since the PCH signal is fed back to the reference model, hence boundedness of the tracking error signal $e(t)$ does not automatically imply boundedness of the system output $y(t)$ unlike the case without PCH. We first show boundedness of the errors in plant states, error observer states and NN weights via Lyapunov analysis regardless of boundedness of the reference model states, and then ensure that the reference model states are bounded using the proven boundedness property of the errors in plant states and NN weights, which is done without assuming boundedness of the reference model. Boundedness analysis is given both for a static actuator with position limits and time delay, and for a dynamic actuator with position/rate limits including time delay. Boundedness of the errors in plant states, error observer states and NN weights can be ensured by one of adaptive laws given in Section 3.4.1 - 3.4.3. Lemmas in this section complete the proofs of boundedness by ensuring that the reference model states are bounded.

Using the mean value theorem, the PCH signal is bounded by

$$\begin{aligned} \|v_h\| &= \frac{1}{|b_1|}\|\hat{h}_r(y,\bar{y},u_{cmd}) - \hat{h}_r(y,\bar{y},\hat{u})\| \\ &\leq \frac{\hat{h}_u}{|b_1|}\|u_{cmd} - \hat{u}\| \end{aligned} \tag{3.5.5}$$

where $\hat{h}_u = \max\left\|\frac{\partial \hat{h}_r}{\partial \bar{u}}\right\|$, $\frac{\partial \hat{h}_r}{\partial \bar{u}} = \frac{\partial \hat{h}_r}{\partial u}|_{u=\bar{u}}$, $\bar{u} = \theta u_{cmd} + (1-\theta)\hat{u}$ and $\theta \in [0,1]$. In the presence of time delay, utilizing the Lipschitz continuity of the bounded function $\hat{u}(t)$,

$$\begin{aligned} \|v_h\| &\leq \frac{\hat{h}_u}{|b_1|}\|u_{cmd}(t) - \hat{u}(t-T_D)\| \\ &\leq \frac{\hat{h}_u}{|b_1|}\left(\|u_{cmd}(t) - \hat{u}(t)\| + \|\hat{u}(t) - \hat{u}(t-T_D)\|\right) \\ &\leq \frac{\hat{h}_u}{|b_1|}\left(\|u_{cmd}(t) - \hat{u}(t)\| + l_3 T_D\right) \end{aligned} \tag{3.5.6}$$

where l_3 is Lipschitz constant for $\hat{u}(t)$, and $T_D \geq 0$ is a time delay used in the actuator model.

Remark 3.5.1. Recall that $\boldsymbol{v}_d(t)$ in (2.4.27) is used only to reconstruct the state $\boldsymbol{x}(t)$. In the case of time delay of T_D in the actuator, $\boldsymbol{v}_d(t-T_D)$ should be used instead of $\boldsymbol{v}_d(t)$.

3.5.1 Static Actuation

For the proof of boundedness we choose linear approximations as stated in the following assumption.

Assumption 3.5.2. Linear models are used for approximate expressions for every derivative of the output up to r^{th} derivative:

$$\begin{aligned} \hat{h}_i(y,\bar{y}) &= c_i y, \quad i = 1, \cdots, r-1 \\ \hat{h}_r(y,\bar{y},u) &= c_r y + d_r u \end{aligned}$$

Then $\hat{h}_u$ in (3.5.5) boils down to d_r.

Assumption 3.5.3. When the true actuator nonlinearity is static, the actuator model satisfies the following property

$$\hat{u}(u_{cmd}) = \text{sgn}(u_{cmd}) \cdot \min(\|u_{cmd}\|, M), \quad M > 0$$

Utilizing Assumption 3.5.2, the commanded control input can be expressed as:

$$\begin{aligned} u_{cmd} &= \frac{1}{d_r}(b_1 v - \sum_{i=0}^{r} a_{i+1} c_i y) \\ &= \frac{1}{d_r}\left(\boldsymbol{\phi}^T \boldsymbol{x}_{rm} + m_1 y_{com} + b_1(v_{dc} - v_{ad}) + \sum_{i=0}^{r} a_{i+1} c_i (e - x_{rm})\right) \end{aligned} \tag{3.5.7}$$

where $\boldsymbol{\phi} = \begin{bmatrix} (a_1 - m_1) & \cdots & (a_r - m_r) \end{bmatrix}^T$, and

$$u_{cmd} = \frac{1}{d_r}\left(\bar{\boldsymbol{\phi}}^T \boldsymbol{x}_{rm} + m_1 y_{com} + b_1(v_{dc} - v_{ad}) + \sum_{i=0}^{r} a_{i+1} c_i e\right) \tag{3.5.8}$$

where $\bar{\boldsymbol{\phi}} = \begin{bmatrix} (a_1 - m_1 - \sum_{i=0}^{r} a_{i+1} c_i) & (a_2 - m_2) & \cdots & (a_r - m_r) \end{bmatrix}^T$.

Assumption 3.5.4. The actuator model $\hat{u}$ follows the input command u_{cmd} closely enough such that

$$\|u_{cmd} - \hat{u}\| \leq \delta_d \|\bar{\boldsymbol{\phi}}\| \|\boldsymbol{x}_{rm}\|$$

where $0 < \delta_d |d_r| < 1$.

Assumption 3.5.4 can be satisfied if the following condition holds.

$$\|m_1 y_{com} + b_1(v_{dc} - v_{ad}) + \sum_{i=0}^{r} a_{i+1} c_i e\| \leq \frac{M}{\delta_d} \tag{3.5.9}$$

where M is the limit value of actuator introduced in Assumption 3.5.3. From (3.2.17) and (3.3.5), v_{dc} and v_{ad} can be bounded by:

$$\begin{aligned} \|v_{dc}\| &\leq \left[\|\boldsymbol{c}_c\|^2 + d_c^2\right]^{\frac{1}{2}} \|\boldsymbol{E}\| \\ \|v_{ad}\| &\leq \sqrt{n_2 + 1}(\|\tilde{Z}\| + Z^*) \end{aligned} \tag{3.5.10}$$

The ultimate boundedness of tracking error signal and NN weights error signal are ensured by one of Theorems 3.4.1, 3.4.2 and 3.4.3. The ultimate bounds can be used to impose a restriction on the magnitude of command signal y_{com} in Assumption 3.5.4.

$$\begin{aligned}\|m_1 y_{com}\| &\leq \frac{M}{\delta_d} - b_1 \left([\|\boldsymbol{c}_c\|^2 + d_c^2]^{\frac{1}{2}} \|\boldsymbol{E}\| + \sqrt{n_2+1}(\|\tilde{Z}\| + Z^*) \right) - \left| \sum_{i=0}^{r} a_{i+1} c_i \right| e \\ &\leq \frac{M}{\delta_d} - b_1 C \sqrt{\frac{\lambda_{\max}(T)}{\lambda_{\min}(T)}} \left([\|\boldsymbol{c}_c\|^2 + d_c^2]^{\frac{1}{2}} + \sqrt{n_2+1} + \left| \sum_{i=0}^{r} a_{i+1} c_i \right| \right) \\ &\quad - b_1 \sqrt{n_2+1} Z^*\end{aligned} \tag{3.5.11}$$

where C is defined in (3.4.12), (3.4.27), or (3.4.42). Applying Assumptions 3.5.2 and 3.5.4 to (3.5.6),

$$\|v_h\| \leq \frac{1}{|b_1|} (\delta_d |d_r| \|\bar{\boldsymbol{\phi}}\| \|\boldsymbol{x}_{rm}\| + l_3 T_D) \tag{3.5.12}$$

Utilizing the above assumptions, the following Lemma ensures the boundedness of reference model states.

Lemma 3.5.1. Let Assumptions 3.5.1, 3.5.2, 3.5.3, and 3.5.4 hold. If $\boldsymbol{E}$ and $\tilde{Z}$ are bounded, then the reference model state, $\boldsymbol{x}_{rm}$, is bounded.

Proof. Introduce a Lyapunov function candidate to show boundedness of $\boldsymbol{x}_{rm}$,

$$L_{rm} = \boldsymbol{x}_{rm}^T P_{rm} \boldsymbol{x}_{rm} \tag{3.5.13}$$

Its time derivative becomes,

$$\begin{aligned}\dot{L}_{rm} &= -\boldsymbol{x}_{rm}^T Q_{rm} \boldsymbol{x}_{rm} + 2\boldsymbol{x}_{rm}^T P_{rm} B_{rm} \begin{bmatrix} m_1 y_{com} \\ -b_1 v_h \end{bmatrix} \\ &\leq -\lambda_{\min}(Q_{rm}) \|\boldsymbol{x}_{rm}\|^2 + 2\|\boldsymbol{x}_{rm}\| \|P_{rm} B_{rm}\| (m_1 y_{com}^* + \delta_d |d_r| \|\bar{\boldsymbol{\phi}}\| \|\boldsymbol{x}_{rm}\| + l_3 T_D) \\ &\leq -\lambda_{\min}(Q_{rm}) \|\boldsymbol{x}_{rm}\|^2 + k_5 \|\boldsymbol{x}_{rm}\|^2 + k_6 \|\boldsymbol{x}_{rm}\| \\ &\leq -\|\boldsymbol{x}_{rm}\| \left[(\lambda_{\min}(Q_{rm}) - k_5) \|\boldsymbol{x}_{rm}\| - k_6 \right]\end{aligned} \tag{3.5.14}$$

where $k_5 = 2\delta_d |d_r| \|\bar{\boldsymbol{\phi}}\| \|P_{rm} B_{rm}\|$, $k_6 = 2(l_3 T_D + y^*_{com}) \|P_{rm} B_{rm}\|$. Choose Q_{rm} so that $\lambda_{min}(Q_{rm}) > k_5$. Then, $\dot{L}_{rm} \leq 0$ when

$$\|\boldsymbol{x}_{rm}\| \geq \gamma_{rm} \triangleq \frac{k_6}{\lambda_{\min}(Q_{rm}) - k_5} \tag{3.5.15}$$

Hence the reference model state $\boldsymbol{x}_{rm}$ is ultimately bounded. The bound on $\boldsymbol{x}_{rm}$ can be calculated as:

$$\begin{aligned} \lambda_{\min}(P_{rm}) \|\boldsymbol{x}_{rm}\|^2 \leq L_{rm} \leq \lambda_{\max}(P_{rm}) \|\boldsymbol{x}_{rm}\|^2 \leq \lambda_{\max}(P_{rm}) \gamma_{rm}^2 \\ \|\boldsymbol{x}_{rm}\| \leq \sqrt{\frac{\lambda_{\max}(P_{rm})}{\lambda_{\min}(P_{rm})}} \gamma_{rm} \end{aligned} \tag{3.5.16}$$

□

Remark 3.5.2. This lemma is applied to the following linear scalar system.

$$\dot{x}(t) = ax(t) + bu(t) \tag{3.5.17}$$

Consider the following approximate model.

$$\begin{aligned} \dot{x}(t) &= c_r x(t) + d_r u(t) + \Delta \\ u_{cmd} &= \frac{1}{d_r}(v - c_r x) \\ v_{dc} &= k_p e \end{aligned} \tag{3.5.18}$$

The PCH signal is

$$v_h = d_r(u_{cmd} - \hat{u})$$

The reference model with PCH is expressed as:

$$\dot{x}_{rm} = -m x_{rm} + m y_{com} - v_h, \quad m > 0 \tag{3.5.19}$$

The inequality (3.5.9) becomes

$$|m y_{com}| \leq \frac{M}{\delta_d} - C\sqrt{\frac{\lambda_{\max}(T)}{\lambda_{\min}(T)}}(|c_r - k_p| + \sqrt{n_2 + 1}) - \sqrt{n_2 + 1} Z^* \tag{3.5.20}$$

Assumption 3.5.4 becomes

$$|u_{cmd} - \hat{u}| \leq \delta_d m |x_{rm}| \tag{3.5.21}$$

In case that the values of a and b are known, (3.5.9) boils down to

$$|my_{com}| \leq \frac{M}{\delta_d} \tag{3.5.22}$$

Consider the following Lyapunov function candidate:

$$L_{rm} = \frac{1}{2}x_{rm}^2 \tag{3.5.23}$$

The time derivative of L_{rm} is

$$\begin{aligned} \dot{L}_{rm} &= x_{rm}(-mx_{rm} + my_{com} - b(u_{cmd} - \hat{u})) \\ &\leq -mx_{rm}^2 + my_{com}x_{rm} + m\delta_d|b|x_{rm}^2 \\ &\leq -m|x_{rm}|[(1 - \delta_d|b|)|x_{rm}| - y_{com}] \end{aligned} \tag{3.5.24}$$

$\dot{L}_{rm} < 0$ when $|x_{rm}| > \frac{y_{com}}{(1-\delta_d|b|)}$. Hence, x_{rm} is ultimately bounded.

3.5.2 Dynamic Actuation

For a dynamic actuator we have the following assumption.

Assumption 3.5.5. The 1^{st}-order dynamic actuator model with position/rate saturations and time delay is expressed in the following form:

$$\begin{aligned} \dot{x}_a(t) &= \text{sat}_R\left(-\frac{1}{\tau}x_a(t) + \frac{1}{\tau}\text{sat}_P(u_c(t))\right) \\ \hat{u}(t) &= x_a(t - T_D) \end{aligned} \tag{3.5.25}$$

The position/rate saturation functions are defined as:

$$\begin{aligned} \text{sat}_P(x) &\triangleq \text{sgn}(x) \cdot \min(\theta_P, |x|) \\ \text{sat}_R(x) &\triangleq \text{sgn}(x) \cdot \min(\theta_R, |x|) \end{aligned} \tag{3.5.26}$$

where θ_P and θ_R denote the position bound and rate bound respectively.

Using (3.5.5), the reference model can be rewritten as:

$$\begin{aligned} \dot{\boldsymbol{x}}_{rm} &= A_{rm}\boldsymbol{x}_{rm} + \boldsymbol{b}(m_1 y_{com} - \frac{\partial \hat{h}_r}{\partial \bar{u}}(u_c(t) - \hat{u}(t))) \\ &= A_{rm}\boldsymbol{x}_{rm} + \boldsymbol{b}(m_1 y_{com} - \frac{\partial \hat{h}_r}{\partial \bar{u}}(u_c(t) - x_a(t) + \dot{x}_a(t - \theta T_D)T_D)) \end{aligned} \tag{3.5.27}$$

where $\boldsymbol{b} = \begin{bmatrix} 0 & \cdots & 0 & 1 \end{bmatrix}^T \in \Re^r$ and $\theta \in [0,1]$. The augmented reference model can be given by:

$$\begin{bmatrix} \dot{\boldsymbol{x}}_{rm} \\ \dot{x}_a \end{bmatrix} = \underbrace{\begin{bmatrix} A_{rm} & \frac{\partial \hat{h}_r}{\partial \bar{u}}\boldsymbol{b} \\ 0_{1\times r} & -\frac{1}{\tau} \end{bmatrix}}_{\bar{A}_{rm}} \underbrace{\begin{bmatrix} \boldsymbol{x}_{rm} \\ x_a \end{bmatrix}}_{\bar{\boldsymbol{x}}_{rm}} + \underbrace{\begin{bmatrix} \boldsymbol{b} & 0_{r\times 1} \\ 0 & 1 \end{bmatrix}}_{\bar{B}_{rm}} \begin{bmatrix} m_1 y_{com} - \frac{\partial \hat{h}_r}{\partial \bar{u}}(u_c + \dot{x}_a(t-\theta T_D)T_D) \\ \text{sat}_R(w) - w + \frac{1}{\tau}\text{sat}_P(u_c) \end{bmatrix} \tag{3.5.28}$$

where $w = -\frac{1}{\tau}x_a(t) + \frac{1}{\tau}\text{sat}_P(u_c(t))$. There exists a unique $\bar{P}_{rm} > 0$ that solves the following Lyapunov equation

$$\bar{A}_{rm}^T \bar{P}_{rm} + \bar{P}_{rm}\bar{A}_{rm} = -\bar{Q}_{rm} \tag{3.5.29}$$

for arbitrary $\bar{Q}_{rm} > 0$.

Lemma 3.5.2. Let Assumptions 3.5.1 and 3.5.5 hold. If $\boldsymbol{E}$ and $\tilde{Z}$ are bounded, the reference model state, $\boldsymbol{x}_{rm}$, is bounded.

Proof. Consider the following Lyapunov function,

$$L_{rm} = \bar{\boldsymbol{x}}_{rm}^T \bar{P}_{rm} \bar{\boldsymbol{x}}_{rm} \tag{3.5.30}$$

Differentiating L_{rm} with respect to time,

$$\begin{aligned} \dot{L}_{rm} &= -\bar{\boldsymbol{x}}_{rm}^T \bar{Q}_{rm} \bar{\boldsymbol{x}}_{rm} + 2\bar{x}_{rm}^T \bar{P}_{rm} \bar{B}_{rm} \begin{bmatrix} m_1 y_{com} - \frac{\partial \hat{h}_r}{\partial \bar{u}}(u_c + \dot{x}_a(t-\theta T_D)T_D) \\ \text{sat}_R(w) - w + \frac{1}{\tau}\text{sat}_P(u_c) \end{bmatrix} \\ &\leq -\lambda_{min}(\bar{Q}_{rm})\|\bar{\boldsymbol{x}}_{rm}\|^2 + \|\bar{\boldsymbol{x}}_{rm}\|(q_1\|\boldsymbol{x}_{rm}\| + q_2\|x_a\| + q_3) \end{aligned} \tag{3.5.31}$$

where $q_1 = 2\|\bar{P}_{rm}\bar{B}_{rm}\|\hat{h}_u l_1(k_1+1)$, $q_2 = 2\|\bar{P}_{rm}\bar{B}_{rm}\|\frac{1}{\tau}$, $q_3 = 2\|\bar{P}_{rm}\bar{B}_{rm}\|\{m_1 y_{com}^* + \hat{h}_u(l_1(E^* + k_2) + l_2) + \theta_R T_D) + \theta_R\}$. Utilizing the following inequality,

$$\left\| \begin{matrix} \boldsymbol{z} \\ \boldsymbol{y} \end{matrix} \right\| \leq \|\boldsymbol{z}\| + \|\boldsymbol{y}\| \leq \sqrt{2} \left\| \begin{matrix} \boldsymbol{z} \\ \boldsymbol{y} \end{matrix} \right\| \tag{3.5.32}$$

$$\dot{L}_{rm} \leq -(\lambda_{min}(\bar{Q}_{rm}) - \sqrt{2}q_4)\|\bar{\boldsymbol{x}}_{rm}\|^2 + q_3\|\bar{\boldsymbol{x}}_{rm}\| \tag{3.5.33}$$

where $q_4 = \max(q_1, q_2)$. L_{rm} is negative when $\|\bar{x}_{rm}\| > \frac{q_3}{\lambda_{min}(\bar{Q}_{rm}) - \sqrt{2}q_4}$. Hence $\boldsymbol{x}_{rm}$ and x_a are bounded. □

Figure 7: R-50 unmanned helicopter

3.6 Design and Performance Results of R-50 Helicopter Model

To demonstrate that the developed approach is adaptive to both parametric uncertainty and unmodeled dynamics (including time delay), we illustrate a design and performance evaluation using a simplified model for the longitudinal dynamics of an R-50 experimental helicopter shown in Figure 7. A linear model is used both for design and simulation so as not to obscure the effects due to unmodeled dynamics and actuation limits. Figure 8 presents the implementation block diagram.

The pitch channel equations of motion of the R-50 helicopter can be expressed as a single-input multi-output system:

$$\dot{x} = f(x, \delta), \quad \begin{bmatrix} \bar{y} \\ y \end{bmatrix} = \begin{bmatrix} q \\ \theta \end{bmatrix} \tag{3.6.1}$$

where $x = [u, q, \theta, \beta, w]^T$ is the state vector , u being the forward velocity, q the pitch rate, θ the pitch angle, β control rotor longitudinal tilt angle, w vertical velocity, δ longitudinal cyclic input (deflection angle of swashplate in radian), $\bar{y}$ is an additional

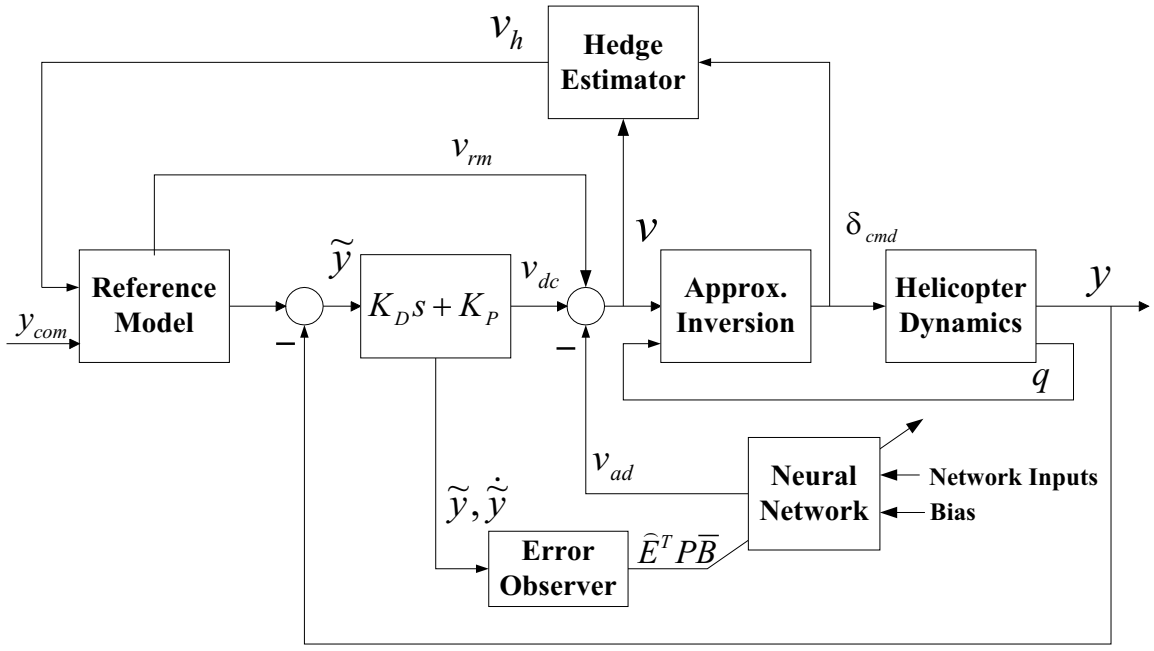

Figure 8: Generic block diagram of single channel of adaptive attitude command system with pseudo control hedging

measurement and y is the controlled output. Note that since only pitch angle and pitch rate are used in the inversion process, the main sources of unmodeled dynamics are the control rotor dynamics and time delay.

The following linearized model was obtained based on flight test data:

$$\begin{bmatrix} \dot{u} \\ \dot{q} \\ \dot{\theta} \\ \dot{\beta} \\ \dot{w} \end{bmatrix} = \begin{bmatrix} X_u & X_q & X_\theta & X_\beta & X_w \\ M_u & M_q & 0 & M_\beta & M_w \\ 0 & 1 & 0 & 0 & 0 \\ B_u & -1 & 0 & B_\beta & 0 \\ Z_u & Z_q & Z_\theta & Z_\beta & Z_w \end{bmatrix} \begin{bmatrix} u \\ q \\ \theta \\ \beta \\ w \end{bmatrix} + \begin{bmatrix} X_\delta \\ M_\delta \\ 0 \\ B_\delta \\ Z_\delta \end{bmatrix} \delta \qquad (3.6.2)$$

where the actual coefficient values are:

$$\begin{aligned} X_u = -0.0553, X_q = 1.413, X_\theta = -32.1731, \\ X_\beta = -19.9033, X_w = 0.0039, M_u = 0.2373, \\ M_q = -6.9424, M_\beta = 68.2896, M_w = 0.002, \\ B_u = 0.0101, B_\beta = -2.1633, Z_u = -0.0027, \\ Z_q = -0.0236, Z_\theta = -0.2358, Z_\beta = -0.1233, \\ Z_w = -0.5727, X_\delta = 11.2579, M_\delta = -38.6267, \\ B_\delta = -4.2184, Z_\delta = 0.0698. \end{aligned} \tag{3.6.3}$$

In Assumption 3.1.3 we have assumed the relative degree of the output is known. If we assume that the actuator responds to the commanded input according to the 1^{st}-order dynamics

$$\tau\dot{\delta}(t) = -\delta(t) + \delta_c(t - T_D) \tag{3.6.4}$$

then θ has relative degree 3. The time delay T_D will be dealt with by PCH.

We choose the desired linearized system in (3.2.4) so that we can stabilize the closed-loop system with the PD (proportional + derivative) controller depicted in Figure 8.

$$G_d(s) = \frac{p}{s^2(s+p)} \tag{3.6.5}$$

This corresponds to $a_1 = p, a_2 = 0, a_3 = 0$ and $b_1 = p$ in (3.2.4), and the error dynamics with $v_{dc} = (K_D s + K_P)e$ in (3.2.16) become

$$(s^3 + ps^2 + pK_D s + pK_P)e = 0 \tag{3.6.6}$$

The PD controller is designed to place the closed-loop poles at $-20, -8 \pm 6i$, which corresponds to that $p = 36, K_P = 55.56$ and $K_D = 11.67$. From (3.2.6), the relationship between pseudo control v and the controlled output y is given by:

$$p(v + \Delta) = \dddot{y} + p\ddot{y} \tag{3.6.7}$$

In order to get the inversion law we are considering only q and θ as in (3.6.8) leaving other states (u, β, w) as unmodeled dynamics.

$$\begin{bmatrix} \dot{q} \\ \dot{\theta} \end{bmatrix} = \begin{bmatrix} \hat{M}_q & 0 \\ 1 & 0 \end{bmatrix} \begin{bmatrix} q \\ \theta \end{bmatrix} + \begin{bmatrix} \hat{M}_\delta \\ 0 \end{bmatrix} \delta \tag{3.6.8}$$

We can get the approximations for $\ddot{y}$ and $\dddot{y}$ from (3.6.8).

$$\begin{aligned} \hat{\ddot{y}} &= \hat{M}_q q \\ \hat{\dddot{y}} &= \hat{M}_q^2 q + \frac{\hat{M}_\delta}{\tau} \delta_{cmd} \end{aligned} \tag{3.6.9}$$

where $\hat{M}_q$ and $\hat{M}_\delta$ are introduced to account for parametric uncertainty in M_q and M_δ, respectively. Utilizing the above approximation, (3.6.7) becomes

$$p(v + \Delta) = \hat{M}_q^2 q + \frac{\hat{M}_\delta}{\tau} \delta_{cmd} + p\hat{M}_q q + \Delta_3 + p\Delta_2 \tag{3.6.10}$$

where $\Delta_3 = \dddot{y} - \hat{\dddot{y}}$ and $\Delta_2 = \ddot{y} - \hat{\ddot{y}}$. Using (3.6.10), the approximate inversion law (3.2.1) becomes

$$\delta_{cmd} = \frac{\tau}{\hat{M}_\delta}(pv - \hat{M}_q(\hat{M}_q + p)q) \tag{3.6.11}$$

and from (3.2.11), the model inversion error Δ can be expressed as

$$\begin{aligned} \Delta &= \frac{1}{p}(\Delta_3 + p\Delta_2) \\ &= \frac{1}{p}\{\dddot{y} - \hat{\dddot{y}} + p(\ddot{y} - \hat{\ddot{y}})\} \end{aligned} \tag{3.6.12}$$

The eigenvalues of $\tilde{A}$ in (3.3.2) have been placed to be 4 times faster than those of $\bar{A}$ in (3.2.21). The weight update laws for the application were chosen to be (3.4.20). The adaptation gains have been set to $\Gamma_V = 20I$, $\Gamma_W = 100I$. The following sigmoidal function

$$\boldsymbol{\sigma}(z) = \frac{1}{1 + e^{-az}} \tag{3.6.13}$$

was implemented in the NN design with five hidden neurons, with activation potentials chosen to be [2, 1.6, 1.2, 0.8, 0.2]. The σ-modification gain k_σ in the NN

update laws (3.4.20) was selected to be 2.5. The σ-modification initial matrices W_0 and V_0 are set to zero since no *a priori* knowledge for estimates of the weight matrices is available. The number of neurons was chosen experimentally by starting with a large number and gradually reducing until a degradation in performance became non-negligible.

As shown in Figure 8, the commanded pitch attitude is processed through a linear 3^{rd}-order reference model,

$$y_{rm} = \frac{2\omega^3}{(s+2\omega)(s^2+2\zeta\omega s+\omega^2)}\, y_{com} \tag{3.6.14}$$

The reference model is incorporated with PCH in state space form.

$$\begin{bmatrix} \dot{x}_{rm} \\ \ddot{x}_{rm} \\ \dddot{x}_{rm} \end{bmatrix} = \begin{bmatrix} 0 & 1 & 0 \\ 0 & 0 & 1 \\ -2w^3 & -(1+4\zeta)w^2 & -2(1+\zeta)w \end{bmatrix} \begin{bmatrix} x_{rm} \\ \dot{x}_{rm} \\ \ddot{x}_{rm} \end{bmatrix} + \begin{bmatrix} 0 & 0 \\ 0 & 0 \\ 2w^3 & -p \end{bmatrix} \begin{bmatrix} y_{com} \\ v_h \end{bmatrix}$$

$$v_{rm} = \frac{1}{p}\begin{bmatrix} -2w^3 & -(1+4\zeta)w^2 & p-2(1+\zeta)w \end{bmatrix} \begin{bmatrix} x_{rm} \\ \dot{x}_{rm} \\ \ddot{x}_{rm} \end{bmatrix} + \frac{2w^3}{p} y_{com}$$

where $\omega = 10$, and $\zeta = 0.8$. Pseudo-control hedging signal v_h is generated as in (3.5.1)

$$v_h = \frac{\hat{M}_\delta}{\tau p}(\delta_{cmd} - \hat{\delta}) \tag{3.6.15}$$

and is multiplied by p and subtracted from the reference model, which becomes the reference model state update ($\dddot{x}_{rm}$) as in (3.5.2).

Figures 9-11 provide simulated performance results of the adaptive controller using the helicopter model in (3.6.2). The simulation includes the control rotor dynamics, actuator dynamics ($\tau = 0.04\ sec$), time delay ($T_D = 0.03\ sec$) and control limits (7.8° in position and $78^\circ/sec$ in rate). The command to the reference model is a sequence of positive, zero and negative steps. The parameter estimates used in (3.6.11) are $\hat{M}_\delta = 0.7M_\delta$ and $\hat{M}_q = 2M_q$. Figure 9 presents the pitch tracking performance without NN

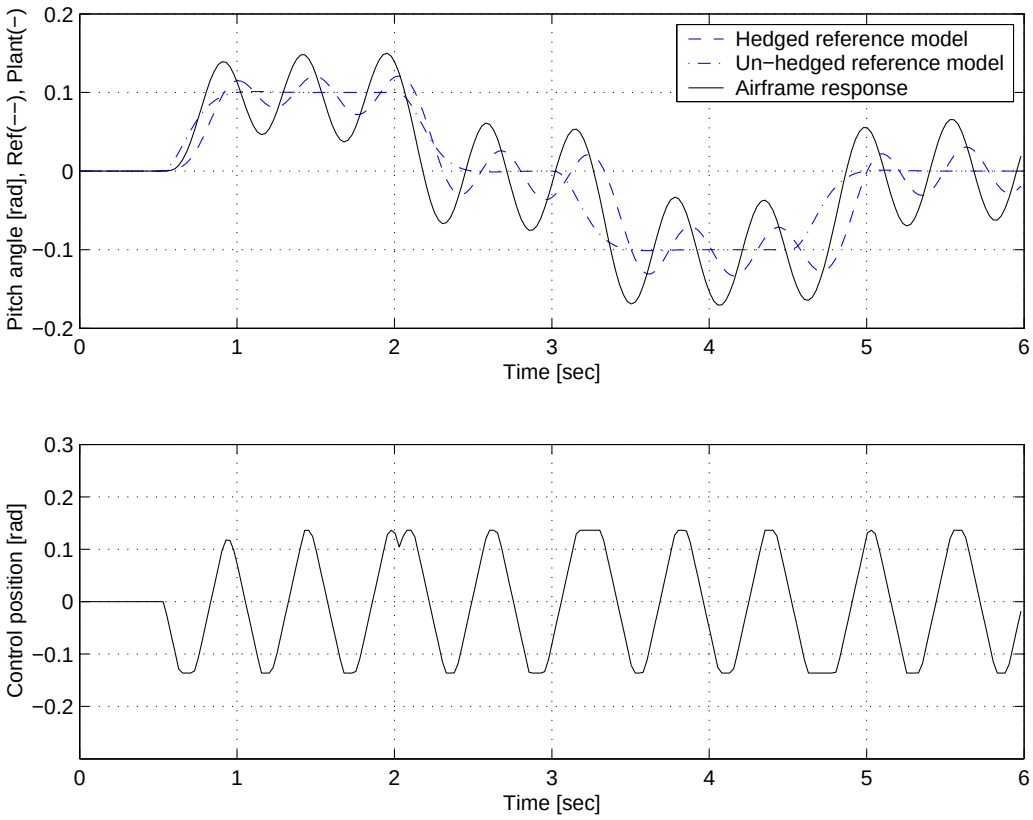

Figure 9: Pitch tracking performance without NN controller

augmentation. The upper plot gives a comparison of the un-hedged reference model output (dash-dotted line), and the hedged reference model output (dashed line), which includes the effect of pseudo-control hedging, with the pitch attitude response of the airframe (solid line). The inversion error causes an unstable attitude response and commands control input (δ_{cmd}) beyond the capacity of the actuator. The pseudo-control hedging modifies the reference model output so that the airframe response appears to follow the hedged reference model within the capacity of the actuator. Note that the actuator response is either position or rate limited throughout the entire time interval. The airframe response without hedging is similar. The main sources of the limit cycle behavior observed here are the unmodeled dynamics and the actuation limits.

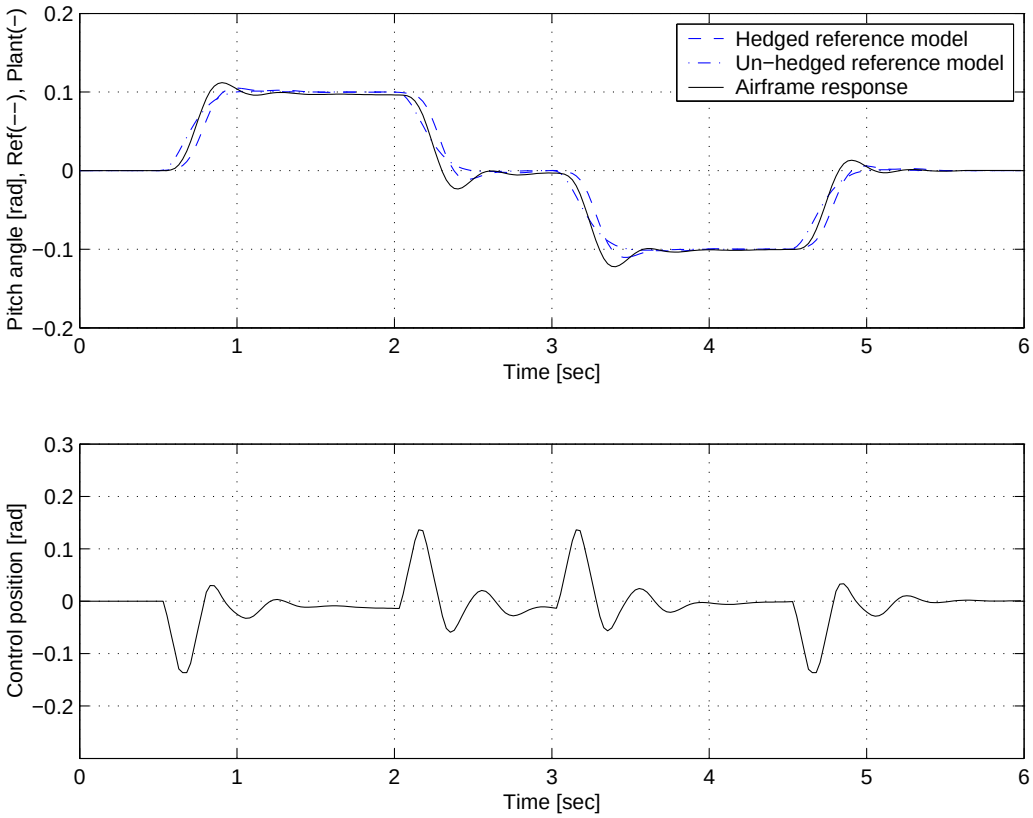

Figure 10: Pitch tracking performance with NN controller and σ-modification

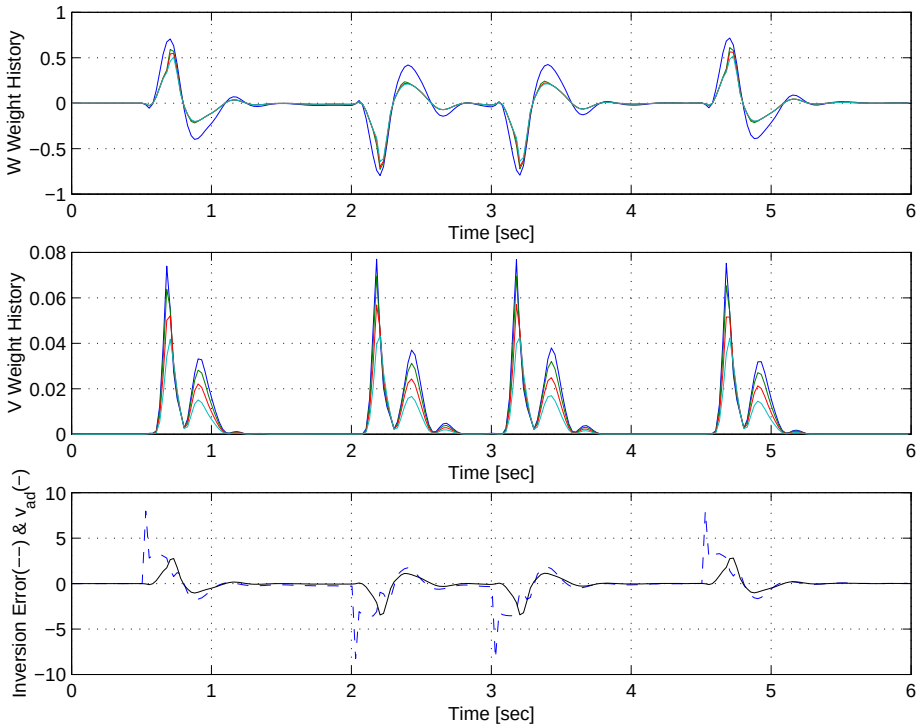

Figure 11: NN weights $(\hat{W}, \hat{V})$ history and Δ vs. v_{ad} with σ-modification

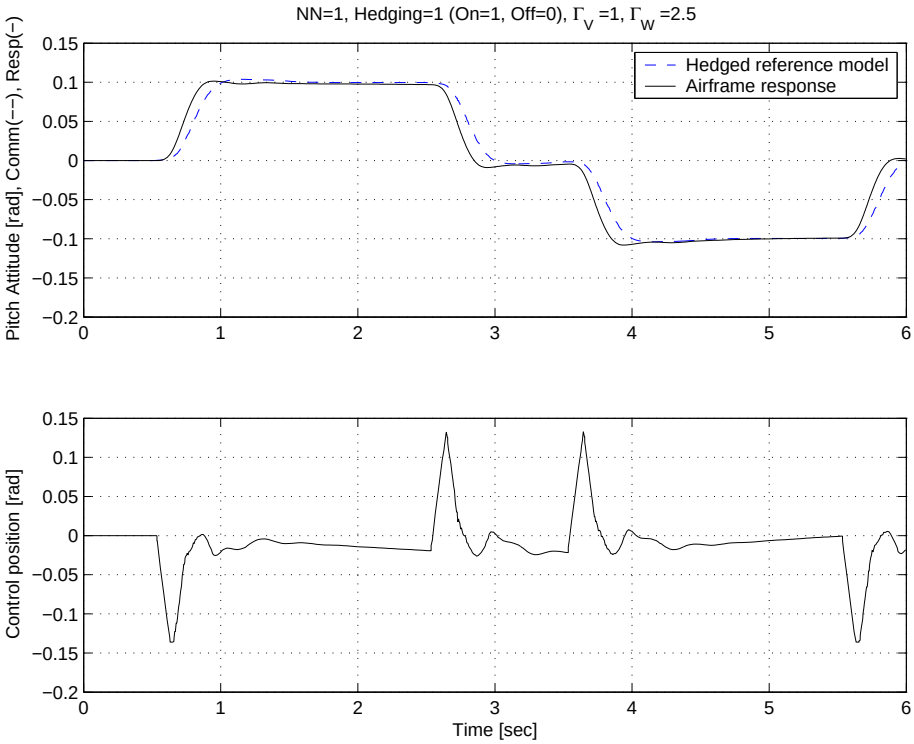

Figure 12: Pitch tracking performance with e-modification

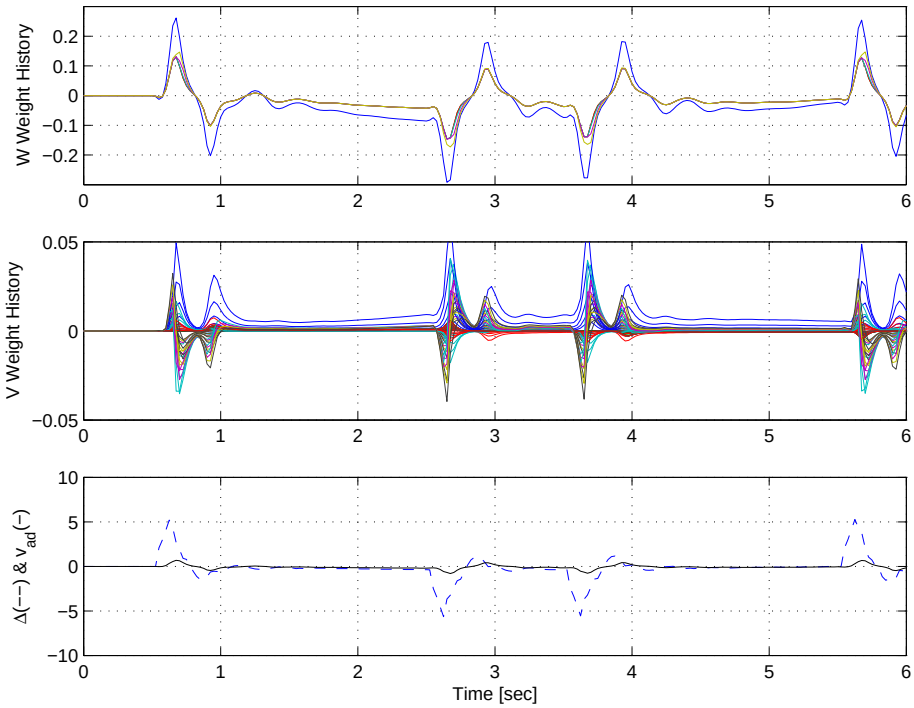

Figure 13: NN weights $(\hat{W}, \hat{V})$ history and Δ vs. v_{ad} with e-modification

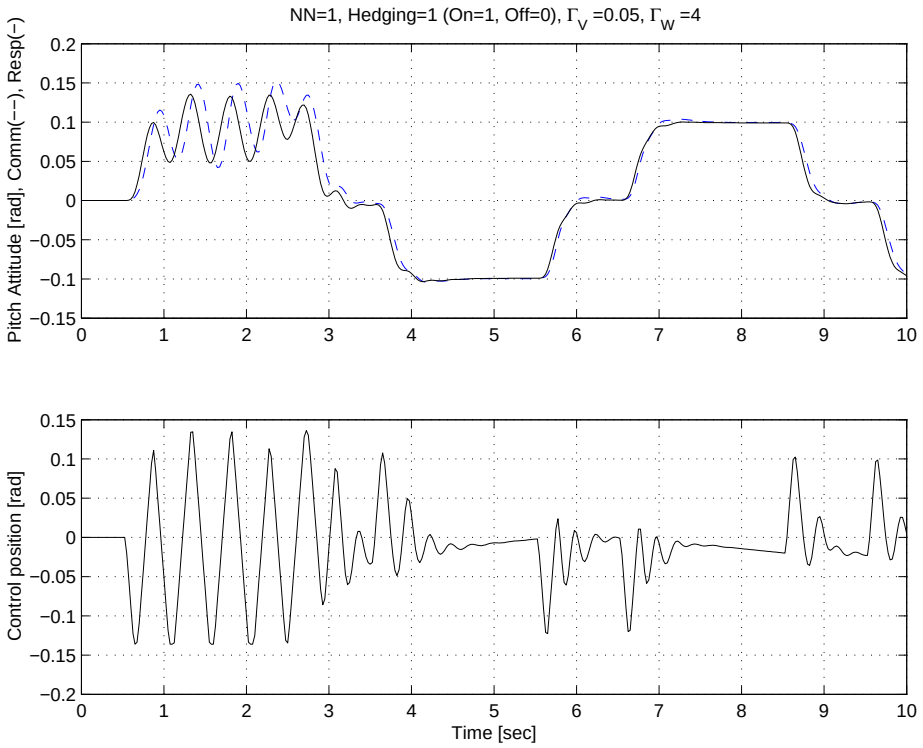

Figure 14: Pitch tracking performance with projection

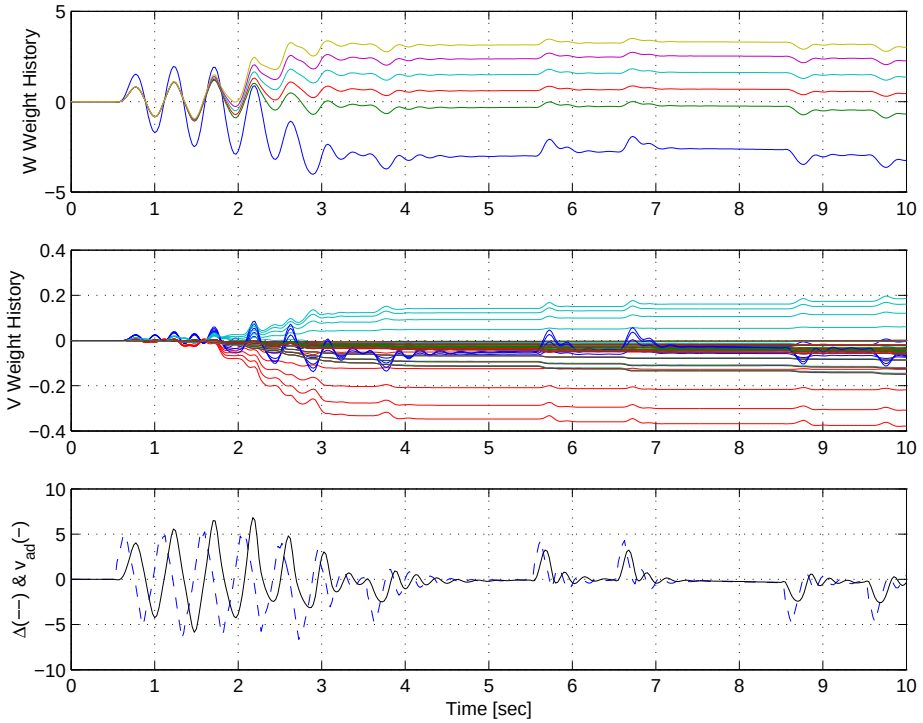

Figure 15: NN weights $(\hat{W}, \hat{V})$ history and Δ vs. v_{ad} with projection

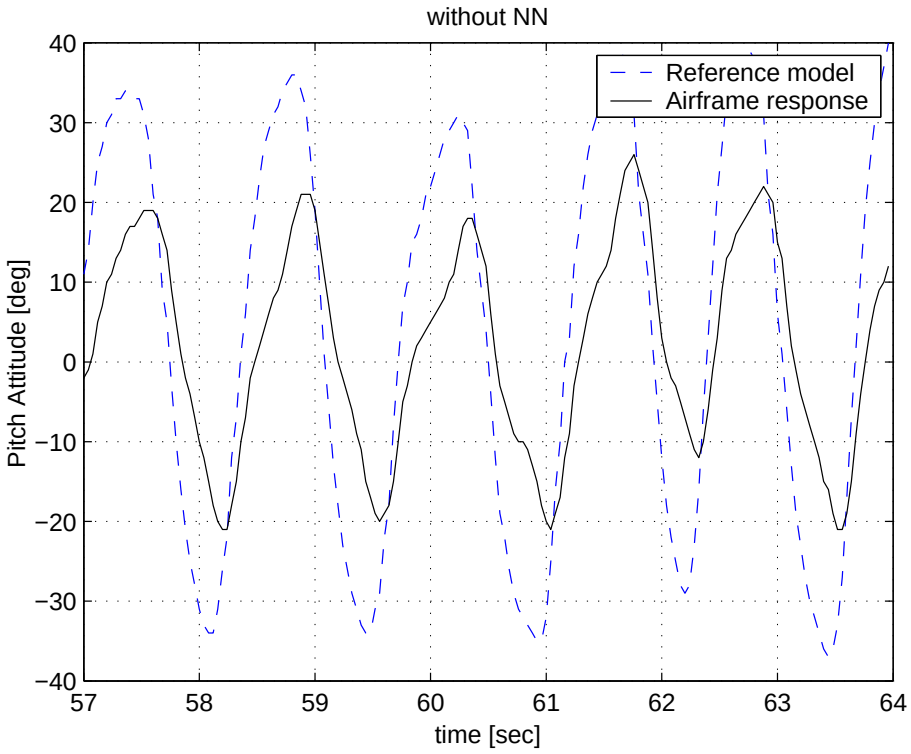

Figure 16: R-50 flight test in attitude control without NN

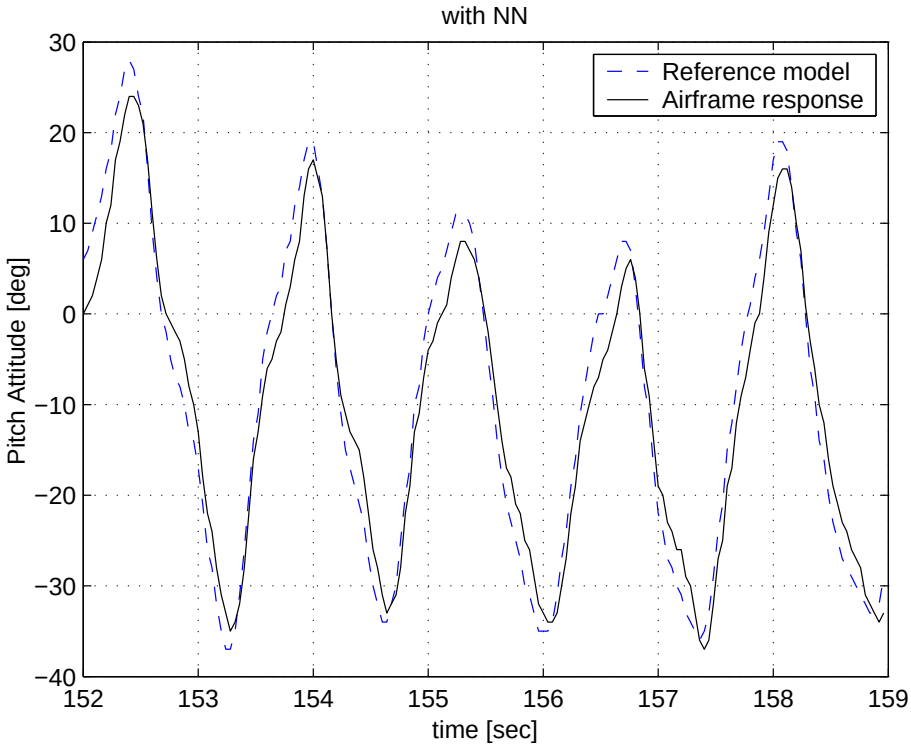

Figure 17: R-50 flight test in attitude control with NN

Figure 10 repeats the plots presented in Figure 9 with NN augmentation. Acceptable tracking of the filtered hedged command is obtained even during brief periods where the position and rate limits are encountered. The results demonstrate the ability of the high-bandwidth flight control system to operate at the physical limits of the aircraft hardware while delivering acceptable tracking performance. This is made possible by the introduction of hedging, that permits correct adaptation to continue while not in control. Note that the un-hedged reference model outputs in Figures 9 and 10 are identical and the airframe response appears to lag the un-hedged command for a period of time, but lead the hedged command. This behavior is a consequence of the feedforward term from the reference model, v_{rm} in Figure 8. Figure 11 shows the NN weights time history $\hat{W}$ (Output layer) in the top and $\hat{V}$ (Input layer) in the middle. The weights have a tendency to return to zero after each step in command due to the σ-modification term in (3.4.20). The bottom plot in Figure 11 shows the inversion error (Δ) and the output of the NN (v_{ad}). The adaptive signal v_{ad} approximates Δ except when the command is initiated. This inability of the NN to immediately adapt causes slight overshoots in the pitch attitude response in Figure 10. This demonstrates the effectiveness of PCH in allowing adaptation to continue during periods of control saturation.

Figures 12 and 13 are the simulation result with e-modification as presented in Section 3.4.2. It has the same simulation conditions as the σ-modification except the adaptation gains $\Gamma_V = I, \Gamma_W = 2.5I$, the e-modification gain $k_e = 10$, and the activation potentials $[1, 2, 4, 8, 16]$. Figure 12 shows a better tracking performance than Figure 10 when the command is initiated. Figure 13 shows that the NN weights are not driven to zero in the steady state.

Figure 14 shows the pitch tracking performance with the projection operator as presented in Section 3.4.3. The adaptation gains are $\Gamma_V = 0.05I, \Gamma_W = 4I$ and the activation potentials are $[13, 13.5, 14, 14.5, 15]$. The estimated bounds on the NN

weights are chosen to be $W_{max} = 5,\ V_{max} = 0.5$. The projection tolerances are set to be $\epsilon_W = 0.1W_{max}^2,\ \epsilon_V = 0.1V_{max}^2$. Although it takes more time to adapt to the uncertainties, it shows better tracking performance after the initial adaptation phase. Figure 15 shows the NN weights history $(\hat{W}, \hat{V})$ are well behaved without the use of σ-modification or e-modification and the output of the NN adapts and cancels approximately the inversion error.

Figures 16 and 17 present the flight test results of attitude command tracking for the pitch channel using the error observer-based design at design bandwidth of 10 rad/sec without NN and with NN, respectively. Sinusoidal type pitch attitude commands are generated directly by a remote pilot. Figure 17 shows that reasonably good tracking of the command is accomplished for the NN. The adaptive control design parameters used for the flight test are $\Gamma_W = 70$, $\Gamma_V = 30$ and $k_\sigma = 1.3$.

3.7 Application to High Bandwidth Longitudinal Flight Control

In this section we consider a 58 state model of a flexible aircraft consisting of rigid body dynamics (short period model) coupled with actuator and flexible modes.[2] The truncated short period dynamics can be expressed as

$$\begin{bmatrix} \dot{\alpha} \\ \dot{q} \end{bmatrix} = \begin{bmatrix} Z_\alpha/U_0 & 1 + Z_q/U_0 \\ M_\alpha & M_q \end{bmatrix} \begin{bmatrix} \alpha \\ q \end{bmatrix} + \begin{bmatrix} Z_\delta/U_0 \\ M_\delta \end{bmatrix} \delta + \begin{bmatrix} \Delta_\alpha \\ \Delta_1 \end{bmatrix} \tag{3.7.1}$$

where α is the angle of attack, q is the pitch rate, δ is the control perturbation input, Δ_α, Δ_1 are approximation errors (representing the functional dependence on states associated with the actuator and flexible dynamics).

[2]For information of the model, refer to James M. Buffington, Ph.D. Branch Specialist Flight Control/Vehicle Management Systems, Lockheed Martin Aeronautics Company PO Box 748 Ft. Worth TX 76101 Mail Zone 9338

3.7.1 Relative Degree = 1 Design

For the relative degree = 1 design, we assume the simplest feedback-linearized system as in (3.2.4)

$$G_d(s) = \frac{1}{s} \tag{3.7.2}$$

From the feedback-linearized system in (3.7.2) the pseudo control/output dependence can be given:

$$\begin{aligned} v + \Delta &= \dot{y} \\ &= \hat{\dot{y}} + \Delta_1 \end{aligned} \tag{3.7.3}$$

where y is the controlled output which is the pitch rate q. Utilizing the short period approximation in (3.7.1) the above equation becomes

$$v + \Delta = M_\alpha \alpha + M_q q + M_\delta \delta + \Delta_1 \tag{3.7.4}$$

From (3.7.4) we can acquire the inversion law and the inversion error as following.

$$\begin{aligned} \delta &= \frac{1}{M_\delta}(v - M_\alpha \alpha - M_q q) \\ \Delta &= \Delta_1 = \dot{y} - \hat{\dot{y}} \end{aligned} \tag{3.7.5}$$

A PI (proportional and integral) controller is designed for the feedback-linearized system to have the both closed-loop poles at $-\frac{w_c}{2}$. The PI controller gains are $K_P = w_c$ and $K_I = \frac{w_c^2}{4}$. To construct the reference model pseudo control signal v_{rm}, a 1^{st}-order reference model is introduced as:

$$y_{rm} = \frac{1}{\frac{2}{w_c}s + 1} y_{com} \tag{3.7.6}$$

where y_{rm} is the output of the reference model and y_{com} is the pre-filtered command. The error dynamics can be presented as in (3.7.7)

$$\begin{aligned}
\dot{y} &= v + \Delta \\
&= v_{dc} + v_{rm} - v_{ad} + \Delta \\
&= K_I \eta + K_P \tilde{y} + \dot{y}_{rm} - v_{ad} + \Delta \\
\begin{bmatrix} \dot{\tilde{y}} \\ \dot{\eta} \end{bmatrix} &= \begin{bmatrix} -K_P & -K_I \\ 1 & 0 \end{bmatrix} \begin{bmatrix} \tilde{y} \\ \eta \end{bmatrix} + \begin{bmatrix} 1 \\ 0 \end{bmatrix} (v_{ad} - \Delta)
\end{aligned} \tag{3.7.7}$$

where $\tilde{y} \triangleq y_{rm} - y$ and η is the state of the PI controller.

The adaptation gains have been set to $\Gamma_V = 5I$, $\Gamma_W = 0.05I$. The following sigmoidal function

$$\sigma(z_i) = \frac{1}{1 + e^{-a_i z_i}} \tag{3.7.8}$$

has been implemented in the NN design with nine hidden neurons, activation potentials chosen to be $\boldsymbol{a} = [1, 2, 3, 4, 5, 6, 7, 8, 9]$. The σ-modification coefficient k_σ in the NN update laws (3.4.20) is selected to be 10. The σ-modification initial matrices W_0 and V_0 are set to zero since no *a priori* knowledge for estimates of the weight matrices is available. Figure 18 presents the implementation block diagram.

The adaptive output feedback approach assumes that the relative degree (r) of the regulated variable is known. What is important is not the theoretical relative degree, but the relative degree over the bandwidth of the design. That is, high frequency poles and zeros can be disregarded. Another way to view this is in terms of the roll-off and phase shift in the vicinity of the gain crossover frequency in a Bode plot. In general, the relative degree may be determined from modeling equations, or it can be experimentally estimated. Taking q as the regulated output variable, and considering only the rigid body dynamics, then $r = 1$. For an $r = 1$ design, the error observer described in the last section is not needed, since $\boldsymbol{E}$ in (3.2.21) involves only the regulated output and the compensator states. In a sense, the output

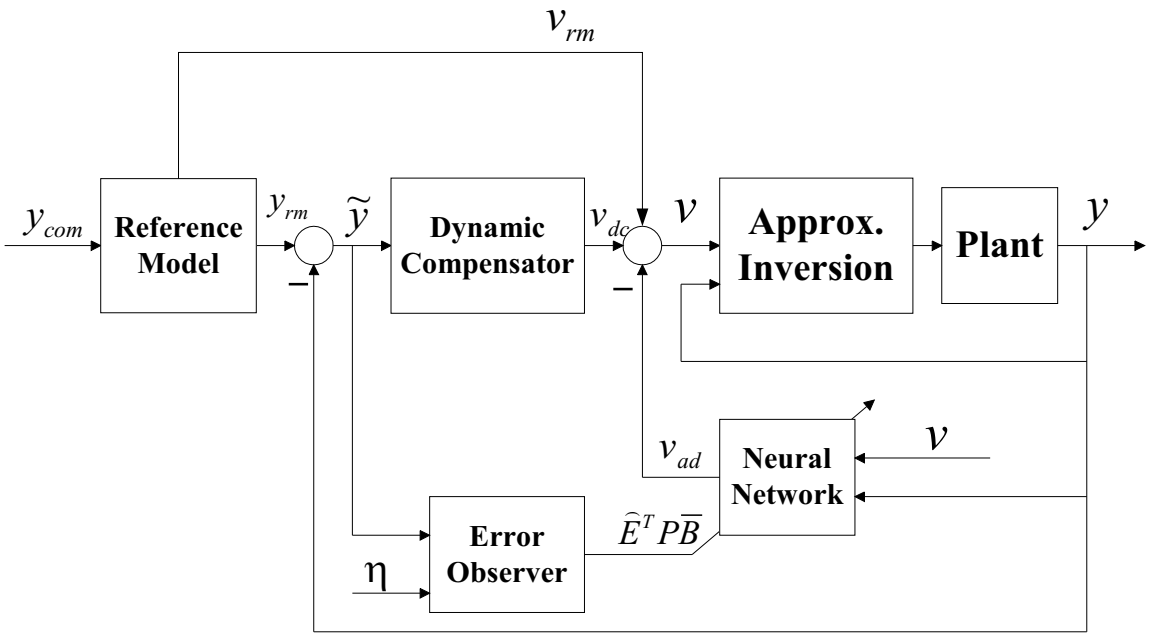

Figure 18: Generic block diagram of single channel of an adaptive rate command system

feedback approach becomes nearly equivalent to the case of state feedback, except that it retains the potential for adaptation to unmodeled dynamics, if these unmodeled dynamics do not significantly affect the assumed relative degree (and therefore become the zero dynamics). The essential difference between this approach and adaptive approaches using full state feedback lies in the use of delayed values at the input side of the adaptive element, as defined in (2.4.27).

3.7.2 Relative Degree = 2 Design

For the relative degree = 2 design, we assume the feedback-linearized system as in (3.2.4)

$$G_d(s) = \frac{p^2}{(s+p)^2} \ , \tag{3.7.9}$$

where $a_2 = 2p, a_1 = p^2$ and $b_1 = p^2$. The reason we have two shifted poles from the origin in (3.7.9) is to keep a PI controller structure. We cannot stabilize $\frac{1}{s^2}$ by using a PI controller. For the approximation of the second derivative of the output (y), a

1^{st}-order actuator model is introduced

$$\delta = \frac{1}{\tau s + 1}\delta_{cmd} \tag{3.7.10}$$

where δ is a state of the actuator dynamics, δ_{cmd} is the control input and τ is the time constant. From the feedback-linearized system in (3.7.9) the pseudo control/output dependence can be given:

$$\begin{aligned} p^2(v + \Delta) &= \ddot{y} + 2p\dot{y} + p^2 y \\ &= \hat{\ddot{y}} + 2p\hat{\dot{y}} + p^2 y + \Delta_2 + 2p\Delta_1 \end{aligned} \tag{3.7.11}$$

where y is the controlled output which is the pitch rate q. Utilizing the short period approximation in (3.7.1) and the actuator model in (3.7.10), the approximation of the second derivative of the output is given by

$$\begin{aligned} \hat{\ddot{y}} = M_\alpha(Z_\alpha\alpha + Z_q q + M_\delta\delta) + M_q(M_\alpha\alpha \\ + M_q q + M_\delta\delta) + M_\delta(-\frac{1}{\tau}\delta + \frac{1}{\tau}\delta_{cmd}) \end{aligned} \tag{3.7.12}$$

Substituting (3.7.12) into (3.7.11), we obtain the following expression for the inversion law and the inversion error:

$$\begin{aligned} \delta_{cmd} &= \frac{\tau}{M_\delta}(p^2 v - C_\alpha\alpha - C_q q) \\ \Delta &= \frac{1}{p^2}(\Delta_2 + 2p\Delta_1) \\ &= \frac{1}{p^2}(\ddot{y} - \hat{\ddot{y}} + 2p(\dot{y} - \hat{\dot{y}})) \end{aligned} \tag{3.7.13}$$

where $C_\alpha = M_\alpha(Z_\alpha + M_q + 2p)$ and $C_q = M_\alpha Z_q + M_q^2 + 2pM_q + p^2$.

The PI controller is designed for the feedback-linearized system to have the both closed-loop poles at $-w_c$. The value of p in (3.7.9) is chosen to be $2\zeta w_c$ and the PI controller gains are $K_P = w_c^2/p^2$ and $K_I = pK_P$. Note that the shifted pole (p) cancels the zero of the PI controller so that the closed-loop system remains second order. To construct the reference model pseudo control signal v_{rm}, a second order reference model is introduced as:

$$y_{rm} = \frac{w_c^2/4}{s^2 + w_c s + w_c^2/4}y_{com} \tag{3.7.14}$$

where y_{rm} is the output of the reference model, y_{com} is the pre-filtered command. The error dynamics can be represented as in (3.7.15)

$$\begin{bmatrix} \dot{\eta} \\ \dot{\tilde{y}} \\ \ddot{\tilde{y}} \end{bmatrix} = \begin{bmatrix} 0 & 1 & 0 \\ 0 & 0 & 1 \\ -p^2 K_I & -p^2(1+K_P) & -2p \end{bmatrix} \begin{bmatrix} \eta \\ \tilde{y} \\ \dot{\tilde{y}} \end{bmatrix} + \begin{bmatrix} 0 \\ 0 \\ 1 \end{bmatrix} p^2(v_{ad} - \Delta) \tag{3.7.15}$$

where $\tilde{y} \triangleq y_{rm} - y$ and η is the state of the PI controller. The error observer poles have been placed to be 4 times faster than those of the error dynamics (3.7.15). The adaptation gains have been set to $\Gamma_V = 20I,\ \Gamma_W = 10I$. The sigmoidal function in (3.7.8) is used with activation potentials $100 \times [1, 2, 3, 4, 5, 6, 7, 8, 9]$. The σ-modification coefficient k_σ in the NN update laws (3.4.20) is selected to be 4. The σ-modification initial matrices W_0 and V_0 are set to zero.

3.7.3 Numerical Results

Figure 19 depicts and quantifies to some degree the effect of the flexible modes in this model. Two responses are shown. The solid line shows the response in pitch rate to a step command for a baseline controller without a structural model filter. The baseline design is a α, q feedback inverting design with PI compensation. The effect of unmodeled dynamics is apparent from the response. To verify that this is due to a structural mode interaction (rather than an interaction with the actuator mode), the following two structural compensation filters were placed in series in the pitch rate feedback path:

$$\frac{s^2 + 1.58s + 1181.2}{s^2 + 6.87s + 1181.2}, \frac{s^2 + 4.87s + 2667.2}{s^2 + 20.66s + 2667.2} \tag{3.7.16}$$

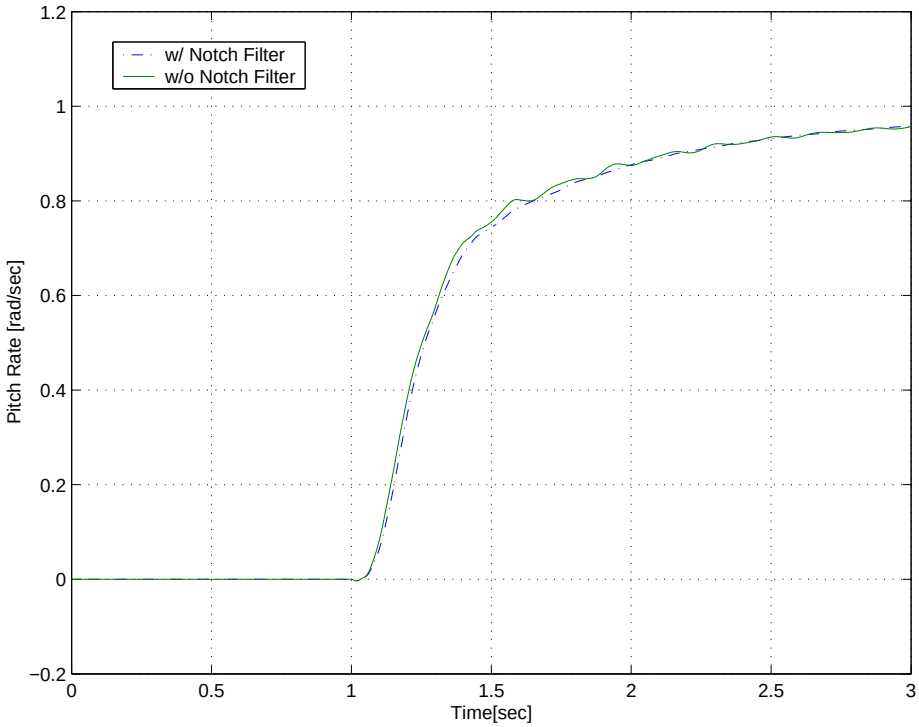

Figure 19: Baseline design performance.

The dashed line in Figure 19 demonstrates that the structural mode interaction is indeed eliminated with the introduction of these filters.

Figure 20 shows the result of the $r = 1$ adaptive design using $w_c = 7$ rad/sec in the reference model. Note that it exhibits even greater interaction with the flexible modes, than does the baseline design of Figure 19. However, this design reaches the command level much faster.

To examine why this design fails to suppress the effect of the flexible modes, we considered the rigid body model and the full plant model by comparing their respective Bode plots. The magnitude plot in Figure 21 shows that the rigid body model is a good approximation over much of the frequency range of interest, but the phase plot shows significant differences in the vicinity of the design bandwidth, as set by the command model frequency. It appears that an additional phase shift of 90 degrees is introduced up to about 20 rad/sec, which lies beyond the bandwidth of our design. A slight change in the slope is also evident in the magnitude plot at

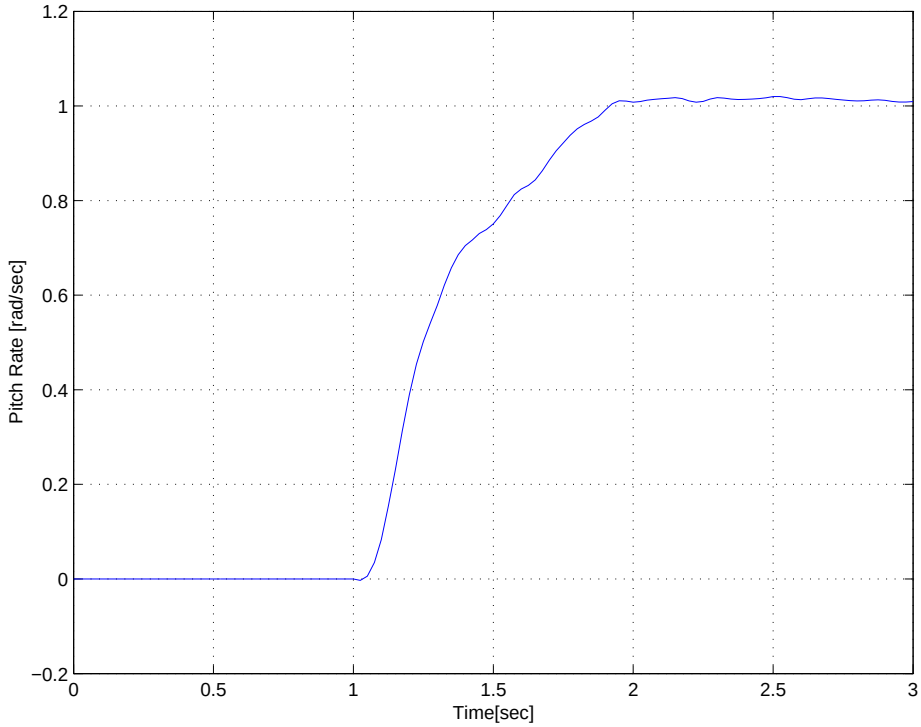

Figure 20: Relative degree = 1 design ($w_c = 7$ rad/sec).

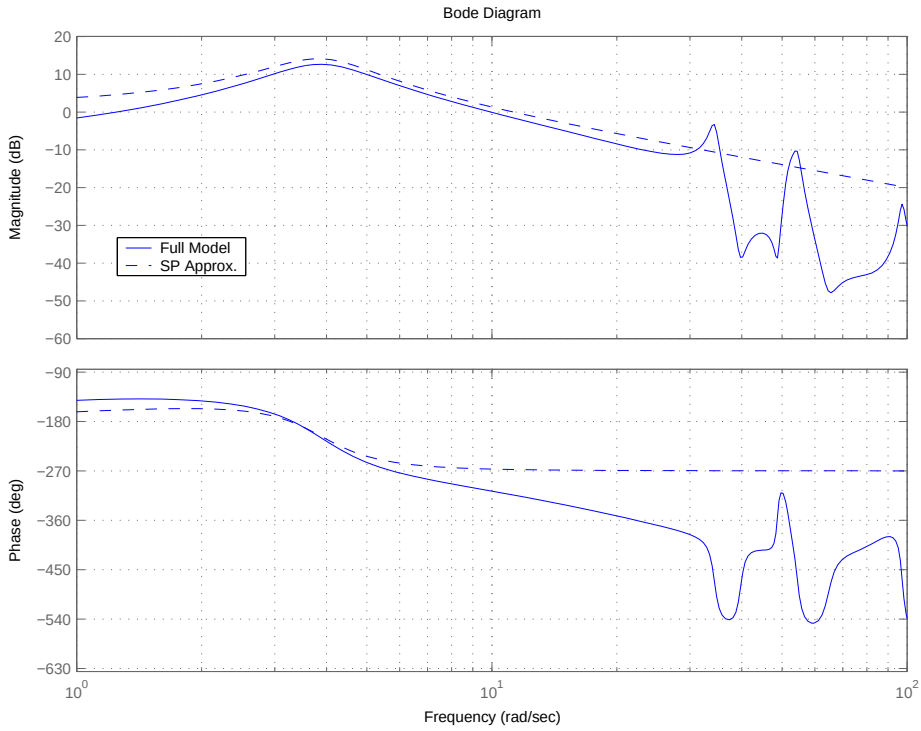

Figure 21: Bode plots of the full model and the short period model.

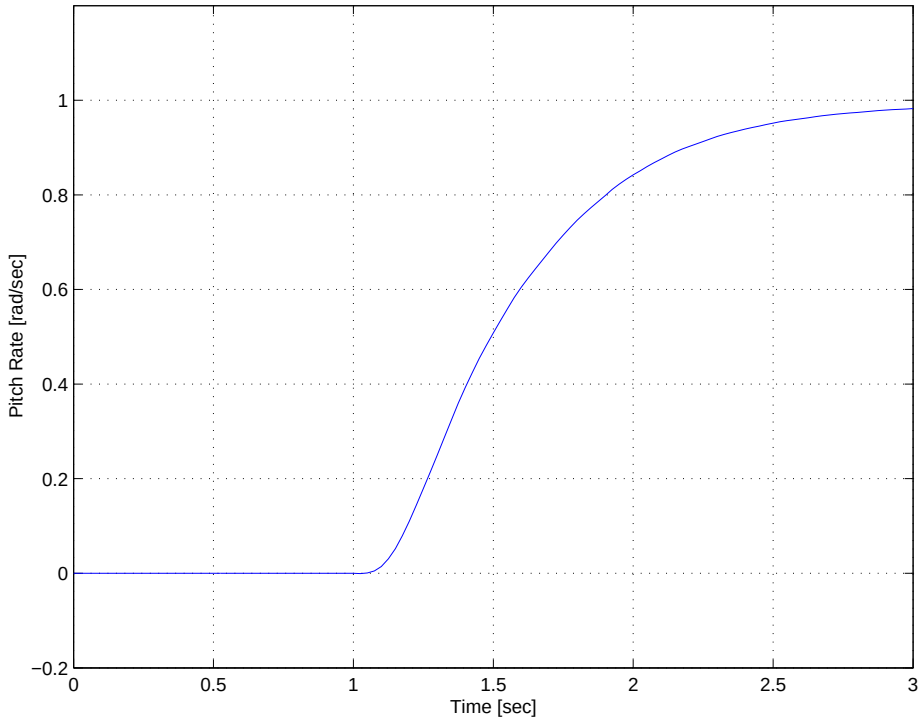

Figure 22: Relative degree = 2 design ($w_c = 7$ rad/sec).

around 10 rad/sec. However, it is evident that the phase plot is a clearer indicator of relative degree than is the magnitude plot. Therefore, we tried an $r = 2$ design, which required the introduction of the error observer in (3.3.1). Figure 22 shows that the $r = 2$ design does eliminate the structural mode interaction, without requiring notch filtering, which was the main objective in this phase of the effort.

3.8 Nonlinearly-Parameterized NN with SPR Approach

As presented in the previous sections, Lyapunov stability analysis results in a NN update law in terms of the error vector. When $r \geq 2$ and the derivatives of the output signal are not available for feedback, we used an error observer in realizing the estimate of the error vector for the use of the update law. Alternatively, we can use a direct adaptive approach that employs a strictly positive real (SPR) filter [38]. It utilizes a low-pass filter so that the error dynamics satisfy an SPR condition, and a scalar

error signal can be directly used in the Lyapunov stability analysis in place of the error vector. In [38] a linearly-parameterized NN controller with SPR approach was introduced by redefining the teaching signal so that the training signal is related to the NN approximation error through an SPR transfer function. In this section, we develop an adaptive law for nonlinearly-parameterized NNs using the SPR approach. This is done by augmenting an auxiliary error signal with the tracking error signal so that the augmented error is associated with the NN approximation error through an SPR transfer function. The idea of augmenting an auxiliary error when $r \geq 2$ was proposed by Sastry et.al. [60]. The performance of the adaptive scheme is demonstrated by a numerical example of a modified Van der Pol oscillator and compared with the approach found in [38]. Moreover, in contrast to the σ-modification term used in [38], we show that it is possible to incorporate an e-modification term in the adaptive law.

3.8.1 Controller Design

Consider the following error dynamics taken from (3.2.27)

$$\begin{aligned} \dot{\boldsymbol{E}} &= A\boldsymbol{E} + \boldsymbol{b}h_{\bar{v}}(\hat{W}^T\hat{\boldsymbol{\sigma}} - W^T\boldsymbol{\sigma} - \epsilon) \\ e &= C\boldsymbol{E} \end{aligned} \tag{3.8.1}$$

where A is Hurwitz and $r \geq 2$. It can be expressed in frequency domain.

$$e = G(s)h_{\bar{v}}(\hat{W}^T\hat{\boldsymbol{\sigma}} - W^T\boldsymbol{\sigma} - \epsilon) \tag{3.8.2}$$

Currently, the boundedness analysis with SPR approach is limited to the following assumption.

Assumption 3.8.1. $h_{\bar{v}}$ is a known constant.

Introduce an auxiliary error signal e_a and a low-pass filter $T(s)$ such that $\bar{G}(s) \triangleq$

$G(s)T^{-1}(s)$ is SPR:

$$\begin{aligned} e_a &\triangleq \bar{G}(s)h_{\bar{v}}\left(\hat{W}^T T(s)\hat{\boldsymbol{\sigma}} - T(s)(\hat{W}^T\hat{\boldsymbol{\sigma}})\right) \\ &= \bar{G}(s)h_{\bar{v}}\left(\hat{W}^T\hat{\boldsymbol{\sigma}}_f - W^T\boldsymbol{\sigma}_f + W^T\boldsymbol{\sigma}_f\right) - G(s)h_{\bar{v}}(\hat{W}^T\hat{\boldsymbol{\sigma}}) \\ &= \bar{G}(s)h_{\bar{v}}\left(\hat{W}^T\hat{\boldsymbol{\sigma}}_f - W^T\boldsymbol{\sigma}_f\right) + G(s)h_{\bar{v}}(W^T\boldsymbol{\sigma} - \hat{W}^T\hat{\boldsymbol{\sigma}}) \end{aligned} \tag{3.8.3}$$

where $\boldsymbol{\sigma}_f = T(s)\boldsymbol{\sigma}$, $\hat{\boldsymbol{\sigma}}_f = T(s)\hat{\boldsymbol{\sigma}}$ and $T(s)$ is called an SPR filter. Note that e_a can be computed since the estimated weight $\hat{W}$ and the activation function $\hat{\boldsymbol{\sigma}}$ are both available online and that e_a goes to zero if $\hat{W}$ is replaced by the optimal weight W. In the controller canonical form it is given by:

$$\begin{aligned} \dot{\boldsymbol{E}}_a &= A\boldsymbol{E}_a + \boldsymbol{b}h_{\bar{v}}\left(\hat{W}^T T(s)\hat{\boldsymbol{\sigma}} - T(s)(\hat{W}^T\hat{\boldsymbol{\sigma}})\right) \\ e_a &= \bar{C}\boldsymbol{E}_a \end{aligned} \tag{3.8.4}$$

Since $\bar{G}(s)$ is SPR, the following equations hold:

$$\begin{aligned} A^T P + PA &= -Q < 0 \\ P\boldsymbol{b} &= \bar{C}^T \end{aligned} \tag{3.8.5}$$

Remark 3.8.1. Assumption 3.8.1 implies that $\frac{\partial h_r}{\partial u}$ is known. Knowledge of $\frac{\partial h_r}{\partial u}$ is needed to generate e_a. It can still be applied to a non-affine system as long as Assumption 3.8.1 holds.

Define the augmented error signal as:

$$\begin{aligned} \bar{e} &\triangleq e + e_a \\ &= \bar{G}(s)h_{\bar{v}}\left(\hat{W}^T\hat{\boldsymbol{\sigma}}_f - W^T\boldsymbol{\sigma}_f - \epsilon_f\right) \end{aligned} \tag{3.8.6}$$

where $\epsilon_f = T(s)\epsilon$ and is bounded by $\|\epsilon_f\| \leq \epsilon_f^*$. For the stability proof we will need

the following representation:

$$\begin{aligned}
&\hat{W}^T\hat{\boldsymbol{\sigma}}_f - W^T\boldsymbol{\sigma}_f - \epsilon_f \\
&\quad = \hat{W}^T\hat{\boldsymbol{\sigma}}_f - W^T\boldsymbol{\sigma}_f - W^T\hat{\boldsymbol{\sigma}}_f + W^T\hat{\boldsymbol{\sigma}}_f - \hat{W}^T\boldsymbol{\sigma} + \hat{W}^T\boldsymbol{\sigma} - \epsilon_f \\
&\quad = \tilde{W}^T\hat{\boldsymbol{\sigma}}_f - W^T\tilde{\boldsymbol{\sigma}}_f - \hat{W}^T(\hat{\boldsymbol{\sigma}} - \hat{\sigma}'\tilde{V}^T\boldsymbol{\mu} + \mathcal{O}(\|\tilde{V}\|^2) + \hat{W}^T\boldsymbol{\sigma} - \epsilon_f \\
&\quad = \tilde{W}^T\hat{\boldsymbol{\sigma}}_f - W^T\hat{\sigma}'V^T\boldsymbol{\mu} + \left(W^T\hat{\sigma}'\hat{V}^T\boldsymbol{\mu} - \hat{W}^T\hat{\sigma}'\hat{V}^T\boldsymbol{\mu}\right) \\
&\quad + \left(\hat{W}^T\hat{\sigma}'\hat{V}^T\boldsymbol{\mu} - \hat{W}^T\hat{\sigma}'V^T\boldsymbol{\mu}\right) + \hat{W}^T\hat{\sigma}'V^T\boldsymbol{\mu} - W^T\mathcal{O}(\|\tilde{V}\|^2) - \epsilon_f \\
&\quad = \tilde{W}^T\left(\hat{\boldsymbol{\sigma}}_f - \hat{\sigma}'\hat{V}^T\boldsymbol{\mu}\right) + \hat{W}^T\hat{\sigma}'\tilde{V}^T\boldsymbol{\mu} + \tilde{W}^T\hat{\sigma}'V^T\boldsymbol{\mu} - W^T\mathcal{O}(\|\tilde{V}\|^2) - \epsilon_f \\
&\quad = \tilde{W}^T\left(\hat{\boldsymbol{\sigma}}_f - \hat{\sigma}'\hat{V}^T\boldsymbol{\mu}\right) + \hat{W}^T\hat{\sigma}'\tilde{V}^T\boldsymbol{\mu} + \bar{w}
\end{aligned} \tag{3.8.7}$$

where $\boldsymbol{\sigma} = \boldsymbol{\sigma}(V^T\boldsymbol{\mu})$, $\hat{\boldsymbol{\sigma}} = \boldsymbol{\sigma}(\hat{V}^T\boldsymbol{\mu})$, $\hat{\sigma}' = \frac{d\boldsymbol{\sigma}}{d\boldsymbol{z}}|_{\boldsymbol{z}=\hat{V}^T\boldsymbol{\mu}}$, $\mathcal{O}(\|\tilde{V}\|^2) = \boldsymbol{\sigma} - \hat{\boldsymbol{\sigma}} + \hat{\sigma}'\tilde{V}^T\boldsymbol{\mu}$ and the disturbance term $\bar{w} = W^T\hat{\boldsymbol{\sigma}}_f - W^T\boldsymbol{\sigma}_f + \hat{W}^T\hat{\sigma}'V^T\boldsymbol{\mu} - W^T\hat{\sigma}'\hat{V}^T\boldsymbol{\mu} - \epsilon_f$ is upper bounded as:

$$\begin{aligned}
\|\bar{w}\| &\leq 2\sqrt{n_2+1}W^* + \delta\sqrt{n_2+1}W^* + \|\hat{W}\|\frac{a^*}{4}V^*\mu^* + \epsilon_f^* \\
&\leq c_1\|\tilde{Z}\|_F + c_2
\end{aligned} \tag{3.8.8}$$

where $c_1 = \frac{a^*}{4}Z^*\mu^*$, $c_2 = ((2+\delta)\sqrt{n_2+1} + c_1)W^* + \epsilon_f^*$. Using (3.8.7), the error dynamics (3.8.6) can be expressed as:

$$\bar{e} = \bar{G}(s)h_{\bar{v}}\left(\tilde{W}^T(\hat{\boldsymbol{\sigma}}_f - \hat{\sigma}'\hat{V}^T\boldsymbol{\mu}) + \hat{W}^T\hat{\sigma}'\tilde{V}^T\boldsymbol{\mu} + \bar{w}\right) \tag{3.8.9}$$

and in the controller canonical form.

$$\begin{aligned}
\dot{\bar{\boldsymbol{E}}} &= A\bar{\boldsymbol{E}} + \boldsymbol{b}h_{\bar{v}}\left(\tilde{W}^T(\hat{\boldsymbol{\sigma}}_f - \hat{\sigma}'\hat{V}^T\boldsymbol{\mu}) + \hat{W}^T\hat{\sigma}'\tilde{V}^T\boldsymbol{\mu} + \bar{w}\right) \\
\bar{e} &= \bar{C}\bar{\boldsymbol{E}}
\end{aligned} \tag{3.8.10}$$

The filter $T(s)$ can be realized in a state space form

$$\begin{aligned}
\dot{\boldsymbol{z}}_f &= A_f\boldsymbol{z}_f + B_f\hat{\boldsymbol{\sigma}} \\
\hat{\boldsymbol{\sigma}}_f &= C_f\boldsymbol{z}_f
\end{aligned} \tag{3.8.11}$$

The signal $\hat{\boldsymbol{\sigma}}_f$ is used in the NN adaptation law

$$\begin{aligned}
\dot{\hat{W}} &= -\Gamma_W\left[\mathrm{sgn}(h_{\bar{v}})(\hat{\boldsymbol{\sigma}}_f - \hat{\sigma}'\hat{V}^T\boldsymbol{\mu})\bar{e} + k_e|\bar{e}|\hat{W}\right] \\
\dot{\hat{V}} &= -\Gamma_V\left[\mathrm{sgn}(h_{\bar{v}})\boldsymbol{\mu}\bar{e}\hat{W}^T\hat{\sigma}' + k_e|\bar{e}|\hat{V}\right]
\end{aligned} \tag{3.8.12}$$

where $\Gamma_V, \Gamma_W > 0$ are the learning rate and $k_e > 0$ is the e-modification gain.

Assumption 3.8.2. Assume

$$R > C\sqrt{\frac{\lambda_{max}(T)}{\lambda_{min}(T)}} \geq C \tag{3.8.13}$$

where $\lambda_{max}(T)$ and $\lambda_{min}(T)$ are the maximum and minimum eigenvalues of the following matrix:

$$T \triangleq \begin{bmatrix} P & 0 & 0 \\ 0 & \Gamma_W^{-1} & 0 \\ 0 & 0 & \Gamma_V^{-1} \end{bmatrix} \tag{3.8.14}$$

which will be used in a Lyapunov function candidate as $L = \boldsymbol{\zeta}^T T \boldsymbol{\zeta}$ with a redefined error vector $\boldsymbol{\zeta} = \begin{bmatrix} \bar{\boldsymbol{E}}^T & \tilde{W}^T & (vec\tilde{V})^T \end{bmatrix}^T$, and

$$C \triangleq \max\Big(\frac{\|\bar{C}\|(c_1^2 + 2c_2 + k_e Z^{*2})}{\lambda_{min}(Q)}, \quad \sqrt{\frac{(c_1^2 + 2c_2 + k_e Z^{*2})}{k_e - 1}}\Big) \tag{3.8.15}$$

is the radius of a ball B_C containing Γ.

Define the Lyapunov function level sets Ω_α and Ω_β

$$\begin{aligned} \Omega_\alpha &= \{\boldsymbol{\zeta} \in B_R \mid L \leq \alpha \triangleq \min_{\|\boldsymbol{\zeta}\|=R} L\} \\ \Omega_\beta &= \{\boldsymbol{\zeta} \in B_R \mid L \leq \beta \triangleq \max_{\|\boldsymbol{\zeta}\|=C} L\} \end{aligned} \tag{3.8.16}$$

Theorem 3.8.1. Let Assumptions 3.1.1, 3.1.2, 3.1.3, 3.1.4, 3.2.1, 3.5.1, 3.8.1 and 3.8.2 hold. If the initial errors belong to the compact set Ω_α defined in (3.8.16), then the feedback control law given by (3.2.1) and the weight update law (3.8.12) ensure that the signals $\bar{\boldsymbol{E}}, \tilde{W}$ and $\tilde{V}$ in the closed-loop system are ultimately bounded with the ultimate bound $C\sqrt{\frac{\lambda_{max}(T)}{\lambda_{min}(T)}}$.

Proof. See Appendix A.5. □

3.8.2 Numerical Example

The efficacy of the adaptive output feedback controller developed in Section 3.8 is demonstrated using a modified Van der Pol oscillator model treated in [38].

$$\begin{aligned}
\dot{x}_1 &= x_2 \\
\dot{x}_2 &= -2(x_1^2 - 1)x_2 - x_1 + u \\
\dot{x}_3 &= x_4 \\
\dot{x}_4 &= -x_3 - 0.2x_4 + x_1 \\
y &= x_1 + x_3
\end{aligned} \tag{3.8.17}$$

The output has relative degree $r = 2$. We assume that we have an approximate model as:

$$\hat{\ddot{y}} = u \tag{3.8.18}$$

The linear controller is designed such that the closed-loop poles of the approximate model in (3.8.18) are placed at $-3, -2 \pm 2i$.

$$v_{dc} = \frac{20(s + 1.2)}{s + 7}\tilde{y} \tag{3.8.19}$$

Then the error dynamics becomes,

$$\begin{aligned}
\tilde{y} &= G(s)(v_{ad} - \Delta), \\
G(s) &= \frac{s + 7}{s^3 + 7s^2 + 20s + 24}
\end{aligned} \tag{3.8.20}$$

where $\Delta = -2(x_1^2 - 1)x_2 - x_3 - 0.2x_4$. We select an SPR filter $T(s)$ so that $G(s)T^{-1}(s)$ is SPR.

$$T(s) = \frac{s + 7}{(s + 1)(s + 2)} \tag{3.8.21}$$

Five hidden layer neurons are used and their activation potentials are $\begin{bmatrix} 1 & 0.9 & 0.8 & 0.7 & 0.6 \end{bmatrix}$. The learning rates for adaptation laws in (3.8.12) are $\Gamma_W = 30, \Gamma_V = 40$ and the e-modification coefficient is $k_e = 0.001$. A second order reference model is selected with a natural frequency of 1 rad/sec and damping ratio of 0.707. The initial condition for the plant is $x_1(0) = 0.5, x_2(0) = 2.5, x_3(0) = 0, x_4(0) = 0$.

The system response without NN augmentation in Figure 23 exhibits a limit-cycle-like oscillation due to unmodeled dynamics. With NN augmentation as developed in Section 3.8, the oscillation is removed after about a 3 second adaptation period as shown in Figure 24. The performance obtained using a linearly-parameterized NN is shown in Figure 25. Figure 24 takes more time to adapt but has better steady state tracking performance than seen in Figure 25. Nonlinearly-parameterized NN weight histories in Figures 27 and 28 show that NN weights approach nearly constant values that are non-zero, in contrast to the linearly-parameterized NN weight histories that tend to return to zero as shown in Figure 26. The control efforts are shown in Figures 29 and 30. Figures 31 and 32 show the degree to which the NN output approximates Δ.

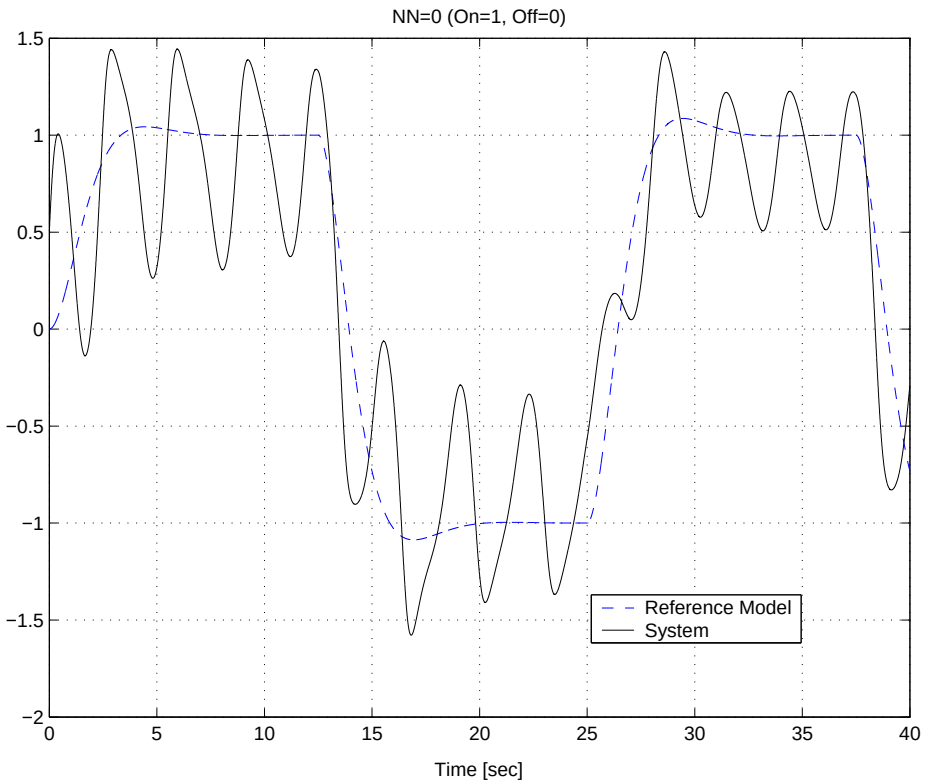

Figure 23: System response with a linear compensator

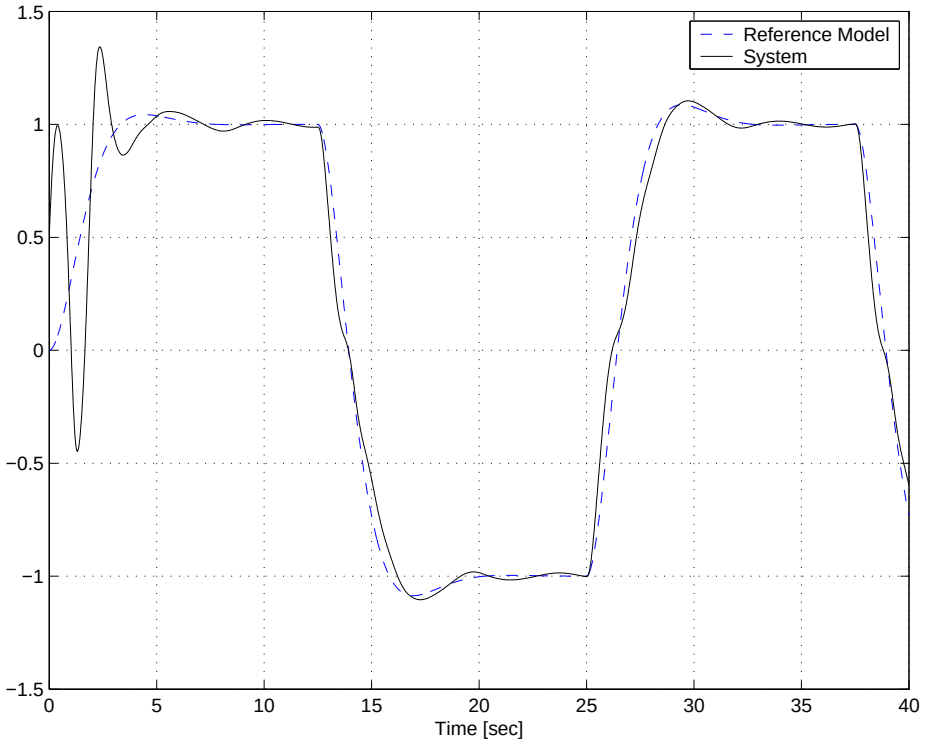

Figure 24: System response with nonlinearly-parameterized NN

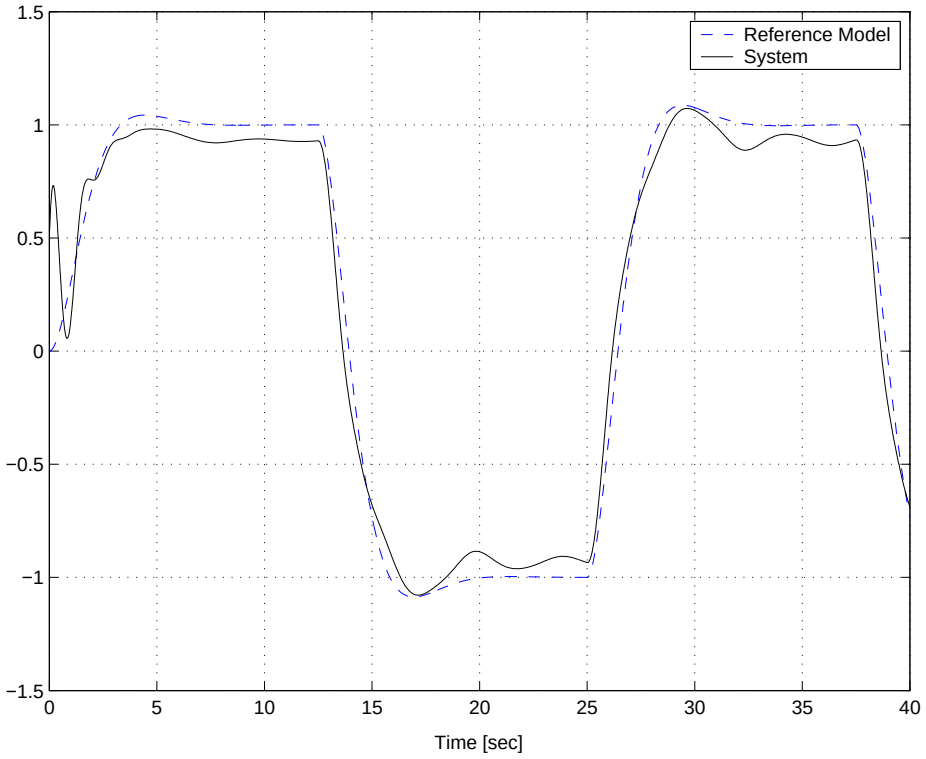

Figure 25: System response with linearly-parameterized NN

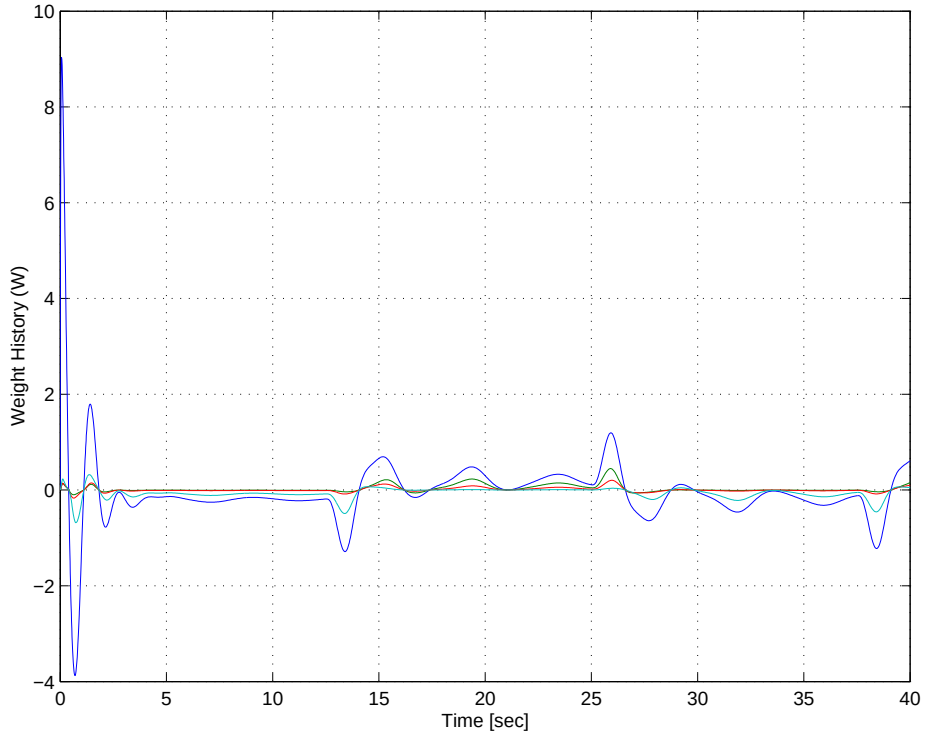

Figure 26: Weight history with linearly-parameterized NN

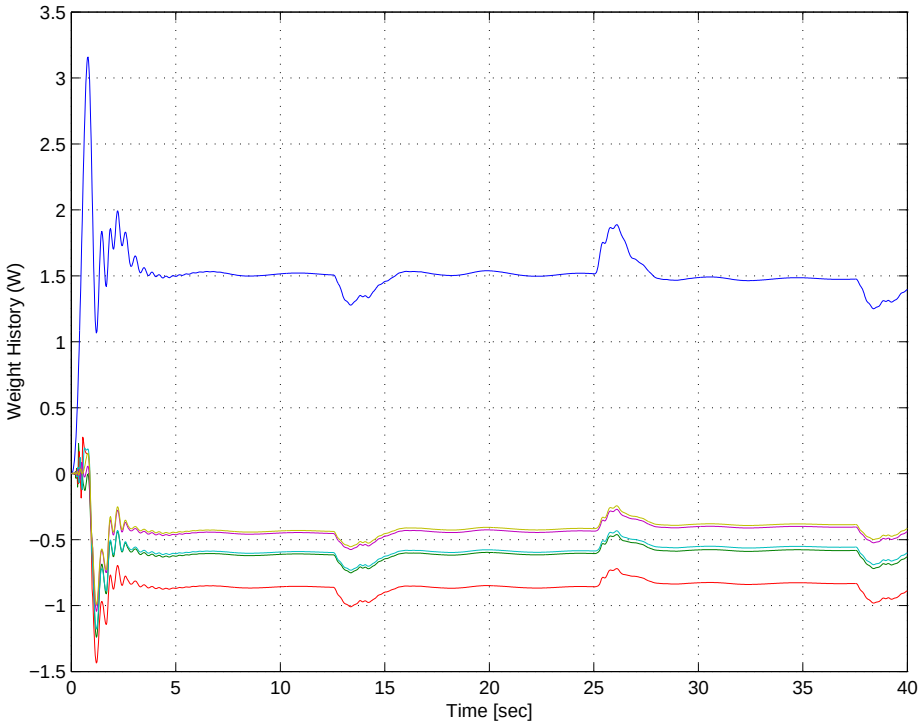

Figure 27: Weight (W) history with nonlinearly-parameterized NN

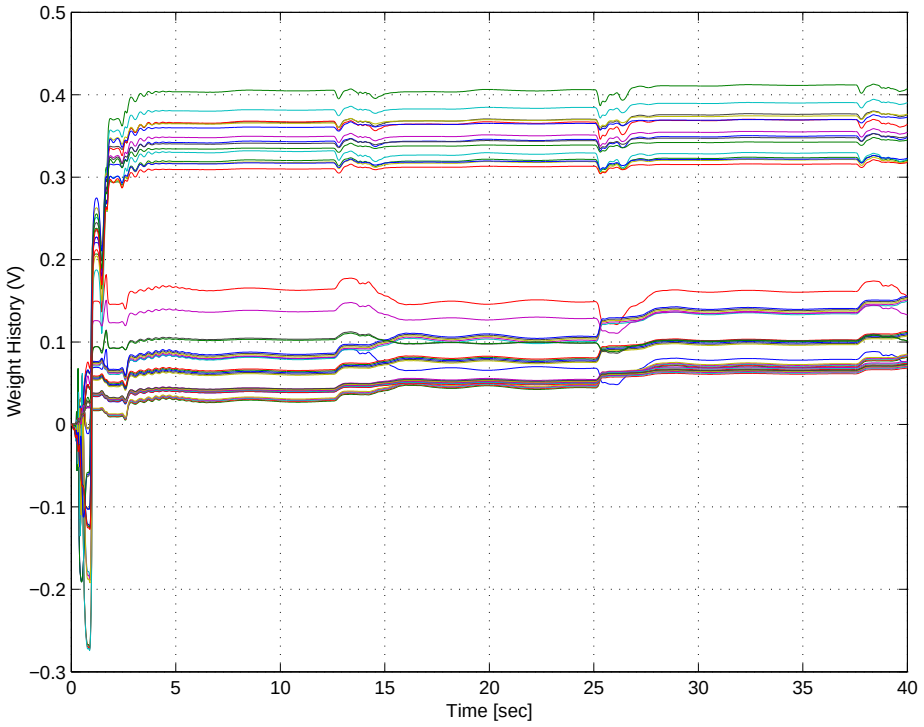

Figure 28: Weight (V) history with nonlinearly-parameterized NN

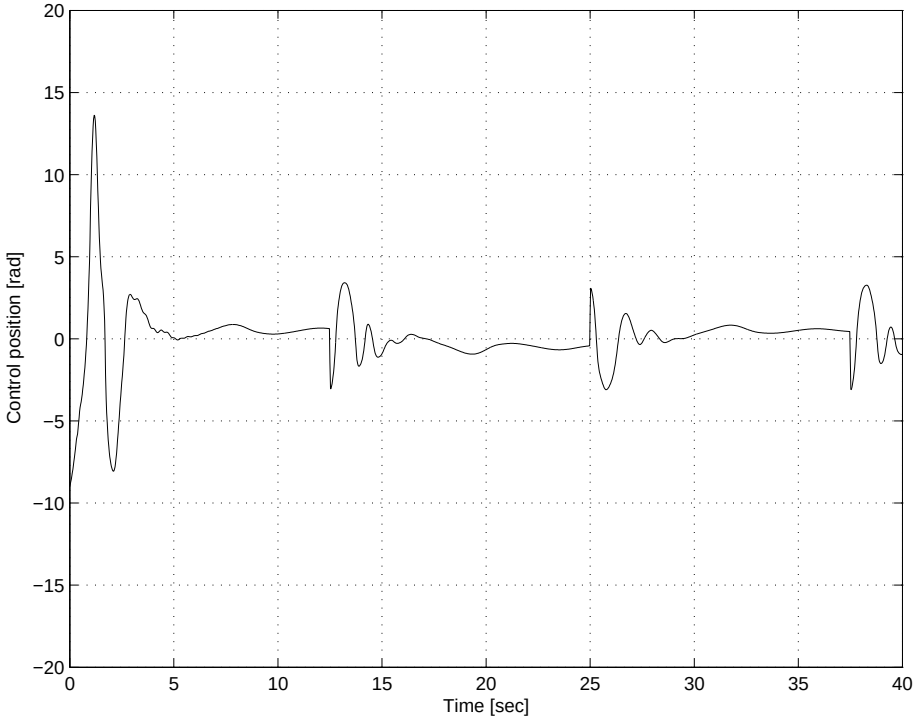

Figure 29: Control position with nonlinearly-parameterized NN

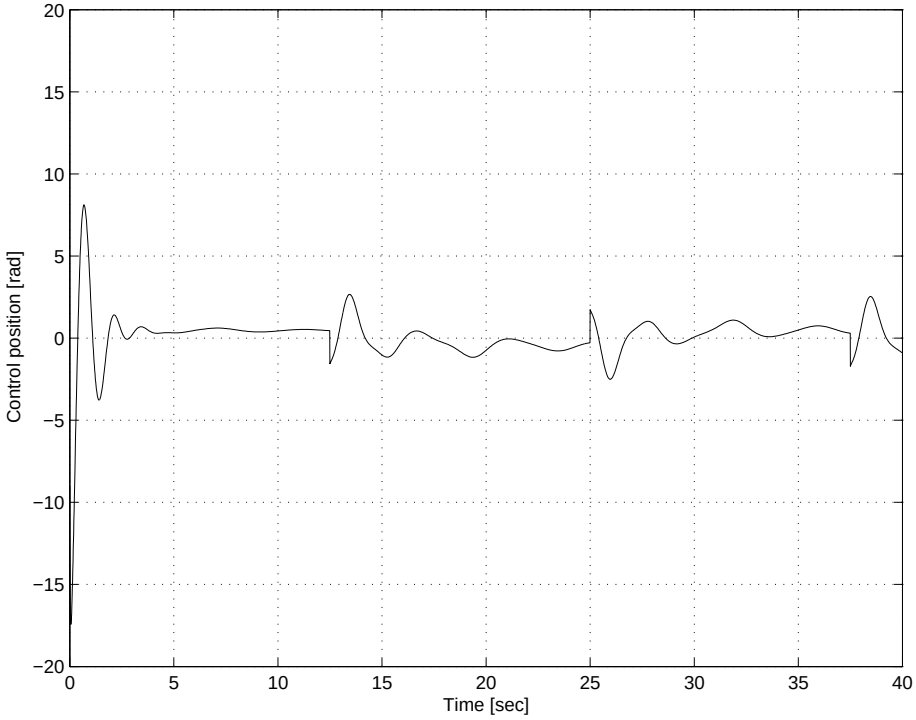

Figure 30: Control position with linearly-parameterized NN

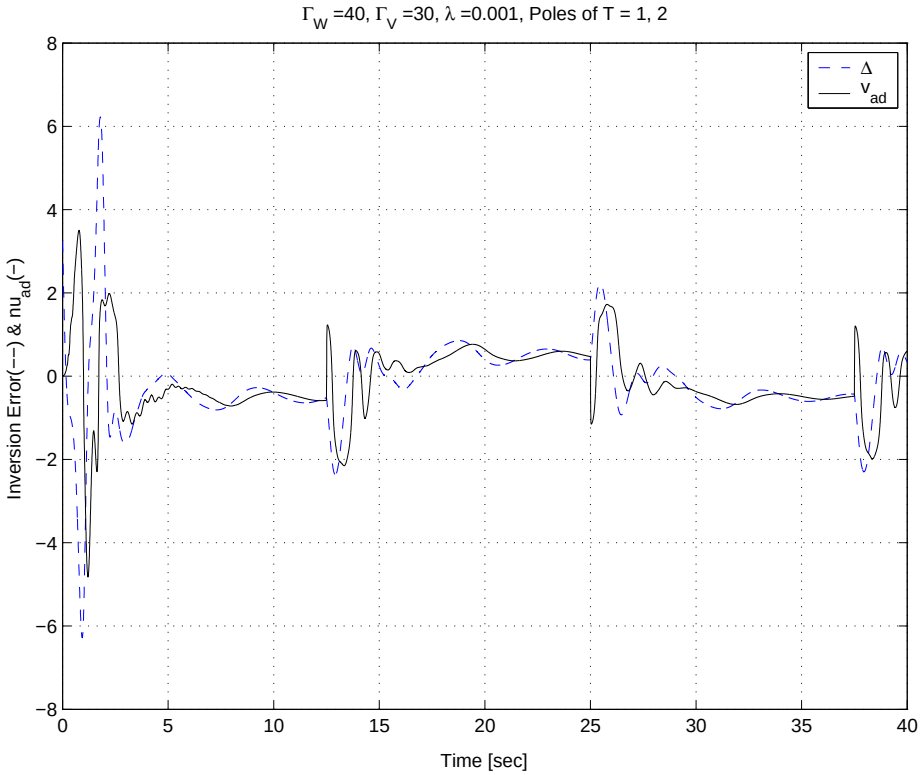

Figure 31: Δ vs. v_{ad} with nonlinearly-parameterized NN

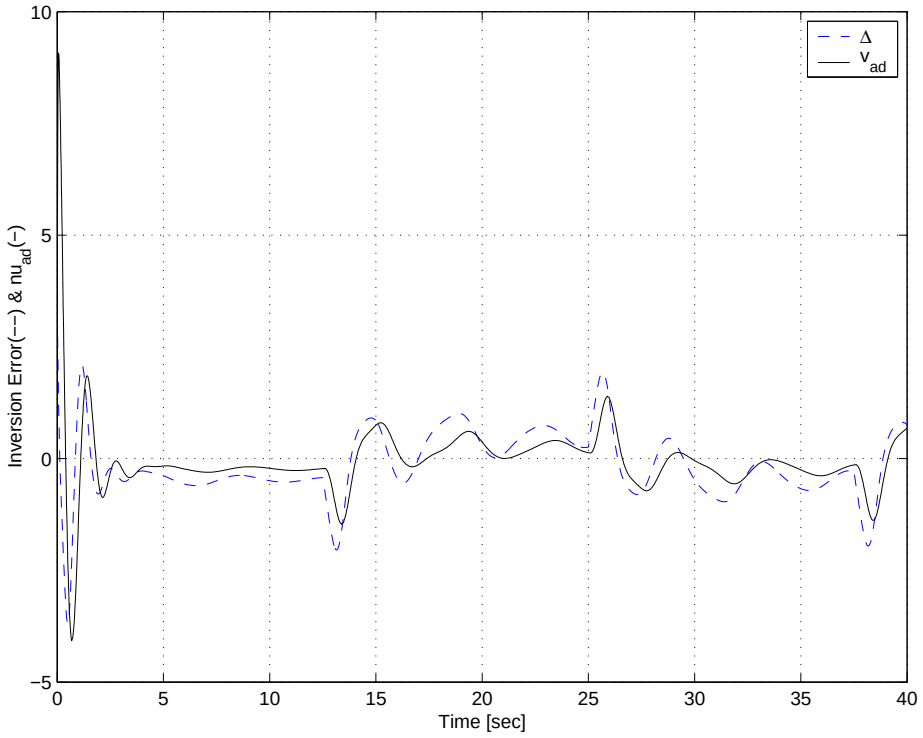

Figure 32: Δ vs. v_{ad} with linearly-parameterized NN

CHAPTER IV

NN AUGMENTATION OF EXISTING CONTROLLERS

This chapter presents an approach to augment existing controllers with a NN. Previous adaptive output feedback control approaches have been applied within a control architecture that uses an inverting type of controller for the non-adaptive portion of the control system. Considering that the vast majority of existing controllers are not based on inversion, it is desirable to retrofit such systems with an adaptive element. Generally, when a complete control system already exists for the nominal plant, one can augment it with an adaptive process to gain the benefits provided by adaptation. In the particular case of aviation applications, the aircraft industry would much prefer to augment flight control architectures that are already certified, rather than replace them with a totally new architecture. In [44] adaptive augmentation of a linear controller is examined for the case of state feedback. References [45, 46, 47] introduced several methods for linear controller augmentation in an output feedback setting. Here we develop an approach for a simple reference model which has the same relative degree as the true plant as depicted in Figure 33. The approach is useful for situations in which one wishes to augment an existing linear controller without knowledge of the process by which the controller was designed. For example, the controller gains may have been obtained by a tuning process while in operation with the true plant, and not obtained (in its operational form) via a model based design approach. This situation is often the case in many practical industrial settings, such as process control, automotive engine and transmission control, and many aircraft,

missile and guided munition flight control applications as well.

First we describe the control system architecture and develop the error equation needed to apply an existing approach to adaptive output feedback augmentation. A reference model is constructed to represent the ideal response characteristics of the closed-loop system. NN augmentation of an existing controller is used to force the plant output to track the reference model trajectory. This approach involves formulating an architecture for which the associated error equations have a form suitable for applying the same NN and update laws as those given in Chapter 3. In addition Section 4.1.2 develops an SPR filter approach for directly using the tracking error signal to update the NN weights. The augmentation methodology is extended to MIMO systems in Section 4.2. The efficacy of the design is demonstrated via application to autopilot design for a guided munition model. In Section 4.3.2, command limiting is introduced to avoid an oscillatory response at high angle of attack in normal acceleration tracking.

4.1 Existing Controller Augmentation Scheme

Consider the following observable and stabilizable SISO nonlinear system:

$$\begin{aligned} \dot{\boldsymbol{x}} &= \boldsymbol{f}(\boldsymbol{x}, u) \\ y &= h(\boldsymbol{x}) \end{aligned} \tag{4.1.1}$$

where $\boldsymbol{x}$ is the state of the system on a domain $\mathcal{D}_x \subset \Re^n$, and $u, y \in \Re$ are the control and regulated output variables, respectively. The functions $\boldsymbol{f}$ and h may be unknown. The regulated output is available for feedback and its relative degree is known to be r.

Assumption 4.1.1. The output y has relative degree r for all $(\boldsymbol{x}, u) \in \mathcal{D}_x \times \Re$.

We assume that the system (4.1.1) can be transformed into a normal form,

$$\begin{aligned} \dot{\boldsymbol{\chi}} &= \boldsymbol{f}_0(\boldsymbol{\xi}, \boldsymbol{\chi}) \\ \dot{\xi}_i &= \xi_{i+1} \qquad i = 1, \cdots, r-1 \\ \dot{\xi}_r &= h_r(\boldsymbol{\xi}, \boldsymbol{\chi}, u) \\ y &= \xi_1 \end{aligned} \tag{4.1.2}$$

where $\boldsymbol{\xi} = [\ \xi_1 \quad \dots \quad \xi_r\ ]^T$, $h_r(\boldsymbol{\xi}, \boldsymbol{\chi}, u) = L_f^r h$, and $\boldsymbol{\chi}$ is the state vector associated with the internal dynamics.

Assumption 4.1.2. The internal dynamics in (3.1.4), with $\boldsymbol{\xi}$ viewed as input, are input-to-state stable. [53]

Assumption 4.1.3. The sign of $\partial h_r / \partial u$ is known.

It is assumed that there already exists a linear controller:

$$\begin{aligned} \dot{\boldsymbol{x}}_c &= A_c \boldsymbol{x}_c + \boldsymbol{b}_c (y_c - y) \\ u_{ec} &= C_c \boldsymbol{x}_c + D_c (y_c - y) \end{aligned} \tag{4.1.3}$$

where $y_c \in \Re$ is a command signal, $\boldsymbol{x}_c \in \Re^{n_c}$ is the state vector of the linear controller and A_c is Hurwitz. However, the process by which this controller was obtained in its final form does not lend itself to a straightforward model-based design method. Consequently, a linear plant model is not available which can be combined with the controller in (4.1.3) to define the desired closed-loop performance.

We suggest using a simple linear performance model $G(s)$ as a reference model

$$G(s) = \frac{b_1}{s^r + a_r s^{r-1} + \cdots + a_1} \tag{4.1.4}$$

as shown in Figure 33. The reference model should be designed to have relative degree r and to satisfy performance requirement of closed-loop system. $G(s)$ has r poles in the open left half plane and can be expressed in state-space form as:

$$\begin{aligned} \dot{\boldsymbol{y}}_m &= A_m \boldsymbol{y}_m + \boldsymbol{b}_m b_1 y_c \\ y_m &= C_m \boldsymbol{y}_m \end{aligned} \tag{4.1.5}$$

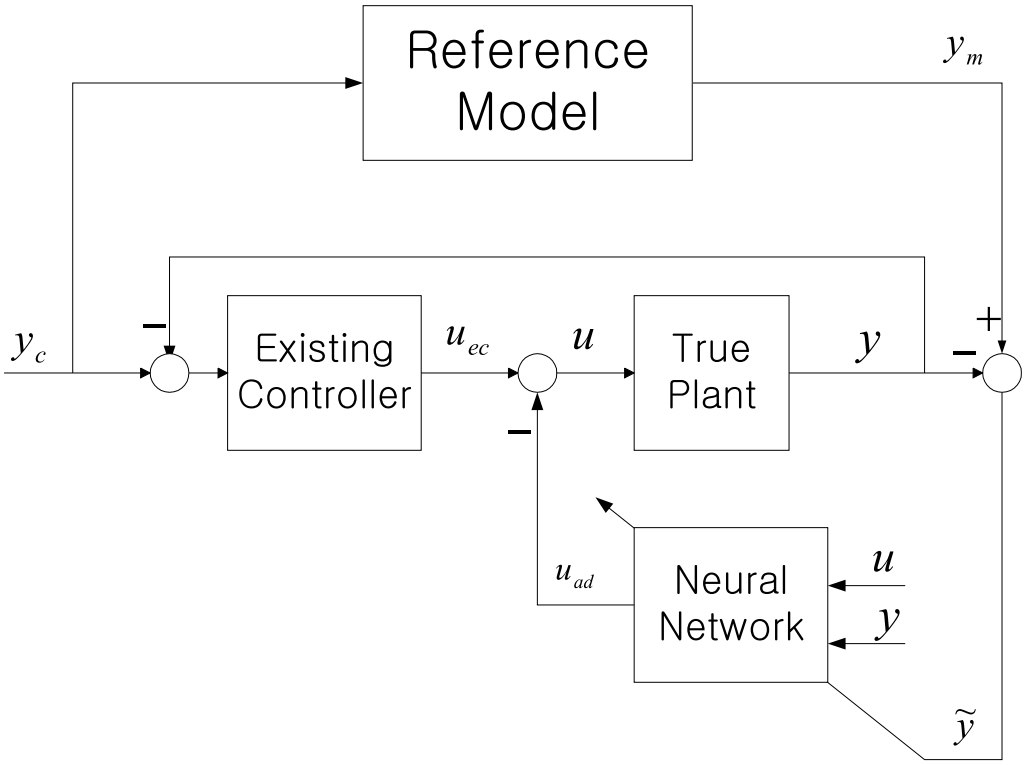

Figure 33: Adaptive control architecture with existing controller augmentation using simple reference model

$$\boldsymbol{y}_m \triangleq \begin{bmatrix} y_m & \dot{y}_m & \cdots & y_m^{(r-1)} \end{bmatrix}^T$$

$$A_m = \begin{bmatrix} 0 & 1 & 0 & \cdots & 0 \\ 0 & 0 & 1 & \cdots & \vdots \\ \vdots & \vdots & \vdots & \ddots & 0 \\ 0 & 0 & \cdots & 0 & 1 \\ -a_1 & -a_2 & -a_3 & \cdots & -a_r \end{bmatrix}, \boldsymbol{b}_m = \begin{bmatrix} 0 \\ 0 \\ 0 \\ \vdots \\ 1 \end{bmatrix},$$

$$C_m = \begin{bmatrix} 1 & 0 & 0 & 0 & \cdots & 0 \end{bmatrix}$$

where A_m is Hurwitz.

Assumption 4.1.4. The command $y_c(t)$ is bounded so that

$$\|y_c(t)\| \leq y_c^*$$

By Assumption 4.1.4, $\boldsymbol{y}_m$ is guaranteed to be bounded. Then the r^{th} derivative of y_m is

$$y_m^{(r)} = C_r \boldsymbol{y}_m + D_r y_c \tag{4.1.6}$$

where $C_r \triangleq C_m A_m^r = \begin{bmatrix} -a_1 & -a_2 & -a_3 & \cdots & -a_r \end{bmatrix}$ and $D_r \triangleq C_m A_m^{r-1} \boldsymbol{b}_m b_1 = b_1$.

The feedback control law is designed as:

$$u = u_{ec} - u_{ad} \tag{4.1.7}$$

$y^{(r)}$ in (4.1.2) can be put in the following form.

$$\begin{aligned} y^{(r)} &= -a_r y^{(r-1)} \cdots - a_1 y + b_1 (y_c - u_{ad} + \Delta) \\ &= C_r \boldsymbol{y} + b_1 (y_c - u_{ad} + \Delta(y_c, \boldsymbol{y}, u)) \end{aligned} \tag{4.1.8}$$

where $\boldsymbol{y} \triangleq \begin{bmatrix} y & \dot{y} & \cdots & y^{(r-1)} \end{bmatrix}^T$ and $\Delta(y_c, \boldsymbol{y}, u) \triangleq \frac{1}{b_1}(y^{(r)} - C_r \boldsymbol{y}) - y_c + u_{ad}$

Its state-space form is given by [1]

$$\begin{aligned} \dot{\boldsymbol{y}} &= A_m \boldsymbol{y} + \boldsymbol{b}_m b_1 (y_c - u_{ad} + \Delta(y_c, \boldsymbol{y}, u)) \\ y &= C_m \boldsymbol{y} \end{aligned} \tag{4.1.9}$$

[1] If additional outputs are available for feedback, which are not regulated, they can easily be incorporated into the design, similar to what was done in Chapter 3.

Let the error be defined as $e \triangleq y_m - y$. Then we have the following tracking error dynamics.

$$\begin{aligned} e^{(r)} &= C_r \boldsymbol{E} + b_1(u_{ad} - \Delta) \\ &= -(a_1 e + a_2 \dot{e} + \cdots + a_r e^{(r-1)}) + b_1(u_{ad} - \Delta) \end{aligned} \tag{4.1.10}$$

where $\boldsymbol{E} = \begin{bmatrix} e & \dot{e} & \cdots & e^{(r-1)} \end{bmatrix}^T$. In state space form it can be represented as:

$$\begin{aligned} \dot{\boldsymbol{E}} &= A_m \boldsymbol{E} + \boldsymbol{b}_m b_1(u_{ad} - \Delta(y_c, \boldsymbol{y}, u)) \\ \boldsymbol{z} &= C_m \boldsymbol{E} \end{aligned} \tag{4.1.11}$$

Define the following signal

$$u^* \triangleq h_r^{-1}(\boldsymbol{x}, b_1 y_c + C_r \boldsymbol{y}) \tag{4.1.12}$$

From (4.1.12), the following equation is satisfied.

$$b_1 y_c + C_r \boldsymbol{y} = h_r(\boldsymbol{x}, u^*) \tag{4.1.13}$$

$u_{ad} - \Delta$ can be expressed as

$$\begin{aligned} u_{ad} - \Delta &= u_{ad} - \frac{1}{b_1}(y^{(r)} - C_r \boldsymbol{y}) + y_c - u_{ad} \\ &= -\frac{1}{b_1}(h_r(\boldsymbol{x}, u) - C_r \boldsymbol{y} - b_1 y_c) \\ &= \frac{1}{b_1}(h_r(\boldsymbol{x}, u^*) - h_r(\boldsymbol{x}, u)) \end{aligned} \tag{4.1.14}$$

Applying the mean value theorem,

$$\begin{aligned} u_{ad} - \Delta &= \frac{h_{\bar{u}}}{b_1}(u^* - u) \\ &= \frac{h_{\bar{u}}}{b_1}(h_r^{-1}(\boldsymbol{x}, b_1 y_c + C_r \boldsymbol{y}) - u_{ec} + u_{ad}) \\ &= \frac{h_{\bar{u}}}{b_1}(u_{ad} - \bar{\Delta}(\boldsymbol{x}, y_c, u_{ec})) \end{aligned} \tag{4.1.15}$$

where $\bar{\Delta} = u_{ec} - h_r^{-1}(\boldsymbol{x}, b_1 y_c + C_r \boldsymbol{y})$ and

$$h_{\bar{u}} \triangleq \left. \frac{\partial h_r}{\partial u} \right|_{u=\bar{u}}, \ \bar{u} = \theta u + (1-\theta) u^*, \text{ and } \ 0 \leq \theta(u) \leq 1 \tag{4.1.16}$$

Using the representation of (4.1.15), we have the following error dynamics.

$$\begin{aligned} \dot{\boldsymbol{E}} &= A_m \boldsymbol{E} + \boldsymbol{b}_m h_{\bar{u}}(u_{ad} - \bar{\Delta}) \\ \boldsymbol{z} &= C_m \boldsymbol{E} \end{aligned} \tag{4.1.17}$$

Define the bounds for $h_{\bar{u}}$ and $\frac{d}{dt}\left(\frac{1}{h_{\bar{u}}}\right)$ in a compact set,

$$h^B \triangleq \max_{\boldsymbol{x}, u \in \mathcal{D}} |h_{\bar{u}}|, \;\; H \triangleq \max_{\boldsymbol{x}, u \in \mathcal{D}} \left| \frac{d}{dt}\left(\frac{1}{h_{\bar{u}}}\right) \right| \tag{4.1.18}$$

Now we design the adaptive term as

$$u_{ad} = \hat{W}^T \boldsymbol{\sigma}(\hat{V}^T \boldsymbol{\mu}) \tag{4.1.19}$$

If the NN output signal u_{ad} perfectly cancels $\bar{\Delta}$, then we have asymptotically stable error dynamics. Since A_m is Hurwitz, there exists a unique $P > 0$ solving the following Lyapunov equation

$$A_m^T P + P A_m = -Q \tag{4.1.20}$$

for arbitrary $Q > 0$. Lyapunov stability analysis of the error dynamics results in update laws for the adaptive element in terms of $\boldsymbol{E}$. However, for $r \geq 2$ it is assumed that $\boldsymbol{E}$ is not available for feedback. We can deal with it by either using the error observer approach [47] or the direct adaptive approach [45, 46], similar to what was done in Chapter 3. These two approaches will be detailed in the sequel.

4.1.1 Error Observer Approach

Here we treat the problem using the error observer approach and the update law with σ-modification as presented in Section 3.4.1. Introducing a linear observer for the tracking error dynamics as in Section 3.3, we have:

$$\begin{aligned} \dot{\hat{\boldsymbol{E}}} &= A_m \hat{\boldsymbol{E}} + K\left(\boldsymbol{z} - \hat{\boldsymbol{z}}\right) \\ \hat{\boldsymbol{z}} &= C_m \hat{\boldsymbol{E}}, \end{aligned} \tag{4.1.21}$$

where K should be chosen in a way to make $A_m - KC_m$ asymptotically stable. Let

$$\tilde{A} \triangleq A_m - KC_m, \quad \tilde{\boldsymbol{E}} \triangleq \hat{\boldsymbol{E}} - \boldsymbol{E}. \tag{4.1.22}$$

Then the observer error dynamics can be written:

$$\dot{\tilde{\boldsymbol{E}}} = \tilde{A}\tilde{\boldsymbol{E}} - \boldsymbol{b}_m h_{\bar{u}}(u_{ad} - \Delta). \tag{4.1.23}$$

Since $\tilde{A}$ is Hurwitz, there exists $\tilde{P} > 0$ satisfying the following Lyapunov equation

$$\tilde{A}^T\tilde{P} + \tilde{P}\tilde{A} = -\tilde{Q}, \tag{4.1.24}$$

for an arbitrary positive definite matrix $\tilde{Q}$. In the same manner as (3.4.5), we have the following representation.

$$u_{ad} - \Delta = \tilde{W}^T\left(\hat{\boldsymbol{\sigma}} - \hat{\sigma}'\hat{V}^T\boldsymbol{\mu}\right) + \hat{W}^T\hat{\sigma}'\tilde{V}^T\boldsymbol{\mu} + \bar{w} \tag{4.1.25}$$

where the disturbance term is bounded by:

$$\|\bar{w}\| \leq \gamma_1\|\tilde{Z}\|_F + \gamma_2 \tag{4.1.26}$$

where $\gamma_1 = \frac{a^*}{4}Z^*\mu^*$, $\gamma_2 = ((2+\delta)\sqrt{n_2+1} + \gamma_1)W^* + \epsilon^*$ and δ as defined in (2.3.11).

Assumption 4.1.5. Assumption 3.4.1 holds with $\boldsymbol{b}_m$ in place of $\bar{\boldsymbol{b}}$.

Theorem 4.1.1. Let assumptions 4.1.1, 4.1.2, 4.1.3, 4.1.4 and 4.1.5 hold. Let the adaptation law be given by:

$$\begin{aligned}\dot{\hat{W}} &= -\Gamma_W\left[\operatorname{sgn}(h_{\bar{u}})(\hat{\boldsymbol{\sigma}} - \hat{\sigma}'\hat{V}^T\boldsymbol{\mu})\hat{\boldsymbol{E}}^T P\boldsymbol{b}_m + k_\sigma(\hat{W} - W_0)\right] \\ \dot{\hat{V}} &= -\Gamma_V\left[\operatorname{sgn}(h_{\bar{u}})\boldsymbol{\mu}\hat{\boldsymbol{E}}^T P\boldsymbol{b}_m\hat{W}^T\hat{\sigma}' + k_\sigma(\hat{V} - V_0)\right]\end{aligned} \tag{4.1.27}$$

where $\Gamma_V, \Gamma_W > 0$. Then there exists a positive invariant set, Ω_α such that if the initial errors belong to Ω_α, then the feedback control law given by (4.1.7) ensures that the signals $\boldsymbol{E}, \tilde{\boldsymbol{E}}, \tilde{W}$ and $\tilde{V}$ in the closed-loop system are ultimately bounded with the ultimate bound $C\sqrt{\frac{\lambda_{max}(T)}{\lambda_{min}(T)}}$.

Proof. The proof is the same as that of Theorem 3.4.1 with $\boldsymbol{b}_m$ in place of $\bar{\boldsymbol{b}}$. □

Remark 4.1.1. Theorem 4.1.1 can be applied to the e-modification as in (3.4.21) or the projection operator as in (3.4.38).

4.1.2 SPR Filter Approach

Reference [38] presents a direct adaptive output feedback design approach employing feedback linearization and a linearly-parameterized NN to compensate for modeling errors without using the error observer. It introduces an additional error signal for training the NN by using a two-output dynamic compensator. The training signal can be interpreted as a filtered tracking error signal. Here we will directly use the tracking error signal to update weights in the linearly-parameterized NN. An extension to a nonlinearly-parameterized NN is given in Section 3.8. The control system is augmented by a low-pass filter designed to meet a SPR condition of a transfer function of error dynamics. The SPR condition is used in the Lyapunov stability analysis to construct the NN adaptation law using only available measurements.

Following [6, 7, 8], Δ can be represented by $W^T\phi + \epsilon$, and with the adaptive element of (4.1.19) the error dynamics in (4.1.11) can be expressed as:

$$e = G(s)h_{\bar{u}}(\tilde{W}^T\boldsymbol{\phi} - \epsilon) \tag{4.1.28}$$

where $G(s)$ is defined in (4.1.4) and $\boldsymbol{\phi}(\boldsymbol{\mu})$ is a radial basis function defined by:

$$\phi_i = e^{-(\boldsymbol{\mu}-\boldsymbol{c}_i)^T(\boldsymbol{\mu}-\boldsymbol{c}_i)/2}, \quad i = 1, 2, \cdots, n_2 \tag{4.1.29}$$

The centers $\boldsymbol{c}_i$ are randomly chosen over a range of possible values of the input vector $\boldsymbol{\mu}$. The proof of ultimate boundedness requires (4.1.28) to be strictly positive real (SPR). If $r \geq 2$, we introduce an $(r-1)^{th}$ order SPR filter $T(s)$ to meet the SPR condition.

$$\begin{aligned} e &= G(s)T^{-1}(s)T(s)h_{\bar{u}}(\tilde{W}^T\boldsymbol{\phi} - \epsilon) \\ &= G(s)T^{-1}(s)h_{\bar{u}}(\tilde{W}^T\boldsymbol{\phi}_f + \delta_f - \epsilon_f) \end{aligned} \tag{4.1.30}$$

where $\boldsymbol{\phi}_f = T(s)\boldsymbol{\phi},\ \delta_f = T(s)(\tilde{W}^T\boldsymbol{\phi}) - \tilde{W}^T\boldsymbol{\phi}_f,\ \epsilon_f = T(s)\epsilon$, and are bounded as:

$$\|\delta_f\| \leq \kappa_1\|\tilde{W}\|_F, \quad \|\epsilon\| \leq \epsilon_f^* \tag{4.1.31}$$

$T(s)$ can be constructed by Kalman-Yakubovich-Popov (KYP) approach [61]. Assume that

$$G(s)T^{-1}(s) = \frac{c_r s^{r-1} + c_{r-1}s^{r-2} + \cdots + c_1}{s^r + a_r s^{r-1} + \cdots + a_1} \tag{4.1.32}$$

The state space realization of the transfer function $G(s)T(s)^{-1}$ is given by

$$\begin{aligned} \dot{\boldsymbol{z}} &= A_m \boldsymbol{z} + \bar{\boldsymbol{b}}(h_{\bar{u}}(\tilde{W}^T \boldsymbol{\phi}_f + \delta_f - \epsilon_f) \\ e &= \bar{C}\boldsymbol{z} \end{aligned} \tag{4.1.33}$$

where

$$\begin{aligned} A_m &= \begin{bmatrix} 0 & 1 & 0 & \cdots & 0 \\ 0 & 0 & 1 & \cdots & \vdots \\ \vdots & \vdots & \vdots & \ddots & 0 \\ 0 & 0 & \cdots & 0 & 1 \\ -a_1 & -a_2 & -a_3 & \cdots & -a_r \end{bmatrix}, \quad \bar{\boldsymbol{b}} = \begin{bmatrix} 0 \\ 0 \\ \vdots \\ 0 \\ 1 \end{bmatrix} \\ \bar{C} &= \begin{bmatrix} c_1 & c_2 & \cdots & c_{r-1} & c_r \end{bmatrix} \end{aligned} \tag{4.1.34}$$

$G(s)T(s)^{-1}$ is SPR if and only if it complies with KYP Lemma, i.e. there exists $Q > 0$ such that the solution P of

$$A_m^T P + P A_m = -Q \tag{4.1.35}$$

is positive definite and

$$\bar{C} = \bar{\boldsymbol{b}}^T P \tag{4.1.36}$$

From the elements of $\bar{C}$ which is the last row of P in this canonical form, we can construct a stable low-pass filter $T(s)$ ensuring $G(s)T(s)^{-1}$ is SPR.

$$T(s) = \frac{b_1}{c_r s^{r-1} + c_{r-1}s^{r-2} + \cdots + c_1} \tag{4.1.37}$$

The filter $T(s)$ can be realized in a state space form.

$$\begin{aligned} \dot{\boldsymbol{z}}_f &= A_f \boldsymbol{z}_f + B_f \boldsymbol{\phi} \\ \boldsymbol{\phi}_f &= C_f \boldsymbol{z}_f \end{aligned} \tag{4.1.38}$$

The signal $\boldsymbol{\phi}_f$ is used in the NN adaptation law

$$\dot{\hat{W}} = -\Gamma_W[\text{sgn}(h_{\bar{u}})e\boldsymbol{\phi}_f + k_\sigma \hat{W}] \tag{4.1.39}$$

where $\Gamma_W > 0$ is the learning rate and $k_\sigma > 0$ is the σ-modification gain. Since the filter is stable, for any positive definite Q_f, there exists P_f satisfying

$$A_f^T P_f + P_f A_f = -Q_f \tag{4.1.40}$$

Assumption 4.1.6. Assume

$$R > C\sqrt{\frac{\lambda_{max}(T)}{\lambda_{min}(T)}} \geq C \tag{4.1.41}$$

where $\lambda_{max}(T)$ and $\lambda_{min}(T)$ are the maximum and minimum eigenvalues of the following matrix:

$$T \triangleq \begin{bmatrix} P & 0 & 0 \\ 0 & P_f & 0 \\ 0 & 0 & \Gamma_W^{-1} \end{bmatrix} \tag{4.1.42}$$

which will be used in a Lyapunov function candidate as $L = \boldsymbol{\zeta}^T T \boldsymbol{\zeta}$ with an error vector $\boldsymbol{\zeta} = \begin{bmatrix} \boldsymbol{z}^T & \boldsymbol{z}_f^T & \tilde{W}^T \end{bmatrix}^T$, and

$$C \triangleq \max\Big(\sqrt{\frac{\Upsilon}{\frac{\lambda_{min}(Q)}{h^B} - H\lambda_{max}(P) - \kappa_2}},\ \sqrt{\frac{\Upsilon}{\lambda_{min}(Q_f) - \kappa_3}},\ \sqrt{\frac{\Upsilon}{k_\sigma - \kappa_4}}\Big) \tag{4.1.43}$$

is a radius of a ball B_C containing Γ (See Figure 2), where

$$\begin{aligned} &\kappa_2 = (\kappa_1 + \epsilon_f^*)\|C\|,\ \ \kappa_3 = \|P_f B_f\|\|\boldsymbol{\phi}\|,\ \ \kappa_4 = \kappa_1\|C\| + k_\sigma W^*, \\ &\Upsilon = \epsilon_f^*\|C\| + \|P_f B_f\|\|\boldsymbol{\phi}\| + k_\sigma W^*, \\ &\lambda_{min}(Q) > h^B(H\lambda_{max}(P) - \kappa_2),\ \ \lambda_{min}(Q_f) > \kappa_3,\ \ k_\sigma > \kappa_4 \end{aligned} \tag{4.1.44}$$

Define the Lyapunov function level sets Ω_α and Ω_β

$$\begin{aligned} \Omega_\alpha &= \{\boldsymbol{\zeta} \in B_R \mid L \leq \alpha \ \triangleq \min_{\|\boldsymbol{\zeta}\|=R} L\} \\ \Omega_\beta &= \{\boldsymbol{\zeta} \in B_R \mid L \leq \beta \ \triangleq \max_{\|\boldsymbol{\zeta}\|=C} L\} \end{aligned} \tag{4.1.45}$$

Theorem 4.1.2. Let assumptions 4.1.1, 4.1.2, 4.1.3, 4.1.4 and 4.1.6 hold. If the initial errors belong to the compact set Ω_α defined in (4.1.45), then the feedback control law given by (4.1.7) and the weight update law (4.1.39) ensure that the signals $\boldsymbol{z}, \boldsymbol{z}_f, \tilde{W}$ in the closed-loop system are ultimately bounded with the ultimate bound $C\sqrt{\frac{\lambda_{max}(T)}{\lambda_{min}(T)}}$.

Proof. See Appendix A.6. □

4.2 Extension to MIMO Systems

Let the dynamics of an *observable* and *stabilizable* nonlinear MIMO system be given by the following equations:

$$\dot{\boldsymbol{x}} = \boldsymbol{f}(\boldsymbol{x}, \boldsymbol{u}), \quad \boldsymbol{y} = \boldsymbol{g}(\boldsymbol{x}) \tag{4.2.1}$$

where $\boldsymbol{x} \in \Omega \subset \Re^n$ is the state of the system, $\boldsymbol{u}, \boldsymbol{y} \in \Re^{n_3}$ are the system input (control) and output (measurement) signals, respectively, and $\boldsymbol{f}(\cdot,\cdot), \boldsymbol{g}(\cdot)$ are unknown functions. Moreover, n need not be known.

Assumption 4.2.1. The dynamic system in (4.2.1) has vector relative degree $[r_1, r_2, \cdots, r_{n_3}]^T$, $r = r_1 + r_2 + \cdots + r_{n_3} \leq n$ [62].

Then there exists a mapping $\boldsymbol{\xi} = \Phi(\boldsymbol{x})$, where

$$\Phi(\boldsymbol{x}) = \begin{bmatrix} \phi_1 \\ \phi_2 \\ \vdots \\ \phi_{n_3} \end{bmatrix}, \quad \phi_i(\boldsymbol{x}) = \begin{bmatrix} g_i \\ L_{\boldsymbol{f}}^1 g_i \\ \vdots \\ L_{\boldsymbol{f}}^{r_i - 1} g_i \end{bmatrix} \triangleq \boldsymbol{\xi}_i \in \Re^{r_i} \tag{4.2.2}$$

with $L_{\boldsymbol{f}}^j g_i$ being the Lie derivatives, g_i's the elements of the vector $\boldsymbol{g}$ in (4.2.1), that

transforms the system (4.2.1) into the so called normal form [62, 63]:

$$\begin{aligned}
\dot{\boldsymbol{\chi}} &= \boldsymbol{f}_0(\boldsymbol{\xi}, \boldsymbol{\chi}) \\
\dot{\xi}_i^1 &= \xi_i^2, \\
&\vdots \\
\dot{\xi}_i^{r_i} &= h_i(\boldsymbol{\xi}, \boldsymbol{\chi}, \boldsymbol{u}) \\
\xi_i^1 &= y_i, \quad i = 1, \cdots, n_3\,,
\end{aligned} \tag{4.2.3}$$

where $h_i(\boldsymbol{\xi}, \boldsymbol{\chi}, \boldsymbol{u}) = L_{\boldsymbol{f}}^{r_i} g_i$, $\boldsymbol{\xi} = \begin{bmatrix} \boldsymbol{\xi}_1^T & \dots & \boldsymbol{\xi}_{n_3}^T \end{bmatrix}^T \in \Re^r$, $\boldsymbol{\xi}_i = \begin{bmatrix} \xi_i^1 & \dots & \xi_i^{r_i} \end{bmatrix}^T$, and $\boldsymbol{\chi} \in \Re^{n-r}$ are the states associated with the internal dynamics.

Assumption 4.2.2. The internal dynamics in (4.2.3), with $\boldsymbol{\xi}$ viewed as input, are input-to-state stable. [53]

The objective is to synthesize a feedback control law that utilizes the available measurements $\boldsymbol{y}$, so that $y_i(t)$ track bounded reference trajectories $y_{c_i}(t)$ within bounded errors.

The reference model should be designed to have the same vector relative degree as the plant dynamics and satisfy closed-loop performance requirements. Define a r^{th}-order block-diagonal matrix reference model as:

$$\begin{aligned}
\dot{\boldsymbol{x}}_m &= A_m \boldsymbol{x}_m + B_m \boldsymbol{y}_c \\
\boldsymbol{y}_m &= C_m \boldsymbol{x}_m
\end{aligned} \tag{4.2.4}$$

where $\boldsymbol{y}_c \in \Re^{n_3}$ is a raw command, $\boldsymbol{y}_m \in \Re^{n_3}$ is the output of the reference model and

$$\boldsymbol{x}_m = \begin{bmatrix} \boldsymbol{x}_{m,1} \\ \boldsymbol{x}_{m,2} \\ \vdots \\ \boldsymbol{x}_{m,n_3} \end{bmatrix}_{r \times 1}, \quad \boldsymbol{x}_{m,i} \in \Re^{r_i}, \quad i = 1, \cdots, n_3 \tag{4.2.5}$$

$$A_m = \begin{bmatrix} A_1 & 0 & \cdots & 0 \\ 0 & A_2 & \cdots & 0 \\ \vdots & \vdots & \ddots & \vdots \\ 0 & \cdots & 0 & A_{n_3} \end{bmatrix}_{r\times r}, \quad A_i = \begin{bmatrix} 0 & 1 & 0 & \cdots & 0 \\ 0 & 0 & 1 & \cdots & \vdots \\ \vdots & \vdots & \vdots & \ddots & 0 \\ 0 & 0 & \cdots & 0 & 1 \\ -a_i^1 & -a_i^2 & -a_i^3 & \cdots & -a_i^{r_i} \end{bmatrix}_{r_i\times r_i},$$

$$B_m = \begin{bmatrix} \boldsymbol{b}_1 & 0 & \cdots & 0 \\ 0 & \boldsymbol{b}_2 & \cdots & 0 \\ \vdots & \vdots & \ddots & \vdots \\ 0 & \cdots & 0 & \boldsymbol{b}_{n_3} \end{bmatrix}_{r\times n_3}, \quad \boldsymbol{b}_i = \begin{bmatrix} 0 \\ 0 \\ \vdots \\ b_i \end{bmatrix}_{r_i\times 1}, \tag{4.2.6}$$

$$C_m = \begin{bmatrix} \boldsymbol{c}_1 & 0 & \cdots & 0 \\ 0 & \boldsymbol{c}_2 & \cdots & 0 \\ \vdots & \vdots & \ddots & \vdots \\ 0 & \cdots & 0 & \boldsymbol{c}_{n_3} \end{bmatrix}_{n_3\times r}, \quad \boldsymbol{c}_i = \begin{bmatrix} 1 & 0 & 0 & \cdots & 0 \end{bmatrix}_{1\times r_i}$$

where every A_i is Hurwitz and so is A_m. (4.2.4) can be decomposed of

$$\begin{aligned} \dot{\boldsymbol{x}}_{m,i} &= A_i \boldsymbol{x}_{m,i} + \boldsymbol{b}_i y_{c,i} \\ y_{m,i} &= \boldsymbol{c}_i \boldsymbol{x}_{m,i} \end{aligned} \tag{4.2.7}$$

Note that given Hurwitz A_m, for all $Q > 0$ there exist a positive definite matrix P solving the following Lyapunov equation,

$$A_m^T P + P A_m = -Q \tag{4.2.8}$$

$\dot{\xi}_i^{r_i}$ in (4.2.3) can be put in the following form:

$$\dot{\xi}_i^{r_i} = -\boldsymbol{a}_i \boldsymbol{\xi}_i + b_i(y_{c,i} - u_{ad,i} + \Delta_i) \tag{4.2.9}$$

where $\Delta_i(\boldsymbol{\xi}, \boldsymbol{\chi}, \boldsymbol{u}) = \frac{1}{b_i}(\dot{\xi}_i^{r_i} + \boldsymbol{a}_i \boldsymbol{\xi}_i) - y_{c,i} - u_i + u_{ec,i}$ and $\boldsymbol{a}_i = \begin{bmatrix} a_i^1 & a_i^2 & \cdots & a_i^{r_i} \end{bmatrix}^T$. It can be expressed in state space form:

$$\begin{aligned} \dot{\boldsymbol{\xi}}_i &= A_i \boldsymbol{\xi}_i + \boldsymbol{b}_i(y_{c,i} - u_{ad,i} + \Delta_i) \\ \xi_i^1 &= \boldsymbol{c}_i \boldsymbol{\xi}_i \end{aligned} \tag{4.2.10}$$

Denote $\boldsymbol{e}_i \triangleq \boldsymbol{x}_{m,i} - \boldsymbol{\xi}_i$, then error dynamics for each block can be represented as:

$$\begin{aligned} \dot{\boldsymbol{e}}_i &= A_i \boldsymbol{e}_i + \boldsymbol{b}_i (u_{ad,i} - \Delta_i) \\ z_i &= \boldsymbol{c}_i \boldsymbol{e}_i \end{aligned} \tag{4.2.11}$$

In the same manner as Section 4.1 we reformulate the modeling error such that a new modeling error is not a function of u_{ad}. Define the following signal

$$u_i^* \triangleq h_i^{-1}(\boldsymbol{x}, u_1, \cdots, u_{i-1}, b_i y_{c,i} - \boldsymbol{a}_i \boldsymbol{\xi}_i, u_{i+1}, \cdots, u_{n_3}) \tag{4.2.12}$$

From (4.2.12), the following equation is satisfied.

$$b_i y_{c,i} - \boldsymbol{a}_i \boldsymbol{\xi}_i = h_i(\boldsymbol{x}, u_1, \cdots, u_{i-1}, u_i^*, u_{i+1}, \cdots, u_{n_3}) \tag{4.2.13}$$

$u_{ad,i} - \Delta_i$ can be expressed as

$$\begin{aligned} u_{ad,i} - \Delta_i &= -\frac{1}{b_1}(h_i(\boldsymbol{x}, \boldsymbol{u}) - \boldsymbol{a}_i \boldsymbol{\xi}_i) + y_{c,i} \\ &= \frac{1}{b_1}\left(h_i(\boldsymbol{x}, u_1, \cdots, u_{i-1}, u_i^*, u_{i+1}, \cdots, u_{n_3}) - h_i(\boldsymbol{x}, \boldsymbol{u})\right) \end{aligned} \tag{4.2.14}$$

Applying the mean value theorem with respect to u_i,

$$\begin{aligned} u_{ad,i} - \Delta_i &= \frac{h_{\bar{u},i}}{b_i}(u_i^* - u_i) \\ &= \frac{h_{\bar{u},i}}{b_i}(h_i^{-1}(\boldsymbol{x}, u_1, \cdots, u_{i-1}, u_i^*, u_{i+1}, \cdots, u_{n_3}) - u_{ec,i} + u_{ad,i}) \\ &= \frac{h_{\bar{u},i}}{b_i}(u_{ad,i} - \bar{\Delta}_i(\boldsymbol{x}, y_{c,i}, u_{ec,i})) \end{aligned} \tag{4.2.15}$$

where $\bar{\Delta}_i = u_{ec} - (h_i^{-1}(\boldsymbol{x}, u_1, \cdots, u_{i-1}, u_i^*, u_{i+1}, \cdots, u_{n_3})$ and

$$h_{\bar{u},i} \triangleq \left.\frac{\partial h_i}{\partial u}\right|_{u_i = \bar{u}_i}, \ \bar{u}_i = \theta u_i + (1-\theta) u_i^*, \text{ and } \ 0 \le \theta(u_i) \le 1 \tag{4.2.16}$$

Using the representation of (4.2.15), the complete error dynamics are given by:

$$\begin{aligned} \dot{\boldsymbol{E}} &= A_m \boldsymbol{E} + \bar{B}_m H_{\bar{u}}(\boldsymbol{u}_{ad} - \bar{\boldsymbol{\Delta}}) \\ \boldsymbol{z} &= C_m \boldsymbol{E} \end{aligned} \tag{4.2.17}$$

where

$$\boldsymbol{E} = \begin{bmatrix} \boldsymbol{e}_1 \\ \boldsymbol{e}_2 \\ \vdots \\ \boldsymbol{e}_{n_3} \end{bmatrix}, \ \boldsymbol{u}_{ad} = \begin{bmatrix} u_{ad,1} \\ u_{ad,2} \\ \vdots \\ u_{ad,n_3} \end{bmatrix}, \ \bar{\boldsymbol{\Delta}} = \begin{bmatrix} \bar{\Delta}_1 \\ \bar{\Delta}_2 \\ \vdots \\ \bar{\Delta}_{n_3} \end{bmatrix}, \ H_{\bar{u}} = \begin{bmatrix} h_{\bar{u},1} & 0 & \cdots & 0 \\ 0 & h_{\bar{u},2} & 0 & \vdots \\ 0 & 0 & \ddots & 0 \\ 0 & \cdots & 0 & h_{\bar{u},n_3} \end{bmatrix},$$

$$\bar{B}_m = \begin{bmatrix} \bar{\boldsymbol{b}}_1 & 0 & \cdots & 0 \\ 0 & \bar{\boldsymbol{b}}_2 & \cdots & 0 \\ \vdots & \vdots & \ddots & \vdots \\ 0 & \cdots & 0 & \bar{\boldsymbol{b}}_{n_3} \end{bmatrix}_{r \times n_3}, \quad \bar{\boldsymbol{b}}_i = \begin{bmatrix} 0 \\ 0 \\ \vdots \\ 1 \end{bmatrix}_{r_i \times 1},$$

and $\boldsymbol{z}$ represents the signals available for feedback.

Assumption 4.2.3. The signs of $h_{\bar{u},i}$'s are known for $i = 1, \cdots, n_3$.

Define the following matrices,

$$|H_{\bar{u}}| \triangleq \begin{bmatrix} |h_{\bar{u},1}| & 0 & \cdots & 0 \\ 0 & |h_{\bar{u},2}| & 0 & \vdots \\ \vdots & 0 & \ddots & 0 \\ 0 & \cdots & 0 & |h_{\bar{u},n_3}| \end{bmatrix},$$

$$|H_{\bar{u}}^{-1}| \triangleq \begin{bmatrix} \frac{1}{|h_{\bar{u},1}|} & 0 & \cdots & 0 \\ 0 & \frac{1}{|h_{\bar{u},2}|} & 0 & \vdots \\ \vdots & 0 & \ddots & 0 \\ 0 & \cdots & 0 & \frac{1}{|h_{\bar{u},n_3}|} \end{bmatrix}, \tag{4.2.18}$$

$$\operatorname{sgn}(H_{\bar{u}}) \triangleq \begin{bmatrix} \operatorname{sgn}(h_{\bar{u},1}) & 0 & \cdots & 0 \\ 0 & \operatorname{sgn}(h_{\bar{u},2}) & 0 & \vdots \\ \vdots & 0 & \ddots & 0 \\ 0 & \cdots & 0 & \operatorname{sgn}(h_{\bar{u},n_3}) \end{bmatrix}$$

and the bounds for the use of boundedness analysis,

$$\begin{aligned} h^B &\triangleq \lambda_{max}(|H_{\bar{u}}|), \\ H &\triangleq \max\left[\max_{\boldsymbol{x},\boldsymbol{u}\in\mathcal{D}}\left|\tfrac{d}{dt}\tfrac{1}{h_{\bar{u},1}}\right|,\ \max_{\boldsymbol{x},\boldsymbol{u}\in\mathcal{D}}\left|\tfrac{d}{dt}\tfrac{1}{h_{\bar{u},2}}\right|,\ \cdots,\ \max_{\boldsymbol{x},\boldsymbol{u}\in\mathcal{D}}\left|\tfrac{d}{dt}\tfrac{1}{h_{\bar{u},n_3}}\right|\right] \end{aligned} \tag{4.2.19}$$

Introduce the following linear error observer for the tracking error dynamic system in (4.2.17):

$$\begin{aligned} \dot{\hat{\boldsymbol{E}}} &= A_m\hat{\boldsymbol{E}} + K\left(\boldsymbol{z} - \hat{\boldsymbol{z}}\right) \\ \hat{\boldsymbol{z}} &= C_m\hat{\boldsymbol{E}}, \end{aligned} \tag{4.2.20}$$

where K should be chosen to ensure asymptotic stability of $A_m - KC_m$. The stability of the closed-loop system should be considered along with the observer error dynamics. Let

$$\tilde{A} \triangleq A_m - KC_m, \quad \tilde{\boldsymbol{E}} \triangleq \hat{\boldsymbol{E}} - \boldsymbol{E}. \tag{4.2.21}$$

Then the observer error dynamics can be written:

$$\dot{\tilde{\boldsymbol{E}}} = \tilde{A}\tilde{\boldsymbol{E}} - \bar{B}_m H_{\bar{u}}(\boldsymbol{u}_{ad} - \bar{\boldsymbol{\Delta}}). \tag{4.2.22}$$

and there exists a positive definite matrix $\tilde{P}$ solving the Lyapunov equation for arbitrary $\tilde{Q} > 0$:

$$\tilde{A}^T\tilde{P} + \tilde{P}\tilde{A} = -\tilde{Q} \tag{4.2.23}$$

We design the adaptive element

$$\boldsymbol{u}_{ad} = \hat{W}^T\boldsymbol{\sigma}(\hat{V}^T\boldsymbol{\mu}),$$

where $\hat{W} \in \Re^{(n_2+1)\times n_3}, \hat{V} \in \Re^{(n_1+1)\times n_2}$ are estimates of NN weights that will be updated online. For the NN weight update law we can choose any of the three adaptive schemes presented in Section 3.4.1-3.4.3. Here we will adopt the e-modification scheme in Section 3.4.2 and show boundedness of all the error signals of the closed-loop system.

For the boundedness proof we need the Taylor series expansion of $W^T\boldsymbol{\sigma}(V^T\boldsymbol{\mu})$ at $W = \hat{W}$ and $V = \hat{V}$.

$$W^T\boldsymbol{\sigma} = \hat{W}^T\hat{\boldsymbol{\sigma}} - \tilde{W}^T\hat{\boldsymbol{\sigma}} - \hat{W}^T\hat{\sigma}'\tilde{V}^T\boldsymbol{\mu} + \mathcal{O}(\|\tilde{Z}\|^2) \tag{4.2.24}$$

where the higher order terms $\mathcal{O}(\|\tilde{Z}\|^2) = -W^T(\hat{\boldsymbol{\sigma}} - \boldsymbol{\sigma}) + \hat{W}^T\hat{\sigma}'\tilde{V}^T\boldsymbol{\mu}$. Then

$$\begin{aligned} \boldsymbol{u}_{ad} - \Delta &= \hat{W}^T\hat{\boldsymbol{\sigma}} - W^T\boldsymbol{\sigma} - \epsilon \\ &= \tilde{W}^T\hat{\boldsymbol{\sigma}} + \hat{W}^T\hat{\sigma}'\tilde{V}^T\boldsymbol{\mu} - \mathcal{O}(\|\tilde{Z}\|^2) - \epsilon \\ &= \tilde{W}^T\hat{\boldsymbol{\sigma}} + \hat{W}^T\hat{\sigma}'\tilde{V}^T\boldsymbol{\mu} + \bar{w} \end{aligned} \tag{4.2.25}$$

where $\bar{w} = -\mathcal{O}(\|\tilde{Z}\|^2) - \epsilon = W^T(\hat{\boldsymbol{\sigma}} - \boldsymbol{\sigma}) - \hat{W}^T\sigma'\tilde{V}^T\boldsymbol{\mu} - \epsilon$ and it is bounded by:

$$\begin{aligned} \|\bar{w}\| &\leq 2\sqrt{n_2+1}W^* + \frac{a^*}{4}\|\tilde{V}\|(\|\tilde{W}\| + W^*)\mu^* + \epsilon^* \\ &\leq \gamma_1\|\tilde{Z}\|^2 + \gamma_2\|\tilde{Z}\| + \gamma_3 \end{aligned} \tag{4.2.26}$$

where $\gamma_1 = \frac{a^*}{4}, \gamma_2 = \frac{a^*}{4}W^*\mu^*, \gamma_3 = 2\sqrt{n_2+1}W^* + \epsilon^*$

Assumption 4.2.4. Assumption 3.4.1 holds, where

$$C \triangleq \max\left(\frac{2}{\bar{q}}\Upsilon,\ \ 2\left(\frac{\theta_1^2}{k_e^2} + \frac{\theta_2}{k_e}\right)^{\frac{1}{2}}\right) \tag{4.2.27}$$

is a radius of a ball B_C containing Γ, and

$$\begin{aligned} \theta_1 &= \left(\sqrt{n_2+1} + \delta + \frac{a^*}{4}V^*\mu^*\right)\|P\bar{B}_m\|, \\ \theta_2 &= \frac{k_e}{2}{Z^*}^2 + \|P\bar{B}_m\|W^*\left(\delta + \frac{a^*}{4}V^*\mu^*\right), \\ k_9 &= \alpha_1(h^B\|\tilde{P}\bar{B}_m\| + \|P\bar{B}_m\|), \\ k_{10} &= 2\alpha_2(h^B\|\tilde{P}\bar{B}_m\| + \|P\bar{B}_m\|), \\ k_{11} &= 2\|P\bar{B}_m\|\gamma_1,\ k_{12} = (2\gamma_3\|P\bar{B}_m\| + k_e{Z^*}^2), \\ k_{14} &= \|P\bar{B}_m\|\gamma_2,\ \Upsilon \triangleq (k_9 + k_{14})^2 + (k_{10} + k_{12}) \end{aligned} \tag{4.2.28}$$

Define the Lyapunov function level sets Ω_α and Ω_β

$$\begin{aligned} \Omega_\alpha &= \{\boldsymbol{\zeta} \in B_R \mid L \leq \alpha \ \triangleq \min_{\|\boldsymbol{\zeta}\|=R} L\} \\ \Omega_\beta &= \{\boldsymbol{\zeta} \in B_R \mid L \leq \beta \ \triangleq \max_{\|\boldsymbol{\zeta}\|=C} L\} \end{aligned} \tag{4.2.29}$$

Theorem 4.2.1. Let the assumption 4.2.1, 4.2.2, 4.2.3 and 4.2.4 hold. Consider the following weight adaptation laws:

$$\begin{aligned}\dot{\hat{W}} &= -\Gamma_W \left[\hat{\boldsymbol{\sigma}}\hat{\boldsymbol{E}}^T P\bar{B}_m \mathrm{sgn}(H_{\bar{u}}) + k_e\|\hat{\boldsymbol{E}}\|\hat{W}\right] \\ \dot{\hat{V}} &= -\Gamma_V \left[\boldsymbol{\mu}\hat{\boldsymbol{E}}^T P\bar{B}_m \mathrm{sgn}(H_{\bar{u}})\hat{W}^T\hat{\sigma}' + k_e\|\hat{\boldsymbol{E}}\|\hat{V}\right]\end{aligned} \tag{4.2.30}$$

for $\Gamma_V, \Gamma_W > 0$. If the initial errors belong to the compact set Ω_α, the signals $\boldsymbol{E}, \tilde{\boldsymbol{E}}, \tilde{W}$ and $\tilde{V}$ in the closed-loop system are ultimately bounded with the ultimate bound $C\sqrt{\frac{\lambda_{max}(T)}{\lambda_{min}(T)}}$.

Proof. See Appendix A.7. □

4.3 Application to Guided Munitions

The Joint Direct Attack Munition (JDAM) is a guidance tail kit that converts existing unguided free-fall bombs into accurate munitions. The unit attaches directly to the iron bomb, and directs it to the target through controlled tail fin movements. With the addition of the tail section that contains an inertial navigational system and a global positioning system guidance control unit, JDAM upgrades the existing inventory of general purpose bombs. A schematic of a JDAM is shown in Figure 34. The design challenge is to synthesize a single adaptive autopilot to provide adequate control and performance for a family of guided munitions using only an approximate aerodynamic data. Ideally, a single controller for these guided munitions would be designed to handle several different configurations without compromising performance, thereby reducing the time required for developing each new JDAM variant as well as minimizing reliance on high-fidelity wind tunnel aerodynamic data for autopilot design. The ability of NN-based adaptive control to correct for parametric uncertainty and unmodeled dynamics leads to the conclusion that it is a promising method for achieving the design goals of the JDAM program. Since JDAM is a tail controlled munition, its transfer function from fin deflection to normal acceleration has a non-minimum phase zero. The approach in [64] was limited to feedback linearization

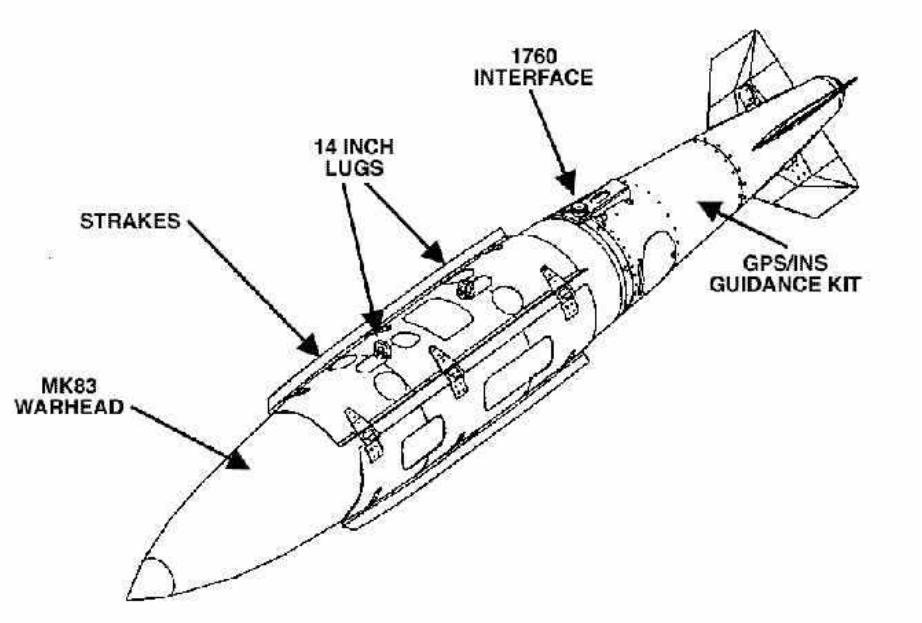

Figure 34: A schematic diagram of JDAM

of the minimum phase inner loop. The non-minimum phase outer loop was closed using a conventional PI controller. The previous work adapted uncertainty only in the moment equation of the inner loop, but did not adapt the force equation of the outer loop. Hence it required accurate knowledge of the force derivative coefficients in the outer loop. Here we implement the controller scheme proposed in Figure 33 which can reduce the dependence on knowledge of force derivatives in the outer loop. Since feedback linearization is not implemented, we can apply a simple control system where the existing controller and the true plant can remain largely unknown; only information required is knowledge of the relative degree of the true plant. Section 4.3.2 presents a method for limiting the command to compensate for poor tracking when control authority is diminished due to high angles of attack flight.

4.3.1 Numerical Results

Consider the following short-period approximation of the vehicle longitudinal dynamics with acceleration at the c.g. as a measured output.

$$\begin{aligned} \begin{bmatrix} \dot{\alpha} \\ \dot{q} \end{bmatrix} &= \begin{bmatrix} Z_\alpha/U_0 & 1 \\ M_\alpha & M_q \end{bmatrix} \begin{bmatrix} \alpha \\ q \end{bmatrix} + \begin{bmatrix} Z_\delta/U_0 \\ M_\delta \end{bmatrix} \delta \\ A_z &= Z_\alpha \alpha + Z_\delta \delta \end{aligned} \tag{4.3.1}$$

This yields the following transfer function from the fin deflection to acceleration.

$$G_{A_z,\,\delta} = \frac{Z_\delta s^2 - Z_\delta M_q s + Z_\alpha M_\delta - M_\alpha Z_\delta}{s^2 - (\frac{Z_\alpha}{U_0} + M_q)s + \frac{Z_\alpha M_q}{U_0} - M_\alpha} \tag{4.3.2}$$

The zeros of this transfer function are determined by the properties of the stability derivatives. In general all of the stability derivatives in (4.3.2) are negative and the following holds

$$|Z_\alpha M_\delta| > |M_\alpha Z_\delta| \tag{4.3.3}$$

Then (4.3.2) has one zero in the LHP and one zero in the RHP and is thus confirmed to be non-minimum phase. The non-minimum phase zeros can be addressed by a "virtual" acceleration sensor; the implementation of which allows us to place the non-minimum zeros far enough from the origin so that they become ignorable in the design [64]. Consider again the short-period approximation of the vehicle's longitudinal dynamics, but now with acceleration measured at a favorable location different from the c.g.

$$\begin{aligned} \begin{bmatrix} \dot{\alpha} \\ \dot{q} \end{bmatrix} &= \begin{bmatrix} Z_\alpha/U_0 & 1 \\ M_\alpha & M_q \end{bmatrix} \begin{bmatrix} \alpha \\ q \end{bmatrix} + \begin{bmatrix} Z_\delta/U_0 \\ M_\delta \end{bmatrix} \delta \\ A_{zIMU} &= A_z + l_x \dot{q} \\ &= (Z_\alpha + l_x M_\alpha)\alpha + l_x M_q q + (Z_\delta + l_x M_\delta)\delta \end{aligned} \tag{4.3.4}$$

where l_x represents the distance $(x_{IMU} - x_{cg})$ i.e. $l_x < 0$ when the Inertial Measurement Unit (IMU) is located forward of the c.g. The transfer function from fin

deflection to acceleration is then given by

$$G_{A_{z_{IMU}},\,\delta} = \frac{(Z_\delta + l_x M_\delta)s^2 + \left(\frac{l_x}{U_0}(M_\alpha Z_\delta - M_\delta Z_\alpha) - Z_\delta M_q\right)s + Z_\alpha M_\delta - M_\alpha Z_\delta}{s^2 - (\frac{Z_\alpha}{U_0} + M_q)s + \frac{Z_\alpha M_q}{U_0} - M_\alpha} \tag{4.3.5}$$

By adjusting l_x, it is possible to ensure that the zeros are sufficiently far from the origin to allow their effects to be neglected in the design. This condition facilitates the use of a low frequency approximation to neglect the zeros entirely, thereby ensuring a stable closed-loop system. Application of the low frequency approximation ($s \approx 0$ in the numerator) results in

$$\hat{G}_{A_{z_{IMU}},\,\delta} = \frac{Z_\alpha M_\delta - M_\alpha Z_\delta}{s^2 - (\frac{Z_\alpha}{U_0} + M_q)s + \frac{Z_\alpha M_q}{U_0} - M_\alpha} \tag{4.3.6}$$

Now we have a relative degree 2 approximate system dynamics from fin deflection to acceleration measured at the virtual IMU. In state space form, it can be expressed as:

$$\begin{aligned} \begin{bmatrix} \dot{\hat{\alpha}} \\ \dot{\hat{q}} \end{bmatrix} &= \begin{bmatrix} Z_\alpha/U_0 & 1 \\ M_\alpha & M_q \end{bmatrix} \begin{bmatrix} \hat{\alpha} \\ \hat{q} \end{bmatrix} + \begin{bmatrix} 0 \\ M_\delta \end{bmatrix} \delta \\ \hat{y} &= (Z_\alpha - \frac{Z_\delta}{M_\delta} M_\alpha)\hat{\alpha} \end{aligned} \tag{4.3.7}$$

where $\hat{\alpha}$ and $\hat{q}$ represent approximate model states and $\hat{y}$ denotes approximate model output. For simplicity let y be $A_{z_{IMU}}$ from now on and (4.3.7) will be used for designing a reference model.

A 10%-to-90% rise time criteria is used as the performance specification in this application. This criteria removes the effect of the time delay and the initial curvature characteristics of systems whose relative degree is greater than one [64]. The desired performance is scheduled according to the dynamic pressure as in Figure 35. The transient-response simulation is performed by commanding ramp inputs in normal acceleration as in Figure 36 to avoid the actuator rate limits (100 deg/sec). The existing controller gains of a representative guided munition [64] for a single flight

Table 1: Flight Conditions for Simulation

Mach Number	Altitude (Kft)	Dynamic Pressure (psf)
0.8	30	281.6
0.8	20	435.7
0.8	10	652
1.0	30	439.9
1.0	20	680.8
1.0	10	1019
1.2	30	633.5
1.2	20	980.4
1.2	10	1467

condition (Mach 1.2 and 10 Kft) were used. Flight conditions where linear simulations of a representative guided munition are performed are listed in Table 1. Thus this study will illustrate that with adaptation it is possible to eliminate the need for gain scheduling. Since r = 2 within the bandwidth of the control design in this application, a simple 2^{nd}-order linear system is used as a reference model.

$$\begin{aligned} y_m &= G(s)y_c \\ \text{where } \ G(s) &= \frac{w^2}{s^2 + 2\zeta w s + w^2} \end{aligned} \tag{4.3.8}$$

$G(s)$ has two poles at $-\zeta w \pm w\sqrt{1-\zeta^2}$ and we used $w = 9.9, \zeta = 0.8$ when the dynamic pressure is over 500 psf, and $w = 3.3, \zeta = 0.8$ when the dynamic pressure is less than 500 psf. Then the 2^{nd} derivative of y_m can be represented as:

$$\ddot{y}_m = -2\zeta w \dot{y}_m - w^2 y_m + w^2 y_c \tag{4.3.9}$$

Let the 2^{nd} derivative of y be

$$\ddot{y} = -2\zeta w \dot{y} - w^2 y + w^2(y_c - u_{ad} + \Delta) \tag{4.3.10}$$

where $\Delta(y_c, y, \dot{y}, u, u_{ec}) = \frac{1}{w^2}(\ddot{y} + 2\zeta w \dot{y} + w^2 y) - y_c - u + u_{ec}$

With the definition of $e \triangleq y_m - y$, we derive the following error dynamics.

$$\begin{aligned} \ddot{e} &= -2\zeta w \dot{e} - w^2 e + w^2(u_{ad} - \Delta) \\ e &= G(s)(u_{ad} - \Delta) \end{aligned} \tag{4.3.11}$$

Reformulating the modeling error as detailed in Section 4.1,

$$e = G(s)h_{\bar{u}}(u_{ad} - \bar{\Delta}) \tag{4.3.12}$$

For the SPR filter approach suggested in Section 4.1.2, the 1^{st}-order low-pass filter $T(s)$ is chosen as:

$$T(s) = \frac{1}{s+1} \tag{4.3.13}$$

It is not difficult to verify that $\bar{G}(s) \triangleq G(s)T^{-1}(s)$ is SPR.

$$\begin{aligned} Re[\bar{G}(jz)] &= Re\left[\frac{w^2(1+jz)(w^2-z^2-2j\zeta wz)}{(w^2-z^2+2j\zeta wz)(w^2-z^2-2j\zeta wz)}\right] \\ &= w^2\frac{w^2+(2\zeta w-1)z^2}{(w^2-z^2)^2+4(\zeta wz)^2} > 0 \quad \text{for all } z \geq 0 \end{aligned} \tag{4.3.14}$$

Then the error dynamic system in (4.3.12) can be given in the form of (4.1.30).

$$e = \bar{G}(s)h_{\bar{u}}(\tilde{W}^T\boldsymbol{\phi} + \delta_f - \epsilon_f) \tag{4.3.15}$$

A Gaussian Radial Basis Function NN with seven neurons and a bias term is used as the adaptive element. The input vector to the NN is composed of the current and delayed values for y and v including a bias term. The learning rate $F = 2$ and the σ-modification coefficient $k_\sigma = 0.005$ are used for the update law. Figure 37 shows one of the simulation results at Mach 1 and 20 Kft. The dash-dotted line is the reference model response to the ramp command in Figure 36, the response with NN (solid line) shows almost the same rise time performance as the reference model while the vehicle shows slow response without the NN. The rise time performance at several flight conditions is summarized in Figure 38. "ECA NN" in the legend stands for existing controller augmentation with NN. "w/o NN" in Figure 38 indicates results of using the existing controller gains given at one flight condition (Mach 1.2 and 10 Kft), where it overlaps with the existing autopilot gain for that flight condition. The NN controller exhibits superior rise time performance in comparison to the response without NN. Figure 39 shows similar transient response using the error observer approach suggested in Section 4.1.1.

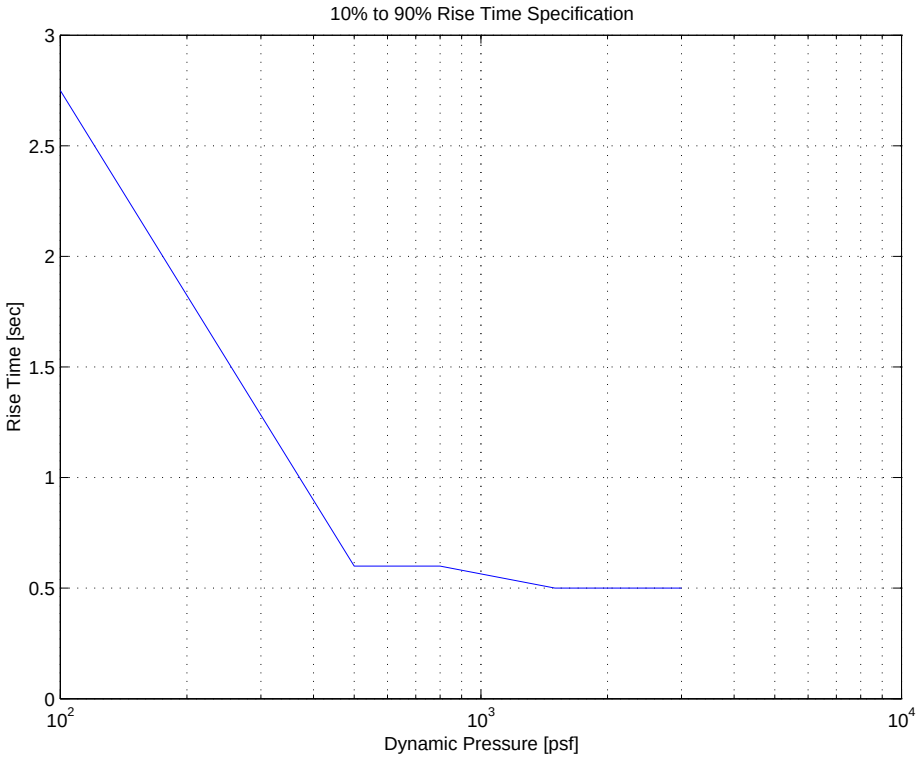

Figure 35: 10%-to-90% rise time specification

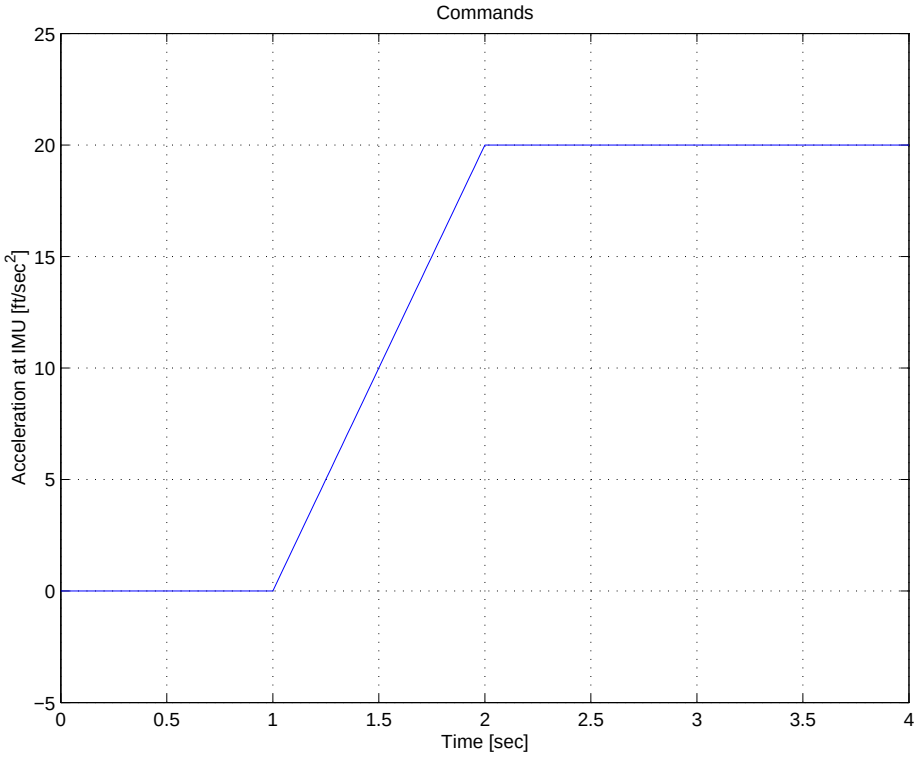

Figure 36: Transient-test commands

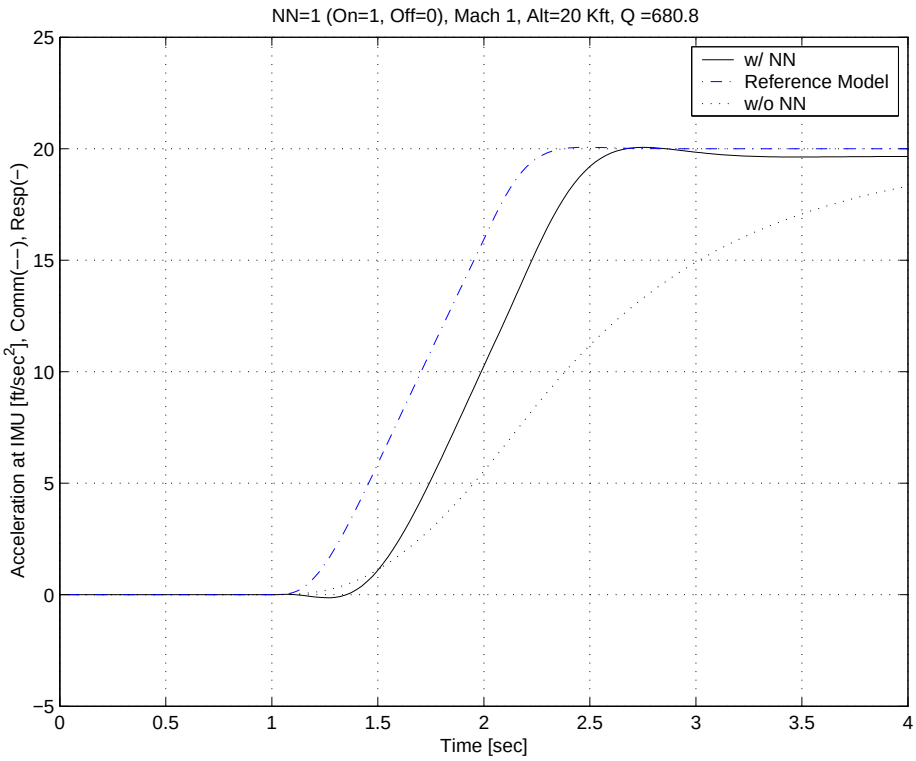

Figure 37: Transient response at Mach 1 and 20 Kft with SPR filter approach

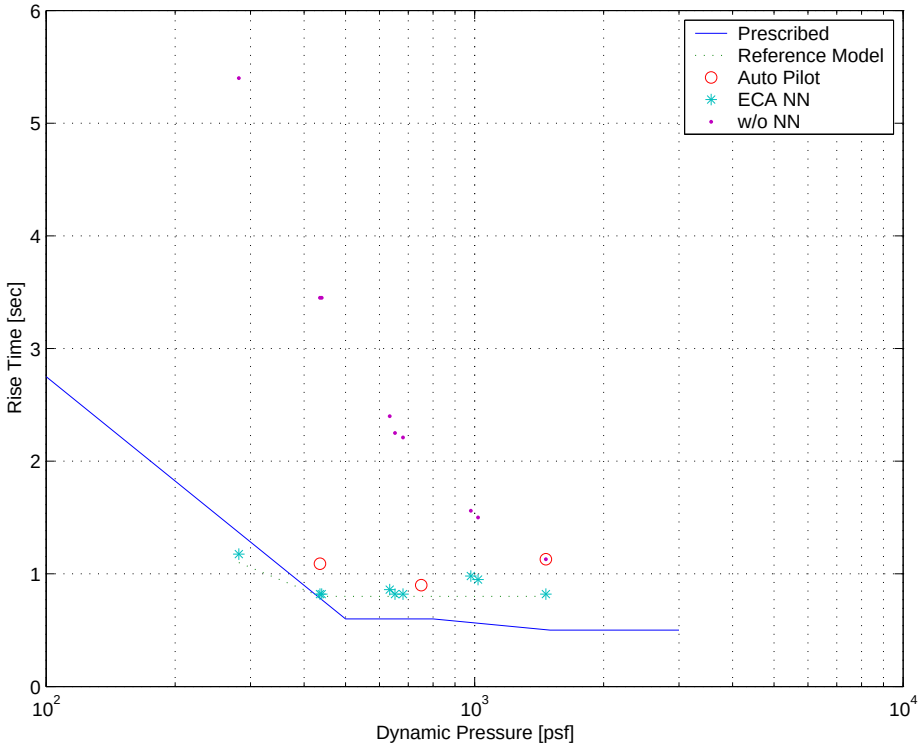

Figure 38: 10%-to-90% rise time comparison

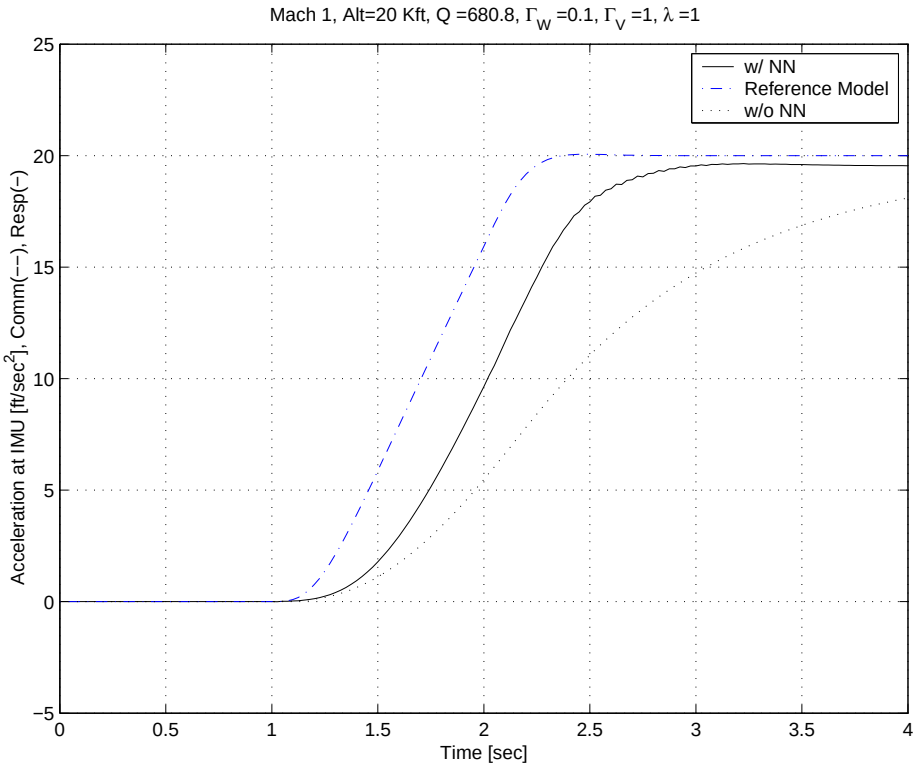

Figure 39: Transient response at Mach 1 and 20 Kft with error observer approach

4.3.2 Command Limiting Using Angle of Attack

Several research projects have demonstrated the necessity of PCH in the case of actuator saturations [41, 40, 57]. As explained in Section 3.5, PCH estimates the control discrepancy between the commanded control and the achievable control due to the actuator limits, and modifies the reference model output so that it is performed within the capacity of the actuator. Inspired by the idea of PCH, we propose to limit a command when a state causes unfavorable output response. In the JDAM application the pitching moment control sensitivity abruptly vanishes and lacks in control power to control at high angle of attack (AoA). As the munition begins to depart, it cannot recover due to this lack of control power. Hence it would be desirable to keep the AoA below a certain level. The earlier work in [64] limited the guidance command to avoid high AoA. This method requires knowledge of the force derivative to design the command limit. In the approach adopted here, the AoA limiting signal is defined as

the AoA excess beyond a prescribed maximum value, and is zero when it is below the prescribed maximum. This signal is used to estimate the amount of output command to be subtracted from the guidance command. The limiting action both reduces the magnitude of the output response by decreasing the reference model output, and ensures bounded response even in the presence of large guidance command inputs. It reduces the dependence of the design on knowledge of the force derivative, Z_α, knowledge of which was required in the existing design. An alternative approach for dealing with this problem can be found in [65, 66, 67].

A nonlinear model data table in the longitudinal channel at Mach 0.8 is considered. It is parameterized by AoA (0 to 26 deg) and longitudinal control deflection angle (-15 to 15 deg). Figure 40 shows results similar to those achieved with a linear model both with and without NN. To simulate the high AoA phenomenon, we choose a model for pitching moment at -20 deg of control surface deflection so that the control power (M_δ) vanishes at high control surface deflection. The control actuator limits are ± 25 deg. A consequence of this choice of model is that the munition does not have sufficient control power to trim at a high AoA flight condition. The objective is to limit the command, y_c, by an amount corresponding to the AoA excess to avoid the oscillatory phenomena due to lack of control power. The limiting signal (α_l) is defined as

$$\alpha_l \triangleq \begin{cases} 0 & \text{if } \alpha \leq \alpha_{max}, \\ \alpha - \alpha_{max} & \text{if } \alpha > \alpha_{max} \end{cases} \tag{4.3.16}$$

where $\alpha_{max} = 22$ deg. The command limiting signal y_l is calculated using the plant model (4.3.7) with parametric uncertainty in the aerodynamic coefficients.

$$y_l = (\hat{Z}_\alpha - \frac{\hat{Z}_\delta}{\hat{M}_\delta}\hat{M}_\alpha)\alpha_l \tag{4.3.17}$$

and is subtracted from y_c as depicted in Figure 41.

We will derive error dynamics incorporated with the command limiting signal. Consider a SISO minimum-phase nonlinear system as in (4.1.1) with relative degree

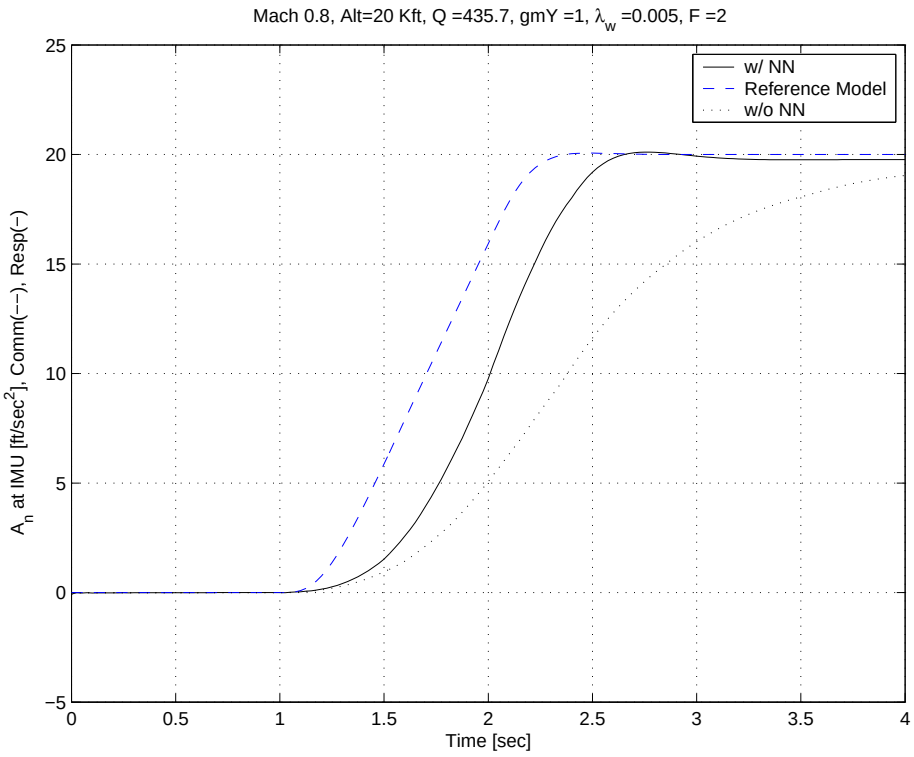

Figure 40: Nonlinear model at Mach 0.8 and 20 Kft

r and an existing controller:

$$\begin{aligned} \dot{\boldsymbol{x}}_c &= A_c \boldsymbol{x}_c + \boldsymbol{b}_c (y_{cl} - y) \\ u_{ec} &= C_c \boldsymbol{x}_c + D_c (y_{cl} - y) \end{aligned} \tag{4.3.18}$$

where $y_{cl} = y_c - y_l$ and A_c is Hurwitz. The system (4.1.1) can be transformed into a normal form as (4.1.2). Let the r^{th}-order reference model be expressed as:

$$\begin{aligned} \dot{\boldsymbol{y}}_m &= A_m \boldsymbol{y}_m + \boldsymbol{b}_m b_1 y_{cl} \\ y_m &= C_m \boldsymbol{y}_m \end{aligned} \tag{4.3.19}$$

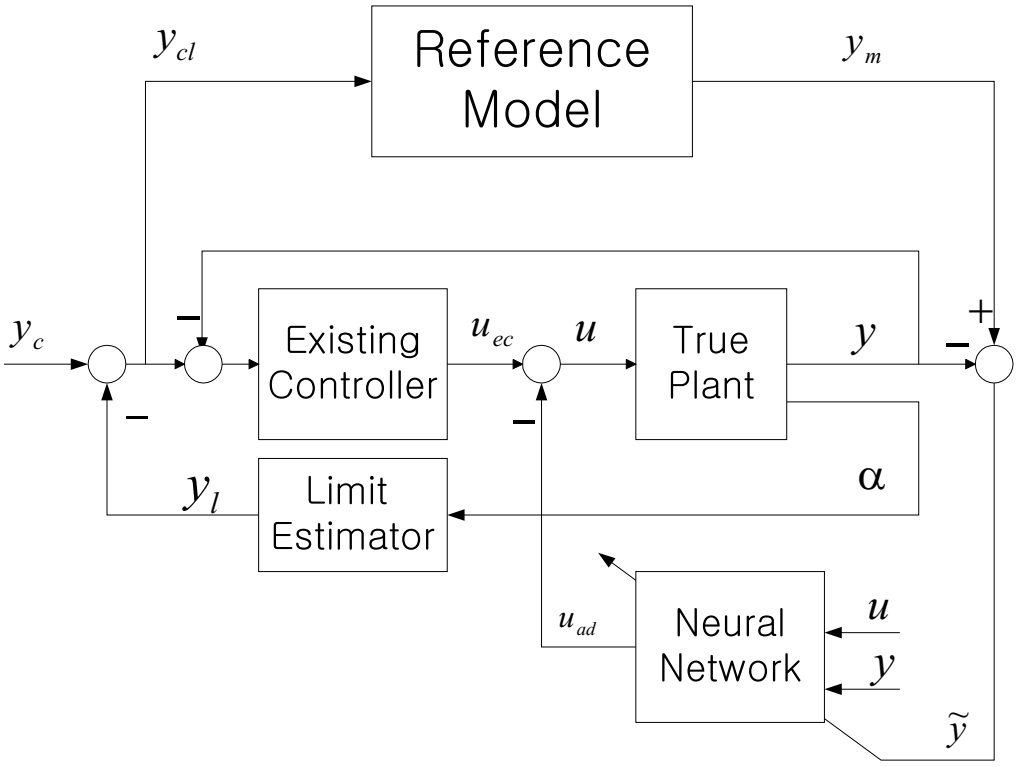

Figure 41: Adaptive control architecture with existing controller augmentation and command limiting

$$\boldsymbol{y}_m \triangleq \begin{bmatrix} y_m & \dot{y}_m & \cdots & y_m^{(r-1)} \end{bmatrix}^T$$

$$A_m = \begin{bmatrix} 0 & 1 & 0 & \cdots & 0 \\ 0 & 0 & 1 & \cdots & 0 \\ \vdots & \vdots & \vdots & \ddots & \vdots \\ 0 & 0 & 0 & 0 & 1 \\ -a_1 & -a_2 & -a_3 & \cdots & -a_r \end{bmatrix}, \boldsymbol{b}_m = \begin{bmatrix} 0 \\ 0 \\ 0 \\ \vdots \\ 1 \end{bmatrix},$$

$$C_m = \begin{bmatrix} 1 & 0 & 0 & \cdots & 0 \end{bmatrix}$$

where A_m is Hurwitz. Then the r^{th} derivative of y_m is

$$y_m^{(r)} = C_r \boldsymbol{y}_m + D_r y_{cl} \tag{4.3.20}$$

where $C_r \triangleq C_m A_m^r = \begin{bmatrix} -a_1 & -a_2 & -a_3 & \cdots & -a_r \end{bmatrix}$ and $D_r = b_1$.
$y^{(r)}$ in (4.1.2) can be put in the following form.

$$\begin{aligned} y^{(r)} &= -a_r y^{(r-1)} \cdots - a_1 y + b_1(y_{cl} - u_{ad} + \Delta) \\ &= C_r \boldsymbol{y} + b_1(y_{cl} - u_{ad} + \Delta) \end{aligned} \tag{4.3.21}$$

where $\boldsymbol{y} \triangleq \begin{bmatrix} y & \dot{y} & \cdots & y^{(r-1)} \end{bmatrix}^T$ and $\Delta(y_{cl}, \boldsymbol{y}, u, u_{ec}) \triangleq \frac{1}{b_1}(y^{(r)} - C_r \boldsymbol{y}) - y_{cl} + u_{ad}$
Its state-space form is given by

$$\begin{aligned} \dot{\boldsymbol{y}} &= A_m \boldsymbol{y} + \boldsymbol{b}_m b_1(y_{cl} - u_{ad} + \Delta) \\ y &= C_m \boldsymbol{y} \end{aligned} \tag{4.3.22}$$

Let the error be defined as $e \triangleq y_m - y$, then we have the identical error dynamics as in (4.1.11).

$$\begin{aligned} \dot{\boldsymbol{E}} &= A_m \boldsymbol{E} + \boldsymbol{b}_m b_1(u_{ad} - \Delta) \\ \boldsymbol{z} &= C_m \boldsymbol{E} \end{aligned} \tag{4.3.23}$$

where $\boldsymbol{E} = \begin{bmatrix} e & \dot{e} & \cdots & e^{(r-1)} \end{bmatrix}^T$. Boundedness of all the error signals can be shown using the error observer approach in Section 4.1.1 or the SPR filter approach in Section 4.1.2, and its proof is omitted here.

A negative ramp command is used to produce a positive AoA, and its amplitude is increased to 35 ft/sec^2 so that a high AoA results in an oscillatory response. Figures 42 and 43 show the simulation results at Mach 0.8 and 20,000 ft (Q=435.7) without NN or command limiting. Its response is slow and starts to depart at around 5 seconds. The response with NN augmentation, but without command limiting is shown in Figures 44 and 45. With NN adaptation, the munition responds more quickly to the command, but encounters the effect of high AoA at around 2.5 seconds. Note the oscillatory response that ensues after 2.5 seconds. Figure 45 shows that the control is saturated after 2.5 seconds. The danger here is that a disturbance can cause a total loss of the munition at this flight condition. Figures 46 and 47 incorporate the NN with command limiting. As the AoA hits its limit, the command is modified to an amplitude of 32 ft/sec^2, and it keeps the AoA at the limit value avoiding control saturation to streamline command tracking within the allowed AoA range. Figures 48 and 49 show the results when parametric uncertainties are included in calculating y_l. Figures 48 and 49 show the acceptable tracking performance with 80% and 150% of the true value of $Z_\alpha - \frac{Z_\delta}{M_\delta} M_\alpha$ in (4.3.17), respectively. However, beyond the range of parametric uncertainty (80% - 150%), the munition falls into the region of oscillation. Thus, a reasonable estimate of the parameter is needed for the method.

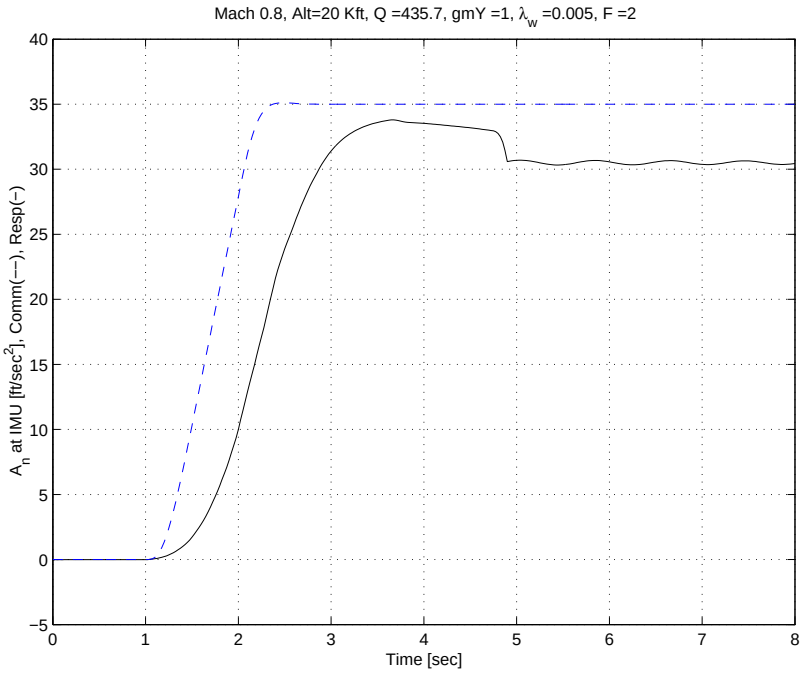

Figure 42: Nonlinear model without command limiting or NN at Mach 0.8 and 20 Kft

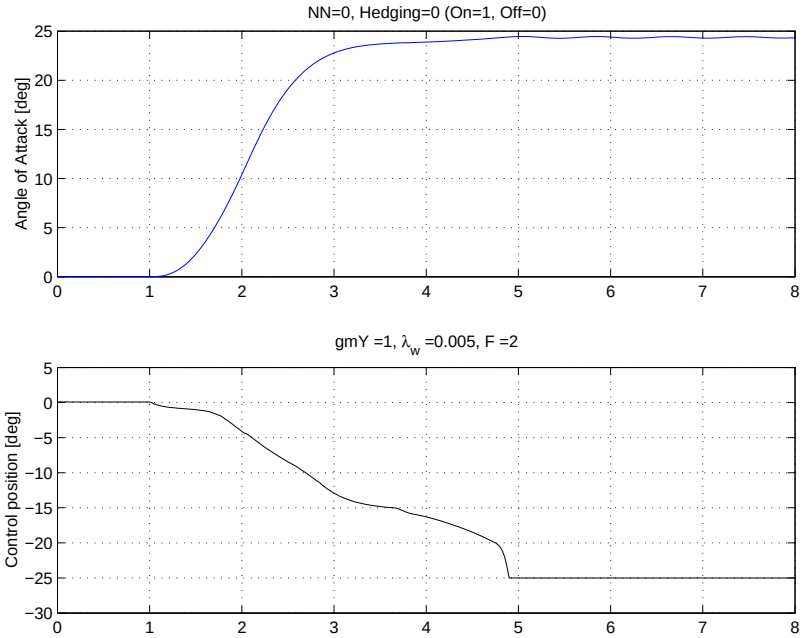

Figure 43: AoA and control effort without command limiting or NN at Mach 0.8 and 20 Kft

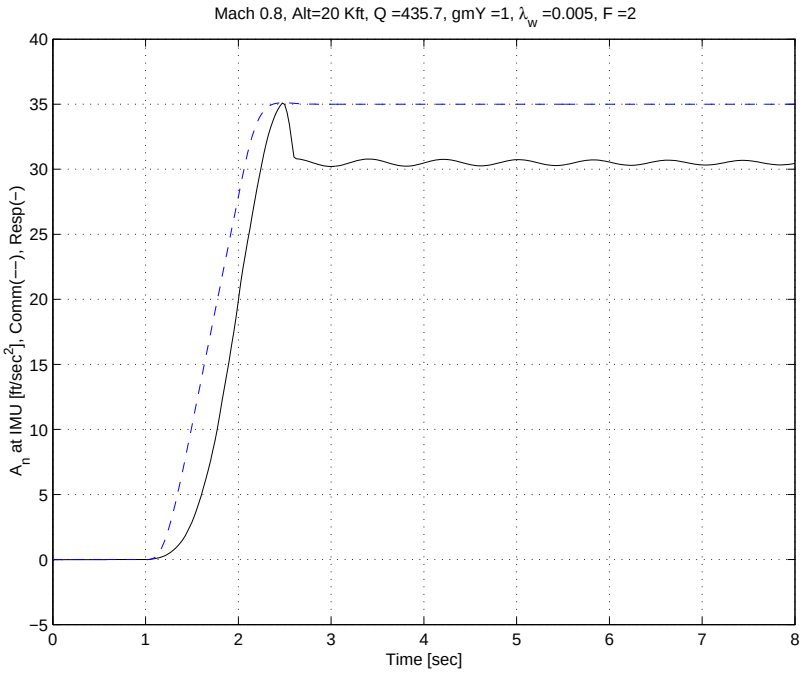

Figure 44: Nonlinear model without command limiting and with NN at Mach 0.8 and 20 Kft

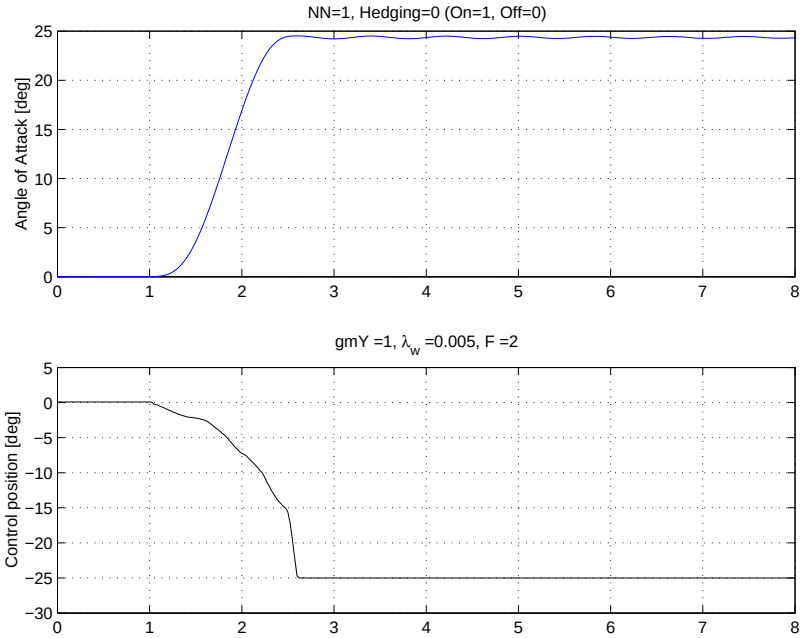

Figure 45: AoA and control effort without command limiting and with NN at Mach 0.8 and 20 Kft

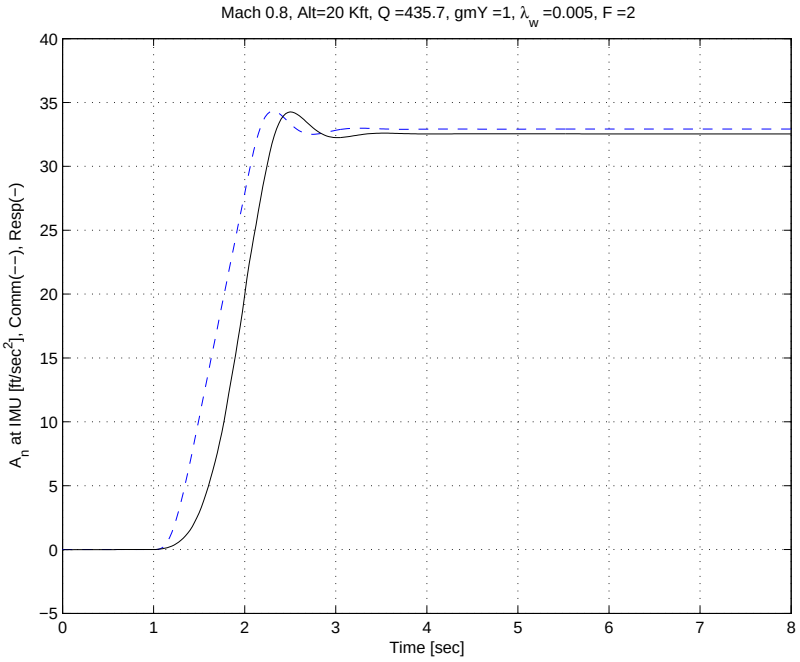

Figure 46: Nonlinear model with command limiting and NN at Mach 0.8 and 20 Kft

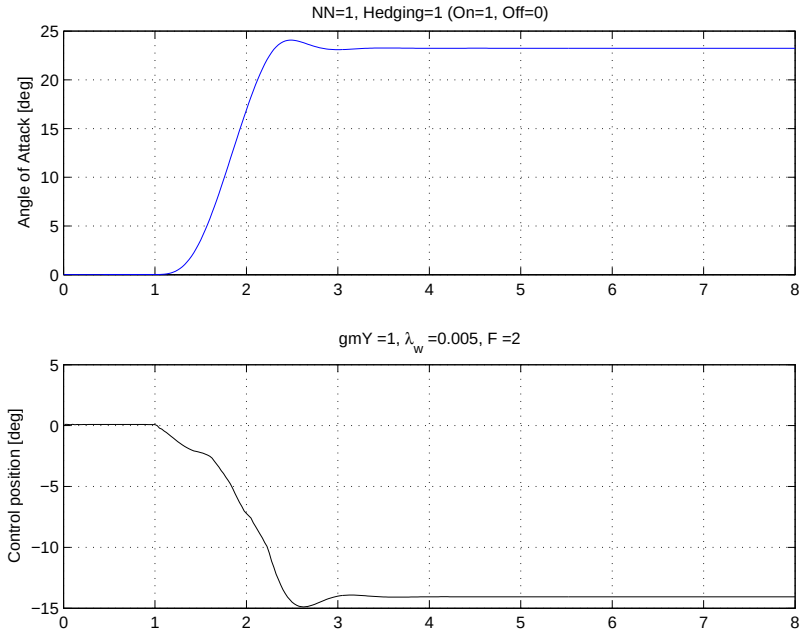

Figure 47: AoA and control effort with command limiting and NN at Mach 0.8 and 20 Kft

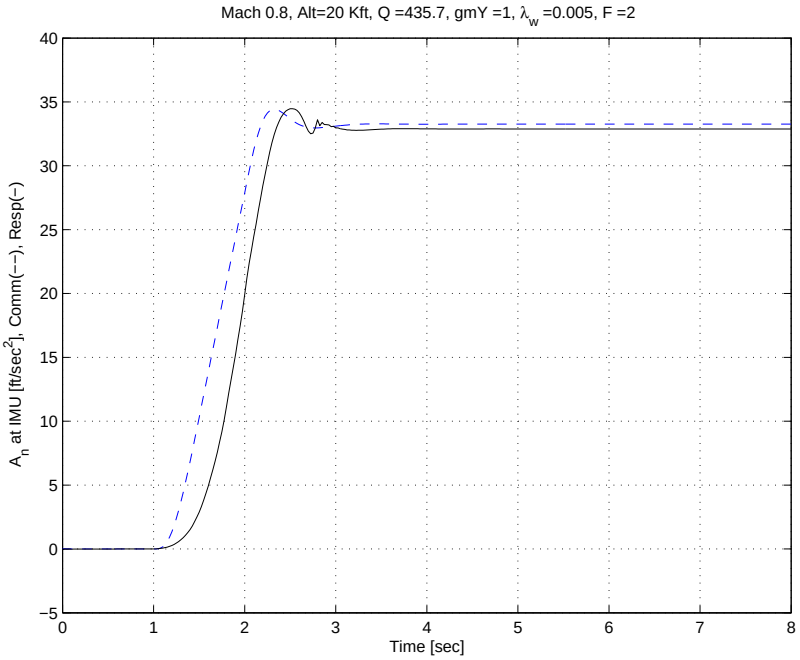

Figure 48: Command limiting and NN at Mach 0.8 and 20 Kft with parametric uncertainty in y_l (80%)

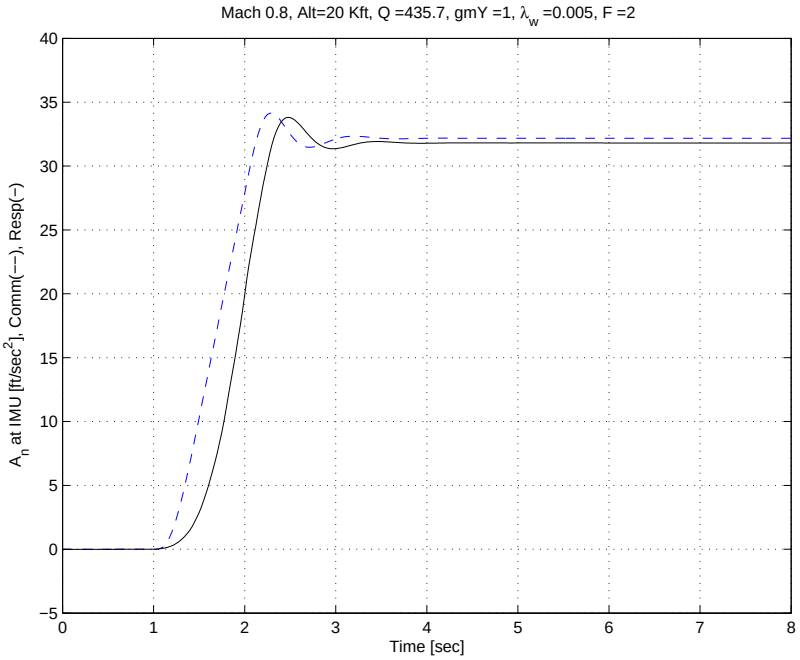

Figure 49: Command limiting and NN at Mach 0.8 and 20 Kft with parametric uncertainty in y_l (150%)

CHAPTER V

NN ADAPTIVE CONTROL WITH ASYMPTOTIC TRACKING

Early results on applications of NNs made use of linearly-parameterized networks to cancel the effect of modeling error on tracking performance. Barbalat's lemma can show that when the NN reconstruction error is zero, the tracking error asymptotically goes to zero. With nonlinearly-parameterized NNs the derivation of adaptive laws entails Taylor series expansion, which necessitates bounding of higher order terms in the derivative of the Lyapunov function [28]. Because of these higher order terms, the limiting result on asymptotic convergence of the tracking error to zero has yet to be obtained.

Here, using the Barbalat's lemma [68], we show that with nonlinearly-parameterized NNs, one can achieve asymptotic convergence of the tracking error to zero. For that we employ a projection operator in the adaptive laws [17] and the notion of adaptive bounding [69, 70].

5.1 System Description and Error Dynamics

For simplicity of presentation, we consider a SISO nonlinear system of the following form:

$$\begin{aligned} \dot{x}_i &= x_{i+1}, \quad i = 1, 2, \cdots, n-1 \\ \dot{x}_n &= f(\boldsymbol{x}, u) \end{aligned} \tag{5.1.1}$$

where $\boldsymbol{x} \in \mathcal{D}_x \subset \Re^n$ are measured, and $u \in \Re$ is the control input. The function $f(\boldsymbol{x}, u)$ may be unknown.

Assumption 5.1.1. $\partial f(\boldsymbol{x}, u)/\partial u$ is continuous and non-zero for every $(\boldsymbol{x}, u) \in \mathcal{D}_x \times \Re$, and its sign is known.

The control objective is to synthesize a state-feedback control law such that $\boldsymbol{x}(t)$ tracks a smooth reference trajectory $\boldsymbol{x}_m(t)$ asymptotically. Let $\hat{f}(\boldsymbol{x}, u)$ denote an approximate model for $f(\boldsymbol{x}, u)$ so that

$$f(\boldsymbol{x}, u) = \hat{f}(\boldsymbol{x}, u) + \Delta \tag{5.1.2}$$

where the modelling error is $\Delta(\boldsymbol{x}, u) = f(\boldsymbol{x}, u) - \hat{f}(\boldsymbol{x}, u)$. The model $\hat{f}(\boldsymbol{x}, u)$ should be chosen to be invertible with respect to its second argument.

Assumption 5.1.2. $\partial \hat{f}(\boldsymbol{x}, u)/\partial u$ is continuous and non-zero for every $(\boldsymbol{x}, u) \in \mathcal{D}_x \times \Re$.

Let the approximate function be recast as

$$v = \hat{f}(\boldsymbol{x}, u) \tag{5.1.3}$$

where v is called pseudo-control. Then the control law can be defined directly from (5.1.3)

$$u = \hat{f}^{-1}(\boldsymbol{x}, v) \tag{5.1.4}$$

The pseudo-control is composed of four signals:

$$v \triangleq x_m^{(n)} + v_c - v_{ad} + v_r \tag{5.1.5}$$

where $x_m^{(n)}$ is the n^{th} time derivative of $x_m(t)$, v_c is the output of a linear controller, and v_{ad} and v_r are adaptive terms used to cancel $\Delta(\boldsymbol{x}, u)$.

The reference model can be expressed in state space form as:

$$\dot{\boldsymbol{x}}_m = A_m \boldsymbol{x}_m + \boldsymbol{b}_m x_c \tag{5.1.6}$$

$$\boldsymbol{x}_m \triangleq \begin{bmatrix} x_m & \dot{x}_m & \cdots & x_m^{(n-1)} \end{bmatrix}^T$$

$$A_m = \begin{bmatrix} 0 & 1 & 0 & \cdots & 0 \\ 0 & 0 & 1 & \cdots & 0 \\ \vdots & \vdots & \vdots & \ddots & \vdots \\ 0 & 0 & 0 & 0 & 1 \\ -a_1 & -a_2 & -a_3 & \cdots & -a_n \end{bmatrix}, \boldsymbol{b}_m = \begin{bmatrix} 0 \\ 0 \\ 0 \\ \vdots \\ a_1 \end{bmatrix},$$

where $\boldsymbol{x}_m \in \Re^n$ are the states of the reference model, $x_c \in \Re$ is a bounded external command signal, and A_m is Hurwitz.

Let $e \triangleq x_m - x_1$. Then

$$e^{(n)} = -v_c + v_{ad} - v_r - \Delta \tag{5.1.7}$$

For simplicity, the linear controller is defined as:

$$v_c = k_1 e + k_2 \dot{e} + \cdots + k_n e^{(n-1)} \tag{5.1.8}$$

where the gains k_i are chosen such that the dynamics in (5.1.8) are asymptotically stable when $v_{ad} - v_r - \Delta = 0$. In state space form:

$$\dot{\boldsymbol{E}} = A\boldsymbol{E} + \boldsymbol{b}(v_{ad} - v_r - \Delta(\boldsymbol{x}, u)) \tag{5.1.9}$$

where $\boldsymbol{E} = \begin{bmatrix} e & \dot{e} & \cdots & e^{(n-1)} \end{bmatrix}^T$, and

$$A = \begin{bmatrix} 0 & 1 & 0 & \cdots & 0 \\ 0 & 0 & 1 & \cdots & 0 \\ \vdots & \vdots & \vdots & \ddots & \vdots \\ 0 & 0 & 0 & 0 & 1 \\ -k_1 & -k_2 & -k_3 & \cdots & -k_n \end{bmatrix}, \boldsymbol{b} = \begin{bmatrix} 0 \\ 0 \\ 0 \\ \vdots \\ 1 \end{bmatrix}.$$

Define the following signals

$$\begin{aligned} v_l &\triangleq x_m^{(n)} + v_c \\ v^* &\triangleq \hat{f}(\boldsymbol{x}, f^{-1}(\boldsymbol{x}, v_l)) \end{aligned} \tag{5.1.10}$$

$v_{ad} - v_r - \Delta$ can be expressed as:

$$\begin{aligned} v_{ad} - v_r - \Delta(\boldsymbol{x}, u) &= v_{ad} - v_r - f(\boldsymbol{x}, u) + \hat{f}(\boldsymbol{x}, u) \\ &= -f(\boldsymbol{x}, \hat{f}^{-1}(\boldsymbol{x}, v)) + v_l \\ &= -f(\boldsymbol{x}, \hat{f}^{-1}(\boldsymbol{x}, v)) + f(\boldsymbol{x}, \hat{f}^{-1}(\boldsymbol{x}, v^*)) \end{aligned} \tag{5.1.11}$$

Applying the mean value theorem,

$$\begin{aligned} v_{ad} - v_r - \Delta &= f_{\bar{v}}(v^* - v) \\ &= f_{\bar{v}}[v_{ad} - v_r - v_l + \hat{f}(x, f^{-1}(\boldsymbol{x}, v_l))] \\ &= f_{\bar{v}}[v_{ad} - v_r - \bar{\Delta}(\boldsymbol{x}, v_l)] \end{aligned} \tag{5.1.12}$$

where $\bar{\Delta} = v_l - \hat{f}(\boldsymbol{x}, f^{-1}(\boldsymbol{x}, v_l))$, and

$$f_{\bar{v}} \triangleq \frac{\partial f}{\partial u}\frac{\partial u}{\partial v}\bigg|_{v=\bar{v}}, \ \bar{v} = \theta v + (1-\theta)v^*, \text{ and } \ 0 \leq \theta(v) \leq 1 \tag{5.1.13}$$

with the following bounds:

$$f^B \triangleq \max_{\boldsymbol{x}, u \in \mathcal{D}} |f_{\bar{v}}|, \quad F \triangleq \max_{\boldsymbol{x}, u \in \mathcal{D}} \left| \frac{d}{dt}\left(\frac{1}{f_{\bar{v}}}\right)\right| \tag{5.1.14}$$

We have the following error dynamics.

$$\dot{\boldsymbol{E}} = A\boldsymbol{E} + \boldsymbol{b} f_{\bar{v}}(v_{ad} - v_r - \bar{\Delta}(\boldsymbol{x}, v_l)) \tag{5.1.15}$$

Since A is Hurwitz, then for any $Q > 0$, there exists a unique $P > 0$ that solves the Lyapunov equation:

$$A^T P + PA = -Q \tag{5.1.16}$$

5.2 Adaptive Control Augmentation

The adaptive term is defined as:

$$v_{ad} = \hat{W}^T \boldsymbol{\sigma}(\hat{V}^T \boldsymbol{\mu}) \tag{5.2.1}$$

where $\boldsymbol{\mu}$ is the input to the NN. The NN weights are updated using the following parameter projection algorithm as in Section 3.4.3.

$$\begin{aligned}\dot{\hat{W}} &= \Gamma_W Proj(\hat{W}, -\text{sgn}(h_{\bar{v}})\hat{\boldsymbol{\sigma}}\hat{\boldsymbol{E}}^T P\boldsymbol{b}) \\ \dot{\hat{V}} &= \Gamma_V Proj(\hat{V}, -\text{sgn}(h_{\bar{v}})\boldsymbol{\mu}\hat{\boldsymbol{E}}^T P\boldsymbol{b}\hat{W}^T\hat{\sigma}')\end{aligned} \tag{5.2.2}$$

where Γ_V, Γ_W are positive definite matrices. Using Taylor series expansion of $W^T\boldsymbol{\sigma}$ at $W = \hat{W}, V = \hat{V}$, one gets:

$$W^T\boldsymbol{\sigma} = W^T\hat{\boldsymbol{\sigma}} - \hat{W}^T\hat{\sigma}'\tilde{V}^T\boldsymbol{\mu} + \mathcal{O}(\|\tilde{Z}\|^2) \tag{5.2.3}$$

where $\mathcal{O}(\|\tilde{Z}\|^2)$ represents the higher order terms. Then

$$\begin{aligned}v_{ad} - \bar{\Delta} &= \hat{W}^T\hat{\boldsymbol{\sigma}} - W^T\boldsymbol{\sigma} - \epsilon \\ &= \tilde{W}^T\hat{\boldsymbol{\sigma}} + \hat{W}^T\hat{\sigma}'\tilde{V}^T\boldsymbol{\mu} - \mathcal{O}(\|\tilde{Z}\|^2) - \epsilon \\ &= \tilde{W}^T\hat{\boldsymbol{\sigma}} + \hat{W}^T\hat{\sigma}'\tilde{V}^T\boldsymbol{\mu} + \bar{w}\end{aligned} \tag{5.2.4}$$

where $\bar{w} = -\mathcal{O}(\|\tilde{Z}\|^2) - \epsilon = W^T(\hat{\boldsymbol{\sigma}} - \boldsymbol{\sigma}) - \hat{W}^T\sigma'\tilde{V}^T\boldsymbol{\mu} - \epsilon$. From (3.4.6) and (3.4.7), we can derive the following bound:

$$\begin{aligned}\|\bar{w}\| &\leq 2\sqrt{n_2+1}W^* + \|\hat{W}\hat{\sigma}'(\hat{V}^T\boldsymbol{\mu} - V^T\boldsymbol{\mu})\| + \epsilon^* \\ &\leq 2\sqrt{n_2+1}W^* + \epsilon^* + \|\hat{W}\|\delta\sqrt{n_2+1} + \frac{a^*}{4}V^*\|\hat{W}\|\|\boldsymbol{\mu}\|\end{aligned} \tag{5.2.5}$$

where a^* is the maximum of activation potentials, and δ is defined in (2.3.11). This implies that

$$\|\bar{w}\| \leq \boldsymbol{s}^T\boldsymbol{\phi} \tag{5.2.6}$$

where $\boldsymbol{s} = \begin{bmatrix}1 & \|\hat{W}\| & \|\boldsymbol{\mu}\|\|\hat{W}\|\end{bmatrix}^T$ is a known vector signal and $\boldsymbol{\phi} = \begin{bmatrix}\phi_0 & \phi_1 & \phi_2\end{bmatrix}^T$ is an unknown constant vector. The following robustifying signal can be used to compensate for $\bar{w}$:

$$v_r \triangleq \text{sgn}(\boldsymbol{E}^T P\boldsymbol{b})\boldsymbol{s}^T\hat{\boldsymbol{\phi}} \tag{5.2.7}$$

where $\hat{\boldsymbol{\phi}}$ is updated according to the following differential equation [71, 70]

$$\dot{\hat{\boldsymbol{\phi}}} = \Gamma\boldsymbol{s}\|\boldsymbol{E}^T P\boldsymbol{b}\| \tag{5.2.8}$$

where $\Gamma > 0$.

With definition of the Lyapunov function level sets,

$$\begin{aligned} \Omega_\alpha &= \{\boldsymbol{\zeta} \in B_R \mid L \leq \alpha \triangleq \min_{\|\boldsymbol{\zeta}\|=R} L\} \\ \Omega_\beta &= \{\boldsymbol{\zeta} \in B_R \mid L \leq \beta \triangleq \max_{\|\boldsymbol{\zeta}\|=C} L\} \end{aligned} \tag{5.2.9}$$

we can now state the following theorem.

Theorem 5.2.1. Let Assumptions 5.1.1 and 5.1.2 hold. Then there exists a positive invariant set $\mathcal{D}_\zeta$ in the space of the error variables $\boldsymbol{\zeta} = \begin{bmatrix} \boldsymbol{E}^T & \tilde{W}^T & (vec\tilde{V})^T & \tilde{\boldsymbol{\phi}}^T \end{bmatrix}^T$ wherein the control law given by (5.1.4), (5.1.5) and the adaptive laws (5.2.2) and (5.2.8) ensure, for all $\boldsymbol{\zeta}(0) \in \Omega_\alpha$, that $\tilde{W}, \tilde{V}, \tilde{\boldsymbol{\phi}}$ are ultimately bounded, and that $\boldsymbol{E}$ asymptotically approaches zero.

Proof. See Appendix A.8. □

CHAPTER VI

CONCLUSIONS AND RECOMMENDATIONS FOR FUTURE RESEARCH

6.1 Conclusion

This thesis introduced several methods of NN-based adaptive output feedback control of uncertain nonlinear systems. It discussed two approaches for augmenting NNs with linear controllers: input/output feedback linearization and augmentation of an existing controller. The former included a novel approach to approximate input/output feedback linearization that employs a pole shifting. The latter introduced a control methodology of the NN augmentation of existing controllers using a simple reference model and extended it to MIMO systems.

Lack of full state information was dealt with by either the error observer approach or the SPR filter approach, with special attention given to improvements and extensions of the adaptation laws that apply to these approaches. The weight adaptation laws were categorized according to a method used to limit growth in the network weights. The methods consisted of σ-modification, e-modification and projection. Any combination of approaches and modifications can be employed with guaranteed ultimate boundedness of all the error signals in the presence of parametric uncertainty and unmodeled dynamics.

One of common assumptions in adaptive control is knowledge of the sign of control effectiveness. This work showed that the knowledge of the sign of control effectiveness is not relevant to the issue of existence of a fixed point solution, which eliminated the fixed point assumption in adaptive control of non-affine systems. It did, however,

show that knowledge of the sign of control effectiveness is indispensable both in the adaptive laws and the proof of boundedness with the use of mean value theorem.

Adaptive control systems are vulnerable to actuator limits. The applicability of PCH, to address nonlinear characteristics of actuator, was extended to an output feedback setting. The nonlinear characteristics of actuator included position limits, rate limits, actuator dynamics, and time delays.

NN-augmented input/output feedback linearization with the error observer approach was used for pitch-attitude tracking control of a linearized representation of R-50 helicopter dynamics along with each case of σ-modification, e-modification, and parameter projection. NN-augmented input/output feedback linearization with the error observer approach and σ-modification was used for pitch-rate tracking control of a flexible aircraft dynamics. NN-augmented input/output feedback linearization with the SPR filter approach was extended to include nonlinearly-parameterized NN and e-modification, and was applied to a modified Van der Pol oscillator. For the guided munition application, NN augmentation of an existing controller with σ-modification was used along with both the error observer approach and the SPR filter approach. A method of command limiting to keep the munition AoA below a certain level was introduced so that the oscillatory phenomena caused by lack of control power at high AoA was avoided. Numerical results from various applications showed that these methods are very promising.

6.2 Recommendations for Future Research

The following presents recommendations for future research.

6.2.1 Relaxation of Assumption 3.5.2

The proof of boundedness in NN adaptive control with PCH is shown using a linear approximation condition placed on $\hat{h}_r(y, \bar{y}, v)$. Consequently it puts a restriction on

selecting an approximate model $\hat{h}(y, \bar{y}, u)$. Relaxation of Assumption 3.5.2 will enable us to choose an approximate model from a wide class of functions but the proof of boundedness will be more involved.

6.2.2 Relaxation of Assumption 3.8.1

Nonlinearly-parameterized NN with SPR approach has been developed under Assumption 3.8.1 which requires that the control effectiveness be known. The assumption restricts the availability of this approach. It is desirable that one should remove the assumption so that an unknown function $h_{\bar{v}}$ with known sign can be used in the boundedness proof.

6.2.3 Extension of Chapter 4 to Non-minimum Phase Systems

All the control methodologies treated in this thesis impose the assumption on input-to-state stability of the internal dynamics, and thus are limited to minimum phase systems. The control architecture in Chapter 4 has similar features as the one in [45, 46, 47], thus an extension to non-minimum phase systems can directly follow augmentation of an existing controller for non-minimum phase systems given in [47].

6.2.4 Extension of Chapter 5 to Output Feedback

Chapter 5 has been treated in a state feedback setting for ease of presentation. Thus, the arguments are limited to the system which relies on full-state information. An extension of these results to output feedback is recommended. For output feedback control, one could use either the error observer approach or the SPR filter approach presented in this thesis to update the NN weights.

APPENDIX A

PROOFS OF BOUNDEDNESS ANALYSIS

A.1 Error Observer Approach with e-modification (Theorem 2.4.2)

Proof. Boundedness of all the error signals is shown in two steps. First, boundedness of weight error signals is shown employing a Lyapunov analysis, and then this result is used to show boundedness of the tracking and observer error signals.

Choose the following Lyapunov function candidate for the weight error signals

$$L_w = \frac{1}{2}\tilde{W}^T\Gamma_W^{-1}\tilde{W} + \frac{1}{2}\mathrm{tr}(\tilde{V}^T\Gamma_V^{-1}\tilde{V}) \tag{A.1.1}$$

The time derivative of L_w is

$$\begin{aligned}
\dot{L}_w =& -\tilde{W}^T\left[\mathrm{sgn}(h_{\bar{v}})\hat{\boldsymbol{\sigma}}\hat{\boldsymbol{E}}^T P\bar{\boldsymbol{b}} + k_e\|\hat{\boldsymbol{E}}\|\hat{W}\right] \\
& - \mathrm{tr}\{\tilde{V}^T\left[\mathrm{sgn}(h_{\bar{v}})\boldsymbol{\mu}\hat{\boldsymbol{E}}^T P\bar{\boldsymbol{b}}\hat{W}^T\hat{\sigma}' + k_e\|\hat{\boldsymbol{E}}\|\hat{V}\right]\} \\
=& -\mathrm{sgn}(h_{\bar{v}})\tilde{W}^T\hat{\boldsymbol{\sigma}}\hat{\boldsymbol{E}}^T P\bar{\boldsymbol{b}} - \mathrm{sgn}(h_{\bar{v}})\hat{\boldsymbol{E}}^T P\bar{\boldsymbol{b}}\hat{W}^T\hat{\sigma}'(\hat{V}^T\boldsymbol{\mu} - V^T\boldsymbol{\mu}) \\
& - k_e\|\hat{\boldsymbol{E}}\|\{\tilde{W}^T\hat{W} + \mathrm{tr}(\tilde{V}^T\hat{V})\}
\end{aligned} \tag{A.1.2}$$

Using (2.3.11) and $-2\mathrm{tr}(\tilde{Z}^T\hat{Z}) \leq -\|\tilde{Z}\|^2 + Z^{*^2}$,

$$\begin{aligned}
\dot{L}_w \leq& \sqrt{n_2+1}\|\tilde{W}\|\|\hat{\boldsymbol{E}}\|\|P\bar{\boldsymbol{b}}\| + \|\hat{\boldsymbol{E}}\|\|P\bar{\boldsymbol{b}}\|\|\hat{W}\|\left(\delta + \frac{a^*}{4}V^*\mu^*\right) \\
& - \frac{k_e}{2}\|\hat{\boldsymbol{E}}\|(\|\tilde{Z}\|^2 - Z^{*^2}) \\
\leq& \theta_1\|\hat{\boldsymbol{E}}\|\|\tilde{W}\| - \frac{k_e}{2}\|\hat{\boldsymbol{E}}\|\|\tilde{Z}\|^2 + \theta_2\|\boldsymbol{E}\| \\
\leq& \theta_1\|\hat{\boldsymbol{E}}\|\|\tilde{Z}\| - \frac{k_e}{2}\|\hat{\boldsymbol{E}}\|\|\tilde{Z}\|^2 + \theta_2\|\boldsymbol{E}\|
\end{aligned} \tag{A.1.3}$$

where $\theta_1 = \left(\sqrt{n_2+1} + \delta + \frac{a^*}{4}V^*\mu^*\right)\|P\bar{\boldsymbol{b}}\|$ and $\theta_2 = \frac{k_e}{2}Z^{*^2} + \|P\bar{\boldsymbol{b}}\|W^*\left(\delta + \frac{a^*}{4}V^*\mu^*\right)$.

Using $\theta_1\|\tilde{Z}\| \leq \frac{k_e}{4}\|\tilde{Z}\|^2 + \frac{\theta_1^2}{k_e}$,

$$\begin{aligned} &\leq -\|\hat{\boldsymbol{E}}\| \left\{ \frac{k_e}{4}\|\tilde{Z}\|^2 - \frac{\theta_1^2}{k_e} - \theta_2 \right\} \\ &< 0 \ \text{ if } \ \|\tilde{Z}\| > 2\sqrt{\frac{\theta_1^2}{k_e^2} + \frac{\theta_2}{k_e}} \end{aligned} \tag{A.1.4}$$

Hence $\tilde{Z}$ is bounded and its bound is denoted as: $\|\tilde{Z}\| \leq \tilde{Z}^*$.

Choose the following Lyapunov function candidate for the entire error system

$$L = \left|\frac{1}{h_{\bar{v}}}\right| \boldsymbol{E}^T P \boldsymbol{E} + \tilde{\boldsymbol{E}}^T \tilde{P} \tilde{\boldsymbol{E}} + 2L_w \tag{A.1.5}$$

Differentiating with respect to time,

$$\begin{aligned} \dot{L} = &\frac{d}{dt}\left|\frac{1}{h_{\bar{v}}}\right| \boldsymbol{E}^T P \boldsymbol{E} + \left|\frac{1}{h_{\bar{v}}}\right| \left(-\boldsymbol{E}^T Q \boldsymbol{E} + 2\boldsymbol{E}^T P \bar{\boldsymbol{b}} h_{\bar{v}} (v_{ad} - \bar{\Delta})\right) \\ &- \tilde{\boldsymbol{E}}^T \tilde{Q} \tilde{\boldsymbol{E}} - 2\tilde{\boldsymbol{E}}^T \tilde{P} \bar{\boldsymbol{b}} h_{\bar{v}} (v_{ad} - \bar{\Delta}) \\ &+ 2\tilde{W}^T \Gamma_W^{-1} \dot{\tilde{W}} + 2\mathrm{tr}(\tilde{V}^T \Gamma_V^{-1} \dot{\tilde{V}}) \end{aligned} \tag{A.1.6}$$

Applying the adaptive law (2.4.34) and the representation (2.3.17),

$$\begin{aligned} \dot{L} = &\frac{d}{dt}\left|\frac{1}{h_{\bar{v}}}\right| \boldsymbol{E}^T P \boldsymbol{E} + \left|\frac{1}{h_{\bar{v}}}\right| \left(-\boldsymbol{E}^T Q \boldsymbol{E} + 2\hat{\boldsymbol{E}}^T P \bar{\boldsymbol{b}} h_{\bar{v}} \bar{w}\right) \\ &- \tilde{\boldsymbol{E}}^T \tilde{Q} \tilde{\boldsymbol{E}} - 2\tilde{\boldsymbol{E}}^T \tilde{P} \bar{\boldsymbol{b}} h_{\bar{v}} (v_{ad} - \bar{\Delta}) - 2\mathrm{sgn}(h_{\bar{v}}) \tilde{\boldsymbol{E}}^T P \bar{\boldsymbol{b}} (v_{ad} - \bar{\Delta}) \\ &- 2k_e \|\hat{\boldsymbol{E}}\| (\tilde{W}^T \hat{W} + \mathrm{tr}(\tilde{V}^T \hat{V})) \\ \leq &\, H\lambda_{max}(P)\|\boldsymbol{E}\|^2 - \frac{1}{h^B}\lambda_{min}(Q)\|\boldsymbol{E}\|^2 + 2\|\hat{\boldsymbol{E}}\|\|P\bar{\boldsymbol{b}}\|(\gamma_1\|\tilde{Z}\| + \gamma_2) \\ &- \lambda_{min}(\tilde{Q})\|\tilde{E}\|^2 + 2\|\tilde{E}\|(h^B\|\tilde{P}\bar{\boldsymbol{b}}\| + \|P\bar{\boldsymbol{b}}\|)(\alpha_1\|\tilde{Z}\| + \alpha_2) \\ &- 2k_e\|\hat{\boldsymbol{E}}\|\mathrm{tr}(\tilde{Z}^T\hat{Z}) \end{aligned} \tag{A.1.7}$$

Using $\bar{q} \triangleq \min[\frac{\lambda_{\min}(Q)}{h^B} - H\lambda_{max}(P),\ \lambda_{\min}(\tilde{Q})]$, $-2\mathrm{tr}(\tilde{Z}^T\hat{Z}) \leq -\|\tilde{Z}\|^2 + Z^{*^2} \leq Z^{*^2}$, and $\|\tilde{Z}\| \leq \tilde{Z}^*$.

$$\begin{aligned} \dot{L} \leq &-\frac{\bar{q}}{2}(\|\boldsymbol{E}\| + \|\tilde{\boldsymbol{E}}\|)^2 + 2\kappa_2(\|\boldsymbol{E}\| + \|\tilde{\boldsymbol{E}}\|)\tilde{Z}^* \\ &+ \kappa_3(\|\boldsymbol{E}\| + \|\tilde{\boldsymbol{E}}\|) \end{aligned} \tag{A.1.8}$$

where $\kappa_2 = \gamma_1\|P\bar{\boldsymbol{b}}\| + \alpha_1(\|\tilde{P}\bar{\boldsymbol{b}}\|h^B + \|P\bar{\boldsymbol{b}}\|),\ \kappa_3 = 2\gamma_2\|P\bar{\boldsymbol{b}}\| + 2\alpha_2(\|\tilde{P}\bar{\boldsymbol{b}}\|h^B + \|P\bar{\boldsymbol{b}}\|) + k_e{Z^*}^2$. Combining terms to obtain

$$\dot{L} \leq -(\|\boldsymbol{E}\| + \|\tilde{\boldsymbol{E}}\|)\Big[\frac{\bar{q}}{2}(\|\boldsymbol{E}\| + \|\tilde{\boldsymbol{E}}\|) - 2\kappa_2\tilde{Z}^* - \kappa_3\Big] \tag{A.1.9}$$

The following condition renders $\dot{L} < 0$.

$$\|\boldsymbol{E}\| + \|\tilde{\boldsymbol{E}}\| > \frac{2}{\bar{q}}\Upsilon \tag{A.1.10}$$

where $\Upsilon = 2\kappa_2\tilde{Z}^* + \kappa_3$. Therefore $\boldsymbol{\zeta}$ remains in Ω_β after a finite time period. The ultimate bound $\sqrt{\frac{\lambda_{max}(T)}{\lambda_{min}(T)}}C$ can be computed as (A.2.16). □

A.2 Error Observer Approach with σ-modification (Theorem 3.4.1)

Proof. Consider the following Lyapunov function candidate:

$$L = \left|\frac{1}{h_{\bar{v}}}\right| \boldsymbol{E}^T P \boldsymbol{E} + \tilde{\boldsymbol{E}}^T \tilde{P} \tilde{\boldsymbol{E}} + (\tilde{W}^T \Gamma_W^{-1} \tilde{W}) + \mathrm{tr}(\tilde{V}^T \Gamma_V^{-1} \tilde{V}), \tag{A.2.1}$$

The derivative of L will be

$$\begin{aligned} \dot{L} = & \frac{d}{dt}\left|\frac{1}{h_{\bar{v}}}\right| \boldsymbol{E}^T P \boldsymbol{E} + \left|\frac{1}{h_{\bar{v}}}\right| \left(-\boldsymbol{E}^T Q \boldsymbol{E} + 2\boldsymbol{E}^T P \bar{\boldsymbol{b}} h_{\bar{v}} (v_{ad} - \bar{\Delta})\right) \\ & - \tilde{\boldsymbol{E}}^T \tilde{Q} \tilde{\boldsymbol{E}} - 2\tilde{\boldsymbol{E}}^T \tilde{P} \bar{\boldsymbol{b}} h_{\bar{v}} (v_{ad} - \bar{\Delta}) \\ & + 2\tilde{W}^T \Gamma_W^{-1} \dot{\tilde{W}} + 2\mathrm{tr}(\tilde{V}^T \Gamma_V^{-1} \dot{\tilde{V}}) \end{aligned} \tag{A.2.2}$$

With the definition of $\tilde{\boldsymbol{E}} = \hat{\boldsymbol{E}} - \boldsymbol{E}$ and (3.4.5), this can be written:

$$\begin{aligned} \dot{L} = & \frac{d}{dt}\left|\frac{1}{h_{\bar{v}}}\right| \boldsymbol{E}^T P \boldsymbol{E} - \left|\frac{1}{h_{\bar{v}}}\right| \boldsymbol{E}^T Q \boldsymbol{E} - \tilde{\boldsymbol{E}}^T \tilde{Q} \tilde{\boldsymbol{E}} \\ & + 2\mathrm{sgn}(h_{\bar{v}}) \hat{\boldsymbol{E}}^T P \bar{\boldsymbol{b}} \left[\tilde{W}^T \left(\hat{\sigma} - \hat{\sigma}' \hat{V}^T \boldsymbol{\mu}\right) + \hat{W}^T \hat{\sigma}' \tilde{V}^T \boldsymbol{\mu} + \bar{w}\right] \\ & - 2\tilde{\boldsymbol{E}}^T (h_{\bar{v}} \tilde{P} \bar{\boldsymbol{b}} + \mathrm{sgn}(h_{\bar{v}}) P \bar{\boldsymbol{b}})(v_{ad} - \bar{\Delta}) + 2(\tilde{W}^T \Gamma_W^{-1} \dot{\tilde{W}}) + 2\mathrm{tr}(\tilde{V}^T \Gamma_V^{-1} \dot{\tilde{V}}). \end{aligned} \tag{A.2.3}$$

Substituting the adaptive laws implies:

$$\begin{aligned} \dot{L} = & \frac{d}{dt}\left|\frac{1}{h_{\bar{v}}}\right| \boldsymbol{E}^T P \boldsymbol{E} - \left|\frac{1}{h_{\bar{v}}}\right| \boldsymbol{E}^T Q \boldsymbol{E} - \tilde{\boldsymbol{E}}^T \tilde{Q} \tilde{\boldsymbol{E}} \\ & + 2\mathrm{sgn}(h_{\bar{v}}) \hat{\boldsymbol{E}}^T P \bar{\boldsymbol{b}} \bar{w} - 2\tilde{\boldsymbol{E}}^T (h_{\bar{v}} \tilde{P} \bar{\boldsymbol{b}} + \mathrm{sgn}(h_{\bar{v}}) P \bar{\boldsymbol{b}})(v_{ad} - \bar{\Delta}) \\ & - 2k_\sigma \left[\tilde{W}(\hat{W} - W_0)\right] - 2k_\sigma \mathrm{tr}\left[\tilde{V}(\hat{V} - V_0)\right] \end{aligned} \tag{A.2.4}$$

Using upper bounds from (3.4.9) and (3.4.8), the derivative of the Lyapunov function candidate can be upper bounded as:

$$\begin{aligned} \dot{L} \leq & H\lambda_{max}(P)\|\boldsymbol{E}\|^2 - \frac{1}{h^B}\lambda_{min}(Q)\|\boldsymbol{E}\|^2 - \lambda_{\min}(\tilde{Q})\|\tilde{\boldsymbol{E}}\|^2 \\ & + 2\|P\bar{\boldsymbol{b}}\|\|\hat{\boldsymbol{E}}\|(\gamma_1\|\tilde{Z}\|_F + \gamma_2) + 2\Theta\|\tilde{\boldsymbol{E}}\|(\alpha_1\|\tilde{Z}\|_F + \alpha_2) \\ & - k_\sigma\left[\|\tilde{W}\|_F^2 + \|\hat{W} - W_0\|_F^2 - \|W - W_0\|_F^2\right] \\ & - k_\sigma\left[\|\tilde{V}\|_F^2 + \|\hat{V} - V_0\|_F^2 - \|V - V_0\|_F^2\right], \end{aligned} \tag{A.2.5}$$

where $\Theta = \|P\bar{\boldsymbol{b}}\| + h^B\|\tilde{P}\bar{\boldsymbol{b}}\|$ and the following property for matrices has been used:

$$2\text{tr}\left[\tilde{W}^T(\hat{W} - W_0)\right] = \|\tilde{W}\|_F^2 + \|\hat{W} - W_0\|_F^2 - \|W - W_0\|_F^2 \,. \tag{A.2.6}$$

Further

$$\begin{aligned}\dot{L} \leq & -\left\{\frac{1}{h^B}\lambda_{min}(Q) - H\lambda_{max}(P)\right\}\|\boldsymbol{E}\|^2 - \lambda_{\min}(\tilde{Q})\|\tilde{\boldsymbol{E}}\|^2 \\ & + 2\|P\bar{\boldsymbol{b}}\|(\|\boldsymbol{E}\| + ||\tilde{\boldsymbol{E}}||)(\gamma_1\|\tilde{Z}\|_F + \gamma_2) + 2\Theta\|\tilde{\boldsymbol{E}}\|(\alpha_1\|\tilde{Z}\|_F + \alpha_2) \\ & - k_\sigma\|\tilde{Z}\|_F^2 + k_\sigma\bar{Z}\,.\end{aligned} \tag{A.2.7}$$

Grouping terms, (A.2.7) can be written:

$$\begin{aligned}\dot{L} \leq & -\left\{\frac{1}{h^B}\lambda_{min}(Q) - H\lambda_{max}(P)\right\}\|\boldsymbol{E}\|^2 - \lambda_{\min}(\tilde{Q})\|\tilde{\boldsymbol{E}}\|^2 \\ & + 2\|P\bar{\boldsymbol{b}}\|\|\boldsymbol{E}\|\left[\gamma_1\|\tilde{Z}\|_F + \gamma_2\right] \\ & + 2\|\tilde{\boldsymbol{E}}\|\left[\Theta\left(\alpha_1\|\tilde{Z}\|_F + \alpha_2\right) + \|P\bar{\boldsymbol{b}}\|\left(\gamma_1\|\tilde{Z}\|_F + \gamma_2\right)\right] \\ & - k_\sigma\|\tilde{Z}\|_F^2 + k_\sigma\bar{Z},\end{aligned} \tag{A.2.8}$$

and further put in the form:

$$\begin{aligned}\dot{L} \leq & -\left\{\frac{1}{h^B}\lambda_{min}(Q) - H\lambda_{max}(P)\right\}\|\boldsymbol{E}\|^2 - \lambda_{\min}(\tilde{Q})\|\tilde{\boldsymbol{E}}\|^2 \\ & + 2\|P\bar{\boldsymbol{b}}\|\|\boldsymbol{E}\|\left[\gamma_1\|\tilde{Z}\|_F + \gamma_2\right] + 2\|\tilde{\boldsymbol{E}}\|\left[\kappa_1\|\tilde{Z}\|_F + \kappa_2\right] \\ & - k_\sigma\|\tilde{Z}\|_F^2 + k_\sigma\bar{Z}\,.\end{aligned} \tag{A.2.9}$$

where $\kappa_1 = \Theta\alpha_1 + \|P\bar{\boldsymbol{b}}\|\gamma_1,\ \kappa_2 = \Theta\alpha_2 + \|P\bar{\boldsymbol{b}}\|\gamma_2$.

Utilizing the following inequalities,

$$\begin{aligned}2\gamma_1\|P\bar{\boldsymbol{b}}\|\|\boldsymbol{E}\|\|\tilde{Z}\|_F &\leq \gamma_1\|P\bar{\boldsymbol{b}}\|(\|\boldsymbol{E}\|^2 + \|\tilde{Z}\|^2) \\ 2\gamma_2\|P\bar{\boldsymbol{b}}\|\|\boldsymbol{E}\| &\leq \gamma_2\|P\bar{\boldsymbol{b}}\|(\|\boldsymbol{E}\|^2 + 1) \\ 2\kappa_1\|\tilde{\boldsymbol{E}}\|\|\tilde{Z}\|_F &\leq \kappa_1(\|\tilde{\boldsymbol{E}}\|^2 + \|\tilde{Z}\|^2) \\ 2\kappa_2\|\tilde{\boldsymbol{E}}\| &\leq \kappa_2(\|\tilde{\boldsymbol{E}}\|^2 + 1)\end{aligned} \tag{A.2.10}$$

Upon completion of squares, we get the following upper bound:

$$\begin{aligned}\dot{L} \leq & -\left(\{\frac{1}{h^B}\lambda_{min}(Q) - H\lambda_{max}(P)\} - (\gamma_1+\gamma_2)\|P\bar{\boldsymbol{b}}\|\right)\|\boldsymbol{E}\|^2 \\ & -\left(\lambda_{\min}(\tilde{Q}) - (\kappa_1+\kappa_2)\right)\|\tilde{\boldsymbol{E}}\|^2 \\ & -\left(k_\sigma - \kappa_1 - \gamma_1\|P\bar{\boldsymbol{b}}\|\right)\|\tilde{Z}\|_F^2 \\ & +\gamma_2\|P\bar{\boldsymbol{b}}\| + \kappa_2 + k_\sigma\bar{Z}.\end{aligned} \tag{A.2.11}$$

One of the following conditions

$$\begin{aligned}\|\boldsymbol{E}\| &> \frac{\Upsilon}{\sqrt{\{\frac{1}{h^B}\lambda_{min}(Q) - H\lambda_{max}(P)\} - (\gamma_1+\gamma_2)\|P\bar{\boldsymbol{b}}\|}} \\ \|\tilde{\boldsymbol{E}}\| &> \frac{\Upsilon}{\sqrt{\lambda_{\min}(\tilde{Q}) - (\kappa_1+\kappa_2)}} \\ \|\tilde{Z}\|_F &> \frac{\Upsilon}{\sqrt{k_\sigma - \kappa_1 - \gamma_1\|P\bar{\boldsymbol{b}}\|}}\end{aligned} \tag{A.2.12}$$

will render $\dot{L} < 0$ outside a compact set, where $\Upsilon^2 = \gamma_2\|P\bar{\boldsymbol{b}}\| + \kappa_2 + k_\sigma\bar{Z}$

To ensure that the conditions (A.2.12) define a compact set in the space of error variables, write (A.2.11) in the following way that the condition $\dot{L} < 0$ is true everywhere in the space of error variables $\boldsymbol{E}, \tilde{\boldsymbol{E}}, \tilde{Z}$, outside the ellipsoid:

$$\begin{aligned}&\left(\{\frac{1}{h^B}\lambda_{min}(Q) - H\lambda_{max}(P)\} - (\gamma_1+\gamma_2)\|P\bar{\boldsymbol{b}}\|\right)\|\boldsymbol{E}\|^2 \\ &+\left(\lambda_{\min}(\tilde{Q}) - (\kappa_1+\kappa_2)\right)\|\tilde{\boldsymbol{E}}\|^2 + \left(k_\sigma - \kappa_1 - \gamma_1\|P\bar{\boldsymbol{b}}\|\right)\|\tilde{Z}\|_F^2 = \Upsilon^2\,.\end{aligned} \tag{A.2.13}$$

Define a compact set in the space of the error variables:

$$B_C = \{\boldsymbol{\zeta} \in B_R \mid \|\boldsymbol{\zeta}\| \leq C\}\,, \tag{A.2.14}$$

outside which $\dot{L} < 0$. Note from (3.4.10) that $B_C \subset B_R$. Consider the Lyapunov function candidate in (A.2.1) and write it as:

$$L(\boldsymbol{\zeta}) = \boldsymbol{\zeta}^T T \boldsymbol{\zeta}\,.$$

and it satisfies the following inequality.

$$\lambda_{min}(T)\|\boldsymbol{\zeta}\|^2 \leq L(\boldsymbol{\zeta}) \leq \lambda_{max}(T)\|\boldsymbol{\zeta}\|^2 \tag{A.2.15}$$

The condition in (3.4.10) ensures that $B_C \subset \Omega_\beta \subset \Omega_\alpha$ and thus ultimate boundedness of $\boldsymbol{\zeta}$. The argument shows that Ω_β is an invariant set and all trajectories starting in Ω_α enter Ω_β within a finite time. To calculate the ultimate bound on $\boldsymbol{\zeta}$, we use the left inequality of (A.2.15) to show

$$\lambda_{min}(T)\|\boldsymbol{\zeta}\|^2 \leq L(\boldsymbol{\zeta}) \leq \beta \Rightarrow \|\boldsymbol{\zeta}\| \leq \sqrt{\frac{\beta}{\lambda_{min}(T)}} = \sqrt{\frac{\lambda_{max}(T)}{\lambda_{min}(T)}}C \tag{A.2.16}$$

Once the trajectory enters Ω_β, it never escapes from Ω_β and the ultimate bound can be taken as $\sqrt{\frac{\lambda_{max}(T)}{\lambda_{min}(T)}}C$. Let $\|\boldsymbol{E}\| \leq E^*$ and $\|\tilde{Z}\| \leq \tilde{Z}^*$. Boundedness of $\boldsymbol{y}_{rm}$ ensured by Lemma 3.5.1 completes the proof. □

A.3 Error Observer Approach with e-modification (Theorem 3.4.2)

Proof. As presented in Section A.1, boundedness of weight error signals is shown first, and this result is used to show boundedness of the tracking and observer error signals.

Consider the following Lyapunov function candidate for the weight error signals

$$L_w = \frac{1}{2}\tilde{W}^T\Gamma_W^{-1}\tilde{W} + \frac{1}{2}\mathrm{tr}(\tilde{V}^T\Gamma_V^{-1}\tilde{V}) \tag{A.3.1}$$

The time derivative of L_w is

$$\begin{aligned}\dot{L}_w =& -\tilde{W}^T\left[\mathrm{sgn}(h_{\bar{v}})\hat{\boldsymbol{\sigma}}\hat{\boldsymbol{E}}^T P\bar{\boldsymbol{b}} + k_e\|\hat{\boldsymbol{E}}\|\hat{W}\right] \\ & - \mathrm{tr}\{\tilde{V}^T\left[\mathrm{sgn}(h_{\bar{v}})\boldsymbol{\mu}\hat{\boldsymbol{E}}^T P\bar{\boldsymbol{b}}\hat{W}^T\hat{\sigma}' + k_e\|\hat{\boldsymbol{E}}\|\hat{V}\right]\} \\ =& -\mathrm{sgn}(h_{\bar{v}})\tilde{W}^T\hat{\boldsymbol{\sigma}}\hat{\boldsymbol{E}}^T P\bar{\boldsymbol{b}} - \mathrm{sgn}(h_{\bar{v}})\hat{\boldsymbol{E}}^T P\bar{\boldsymbol{b}}\hat{W}^T\hat{\sigma}'(\hat{V}^T\boldsymbol{\mu} - V^T\boldsymbol{\mu}) \\ & - k_e\|\hat{\boldsymbol{E}}\|\{\tilde{W}^T\hat{W} + \mathrm{tr}(\tilde{V}^T\hat{V})\}\end{aligned} \tag{A.3.2}$$

Using (2.3.11) and $-2\mathrm{tr}(\tilde{Z}^T\hat{Z}) \le -\|\tilde{Z}\|^2 + Z^{*^2}$,

$$\begin{aligned}\dot{L}_w \le& \sqrt{n_2+1}\|\tilde{W}\|\|\hat{\boldsymbol{E}}\|\|P\bar{\boldsymbol{b}}\| + \|\hat{\boldsymbol{E}}\|\|P\bar{\boldsymbol{b}}\|\|\hat{W}\|\left(\delta + \frac{a^*}{4}V^*\mu^*\right) \\ & - \frac{k_e}{2}\|\hat{\boldsymbol{E}}\|(\|\tilde{Z}\|^2 - Z^{*^2}) \\ \le& \theta_1\|\hat{\boldsymbol{E}}\|\|\tilde{W}\| - \frac{k_e}{2}\|\hat{\boldsymbol{E}}\|\|\tilde{Z}\|^2 + \theta_2\|\boldsymbol{E}\| \\ \le& \theta_1\|\hat{\boldsymbol{E}}\|\|\tilde{Z}\| - \frac{k_e}{2}\|\hat{\boldsymbol{E}}\|\|\tilde{Z}\|^2 + \theta_2\|\boldsymbol{E}\|\end{aligned} \tag{A.3.3}$$

where $\theta_1 = \left(\sqrt{n_2+1} + \delta + \frac{a^*}{4}V^*\mu^*\right)\|P\bar{\boldsymbol{b}}\|$ and $\theta_2 = \frac{k_e}{2}Z^{*^2} + \|P\bar{\boldsymbol{b}}\|W^*\left(\delta + \frac{a^*}{4}V^*\mu^*\right)$. Using $\theta_1\|\tilde{Z}\| \le \frac{k_e}{4}\|\tilde{Z}\|^2 + \frac{\theta_1^2}{k_e}$,

$$\begin{aligned}& \le -\|\hat{\boldsymbol{E}}\|\left\{\frac{k_e}{4}\|\tilde{Z}\|^2 - \frac{\theta_1^2}{k_e} - \theta_2\right\} \\ & < 0 \ \text{ if } \ \|\tilde{Z}\| > 2\sqrt{\frac{\theta_1^2}{k_e^2} + \frac{\theta_2}{k_e}}\end{aligned} \tag{A.3.4}$$

Hence $\tilde{Z}$ is bounded and its bound is denoted as: $\|\tilde{Z}\| \le \tilde{Z}^*$.

Consider the following Lyapunov function candidate for the entire error system

$$L = \left|\frac{1}{h_{\bar{v}}}\right|\boldsymbol{E}^T P\boldsymbol{E} + \tilde{\boldsymbol{E}}^T\tilde{P}\tilde{\boldsymbol{E}} + 2L_w \tag{A.3.5}$$

The time derivative of L will be

$$\begin{aligned}\dot{L} = & \frac{d}{dt}\left|\frac{1}{h_{\bar{v}}}\right| \boldsymbol{E}^T P \boldsymbol{E} + \left|\frac{1}{h_{\bar{v}}}\right| \left(-\boldsymbol{E}^T Q \boldsymbol{E} + 2\boldsymbol{E}^T P \bar{\boldsymbol{b}} h_{\bar{v}}(v_{ad} - \bar{\Delta})\right) \\ & - \tilde{\boldsymbol{E}}^T \tilde{Q} \tilde{\boldsymbol{E}} - 2\tilde{\boldsymbol{E}}^T \tilde{P} \bar{\boldsymbol{b}} h_{\bar{v}}(v_{ad} - \bar{\Delta}) \\ & + 2\tilde{W}^T \Gamma_W^{-1} \dot{\tilde{W}} + 2\mathrm{tr}(\tilde{V}^T \Gamma_V^{-1} \dot{\tilde{V}})\end{aligned} \tag{A.3.6}$$

Using (3.4.23), this can be written:

$$\begin{aligned}\dot{L} = & \frac{d}{dt}\left|\frac{1}{h_{\bar{v}}}\right| \boldsymbol{E}^T P \boldsymbol{E} - \left|\frac{1}{h_{\bar{v}}}\right| \boldsymbol{E}^T Q \boldsymbol{E} - \tilde{\boldsymbol{E}}^T \tilde{Q} \tilde{\boldsymbol{E}} \\ & + 2\mathrm{sgn}(h_{\bar{v}}) \hat{\boldsymbol{E}}^T P \bar{\boldsymbol{b}} \left[\tilde{W}^T \hat{\sigma} + \hat{W}^T \hat{\sigma}' \tilde{V}^T \boldsymbol{\mu} + \bar{w}\right] \\ & - 2\tilde{\boldsymbol{E}}^T (h_{\bar{v}} \tilde{P} \bar{\boldsymbol{b}} + \mathrm{sgn}(h_{\bar{v}}) P \bar{\boldsymbol{b}})(v_{ad} - \bar{\Delta}) + 2(\tilde{W}^T \Gamma_W^{-1} \dot{\tilde{W}}) + 2\mathrm{tr}(\tilde{V}^T \Gamma_V^{-1} \dot{\tilde{V}}).\end{aligned} \tag{A.3.7}$$

Substituting the adaptive laws implies:

$$\begin{aligned}\dot{L} = & \frac{d}{dt}\left|\frac{1}{h_{\bar{v}}}\right| \boldsymbol{E}^T P \boldsymbol{E} - \left|\frac{1}{h_{\bar{v}}}\right| \boldsymbol{E}^T Q \boldsymbol{E} - \tilde{\boldsymbol{E}}^T \tilde{Q} \tilde{\boldsymbol{E}} \\ & + 2\mathrm{sgn}(h_{\bar{v}}) \hat{\boldsymbol{E}}^T P \bar{\boldsymbol{b}} \bar{w} - 2\tilde{\boldsymbol{E}}^T (h_{\bar{v}} \tilde{P} \bar{\boldsymbol{b}} + \mathrm{sgn}(h_{\bar{v}}) P \bar{\boldsymbol{b}})(v_{ad} - \bar{\Delta}) \\ & - 2k_e \left[\tilde{W}^T \hat{W} \|\hat{\boldsymbol{E}}\|\right] - 2k_e \mathrm{tr}\left[\tilde{V}^T \hat{V} \|\hat{\boldsymbol{E}}\|\right].\end{aligned} \tag{A.3.8}$$

Using upper bounds from (3.4.9) and (3.4.24), the derivative of the Lyapunov function candidate can be upper bounded as:

$$\begin{aligned}\dot{L} \leq & H\lambda_{max}(P)\|\boldsymbol{E}\|^2 - \frac{1}{h^B}\lambda_{min}(Q)\|\boldsymbol{E}\|^2 - \lambda_{\min}(\tilde{Q})\|\tilde{\boldsymbol{E}}\|^2 \\ & + 2\|P\bar{\boldsymbol{b}}\|\|\hat{\boldsymbol{E}}\|(\gamma_1\|\tilde{Z}\|_F + \gamma_2) + 2\Theta\|\tilde{\boldsymbol{E}}\|(\alpha_1\|\tilde{Z}\|_F + \alpha_2) \\ & - k_e\|\hat{\boldsymbol{E}}\|\left[\|\tilde{Z}\|_F^2 - Z^{*^2}\right]\end{aligned} \tag{A.3.9}$$

Further

$$\begin{aligned}\dot{L} \leq & H\lambda_{max}(P)\|\boldsymbol{E}\|^2 - \frac{1}{h^B}\lambda_{min}(Q)\|\boldsymbol{E}\|^2 - \lambda_{\min}(\tilde{Q})\|\tilde{\boldsymbol{E}}\|^2 \\ & + \|\tilde{\boldsymbol{E}}\|(2\kappa_9\|\tilde{Z}\|_F + \kappa_{10}) \\ & + \kappa_{12}(\|\boldsymbol{E}\| + \|\tilde{\boldsymbol{E}}\|) + 2\kappa_{14}(\|\boldsymbol{E}\| + \|\tilde{\boldsymbol{E}}\|)\|\tilde{Z}\|\end{aligned} \tag{A.3.10}$$

where $\Theta = \|P\bar{\boldsymbol{b}}\| + h^B\|\tilde{P}\bar{\boldsymbol{b}}\|, \kappa_9 = \alpha_1\Theta,\ \kappa_{10} = 2\alpha_2\Theta,\ \kappa_{12} = 2\|P\bar{\boldsymbol{b}}\|\gamma_2 + k_e Z^{*^2}$, $\kappa_{14} = \|P\bar{\boldsymbol{b}}\|\gamma_1$.

Grouping terms, (A.3.10) can be written:

$$\begin{aligned}\dot{L} \leq & H\lambda_{max}(P)\|\boldsymbol{E}\|^2 - \frac{1}{h^B}\lambda_{min}(Q)\|\boldsymbol{E}\|^2 - \lambda_{\min}(\tilde{Q})\|\tilde{\boldsymbol{E}}\|^2 \\ & + 2(\kappa_9+\kappa_{14})(\|\boldsymbol{E}\|+\|\tilde{\boldsymbol{E}}\|)\tilde{Z}^* + (\kappa_{10}+\kappa_{12})(\|\boldsymbol{E}\|+\|\tilde{\boldsymbol{E}}\|)\end{aligned} \tag{A.3.11}$$

Using $2(x^2+y^2) \geq (x+y)^2$ and $\bar{q} \triangleq \min[\frac{\lambda_{\min}(Q)}{h^B} - H\lambda_{max}(P),\ \lambda_{\min}(\tilde{Q})]$,

$$\begin{aligned}\dot{L} &\leq -\frac{\bar{q}}{2}(\|\boldsymbol{E}\|+\|\tilde{\boldsymbol{E}}\|)^2 + \Upsilon(\|\boldsymbol{E}\|+\|\tilde{\boldsymbol{E}}\|) \\ &\leq -(\|\boldsymbol{E}\|+\|\tilde{\boldsymbol{E}}\|)\Big[\frac{\bar{q}}{2}(\|\boldsymbol{E}\|+\|\tilde{\boldsymbol{E}}\|) - \Upsilon\Big]\end{aligned} \tag{A.3.12}$$

where $\Upsilon \triangleq 2(\kappa_9+\kappa_{14})\tilde{Z}^* + (\kappa_{10}+\kappa_{12})$. The following condition

$$\|\boldsymbol{E}\|+\|\tilde{\boldsymbol{E}}\| > \frac{2}{\bar{q}}\Upsilon \tag{A.3.13}$$

will render $\dot{L} < 0$ outside a compact set. In the same manner as in Theorem 3.4.1, it is ensured that $\boldsymbol{E}, \tilde{\boldsymbol{E}}, \tilde{Z}$ are ultimately bounded and the ultimate bound $\sqrt{\frac{\lambda_{max}(T)}{\lambda_{min}(T)}}C$ can be calculated as (A.2.16). In the case when PCH is implemented, boundedness of $\boldsymbol{y}_{rm}$ can be shown by using Lemma 3.5.1. □

A.4 Error Observer Approach with Projection (Theorem 3.4.3)

Proof. Define a Lyapunov function of the NN weight $\hat{W}$.

$$L_W = g(\Gamma_W^{-1}\hat{W}) + \frac{W_{max}^2}{\epsilon_W} = \frac{(\Gamma_W^{-1}\hat{W})^T\Gamma_W^{-1}\hat{W}}{\epsilon_W} \tag{A.4.1}$$

Differentiating with respect to time,

$$\begin{aligned}\dot{L}_W &= \nabla g^T \Gamma_W^{-1}\dot{\hat{W}} \\ &= \begin{cases} g^T\xi & \text{if } g(\hat{W}) \le 0, \\ g^T\xi & \text{if } g(\hat{W}) > 0 \text{ and } \nabla g^T\xi \le 0, \\ g^T\xi(1-g) & \text{if } g(\hat{W}) > 0 \text{ and } \nabla g^T\xi > 0 \end{cases}\end{aligned} \tag{A.4.2}$$

We can see that $\dot{L}_W \le 0$ outside Π_1 and $\hat{W}$ is bounded in a compact set Π_1. We denote the maximum value of the norm of $\hat{W}$:

$$\hat{W}^* \triangleq \max_{\hat{W}\in\ \Pi_1} \|\hat{W}(t)\| \tag{A.4.3}$$

In the same manner, $\hat{V}$ is bounded and the maximum value of its norm is denoted as:

$$\hat{V}^* \triangleq \max_{\hat{V}\in\ \Pi_1} \|\hat{V}(t)\| \tag{A.4.4}$$

Using the bound on $\hat{W}$ in (A.4.3) and $\hat{V}$ in (A.4.4), $\bar{w}$ in (3.4.23) can be bounded by a constant:

$$\begin{aligned}\|\bar{w}\| &\le 2\sqrt{n_2+1}W^* + \frac{a^*}{4}\|\hat{W}\|(\|\hat{V}\| + V^*)\|\boldsymbol{\mu}\| + \epsilon^* \\ &\le \bar{w}^* \triangleq 2\sqrt{n_2+1}W^* + \frac{a^*}{4}\hat{W}^*(\hat{V}^* + V^*)\boldsymbol{\mu}^* + \epsilon^*\end{aligned} \tag{A.4.5}$$

where a^* is the maximum value of activation potentials in the NN hidden layer. $v_{ad} - \bar{\Delta}$ can be shown to be bounded by a constant:

$$\begin{aligned}\|v_{ad} - \bar{\Delta}\| &= \|\hat{W}^T\hat{\boldsymbol{\sigma}} - W^T\boldsymbol{\sigma} - \epsilon\| \\ &\le \theta^* \triangleq \sqrt{n_2+1}(\hat{W}^* + W^*) + \epsilon^*\end{aligned} \tag{A.4.6}$$

Consider the following Lyapunov candidate of $E, \tilde{E}, \hat{W}, \hat{V}$:

$$L = \left|\frac{1}{h_{\bar{v}}}\right| \boldsymbol{E}^T P \boldsymbol{E} + \tilde{\boldsymbol{E}}^T \tilde{P} \tilde{\boldsymbol{E}} + \tilde{W}^T \Gamma_W^{-1} \tilde{W} + \mathrm{tr}(\tilde{V}^T \Gamma_V^{-1} \tilde{V}) \tag{A.4.7}$$

Differentiating with respect to time,

$$\begin{aligned} \dot{L} = & \frac{d}{dt}\left|\frac{1}{h_{\bar{v}}}\right| \boldsymbol{E}^T P \boldsymbol{E} + \left|\frac{1}{h_{\bar{v}}}\right| \left(-\boldsymbol{E}^T Q \boldsymbol{E} + 2\boldsymbol{E}^T P \bar{\boldsymbol{b}} h_{\bar{v}} (v_{ad} - \bar{\Delta})\right) \\ & - \tilde{\boldsymbol{E}}^T \tilde{Q} \tilde{\boldsymbol{E}} - 2\tilde{\boldsymbol{E}}^T \tilde{P} \bar{\boldsymbol{b}} h_{\bar{v}} (v_{ad} - \bar{\Delta}) \\ & + 2\tilde{W}^T \Gamma_W^{-1} \dot{\tilde{W}} + 2\mathrm{tr}(\tilde{V}^T \Gamma_V^{-1} \dot{\tilde{V}}) \end{aligned} \tag{A.4.8}$$

Using (3.2.21),(3.3.1) and the update laws in (3.4.38) ,

$$\begin{aligned} \dot{L} = & \frac{d}{dt}\left|\frac{1}{h_{\bar{v}}}\right| \boldsymbol{E}^T P \boldsymbol{E} - \left|\frac{1}{h_{\bar{v}}}\right| \boldsymbol{E}^T Q \boldsymbol{E} - \tilde{\boldsymbol{E}}^T \tilde{Q} \tilde{\boldsymbol{E}} \\ & + 2\mathrm{sgn}(h_{\bar{v}}) \hat{\boldsymbol{E}}^T P \boldsymbol{b} \left[\tilde{W}^T \hat{\boldsymbol{\sigma}} + \hat{W}^T \hat{\sigma}' \tilde{V}^T \boldsymbol{\mu} + \bar{w}\right] \\ & + 2\tilde{\boldsymbol{E}}^T (\mathrm{sgn}(h_{\bar{v}}) P \boldsymbol{b} + h_{\bar{v}} \tilde{P} \boldsymbol{b})(v_{ad} - \bar{\Delta}) \\ & + 2\tilde{W}^T Proj(\hat{W}, -\mathrm{sgn}(h_{\bar{v}}) \hat{\boldsymbol{\sigma}} \hat{\boldsymbol{E}}^T P \boldsymbol{b}) \\ & + 2\mathrm{tr}\tilde{V}^T \left[Proj(\hat{V}, -\mathrm{sgn}(h_{\bar{v}}) \boldsymbol{\mu} \hat{\boldsymbol{E}}^T P \boldsymbol{b} \hat{W}^T \hat{\sigma}')\right] \\ = & - \boldsymbol{E}^T Q \boldsymbol{E} - \tilde{\boldsymbol{E}}^T \tilde{Q} \tilde{\boldsymbol{E}} + 2\mathrm{sgn}(h_{\bar{v}}) \bar{w} \boldsymbol{E}^T P \boldsymbol{b} \\ & + 2\tilde{\boldsymbol{E}}^T (\mathrm{sgn}(h_{\bar{v}}) P \boldsymbol{b} + h_{\bar{v}} \tilde{P} \boldsymbol{b})(v_{ad} - \bar{\Delta}) \\ & + 2\tilde{W}^T \left[Proj(\hat{W}, -\mathrm{sgn}(h_{\bar{v}}) \hat{\boldsymbol{\sigma}} \hat{\boldsymbol{E}}^T P \boldsymbol{b}) + \mathrm{sgn}(h_{\bar{v}}) \hat{\boldsymbol{\sigma}} \hat{\boldsymbol{E}}^T P \boldsymbol{b}\right] \\ & + 2\mathrm{tr}\tilde{V}^T \left[Proj(\hat{V}, -\mathrm{sgn}(h_{\bar{v}}) \boldsymbol{\mu} \hat{\boldsymbol{E}}^T P \boldsymbol{b} \hat{W}^T \hat{\sigma}') + \mathrm{sgn}(h_{\bar{v}}) \boldsymbol{\mu} \hat{\boldsymbol{E}}^T P \boldsymbol{b} \hat{W}^T \hat{\sigma}'\right] \\ \leq & - \boldsymbol{E}^T Q \boldsymbol{E} - \tilde{\boldsymbol{E}}^T \tilde{Q} \tilde{\boldsymbol{E}} + 2\mathrm{sgn}(h_{\bar{v}}) \bar{w} \boldsymbol{E}^T P \boldsymbol{b} \\ & + 2\tilde{\boldsymbol{E}}^T (\mathrm{sgn}(h_{\bar{v}}) P \boldsymbol{b} + h_{\bar{v}} \tilde{P} \boldsymbol{b})(v_{ad} - \bar{\Delta}) \end{aligned} \tag{A.4.9}$$

where $c_1 = \bar{w}^* \|P\boldsymbol{b}\|,\ c_2 = (\|P\boldsymbol{b}\| + h^B \|\tilde{P}\boldsymbol{b}\|)\theta^*$.

Utilizing the boundedness of (A.4.5, A.4.6),

$$\begin{aligned}
\dot{L} \leq & -\lambda_{\min}(Q)\|\boldsymbol{E}\|^2 - \lambda_{\min}(\tilde{Q})\|\tilde{\boldsymbol{E}}\|^2 + 2c_1\|\boldsymbol{E}\| + 2c_2\|\tilde{\boldsymbol{E}}\| \\
\leq & -\lambda_{\min}(Q)\left(\|\boldsymbol{E}\| - \frac{c_1}{\lambda_{\min}(Q)}\right)^2 + \frac{c_1^2}{\lambda_{\min}(Q)} \\
& -\lambda_{\min}(\tilde{Q})\left(\|\tilde{\boldsymbol{E}}\| - \frac{c_2}{\lambda_{\min}(\tilde{Q})}\right)^2 + \frac{c_2^2}{\lambda_{\min}(\tilde{Q})} \\
\leq & -\lambda_{\min}(Q)\left(\|\boldsymbol{E}\| - \frac{c_1}{\lambda_{\min}(Q)}\right)^2 \\
& -\lambda_{\min}(\tilde{Q})\left(\|\tilde{\boldsymbol{E}}\| - \frac{c_2}{\lambda_{\min}(\tilde{Q})}\right)^2 + \Upsilon
\end{aligned} \tag{A.4.10}$$

$\dot{L}$ is rendered negative when

$$\|\boldsymbol{E}\| > \frac{c_1}{\lambda_{\min}(Q)} + \sqrt{\frac{\Upsilon}{\lambda_{\min}(Q)}} \quad \text{or} \quad \|\tilde{\boldsymbol{E}}\| > \frac{c_2}{\lambda_{\min}(\tilde{Q})} + \sqrt{\frac{\Upsilon}{\lambda_{\min}(\tilde{Q})}}$$

where $\Upsilon = \frac{c_1^2}{\lambda_{\min}(Q)} + \frac{c_2^2}{\lambda_{\min}(\tilde{Q})}$. Hence ultimate boundedness of $E, \tilde{E}, \hat{W}, \hat{V}$ is established. The ultimate bound $\sqrt{\frac{\lambda_{max}(T)}{\lambda_{min}(T)}}C$ can be obtained in the same manner as (A.2.16). When PCH is implemented, Lemma 3.5.1 can be used to ensure boundedness of $\boldsymbol{x}_{rm}$ as in Section 3.4.1. □

A.5 SPR Filter Approach with e-modification (Theorem 3.8.1)

Proof. Choose the following Lyapunov function candidate,

$$L = \left|\frac{1}{h_{\bar{v}}}\right| \bar{\boldsymbol{E}}^T P \bar{\boldsymbol{E}} + \tilde{W}^T \Gamma_W^{-1} \tilde{W} + \mathrm{tr}(\tilde{V}^T \Gamma_V^{-1} \tilde{V}) \tag{A.5.1}$$

The time derivative of L will be

$$\begin{aligned}
\dot{L} =& -\left|\frac{1}{h_{\bar{v}}}\right| \bar{\boldsymbol{E}}^T Q \bar{\boldsymbol{E}} + 2\mathrm{sgn}(h_{\bar{v}}) \bar{\boldsymbol{E}}^T P \boldsymbol{b} (\tilde{W}^T (\hat{\boldsymbol{\sigma}}_f - \hat{\sigma}' \hat{V}^T \boldsymbol{\mu}) + \hat{W}^T \hat{\sigma}' \tilde{V}^T \boldsymbol{\mu} + \bar{w}) \\
&+ 2(\tilde{W}^T \Gamma_W^{-1} \dot{\tilde{W}}) + 2\mathrm{tr}(\tilde{V}^T \Gamma_V^{-1} \dot{\tilde{V}}) \\
=& -\left|\frac{1}{h_{\bar{v}}}\right| \bar{\boldsymbol{E}}^T Q \bar{\boldsymbol{E}} + 2\mathrm{sgn}(h_{\bar{v}}) \bar{e} (\tilde{W}^T (\hat{\boldsymbol{\sigma}}_f - \hat{\sigma}' \hat{V}^T \boldsymbol{\mu}) + \hat{W}^T \hat{\sigma}' \tilde{V}^T \boldsymbol{\mu} + \bar{w}) \\
&- 2\tilde{W}^T \left[\mathrm{sgn}(h_{\bar{v}}) (\hat{\boldsymbol{\sigma}}_f - \hat{\sigma}' \hat{V}^T \boldsymbol{\mu}) \bar{e} + k_e |\bar{e}| \hat{W}\right] \\
&- 2\mathrm{tr}(\tilde{V}^T \left[\mathrm{sgn}(h_{\bar{v}}) \boldsymbol{\mu} \bar{e} \hat{W}^T \hat{\sigma}' + k_e |\bar{e}| \hat{V}\right]) \\
=& -\left|\frac{1}{h_{\bar{v}}}\right| \bar{\boldsymbol{E}}^T Q \bar{\boldsymbol{E}} + 2\mathrm{sgn}(h_{\bar{v}}) \bar{e} \bar{w} - 2k_e |\bar{e}| (\tilde{W}^T \hat{W} + \mathrm{tr}(\tilde{V}^T \hat{V}))
\end{aligned} \tag{A.5.2}$$

Using the bound of $\bar{w}$ in (3.8.8),

$$\begin{aligned}
\dot{L} \leq& -\left|\frac{1}{h_{\bar{v}}}\right| \bar{\boldsymbol{E}}^T Q \bar{\boldsymbol{E}} + 2\|\bar{e}\|(c_1 \|\tilde{Z}\| + c_2) - 2k_e |\bar{e}| (\tilde{W}^T \hat{W} + \mathrm{tr}(\tilde{V}^T \hat{V})) \\
\leq& -\frac{\lambda_{min}(Q)}{|h_{\bar{v}}|} \|\bar{\boldsymbol{E}}\|^2 + 2\|\bar{C}\| \|\bar{\boldsymbol{E}}\| (c_1 \|\tilde{Z}\| + c_2) - k_e \|\bar{C}\| \|\bar{\boldsymbol{E}}\| (\|\tilde{Z}\|^2 - Z^{*^2}) \\
\leq& -\frac{\lambda_{min}(Q)}{|h_{\bar{v}}|} \|\bar{\boldsymbol{E}}\|^2 + \|\bar{C}\| \|\bar{\boldsymbol{E}}\| \left(2c_1 \|\tilde{Z}\| + 2c_2 - k_e \|\tilde{Z}\|^2 + k_e Z^{*^2}\right) \\
\leq& -\frac{\lambda_{min}(Q)}{|h_{\bar{v}}|} \|\bar{\boldsymbol{E}}\|^2 + \|\bar{C}\| \|\bar{\boldsymbol{E}}\| \left(c_1^2 + \|\tilde{Z}\|^2 + 2c_2 - k_e \|\tilde{Z}\|^2 + k_e Z^{*2}\right) \\
\leq& -\|\bar{\boldsymbol{E}}\| \left[\frac{\lambda_{min}(Q)}{|h_{\bar{v}}|} \|\bar{\boldsymbol{E}}\| + \|\bar{C}\| \left\{(k_e - 1)\|\tilde{Z}\|^2 - c_1^2 - 2c_2 - k_e Z^{*2}\right\}\right]
\end{aligned} \tag{A.5.3}$$

Then $\dot{L} \leq 0$ when one of the following conditions is satisfied.

$$\begin{aligned}
\|\bar{\boldsymbol{E}}\| &\geq \frac{|h_{\bar{v}}| \|\bar{C}\| (c_1^2 + 2c_2 + k_e Z^{*2})}{\lambda_{min}(Q)} \\
\|\tilde{Z}\| &\geq \sqrt{\frac{(c_1^2 + 2c_2 + k_e Z^{*2})}{k_e - 1}}
\end{aligned} \tag{A.5.4}$$

Ultimate boundedness of $\bar{\boldsymbol{E}}$ and $\tilde{Z}$ has been shown. The ultimate bound $\sqrt{\frac{\lambda_{max}(T)}{\lambda_{min}(T)}}C$ can be obtained in the same manner as (A.2.16). From (3.8.4) $\boldsymbol{E}_a$ is bounded with bounded signal $\tilde{Z}$. Hence boundedness of $\boldsymbol{E}$ is established. □

A.6 Augmentation of Existing Controllers with SPR Filter and σ-modification (Theorem 4.1.2)

Proof. Consider the following Lyapunov function candidate.

$$L = \left|\frac{1}{h_{\bar{u}}}\right| \boldsymbol{z}^T P \boldsymbol{z} + \boldsymbol{z}_f^T P_f \boldsymbol{z}_f + \tilde{W}^T F^{-1} \tilde{W} \tag{A.6.1}$$

Then the derivative of L is expressed as

$$\begin{aligned}
\dot{L} =& \frac{d}{dt}\left|\frac{1}{h_{\bar{u}}}\right| \boldsymbol{z}^T P \boldsymbol{z} + \left|\frac{1}{h_{\bar{u}}}\right| \left[-\boldsymbol{z}^T Q \boldsymbol{z} + 2\boldsymbol{z}^T P \bar{\boldsymbol{b}} h_{\bar{u}} (\tilde{W}^T \boldsymbol{\phi}_f + \delta_f - \epsilon_f)\right] \\
& - \boldsymbol{z}_f^T Q_f \boldsymbol{z}_f + 2 z_f^T P_f B_f \boldsymbol{\phi} - 2\tilde{W}^T (\mathrm{sgn}(h_{\bar{u}}) e \boldsymbol{\phi}_f + k_\sigma W) \\
=& - \boldsymbol{z}^T Q \boldsymbol{z} + 2\mathrm{sgn}(h_{\bar{u}}) e (\tilde{W}^T \boldsymbol{\phi}_f + \delta_f - \epsilon_f) \\
& - \boldsymbol{z}_f^T Q_f \boldsymbol{z}_f + 2 z_f^T P_f B_f \boldsymbol{\phi} - 2\tilde{W}^T (\mathrm{sgn}(h_{\bar{u}}) e \boldsymbol{\phi}_f + k_\sigma \hat{W})
\end{aligned} \tag{A.6.2}$$

Utilizing the property of (4.1.31), we get the following inequality

$$\begin{aligned}
\dot{L} \leq & - \left(\frac{\lambda_{min}(Q)}{h^B} - H\lambda_{max}(P)\right) \|\boldsymbol{z}\|^2 + 2\|C\|\|\boldsymbol{z}\|(\kappa_1 \|\tilde{W}\| + \epsilon_f^*) \\
& - \lambda_{min}(Q_f)\|\boldsymbol{z}_f\|^2 \\
& + 2\|z_f\|\|P_f B_f\|\|\boldsymbol{\phi}\| - k_\sigma \|\tilde{W}\|^2 + k_\sigma W^{*^2} \\
\leq & - \left(\frac{\lambda_{min}(Q)}{h^B} - H\lambda_{max}(P)\right) \|\boldsymbol{z}\|^2 + \kappa_1 \|C\|(\|\boldsymbol{z}\|^2 + \|\tilde{W}\|^2) + \epsilon_f^* \|C\|(\|\boldsymbol{z}\|^2 + 1) \\
& - \lambda_{min}(Q_f)\|\boldsymbol{z}_f\|^2 + \|P_f B_f\|\|\boldsymbol{\phi}\|(\|z_f\|^2 + 1) \\
& - k_\sigma \|\tilde{W}\|^2 + k_\sigma W^{*^2} \\
\leq & - \left(\frac{\lambda_{min}(Q)}{h^B} - H\lambda_{max}(P) - \kappa_2\right) \|\boldsymbol{z}\|^2 - (\lambda_{min}(Q_f) - \kappa_3)\|\boldsymbol{z}_f\|^2 \\
& - (k_\sigma - \kappa_4)\|\tilde{W}\|^2 + \Upsilon
\end{aligned} \tag{A.6.3}$$

where $\kappa_2 = (\kappa_1 + \epsilon_f^*)\|C\|,\ \kappa_3 = \|P_f B_f\|\|\boldsymbol{\phi}\|,\ \kappa_4 = \kappa_1\|C\|,\ \Upsilon = \epsilon_f^*\|C\| + \|P_f B_f\|\|\boldsymbol{\phi}\| + k_\sigma {W^*}^2$. One of the following conditions

$$\begin{aligned} \|\boldsymbol{z}\| &> \sqrt{\frac{\Upsilon}{\frac{\lambda_{min}(Q)}{h^B} - H\lambda_{max}(P) - \kappa_2}} \\ \|\boldsymbol{z}_f\| &> \sqrt{\frac{\Upsilon}{\lambda_{min}(Q_f) - \kappa_3}} \\ \|\hat{W}\| &> \sqrt{\frac{\Upsilon}{2k_\sigma - \kappa_4}} \end{aligned} \tag{A.6.4}$$

will render $\dot{L} < 0$ outside a compact set provided the following conditions hold

$$\lambda_{min}(Q) > h^B(H\lambda_{max}(P) - \kappa_2), \quad \lambda_{min}(Q_f) > \kappa_3, \quad k_\sigma > \kappa_4 \tag{A.6.5}$$

The ultimate bound $\sqrt{\frac{\lambda_{max}(T)}{\lambda_{min}(T)}}C$ can be computed in the same manner as (A.2.16). □

A.7 Augmentation of Existing Controllers in MIMO Systems with Error Observer and e-modification (Theorem 4.2.1)

Proof. As presented in Section A.1, boundedness of weight error signals is shown first, and this result is used to show boundedness of the tracking and observer error signals.

Consider the following Lyapunov function candidate for the weight error signals

$$L_w = \frac{1}{2}\mathrm{tr}(\tilde{W}^T\Gamma_W^{-1}\tilde{W}) + \frac{1}{2}\mathrm{tr}(\tilde{V}^T\Gamma_V^{-1}\tilde{V}) \tag{A.7.1}$$

The time derivative of L_w is

$$\begin{aligned}
\dot{L}_w =& -\mathrm{tr}\{\tilde{W}^T\left[\hat{\boldsymbol{\sigma}}\hat{\boldsymbol{E}}^T P\bar{B}_m\mathrm{sgn}(H_{\bar{u}}) + k_e\|\hat{\boldsymbol{E}}\|\hat{W}\right]\} \\
&-\mathrm{tr}\{\tilde{V}^T\left[\boldsymbol{\mu}\hat{\boldsymbol{E}}^T P\bar{B}_m\mathrm{sgn}(H_{\bar{u}})\hat{W}^T\hat{\sigma}' + k_e\|\hat{\boldsymbol{E}}\|\hat{V}\right]\} \\
=& -\mathrm{tr}\{\tilde{W}^T\hat{\boldsymbol{\sigma}}\hat{\boldsymbol{E}}^T P\bar{B}_m\mathrm{sgn}(H_{\bar{u}})\} - \mathrm{tr}\{\hat{\boldsymbol{E}}^T P\bar{B}_m\mathrm{sgn}(H_{\bar{u}})\hat{W}^T\hat{\sigma}'(\hat{V}^T\boldsymbol{\mu} - V^T\boldsymbol{\mu})\} \\
&-k_e\|\hat{\boldsymbol{E}}\|\{\mathrm{tr}(\tilde{W}^T\hat{W}) + \mathrm{tr}(\tilde{V}^T\hat{V})\}
\end{aligned} \tag{A.7.2}$$

Using (2.3.11) and $-2\mathrm{tr}(\tilde{Z}^T\hat{Z}) \le -\|\tilde{Z}\|^2 + Z^{*^2}$,

$$\begin{aligned}
\dot{L}_w \le& \sqrt{n_2+1}\|\tilde{W}\|\|\hat{\boldsymbol{E}}\|\|P\bar{B}_m\| + \|\hat{\boldsymbol{E}}\|\|P\bar{B}_m\|\|\hat{W}\|\left(\delta + \frac{a^*}{4}V^*\mu^*\right) \\
&-\frac{k_e}{2}\|\hat{\boldsymbol{E}}\|(\|\tilde{Z}\|^2 - Z^{*^2}) \\
\le& \theta_1\|\hat{\boldsymbol{E}}\|\|\tilde{W}\| - \frac{k_e}{2}\|\hat{\boldsymbol{E}}\|\|\tilde{Z}\|^2 + \theta_2\|\boldsymbol{E}\| \\
\le& \theta_1\|\hat{\boldsymbol{E}}\|\|\tilde{Z}\| - \frac{k_e}{2}\|\hat{\boldsymbol{E}}\|\|\tilde{Z}\|^2 + \theta_2\|\boldsymbol{E}\|
\end{aligned} \tag{A.7.3}$$

where $\theta_1 = \left(\sqrt{n_2+1} + \delta + \frac{a^*}{4}V^*\mu^*\right)\|P\bar{B}_m\|$ and $\theta_2 = \frac{k_e}{2}Z^{*^2} + \|P\bar{B}_m\|W^*\left(\delta + \frac{a^*}{4}V^*\mu^*\right)$. Using $\theta_1\|\tilde{Z}\| \le \frac{k_e}{4}\|\tilde{Z}\|^2 + \frac{\theta_1^2}{k_e}$,

$$\begin{aligned}
&\le -\|\hat{\boldsymbol{E}}\|\left\{\frac{k_e}{4}\|\tilde{Z}\|^2 - \frac{\theta_1^2}{k_e} - \theta_2\right\} \\
&< 0 \quad \text{if} \quad \|\tilde{Z}\| > 2\sqrt{\frac{\theta_1^2}{k_e^2} + \frac{\theta_2}{k_e}}
\end{aligned} \tag{A.7.4}$$

Hence $\tilde{Z}$ is bounded and its bound is denoted as: $\|\tilde{Z}\| \leq \tilde{Z}^*$.

Consider the following Lyapunov function candidate:

$$L = \sum_{i=1}^{n_3} \left[\left| \frac{1}{h_{\bar{u},i}} \right| \boldsymbol{e}_i^T P_i \boldsymbol{e}_i \right] + \tilde{\boldsymbol{E}}^T \tilde{P} \tilde{\boldsymbol{E}} + 2L_w \tag{A.7.5}$$

The derivative of L will be

$$\begin{aligned}
\dot{L} &= \sum_{i=1}^{n_3} \left[\frac{d}{dt} \left| \frac{1}{h_{\bar{u},i}} \right| \boldsymbol{e}_i^T P_i \boldsymbol{e}_i + \left| \frac{1}{h_{\bar{u},i}} \right| [-\boldsymbol{e}_i^T Q_i \boldsymbol{e}_i + 2\boldsymbol{e}_i^T P_i \boldsymbol{b}_i h_{\bar{u},i} (u_{ad,i} - \bar{\Delta}_i)] \right] \\
&- \tilde{\boldsymbol{E}}^T \tilde{Q} \tilde{\boldsymbol{E}} - 2\tilde{\boldsymbol{E}}^T \tilde{P} \bar{B}_m H_{\bar{u}} (\boldsymbol{u}_{ad} - \boldsymbol{\Delta}) + 2\mathrm{tr}(\tilde{W}^T \Gamma_W^{-1} \dot{\tilde{W}}) + 2\mathrm{tr}(\tilde{V}^T \Gamma_V^{-1} \dot{\tilde{V}}) \\
&= \sum_{i=1}^{n_3} \left[\frac{d}{dt} \left| \frac{1}{h_{\bar{u},i}} \right| \boldsymbol{e}_i^T P_i \boldsymbol{e}_i - \left| \frac{1}{h_{\bar{u},i}} \right| [\boldsymbol{e}_i^T Q_i \boldsymbol{e}_i] \right] + 2\boldsymbol{E}^T P \bar{B}_m \mathrm{sgn}(H_{\bar{u}}) (\boldsymbol{u}_{ad} - \bar{\boldsymbol{\Delta}}) \\
&- \tilde{\boldsymbol{E}}^T \tilde{Q} \tilde{\boldsymbol{E}} - 2\tilde{\boldsymbol{E}}^T \tilde{P} \bar{B}_m H_{\bar{u}} (\boldsymbol{u}_{ad} - \boldsymbol{\Delta}) + 2\mathrm{tr}(\tilde{W}^T \Gamma_W^{-1} \dot{\tilde{W}}) + 2\mathrm{tr}(\tilde{V}^T \Gamma_V^{-1} \dot{\tilde{V}})
\end{aligned} \tag{A.7.6}$$

Substituting (4.2.25) and the adaptive laws, this can be written as:

$$\begin{aligned}
\dot{L} &= \sum_{i=1}^{n_3} \left[\frac{d}{dt} \left| \frac{1}{h_{\bar{u},i}} \right| \boldsymbol{e}_i^T P_i \boldsymbol{e}_i - \left| \frac{1}{h_{\bar{u},i}} \right| [\boldsymbol{e}_i^T Q_i \boldsymbol{e}_i] \right] \\
&+ 2\hat{\boldsymbol{E}}^T P B_m \mathrm{sgn}(H_{\bar{u}}) \left[\tilde{W}^T \hat{\boldsymbol{\sigma}} + \hat{W}^T \hat{\sigma}' \tilde{V}^T \boldsymbol{\mu} + \bar{\boldsymbol{w}} \right] \\
&- \tilde{\boldsymbol{E}}^T \tilde{Q} \tilde{\boldsymbol{E}} - 2\tilde{\boldsymbol{E}}^T (P \bar{B}_m \mathrm{sgn}(H_{\bar{u}}) + \tilde{P} \bar{B}_m H_{\bar{u}}) (\boldsymbol{u}_{ad} - \boldsymbol{\Delta}) \\
&- 2\mathrm{tr}(\tilde{W}^T \hat{\boldsymbol{\sigma}} \hat{\boldsymbol{E}}^T P \bar{B}_m \mathrm{sgn}(H_{\bar{u}}) + k_e \|\hat{\boldsymbol{E}}\| \tilde{W}^T \hat{W}) \\
&- 2\mathrm{tr}(\tilde{V}^T \boldsymbol{\mu} \hat{\boldsymbol{E}}^T P \bar{B}_m \mathrm{sgn}(H_{\bar{u}}) \hat{W}^T \hat{\sigma}' + k_e \|\hat{\boldsymbol{E}}\| \tilde{V}^T \hat{V}).
\end{aligned} \tag{A.7.7}$$

$$\begin{aligned}
\dot{L} &= \sum_{i=1}^{n_3} \left[\frac{d}{dt} \left| \frac{1}{h_{\bar{u},i}} \right| \boldsymbol{e}_i^T P_i \boldsymbol{e}_i - \left| \frac{1}{h_{\bar{u},i}} \right| [\boldsymbol{e}_i^T Q_i \boldsymbol{e}_i] \right] \\
&- \tilde{\boldsymbol{E}}^T \tilde{Q} \tilde{\boldsymbol{E}} + 2\hat{\boldsymbol{E}}^T P B_m \mathrm{sgn}(H_{\bar{u}}) \bar{\boldsymbol{w}} \\
&- 2\tilde{\boldsymbol{E}}^T (P \bar{B}_m \mathrm{sgn}(H_{\bar{u}}) + \tilde{P} \bar{B}_m H_{\bar{u}}) (\boldsymbol{u}_{ad} - \boldsymbol{\Delta}) \\
&- 2k_e \mathrm{tr} \left[\tilde{W}^T \hat{W} \|\hat{\boldsymbol{E}}\| \right] - 2k_e \mathrm{tr} \left[\tilde{V}^T \hat{V} \|\hat{\boldsymbol{E}}\| \right].
\end{aligned} \tag{A.7.8}$$

Using upper bounds from (3.4.9) and (3.4.8), the derivative of the Lyapunov function

candidate can be upper bounded as:

$$\begin{aligned}\dot{L} \leq & -\left(\frac{\lambda_{\min}(Q)}{h^B} - H\lambda_{max}(P)\right)\|\boldsymbol{E}\|^2 - \lambda_{\min}(\tilde{Q})\|\tilde{\boldsymbol{E}}\|^2 \\ & + 2(h^B\|\tilde{P}\bar{B}_m\| + \|P\bar{B}_m\|)\|\tilde{\boldsymbol{E}}\|(\alpha_1\|\tilde{Z}\|_F + \alpha_2) \\ & + 2\|P\bar{B}_m\|\|\hat{\boldsymbol{E}}\|(\gamma_1\|\tilde{Z}\|^2 + \gamma_2\|\tilde{Z}\| + \gamma_3) \\ & - k_e\|\hat{\boldsymbol{E}}\|\left[\|\tilde{Z}\|_F^2 - Z^{*^2}\right]\end{aligned} \tag{A.7.9}$$

Further

$$\begin{aligned}\dot{L} \leq & -\left(\frac{\lambda_{\min}(Q)}{h^B} - H\lambda_{max}(P)\right)\|\boldsymbol{E}\|^2 - \lambda_{\min}(\tilde{Q})\|\tilde{\boldsymbol{E}}\|^2 \\ & + \|\tilde{\boldsymbol{E}}\|(2k_9\|\tilde{Z}\|_F + k_{10}) + k_{11}(\|\boldsymbol{E}\| + \|\tilde{\boldsymbol{E}}\|)\|\tilde{Z}\|^2 \\ & + k_{12}(\|\boldsymbol{E}\| + \|\tilde{\boldsymbol{E}}\|) - k_{13}(\|\boldsymbol{E}\| + \|\tilde{\boldsymbol{E}}\|)\|\tilde{Z}\|^2 + 2k_{14}(\|\boldsymbol{E}\| + \|\tilde{\boldsymbol{E}}\|)\|\tilde{Z}\|\end{aligned} \tag{A.7.10}$$

where $k_9 = \alpha_1(h^B\|\tilde{P}\bar{B}_m\| + \|P\bar{B}_m\|),\ k_{10} = 2\alpha_2(h^B\|\tilde{P}\bar{B}_m\| + \|P\bar{B}_m\|),$
$k_{11} = 2\|P\bar{B}_m\|\gamma_1,\ k_{12} = (2\gamma_3\|P\bar{B}_m\| + k_e Z^{*^2}),\ k_{13} = k_e,\ k_{14} = \|P\bar{B}_m\|\gamma_2.$
Grouping terms, (A.7.10) can be written:

$$\begin{aligned}\dot{L} \leq & -\left(\frac{\lambda_{\min}(Q)}{h^B} - H\lambda_{max}(P)\right)\|\tilde{\boldsymbol{E}}\|^2 - (k_{13} - k_{11})(\|\boldsymbol{E}\| + \|\tilde{\boldsymbol{E}}\|)\|\tilde{Z}\|^2 \\ & + 2(k_9 + k_{14})(\|\boldsymbol{E}\| + \|\tilde{\boldsymbol{E}}\|)\|\tilde{Z}\| + (k_{10} + k_{12})(\|\boldsymbol{E}\| + \|\tilde{\boldsymbol{E}}\|)\end{aligned} \tag{A.7.11}$$

Using $2(x^2 + y^2) \geq (x + y)^2$ and $\bar{q} \triangleq \min[\frac{\lambda_{\min}(Q)}{h^B} - H\lambda_{max}(P), \lambda_{\min}(\tilde{Q})]$,

$$\begin{aligned}\dot{L} \leq & -\frac{\bar{q}}{2}(\|\boldsymbol{E}\| + \|\tilde{\boldsymbol{E}}\|)^2 - (k_{13} - k_{11})(\|\boldsymbol{E}\| + \|\tilde{\boldsymbol{E}}\|)\|\tilde{Z}\|^2 \\ & + 2(k_9 + k_{14})(\|\boldsymbol{E}\| + \|\tilde{\boldsymbol{E}}\|)\|\tilde{Z}\| + (k_{10} + k_{12})(\|\boldsymbol{E}\| + \|\tilde{\boldsymbol{E}}\|) \\ & \leq -(\|\boldsymbol{E}\| + \|\tilde{\boldsymbol{E}}\|)[\frac{\bar{q}}{2}(\|\boldsymbol{E}\| + \|\tilde{\boldsymbol{E}}\|) - (k_{13} - k_{11})\|\tilde{Z}\|^2 \\ & + 2(k_9 + k_{14})\|\tilde{Z}\| + (k_{10} + k_{12})] \\ & \leq -(\|\boldsymbol{E}\| + \|\tilde{\boldsymbol{E}}\|)[\frac{\bar{q}}{2}(\|\boldsymbol{E}\| + \|\tilde{\boldsymbol{E}}\|) - (k_{13} - k_{11} - 1)\|\tilde{Z}\|^2 \\ & + (k_9 + k_{14})^2 + (k_{10} + k_{12})]\end{aligned} \tag{A.7.12}$$

The e-modification coefficient k_e should be large enough so that $k_{13} > k_{11} + 1$, equivalently $k_e > \frac{a^* \|P\bar{B}_m\|}{2} + 1$. One of the following conditions

$$\begin{aligned} \|\boldsymbol{E}\| &> \frac{2}{\bar{q}}\Upsilon \\ \|\tilde{\boldsymbol{E}}\| &> \frac{2}{\bar{q}}\Upsilon \\ \|\tilde{Z}\|_F &> \left(\frac{\Upsilon}{k_{13} - k_{11} - 1}\right)^{\frac{1}{2}} \end{aligned} \tag{A.7.13}$$

will render $\dot{L} < 0$ outside a compact set, where $\Upsilon \triangleq (k_9 + k_{14})^2 + (k_{10} + k_{12})$. In the same manner as in Theorem 3.4.1, it is ensured that $\boldsymbol{E}, \tilde{\boldsymbol{E}}, \tilde{Z}$ are ultimately bounded. The ultimate bound $\sqrt{\frac{\lambda_{max}(T)}{\lambda_{min}(T)}}C$ can be obtained in the same manner as (A.2.16). Consequently $\hat{\boldsymbol{E}}, \hat{Z}$ are also bounded. □

A.8 Asymptotic Tracking with Adaptive Bounding (Theorem 5.2.1)

Proof. Consider the following Lyapunov function candidate:

$$L = \left|\frac{1}{f_{\bar{v}}}\right| \boldsymbol{E}^T P \boldsymbol{E} + \tilde{W}^T \Gamma_W^{-1} \tilde{W} + \mathrm{tr}(\tilde{V}^T \Gamma_V^{-1} \tilde{V}) + \tilde{\boldsymbol{\phi}}^T \Gamma^{-1} \tilde{\boldsymbol{\phi}} \tag{A.8.1}$$

where $\tilde{\boldsymbol{\phi}} \triangleq \hat{\boldsymbol{\phi}} - \boldsymbol{\phi}$. The derivative of L will be,

$$\begin{aligned} \dot{L} = &\frac{d}{dt}\left|\frac{1}{f_{\bar{v}}}\right| \boldsymbol{E}^T P \boldsymbol{E} + \left|\frac{1}{f_{\bar{v}}}\right| \left(-\boldsymbol{E}^T Q \boldsymbol{E} + 2\boldsymbol{E}^T P \boldsymbol{b} f_{\bar{v}} (v_{ad} - \bar{\Delta})\right) \\ &+ 2\tilde{W}^T \Gamma_W^{-1} \dot{\tilde{W}} + 2\mathrm{tr}(\tilde{V}^T \Gamma_V^{-1} \dot{\tilde{V}}) + 2\tilde{\boldsymbol{\phi}}^T \Gamma^{-1} \dot{\tilde{\boldsymbol{\phi}}} \end{aligned} \tag{A.8.2}$$

Using (5.2.3) and the update laws in (3.4.38) and (5.2.8),

$$\begin{aligned} \dot{L} =& \frac{d}{dt}\left|\frac{1}{f_{\bar{v}}}\right| \boldsymbol{E}^T P \boldsymbol{E} - \left|\frac{1}{f_{\bar{v}}}\right| \boldsymbol{E}^T Q \boldsymbol{E} \\ &+ 2\mathrm{sgn}(f_{\bar{v}}) \boldsymbol{E}^T P \boldsymbol{b} \left[\tilde{W}^T \hat{\boldsymbol{\sigma}} + \hat{W}^T \hat{\sigma}' \tilde{V}^T \boldsymbol{\mu} + \bar{w} - v_r\right] \\ &+ 2\tilde{W}^T Proj(\hat{W}, -\mathrm{sgn}(f_{\bar{v}}) \hat{\boldsymbol{\sigma}} \boldsymbol{E}^T P \boldsymbol{b}) + 2\tilde{\boldsymbol{\phi}}^T s \|\boldsymbol{E}^T P \boldsymbol{b}\| \\ &+ 2\mathrm{tr}\tilde{V}^T \left[Proj(\hat{V}, -\mathrm{sgn}(f_{\bar{v}}) \boldsymbol{\mu} \boldsymbol{E}^T P \boldsymbol{b} \hat{W}^T \hat{\sigma}')\right] \\ =& \frac{d}{dt}\left|\frac{1}{f_{\bar{v}}}\right| \boldsymbol{E}^T P \boldsymbol{E} - \left|\frac{1}{f_{\bar{v}}}\right| \boldsymbol{E}^T Q \boldsymbol{E} \\ &+ 2\mathrm{sgn}(f_{\bar{v}}) \boldsymbol{E}^T P \boldsymbol{b} (\bar{w} - v_r) \\ &+ 2\tilde{W}^T \left[Proj(\hat{W}, -\mathrm{sgn}(f_{\bar{v}}) \hat{\boldsymbol{\sigma}} \boldsymbol{E}^T P \boldsymbol{b}) + \mathrm{sgn}(f_{\bar{v}}) \hat{\boldsymbol{\sigma}} \boldsymbol{E}^T P \boldsymbol{b}\right] \\ &+ 2\mathrm{tr}\tilde{V}^T \left[Proj\{\hat{V}, -\mathrm{sgn}(f_{\bar{v}}) \boldsymbol{\mu} \boldsymbol{E}^T P \boldsymbol{b} \hat{W}^T \hat{\sigma}'\} + \mathrm{sgn}(f_{\bar{v}}) \boldsymbol{\mu} \boldsymbol{E}^T P \boldsymbol{b} \hat{W}^T \hat{\sigma}'\right] \end{aligned} \tag{A.8.3}$$

Utilizing the property of the projection operator of (3.4.35) and (3.4.37),

$$\begin{aligned} \dot{L} \leq& -\left(\frac{\lambda_{min}(Q)}{f^B} - F\lambda_{max}(P)\right) \|\boldsymbol{E}\|^2 + 2\|\bar{w}\| \|\boldsymbol{E}^T P \boldsymbol{b}\| - 2\boldsymbol{\phi}^T s \|\boldsymbol{E}^T P \boldsymbol{b}\| \\ \leq& -\left(\frac{\lambda_{min}(Q)}{f^B} - F\lambda_{max}(P)\right) \|\boldsymbol{E}\|^2 \end{aligned} \tag{A.8.4}$$

$\dot{L}$ is rendered non-positive provided that $\frac{\lambda_{min}(Q)}{\lambda_{max}(P)} > f^B F$, i.e. A is sufficiently stable. Then all the error signals are bounded and the error dynamics are Lyapunov stable. We will show the asymptotic tracking performance of $\boldsymbol{E}$ using the Barbalat's Lemma

[68]. Let η be

$$\eta \triangleq -\left(\frac{\lambda_{min}(Q)}{f^B} - F\lambda_{max}(P)\right)\|\boldsymbol{E}\|^2 \leq 0 \tag{A.8.5}$$

We show that η is integrable and uniformly continuous. Notice that

$$L(\infty) - L(0) = \int_0^\infty \dot{L}dt \leq \int_0^\infty \eta dt \leq 0 \tag{A.8.6}$$

Since $\boldsymbol{E}, \hat{W}, \hat{V}, \hat{\phi}$ are bounded, $\dot{\boldsymbol{E}}$ is bounded (See (5.1.9)). Therefore,

$$\dot{\eta} = -2\left(\frac{\lambda_{min}(Q)}{f^B} - F\lambda_{max}(P)\right)\boldsymbol{E}^T\dot{\boldsymbol{E}} \in \mathcal{L}_\infty \tag{A.8.7}$$

Hence η is uniformly continuous. Using the Barbalat's Lemma, η tends to zero as t goes to infinity. This implies the tracking error asymptotically converges to the origin. □

REFERENCES

[1] Isidori, A., Nonlinear Control Systems, chap. 4, Springer, Berlin, 1995.

[2] Khalil, H., Nonlinear Systems, chap. 13, Prentice Hall, New Jersey, 3rd ed., 2002.

[3] Lee, A. and Hedrick, J., "Application of Approximate I/O Linearization to Aircraft Flight Control," *Journal of Dynamic Systems, Measurement,and Control*, Vol. 116, 1994, pp. 429–436.

[4] Enns, D., Bugajski, D., Hendrick, R., and Stein, G., "Dynamic inversion: an evolving methodology for flight control design," *International Journal of Control*, Vol. 59, No. 1, 1994, pp. 71–91.

[5] Brinker, J. and Wise, K., "Stability and Flying Quality Robustness of a Dynamic Inversion Aircraft Control Law," *Journal of Guidance,Control and Dynamics*, Vol. 19, No. 6, 1996, pp. 1270–1277.

[6] Cybenko, G., "Approximation by Superpositions of Sigmoidal Function," *Mathematics of Control, Signals, and Systems*, Vol. 2, No. 4, 1989, pp. 303–314.

[7] Funahashi, K., "On the Approximate Realization of Continuous Mappings by Neural Networks," *IEEE Transactions on Neural Networks*, Vol. 2, 1989, pp. 183–192.

[8] Hornik, K., Stinchcombe, M., and White, H., "Multi-layer Feed-forward Networks are Universal Approximators," *IEEE Transactions on Neural Networks*, Vol. 2, 1989, pp. 359–366.

[9] Wang, L., "Fuzzy systems are universal approximators," *IEEE Conference on Fuzzy Systems*, March 1992, pp. 1163–1170.

[10] Castro, J., "Fuzzy logic controllers are universal approximators," *IEEE Transactions on System, Man, and Cybernetics*, Vol. 25, No. 4, 1995, pp. 629–635.

[11] Sjoberg, J., Qinghua, Z., Ljung, L., Benveniste, A., Delyon, B., Glorennec, P., Hjalmarsson, H., and Juditsky, A., "Nonlinear Black-box Models in System Identification: a Unified Overview," *Automatica*, Vol. 31, No. 12, 1995, pp. 1691–1724.

[12] Ioannou, P. and Kokotovic, P., Adaptive Systems with Reduced Models, Springer-Verlag, New York, 1983.

[13] Ioannou, P. and Kokotovic, P., "Instability Analysis and Improvement of Robustness of Adaptive Control," *Automatica*, Vol. 20, No. 5, 1984, pp. 583–594.

[14] Narendra, K. and Annaswamy, A., "A New Adaptive Law for Robust Adaptation Without Persistent Excitation," *IEEE Transactions on Automatic Control*, Vol. 32, No. 2, 1987, pp. 134–145.

[15] Narendra, K. and Annaswamy, A., Stable Adaptive Control, chap. 8, Prentice Hall, 1989.

[16] Naik, S., Kumar, P., and Ydstie, B., "Robust continuous time adaptive control by parameter projection," *IEEE Transactions on Automatic Control*, Vol. 37, No. 2, 1992, pp. 182–198.

[17] Pomet, J. and Praly, L., "Adaptive Nonlinear Regulation: Estimation from the Lyapunov Equation," *IEEE Transactions on Automatic Control*, Vol. 37, No. 6, 1992, pp. 729–740.

[18] Egardt, B., *Stability of Adaptive Controller*, Springer-Verlag, New York, 1979.

[19] Peterson, B. and Narendra, K., "Bounded error adaptive control," *IEEE Transactions on Automatic Control*, Vol. AC-27, 1982, pp. 1161–1168.

[20] Ioannou, P. and Sun, J., Robust Adaptive Control, chap. 8, Prentice Hall, New Jersey, 1996.

[21] Ortega, R. and Tang, Y., "Robustness of Adaptive Controllers-a Survey," *Automatica*, Vol. 25, No. 5, 1989, pp. 651–677.

[22] Kim, B. and Calise, A., "Nonlinear Flight Control Using Neural Networks," *Journal of Guidance,Control and Dynamics*, Vol. 20, No. 1, 1997, pp. 26–33.

[23] Rysdyk, R. and Calise, A. J., "Adaptive model inversion flight control for tiltrotor aircraft," *Journal of Guidance,Control and Dynamics*, Vol. 22, No. 3, Feb. 1999, pp. 402–407.

[24] Calise, A., Lee, S., and Sharma, M., "Development of a reconfigurable flight control law for a tailless aircraft," *Journal of Guidance,Control and Dynamics*, Vol. 24, No. 5, Sep.-Oct. 2001, pp. 896–902.

[25] Chen, F. C. and Khalil, H. K., "Adaptive control of nonlinear systems using neural networks," *International Journal of Control*, Vol. 55, No. 6, 1992, pp. 1299–1317.

[26] Yesildirek, A. and Lewis, F., "Feedback Linearization using Neural Networks," *Automatica*, Vol. 31, No. 11, 1995, pp. 1659–1664.

[27] Lewis, F., Liu, K., and Yesildirek, A., "Neural-Net Robot Controller with Guaranteed Tracking Performance," *International Symposium on intelligent control, Chicago, IL*, Aug. 1993, pp. 225–231.

[28] Lewis, F., Yesildirek, A., and Liu, K., "Multilayer Neural-Net Robot Controller with Guaranteed Tracking Performance," *IEEE Transactions on Neural Networks*, Vol. 7, No. 2, 1996, pp. 388–399.

[29] Lewis, F., "Neural Network Control of Robot Manipulators," *Expert, IEEE*, Vol. 11, No. 3, June 1996, pp. 64–75.

[30] Leitner, J., Calise, A., and Prasad, J., "Analysis of Adaptive Neural Networks for Helicopter Flight Control," *Journal of Guidance,Control and Dynamics*, Vol. 20, No. 5, 1997, pp. 972–979.

[31] McFarland, M. and Calise, A., "Multilayer neural networks and adaptive control of agile anti-air missile," *Journal of Guidance,Control and Dynamics*, Vol. 23, No. 3, 2000, pp. 547–553.

[32] Widrow, B. and Lehr, M., "30 years of adaptive neural networks: Perceptron, madaline, and backpropagation," *'Proceedings of the IEEE'*, Vol. 78, No. 9, 1990, pp. 1415–1442.

[33] Hunt, K., Sbarbaro, D., Zbikowski, R., and Gawthrop, P., "Neural networks for control systems-A survey," *Automatica*, Vol. 28, No. 6, 1992, pp. 1083–1112.

[34] Lewis, F., "Nonlinear network Structures for Feedback Control," *Asian Journal of Control*, Vol. 1, No. 4, Dec. 1999, pp. 205–228.

[35] Kim, Y. and Lewis, F., "Neural Network Output Feedback Control for Robot Manipulators," *IEEE Transactions on Robotics and Automation*, Vol. 15, No. 2, April 1999, pp. 301–309.

[36] Hovakimyan, N., Rysdyk, R., and Calise, A., "Dynamic neural networks for output feedback control," *Proceedings of the IEEE Conference for Decision and Control*, Vol. 2, 1999, pp. 1685–1690.

[37] Hovakimyan, N., Nardi, F., Calise, A., and Lee, H., "Adaptive Output Feedback Control of a Class of Nonlinear Systems," *International Journal of Control*, Vol. 74, No. 12, 2001, pp. 1161–1169.

[38] Calise, A., Hovakimyan, N., and Idan, M., "Adaptive Output Feedback Control of Nonlinear Systems using Neural Networks," *Automatica*, Vol. 37, No. 8, 2001, pp. 1201–1211.

[39] Hovakimyan, N., Nardi, F., Calise, A., and Kim, N., "Adaptive Output Feedback Control of Uncertain Systems using Single Hidden Layer Neural Networks," *IEEE Transactions on Neural Networks*, Vol. 13, No. 6, Nov. 2002.

[40] Johnson, E. and Calise, A., "Neural Network Adaptive Control of Systems with Input Saturation," *Proceedings of the IEEE American Control Conference*, 2001, pp. 3527–3532.

[41] Johnson, E., Calise, A., El-Shirbiny, H., and Rysdyk, R., "Feedback Linearization with Neural Network Augmentation Applied to X-33 Attitude Control," *Proceedings of the AIAA Guidance, Navigation and Control Conference*, Aug. 2000.

[42] Kim, Y. and Lewis, F., High Level Feedback Control with Neural Networks, chap. 3, World Scientific, Singapore, 1998.

[43] McFarland, M. and Stansbery, D., "Adaptive nonlinear autopilot for anti-air missiles," *AIAA Missile Science Conference*, Monterey, CA, 1998.

[44] Sharma, M. and Calise, A., "Neural Network Augmentation of Existing Linear Controllers," Proceedings of the AIAA Guidance, Navigation and Control Conference, Aug. 2001.

[45] Calise, A., Yang, B.-J., and Craig, J., "Augmentation of an Existing Linear Controller with an Adaptive Element," *Proceedings of the IEEE American Control Conference, Ankorage, AK, May 8-10*, 2002.

[46] Yang, B., Calise, A., and Craig, J., "An Augmenting Adaptive Approach to Control of Flexible Systems," *Proceedings of the AIAA Guidance, Navigation and Control Conference*, 2002.

[47] Hovakimyan, N., Yang, B.-J., and Calise, A., "An adaptive output feedback control methodology for non-minimum phase systems," *Proceedings of the IEEE Conference for Decision and Control*, 2002.

[48] Kim, N., Calise, A., Hovakimyan, N., Prasad, J., and Corban, E., "Adaptive Output Feedback for High-Bandwidth Flight Control," *Journal of Guidance,Control and Dynamics*, Vol. 25, No. 6, 2002, pp. 993–1002.

[49] Zhang, T., Ge, S., and Hang, C., "Direct Adaptive Control of Non-affine Nonlinear Systems Using Multilayer Neural Networks," *Proceedings of the IEEE American Control Conference*, June 1998, pp. 515–519.

[50] Bartle, R., The Elements of Real Analysis, Wiley & Sons, 1964.

[51] Narendra, K. S., "Neural networks for control: Theory and practice," *Proceedings of the IEEE*, Vol. 84, No. 10, Oct. 1996, pp. 1385–1406.

[52] Zhang, T., Ge, S., and Hang, C., "Design and performance analysis of a direct adaptive controller for nonlinear systems," *Automatica*, Vol. 35, 1999, pp. 1809–1817.

[53] Khalil, H., Nonlinear Systems, chap. 4, Prentice Hall, New Jersey, 3rd ed., 2002.

[54] Lavretsky, E., Hoavakimyan, N., and Calise, A., "Upper bounds for approximation of continuous-time dynamics using delayed outputs and feedforward neural networks," *IEEE Transactions on Automatic Control*, Vol. 48, No. 9, Sept. 2003, pp. 1606–1610.

[55] Hovakimyan, N., Nardi, F., and Calise, A., "A Novel Observer based Adaptive Output Feedback Approach for Control of Uncertain Systems," *Proceedings of the IEEE American Control Conference*, 2001, pp. 2444–2449.

[56] Hovakimyan, N., Nardi, F., and Calise, A., "A Novel Error Observer based Adaptive Output Feedback Approach for Control of Uncertain Systems," *IEEE Transactions on Automatic Control*, Vol. 47, No. 8, 2002, pp. 1310–1314.

[57] Corban, J. E., Calise, A., Prasad, J., Hur, J., and Kim, N., "Flight Evaluation of Adaptive High-Bandwidth Control Methods for Unmanned Helicopters," *Proceedings of the AIAA Guidance, Navigation and Control Conference*, 2002-4441.

[58] Kutay, A. T., Calise, A. J., and Hovakimyan, N., "Adaptive Output Feedback Control with Reduced Sensitivity to Sensor Noise," *Proceedings of the IEEE American Control Conference,* ACC03-AIAA0031, June 2003.

[59] Lewis, F., Jagannathan, S., and Yesildirek, A., Neural Network Control of Robot Manipulators and Nonlinear Systems, chap. 4, Taylor & Francis, Philadelphia, PA, 1999.

[60] Sastry, S. and Bodson, M., Adaptive Control: Stability, Convergence and Robustness, chap. 7, Prentice Hall, Englewood Cliffs, NJ, 1989.

[61] Khalil, H., Nonlinear Systems, chap. 6, Prentice Hall, New Jersey, 3rd ed., 2002.

[62] Isidori, A., Nonlinear Control Systems, chap. 5, Springer, Berlin, 1995.

[63] Sastry, S., Nonlinear Systems, chap. 9, Springer, 1999.

[64] Sharma, M., *A Neuro-Adaptive Autopilot Design for Guided Munitions*, Ph.D. thesis, School of Aerospace Engineering, Georgia Institute of Technology, 2001.

[65] Yavrucuk, I. and Prasad, J., "Adaptive Limit Margin Prediction and Control Cueing for Carefree Maneuvering of VTOL Aircraft," *AHS Flight Controls and Crew System Design Technical Specialists Meeting, Philadelphia, PA*, Oct. 2002.

[66] Prasad, J. and Yavrucuk, I., "Adaptive Limit Prediction and Avoidance for Rotorcraft," *28th European Rotorcraft Forum, Bristol, UK*, Sept. 2002.

[67] Yavrucuk, I., Unnikrishnan, S., and Prasad, J., "Carefree Maneuvering Using Neural Networks," *AIAA Atmospheric Flight Mechanics Conference, Monterey, CA*, Aug. 2002.

[68] Slotine, J. and Li, W., Applied Nonlinear Control, chap. 4, Prentice Hall, New Jersey, 1991.

[69] Polycarpou, M., "Stable adaptive neural control scheme for nonlinear systems," *IEEE Transactions on Automatic Control*, Vol. 41, No. 3, 1996, pp. 447–451.

[70] Polycarpou, M. and Mears, M., "Stable adaptive tracking of uncertain systems using nonlinearly parameterized online approximators," *International Journal of Control*, Vol. 70, No. 3, 1998, pp. 363–384.

[71] Nardi, F., *Neural Network based Adaptive Algorithms for Nonlinear Control*, Ph.D. thesis, School of Aerospace Engineering, Georgia Institute of Technology, 2000.

VITA

Nakwan Kim, born in Seoul, Korea, was awarded a Bachelor of Science degree in Aerospace Engineering from Seoul National University in 1995. He worked at the Aerospace Research & Development Center of Daewoo Heavy Industries from 1995 to 1998. He joined the School of Aerospace Engineering at the Georgia Institute of Technology in 1998, where he received a Master of Science degree in Aerospace Engineering in 1999 and began a Ph.D. in 2000. His research interests include nonlinear control, robust adaptive control, neural network control, and simulation.